

AIX-MARSEILLE UNIVERSITÉ
FACULTÉ DE MÉDECINE DE MARSEILLE
ÉCOLE DOCTORALE DES SCIENCES DE LA VIE ET DE LA SANTÉ

THÈSE DE DOCTORAT

Présentée et publiquement soutenue devant

L'IHU MÉDITERRANÉE INFÉCTION

Le 24 Novembre 2017

Par Mme Feriel BOUZID

Née le 27 Janvier 1990 à Sfax, TUNISIE

**La Canettose, une maladie infectieuse émergente
dans la corne de l'Afrique**

Pour obtenir le grade de DOCTEUR d'AIX-MARSEILLE UNIVERSITÉ

SPÉCIALITÉ: Microbiologie

Membres du Jury de la Thèse:

Président du Jury	Professeur Florence FENOLLAR,	Marseille
Rapporteur	Professeur Jean Louis HERRMANN,	Paris
Rapporteur	Docteur Priscille BRODIN,	Lille
Examineur	Docteur Laurent KREMER,	Montpellier
Directeur de Thèse	Professeur Michel DRANCOURT,	Marseille
Co-directeur de Thèse	Docteur Stéphane CANAAN,	Marseille

Unité de Recherche sur les Maladies Infectieuses et Tropicales Émergentes (URMITE)
Directeur : Professeur Didier RAOULT

2017

AVANT PROPOS

Le format de présentation de cette thèse correspond à une recommandation de la spécialité Maladies Infectieuses et Microbiologie, à l'intérieur du Master des Sciences de la Vie et de la Santé qui dépend de l'École Doctorale des Sciences de la Vie de Marseille.

Le candidat est amené à respecter des règles qui lui sont imposées et qui comportent un format de thèse utilisé dans le Nord de l'Europe et qui permet un meilleur rangement que les thèses traditionnelles. Par ailleurs, la partie introduction et bibliographie est remplacée par une revue publiée dans un journal scientifique afin de permettre une évaluation extérieure de la qualité de la revue et de permettre à l'étudiant de commencer le plus tôt possible une bibliographie exhaustive sur le domaine de cette thèse. Par ailleurs, la thèse est présentée sur article publié, accepté ou soumis associé d'un bref commentaire donnant le sens général du travail. Cette forme de présentation a paru plus en adéquation avec les exigences de la compétition internationale et permet de se concentrer sur des travaux qui bénéficieront d'une diffusion internationale.

Pr. Didier Raoult

REMERCIEMENTS

Je manque de mots pour remercier et témoigner de toute ma gratitude pour toute personne qui m'a soutenue au cours de ma thèse.

"Les mots manquent aux émotions" (Victor Hugo)

Monsieur **Michel Drancourt**, travailler avec vous était une expérience de vie. Vos conseils scientifiques, votre confiance et vos encouragements vont m'accompagner tout au long de ma vie professionnelle et personnelle. Trouvez là l'expression de ma forte gratitude.

"Le vrai patron est quelqu'un qui se mêle passionnément de votre travail, qui le fait avec vous, par vous" (Jules Romains)

Monsieur **Stéphane Canaan**, vous m'avez accompagné dès mes premières heures à Marseille et vous m'avez fourni encadrement, encouragement et motivation tout le long de ma thèse. Je vous remercie et vous suis très reconnaissante.

"La reconnaissance est la mémoire du cœur" (Hans Christian Andersen)

Monsieur **Didier Raoult**, à travers vous j'ai appris que le succès n'est pas un hasard, c'est le fruit du travail acharné. Merci d'avoir accepté de financer ma thèse et m'offrir l'opportunité de travailler au sein de votre laboratoire.

"La valeur d'un homme tient dans sa capacité à donner et non dans sa capacité à recevoir" (Albert Einstein)

Papa, Maman, Fares, Hassen et Dorra, vous m'avez tant encouragé et soutenu pour la thèse et pour toute la vie. Je vous aime et j'espère que je vous ai rendus fiers de moi. **Norane**, à toi le flambeau ma petite!

"L'amour d'une famille, le centre autour duquel tout gravite et tout brille" (Victor Hugo)

Je n'oublierai jamais tous les moments de partage avec des gens riches par leurs différences, je cite mes amis jeunes **doctorants**, les **ingénieurs** et les **techniciens** de l'URMITE et l'EIPL. J'ai eu la chance d'être bien entourée par vous. Merci et gardez le sourire !

*Un sourire ne coûte rien et produit beaucoup
Il enrichit ceux qui le reçoivent, sans appauvrir ceux qui le donnent
Il ne dure qu'un instant mais son souvenir est parfois éternel
(Raoul Follereau)*

SOMMAIRE

1. Résumé	1
2. Abstract	4
3. Introduction et objectifs	8
4. CHAPITRE I : Les bacilles tuberculeux lisses: revue de la littérature	14
Article : Smooth Tubercle Bacilli: Neglected Opportunistic Tropical Pathogens	16
5. CHAPITRE II : Étude microbiologique de la tuberculose pulmonaire à Djibouti	33
5.1. Article 1 : Extended spectrum of antibiotic susceptibility for tuberculosis, Djibouti	36
5.2. Article 2 : Multi-drug resistant “ <i>Mycobacterium occultatum</i> posttuberculosis” and <i>Mycobacterium tuberculosis</i> lung co-infection, the Horn of Africa	53
6. CHAPITRE III : Modèle murin d’infection à <i>Mycobacterium canettii</i> par voie digestive	80
Article : Ready experimental translocation of <i>Mycobacterium canettii</i> yields pulmonary tuberculosis	83
7. CHAPITRE IV : Infection des tissus adipeux par <i>Mycobacterium canettii</i>	114
Article : <i>Mycobacterium canettii</i> infection of adipose tissues	117
8. CHAPITRE V : Approches expérimentales pour l’étude du métabolisme des lipides des bacilles tuberculeux: revue de la littérature	133
Article : Experimental models of foamy macrophages and approaches for dissecting the mechanisms of lipid accumulation and consumption during dormancy and reactivation of tuberculosis	135
9. Conclusions et perspectives	152
10. Références	160

1. Résumé

La tuberculose est l'une des maladies infectieuses mortelles les plus fréquentes ayant causé 10,4 million de nouveaux cas et 1,4 million de morts en 2015 selon l'Organisation Mondiale de Santé. Cette maladie est causée par des mycobactéries tuberculeuses génétiquement apparentées qui forment le complexe *Mycobacterium tuberculosis* dont principalement *M. tuberculosis*.

Notre thèse a porté sur la compréhension des sources et modes de transmission de *Mycobacterium canettii*, qui est le taxon le plus proche de l'ancêtre commun du complexe *M. tuberculosis*, caractérisé par un morphotype lisse et un temps de génération plus court que *M. tuberculosis*.

Notre revue de la littérature a montré que moins d'une centaine de cas d'infection à *M. canettii* ont été rapportés chez des patients majoritairement exposés à la République de Djibouti située dans la Corne de l'Afrique. Cette revue a synthétisé les données cliniques, microbiologiques et moléculaires et nous a fait émettre l'hypothèse d'une porte d'entrée digestive.

Afin d'actualiser les données épidémiologiques, notre étude microbiologique prospective de la tuberculose pulmonaire à Djibouti a mesuré une prévalence d'infections à *M. canettii* de 4% qui reste faible par rapport à celle de *M. tuberculosis* (94%). Au cours de cette étude, nous avons isolé pour la première fois à Djibouti et pour la seconde fois dans le monde, une mycobactérie non-tuberculeuse antérieurement dénommée "*Mycobacterium simulans*". Sa description phénotypique et génétique complète nous a amenés à la renommer "*Mycobacterium occultatumposttuberculosis*" signifiant « mycobactérie cachée derrière la tuberculose ».

Également, nous avons observé que 100% des souches testées (73 *M. tuberculosis* dont neuf isolats multi-résistants, trois *M. canettii*, une "*M. occultatumposttuberculosis*" et une

Mycobacterium kansasii) étaient inhibées par la clofazimine, la minocycline et le chloramphénicol ; et 94% par la sulfadiazine ; suggérant l'ajout de ces antibiotiques dans le traitement de la tuberculose pulmonaire surtout en cas de résistance aux antibiotiques anti-tuberculeux de première ligne.

Pour étudier notre hypothèse d'une porte d'entrée digestive de *M. canettii*, nous avons développé un modèle murin d'infection par gavage. Nous avons observé la translocation de *M. canettii* des intestins vers la circulation lymphatique et sanguine ; suivie par une dissémination principalement vers les poumons et les ganglions lymphatiques. Cette étude a alors démontré que *M. canettii* peut infecter les individus à partir du tractus digestif et a révélé que *M. canettii* peut interagir avec le tissu adipeux brun.

Nous avons approfondi ces observations en développant des modèles d'infection *ex vivo* : *i*) les pré-adipocytes blancs et bruns extraits à partir de tissus adipeux murins et *ii*) les pré-adipocytes et adipocytes matures de la lignée cellulaire continue 3T3-L1. Ces travaux expérimentaux ont montré que les pré-adipocytes bruns pourraient constituer une cible potentielle des mycobactéries tuberculeuses. Nous avons également constaté que *M. canettii* intra-adipocyte accumule dans inclusions lipidiques intra-cytoplasmiques mais ne persiste pas dans les cellules contrairement à *M. tuberculosis*.

Sur cette base, nous avons revu les modèles *in vitro* et *in vivo* qui permettent d'étudier le mécanisme d'accumulation des lipides chez les mycobactéries. Les avantages et les limites de chaque modèle ont été discutés dans une revue qui constitue désormais un outil de travail pour les chercheurs spécialisés dans ce domaine.

En conclusion, ce travail de thèse nous a permis d'apporter de connaissances nouvelles sur l'infection à *M. canettii* : sa prévalence, son mode de transmission ainsi que de nouvelles pistes sur de possibles réservoirs environnementaux. L'ensemble de ces données suggèrent

que l'infection à *M. canettii* doit être considérée comme une entité clinique distincte de la tuberculose à *M. tuberculosis* que nous proposons de nommer « Canettose ».

Mots clés: *Mycobacterium canettii*, bacilles tuberculeux lisses, canettose, *Mycobacterium tuberculosis*, tuberculose, modèle murin, infection, tractus digestif, aliments, tissu adipeux, adipocytes, lipides, "*Mycobacterium occultatum posttuberculosis*".

2. Abstract

Tuberculosis is one of the most frequent deadly infectious diseases worldwide which claimed 10.4 million new cases and 1.4 million deaths in 2015 according to the World Health Organization. This disease is caused by genetically related tuberculous mycobacteria that form the *Mycobacterium tuberculosis* complex including mainly *M. tuberculosis*.

Our thesis focused on understanding the sources and modes of transmission of *Mycobacterium canettii*, which is the taxon closest to the common ancestor of the *M. tuberculosis* complex, characterized by a smooth morphotype and a shorter generation time than *M. tuberculosis*.

Our review of the literature showed that less than one hundred cases of *M. canettii* infection have been reported in patients predominantly exposed to the Republic of Djibouti in the Horn of Africa. This work allowed us to synthesize the clinical, microbiological and molecular data on *M. canettii* raising the hypothesis of a digestive borne of infection.

In order to update the epidemiological data, our prospective microbiological study of pulmonary tuberculosis in Djibouti measured a prevalence of *M. canettii* lung infections of 4%, lower than that of *M. tuberculosis* (94%). In the same study, we isolated for the first time in Djibouti and for the second time in the world a non-tuberculous mycobacterium previously named "*Mycobacterium simulans*". After a complete phenotypic and genetic description of this species, we proposed to rename it as "*Mycobacterium occultatumposttuberculosis*" meaning "hidden behind tuberculosis".

We also observed that 100% of the tested strains (73 *M. tuberculosis* including 9 multi drug resistant isolates, three *M. canettii*, one "*M. occultatumposttuberculosis*" and one *M. kansasii*) were inhibited by clofazimine, minocycline and chloramphenicol; and 94% by

sulfadiazine. These results support including these antibiotics in the treatment of pulmonary tuberculosis especially in the case of resistance to first-line anti-tuberculosis drugs.

To study our hypothesis of a digestive entry of *M. canettii*, we developed murine model of *M. canettii* infection by gavage. We then observed the translocation of *M. canettii* from the intestines to the lymphatic and blood circulation; followed by dissemination mainly to the lungs and lymph nodes. In conclusion, this study demonstrated that *M. canettii* can follow the digestive tract to infect individuals and revealed also that *M. canettii* can interact with brown adipose tissue.

We have explored these observations by developing *ex-vivo* cell infection models using: *i*) white and brown pre-adipocytes extracted from murine adipose tissues and *ii*) pre-adipocytes and mature adipocytes of 3T3-L1 continuous cell line. In summary, we have shown that brown pre-adipocytes may be a potential target for tuberculous mycobacteria. We also found that intra-adipocyte *M. canettii* accumulates intra-cytoplasmic lipid inclusions but does not persist contrary to *M. tuberculosis*.

Finally, we reviewed the *in vitro* and *in vivo* models to study the mechanism of lipid accumulation in mycobacteria. The advantages and limitations of each model have been discussed and this review is now a working tool for researchers specialized in this field.

In conclusion, this work allowed to bring new knowledge about *M. canettii* infection: its prevalence, its mode of transmission as well as new avenues on possible environmental reservoirs. All of these data suggest that *M. canettii* infection should be considered as a distinct clinical entity from *M. tuberculosis* tuberculosis. We propose to name "Canettosis" the *M. canettii* infection.

Key words: *Mycobacterium canettii*, smooth tubercle bacilli, canettosis, *Mycobacterium tuberculosis*, tuberculosis, murine model, infection, digestive tract, food, adipose tissue, adipocytes, lipids, “*Mycobacterium occultatum*posttuberculosis”.



INTRODUCTION & OBJECTIFS

3. Introduction et objectifs

La tuberculose est une maladie infectieuse bactérienne contagieuse qui constitue une cause majeure de mortalité à travers le monde (WHO, 2016). En 2015, 10,4 million de nouveaux cas de tuberculose humaine et 1,4 million de morts ont été recensés par l'Organisation Mondiale de Santé (WHO, 2016). Cette infection est caractérisée par une longue phase de latence au cours de laquelle les mycobactéries restent dormantes dans des granulomes pulmonaires (Russell et al., 2009) ou dans des sanctuaires adipeux (Neyrolles et al., 2006). Des estimations récentes ont montré que près d'un tiers de la population mondiale est actuellement atteint de tuberculose latente (WHO, 2016). Toutefois, seuls 5% à 10% des personnes infectées risquent de développer une tuberculose active au cours de leur vie.

La microbiologie de la tuberculose a été déchiffrée pour la première fois par Robert Koch qui, en 1882, a isolé et cultivé la bactérie responsable des infections tuberculeuses (Koch, 1882; Cambau and Drancourt, 2014). Il s'agit de *Mycobacterium tuberculosis*; l'agent étiologique de la maladie qui cause la majorité des cas d'infections humaines. Les plus anciens cas d'infections d'*Homo sapiens* à *M. tuberculosis* ont été documentés à Dja'de el Mughara (Syrie) et daté de -11.000 ans (Baker et al., 2015) et à Atlit-Yam (Israël) dans un site daté de -9.000 ans (Hershkovitz et al., 2008). Ces découvertes témoignent de la longue co-évolution de *M. tuberculosis* avec les populations humaines.

M. tuberculosis est un bacille acido-alcool-résistant à croissance lente caractérisé par ses colonies sèches et rugueuses sur milieu solide (Figure 1). La coloration de Ziehl-Neelsen (Koch and Cote, 1965) donne des bacilles roses adoptant une disposition en corde (Figure 1). Ces caractéristiques phénotypiques constituent la base du diagnostic microbiologique de *M. tuberculosis* par examen microscopique direct. Dans certains pays à ressources limitées dans lesquels la prévalence et l'incidence de la tuberculose pulmonaire sont élevées, la tuberculose

est documenté seulement sur la base de cet examen microscopique; tel est le cas des pays de la corne de l'Afrique, dont la République de Djibouti (Boyer-Cazajous et al., 2014). D'un point de vue clinique, l'infection par *M. tuberculosis* se manifeste le plus souvent sous forme d'infections pulmonaires graves et son traitement repose essentiellement sur l'administration d'une combinaison d'antibiotiques anti-tuberculeux développés dans les années cinquante (Mitchison, 2005). Cependant, l'impact de la tuberculose sur la santé publique est de plus en plus préoccupant avec l'émergence des souches multi-résistantes aux antituberculeux (MDR) définies par leur résistance simultanée au moins à la rifampicine et l'isoniazide (CDC, 2006). En effet, en 2015, 480.000 nouveaux cas de tuberculoses multi-résistantes ont été estimés (WHO, 2016). Par ailleurs, la lutte contre la tuberculose latente reste plus problématique car aucune stratégie thérapeutique n'est proposée à ce jour. De ce fait, l'infection tuberculeuse latente peut être considérée comme une véritable bombe à retardement car le développement ultérieur d'une tuberculose active chez une personne infectée ne peut pas être évité.

Depuis la découverte de *M. tuberculosis*, d'autres mycobactéries génétiquement apparentées ont été identifiées et regroupées au sein du complexe *M. tuberculosis* qui comprend désormais 13 espèces (Coscolla et al., 2013; Ghodbane and Drancourt, 2013; Parsons et al., 2013). En 1968, Georges Canetti, médecin-chercheur à l'Institut Pasteur de Paris, a isolé des colonies lisses d'une mycobactérie à partir d'un échantillon clinique d'un fermier français de 20 ans présentant des symptômes de tuberculose pulmonaire (Asselineau et al., 1969; Aboubaker Osman et al., 2015). Cette souche est actuellement connue sous le nom de *Mycobacterium canettii* CIPT 140010059 et fait partie de la collection d'Institut Pasteur. Deux ans plus tard, il a obtenu un second isolat d'un autre fermier souffrant de tuberculose pulmonaire à Madagascar ; puis une troisième souche chez un patient souffrant d'adénite tuberculeuse à Papeete, Tahiti (Bruno, 2006; Aboubaker Osman et al., 2015). En 1993, une nouvelle souche lisse nommée « So93 » a été isolée à partir d'une adénopathie d'un

enfant Somalien âgé de deux ans (van Soolingen et al., 1997). Le séquençage du gène ribosomique ARNr 16S et de quatre gènes de ménage (*rpoB*, *katG*, *rpsL* et *gyrA*) a montré que les deux isolats *M. canettii* CIPT 140010059 et So93 étaient génétiquement identiques et faisaient partie du complexe *M. tuberculosis* (van Soolingen et al., 1997). Depuis, une centaine de souches de *M. canettii* ont été rapportées dans la littérature. De façon surprenante, la majorité des isolats ont été obtenus à partir de patients habitants ou ayant séjournés dans la Corne de l’Afrique (Djibouti, Ethiopie, Somalie et Erythrée) et principalement à la République de Djibouti (Aboubaker Osman et al., 2015). De point de vue phénotypique, *M. canettii* se caractérise par une morphologie lisse de ses colonies contrairement au morphotype rugueux de *M. tuberculosis* (Figure 1) et par un temps de dédoublement plus court (17h pour *M. canettii* versus 25h pour *M. tuberculosis*) (Aboubaker Osman et al., 2015).


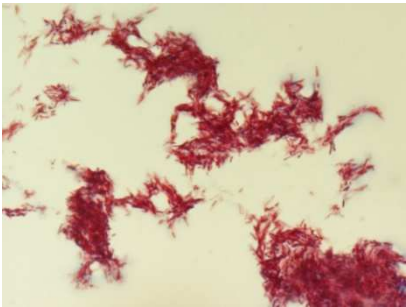

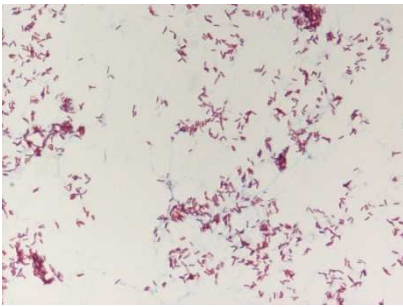
	Culture sur milieu Löwenstein-Jensen	Coloration Ziehl-Neelsen
<i>M. tuberculosis</i> H37Rv		
<i>M. canettii</i> CIPT 140010059		

Figure 1 : Différences phénotypiques entre *M. tuberculosis* et *M. canettii*

Récemment, il a été montré que l'évolution du phénotype lisse au phénotype rugueux était liée à une perte de la biosynthèse des lipooligosaccharides résultant de réarrangements

génomiques du locus codant pour la polyketide-synthase pks5 (Boritsch et al., 2016a). D'autre part, les bacilles révélés par la coloration de Ziehl-Neelsen présentent un aspect plus dispersé et moins cordé que celui obtenu avec *M. tuberculosis* (Koeck et al., 2011) (Figure 1).

De point de vue clinique, les données disponibles indiquent que l'infection par *M. canettii* est responsable de tuberculose pulmonaire chez 52% des patients et de formes extra-pulmonaires chez 48% des patients dont 32% de patients présentant des adénopathies (Aboubaker Osman et al., 2015). Contrairement à *M. tuberculosis*, il n'y a pas d'évidence de transmission inter-humaine de *M. canettii* (Koeck et al., 2011); suggérant la présence d'un réservoir environnemental encore inconnu et laissant une place à la discussion sur le mode de transmission de *M. canettii*. Dans ce cadre, des investigations dans notre laboratoire ont montré que *M. canettii* est capable de survivre dans le sol durant plus d'une année (Ghodbane et al., 2014), résiste à une salinité inférieure ou égale à 3% (Asmar et al., 2016) ainsi qu'à un pH acide entre 2 et 5 après une exposition de deux heures (Bouزيد et al., 2017b) mais est inactivée par une température supérieure ou égale à 45°C (Aboubaker Osman et al., 2017). De point de vue moléculaire, cinq génomes complets de *M. canettii* sont disponibles et ils présentent une taille de $4,48 \pm 0,05$ Mb, qui est légèrement supérieure à celle des autres membres du complexe *M. tuberculosis* (4,4115 Mb pour *M. tuberculosis* H37Rv) (Supply et al., 2013). Ces génomes sont caractérisés par un mosaïcisme génétique (Gutierrez et al., 2005) avec des traces de transferts horizontaux de gènes intra-espèce (Boritsch et al., 2016b). De plus, quatre prophages, probablement responsables de ces transferts, ont été décrits dans quatre différentes souches de *M. canettii* mais aucun phage n'a été observé (Supply et al., 2013; Fan et al., 2014). Enfin, l'analyse des régions variables résultantes des événements d'insertion/délétion a mis en évidence des régions de délétion caractéristiques. En particulier, la région de délétion 1 spécifique de *M. tuberculosis* (TbD1) est absente dans les lignées « modernes » de *M. tuberculosis* et présente dans *M. canettii* (Brosch et al., 2002). Sur ces

bases, *M. canettii* est considérée comme l'espèce cultivée la plus proche génétiquement de l'ancêtre commun putatif du complexe *M. tuberculosis* (Wang et al., 2015). De ce fait, *M. canettii* est le premier membre reconnaissable associé au complexe *M. tuberculosis* et joue donc un rôle central dans l'évolution de la tuberculose humaine.

Dans ce travail de thèse, nous avons comme objectif de mieux comprendre les infections à *M. canettii*. Nous avons réalisé un premier travail bibliographique pour faire le point des connaissances sur les bacilles tuberculeux lisses. Dans un deuxième temps, nous avons étudié la prévalence actuelle des infections pulmonaires à *M. canettii* à travers une étude microbiologique prospective de la tuberculose pulmonaire à Djibouti. Dans un troisième temps, nous avons étudié l'hypothèse de la voie digestive comme voie d'infection possible par *M. canettii*. Enfin, nous avons étudié l'interaction de *M. canettii* avec les tissus adipeux qui seraient des sanctuaires de mycobactéries tuberculeuses. L'ensemble de nos résultats nous a permis de fixer un objectif final, celui de démontrer que l'infection humaine à *M. canettii* serait une entité nosologique en soi que nous proposons d'appeler « Canettose ». Cette maladie présente en effet des différences épidémiologiques, cliniques et microbiologiques avec la tuberculose à *M. tuberculosis* qui confortent notre proposition de création d'une entité nosologique distincte.

CHAPITRE I

Les bacilles tuberculeux lisses

Smooth Tubercle Bacilli: Neglected Opportunistic Tropical Pathogens

Osman AD, Bouzid F, Canaan S, Drancourt M.

Front Public Health. 2016. Review.

4. CHAPITRE I : Les bacilles tuberculeux lisses : revue de la littérature

Georges Canetti est le premier médecin chercheur à avoir isolé les bacilles tuberculeux lisses à la fin des années soixante, mais il n'a jamais décrit officiellement l'espèce. De plus, l'histoire des premiers isolats de *M. canettii* est mal tracée et l'accès aux données cliniques et personnelles des trois premiers patients s'est avéré très difficile (Bruno, 2006). Depuis lors, les cas d'infection à *M. canettii* ont été rapportés dans des études sporadiques et les mêmes collections de souches ont été utilisées par des équipes différentes proposant parfois des nomenclatures de souche différentes.

Dans ce contexte, notre travail avait pour principal objectif de présenter une bibliographie exhaustive sur *M. canettii* en croisant toutes les données de la littérature afin de faciliter l'accès à l'information et présenter les données de manière fidèle. Pour cela, nous avons joint plusieurs équipes de recherche par téléphone ou par e-mail pour avoir des compléments d'information sur la provenance et la traçabilité de certains isolats.

Dans cette revue bibliographique, nous avons recensé 93 isolats de *M. canettii* obtenus à partir de patients exposés aux pays qui composent la Corne de l'Afrique, principalement Djibouti ; à l'exception des trois premiers cas rapportés par Georges Canetti en France, la Polynésie Française et Madagascar. Selon les propos du Professeur Jacques H. Grosset qui travaillait dans les années 1960s sous l'encadrement de G. Canetti à l'Institut Pasteur de Paris, ces exceptions s'expliquent essentiellement par une mauvaise transmission de l'information et proviendraient elles aussi de patients exposés à Djibouti. Ces données suggèrent donc que l'infection à *M. canettii* est une maladie émergente spécifique à la Corne de l'Afrique. Notre travail nous a également permis d'analyser les données cliniques disponibles et de mettre en lumière pour la première fois que la prévalence des infections ganglionnaires causés par *M. canettii* était significativement plus élevée que celle obtenue par *M. tuberculosis* à la même

époque à Djibouti ($P < 0.05$). De plus, ce travail bibliographique nous a conduits à émettre l'hypothèse d'une porte d'entrée digestive de *M. canettii* à partir de l'environnement. D'autre part, l'ensemble des spécificités cliniques, microbiologiques et génomiques présenté dans cette revue est un point de départ extrêmement important pour dégager des pistes sur le mode de transmission et le réservoir potentiel de ces mycobactéries.



Smooth Tubercle Bacilli: Neglected Opportunistic Tropical Pathogens

Djalton Aboubaker Osman^{1,2†}, Ferial Bouzid^{1,3†}, Stéphane Canaan³ and Michel Drancourt^{1*}

¹Aix-Marseille Université, URMITE, UMR CNRS 7278, IRD 198, INSERM 1095, Marseille, France, ²Centre d'Études et de Recherche de Djibouti (CERD), Institut de Recherche Médicinale (IRM), Djibouti, Republic of Djibouti, ³Enzymologie Interfaciale et Physiologie de la Lipolyse UMR7282, Centre National de la Recherche Scientifique (CNRS), Aix-Marseille Université, Marseille, France

OPEN ACCESS

Edited by:

Ying Zhang,
Johns Hopkins University, USA

Reviewed by:

Gyanu Lamichhane,
Johns Hopkins University, USA
Wing Cheong Yam,
The University of Hong Kong,
Hong Kong

*Correspondence:

Michel Drancourt
michel.drancourt@univ-amu.fr

[†]Djalton Aboubaker Osman and
Ferial Bouzid have contributed
equally to this work.

Specialty section:

This article was submitted to
Infectious Diseases,
a section of the journal
Frontiers in Public Health

Received: 17 August 2015

Accepted: 18 December 2015

Published: 11 January 2016

Citation:

Aboubaker Osman D, Bouzid F,
Canaan S and Drancourt M (2016)
Smooth Tubercle Bacilli: Neglected
Opportunistic Tropical Pathogens.
Front. Public Health 3:283.
doi: 10.3389/fpubh.2015.00283

Smooth tubercle bacilli (STB) including “*Mycobacterium canettii*” are members of the *Mycobacterium tuberculosis* complex (MTBC), which cause non-contagious tuberculosis in human. This group comprises <100 isolates characterized by smooth colonies and cordless organisms. Most STB isolates have been obtained from patients exposed to the Republic of Djibouti but seven isolates, including the three seminal ones obtained by Georges Canetti between 1968 and 1970, were recovered from patients in France, Madagascar, Sub-Sahara East Africa, and French Polynesia. STB form a genetically heterogeneous group of MTBC organisms with large 4.48 ± 0.05 Mb genomes, which may link *Mycobacterium kansasii* to MTBC organisms. Lack of inter-human transmission suggested a yet unknown environmental reservoir. Clinical data indicate a respiratory tract route of contamination and the digestive tract as an alternative route of contamination. Further epidemiological and clinical studies are warranted to elucidate areas of uncertainty regarding these unusual mycobacteria and the tuberculosis they cause.

Keywords: *Mycobacterium tuberculosis* complex, “*Mycobacterium canettii*”, smooth tubercle bacilli, Djibouti, Horn of Africa, amoebas, cellulases

INTRODUCTION

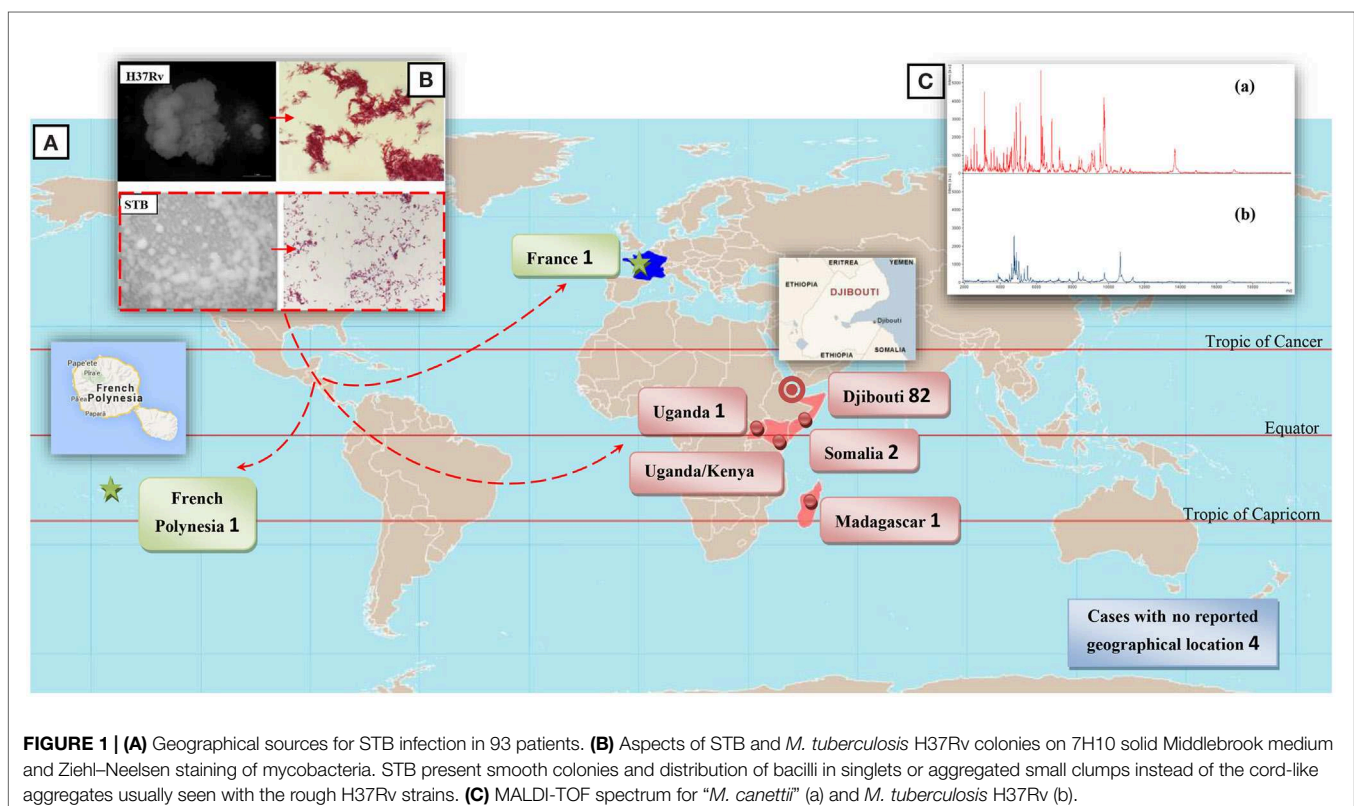
In 2013, 9 million people developed tuberculosis (TB) and 1.5 million people infected with TB died (1). The vast majority of cases were caused by *Mycobacterium tuberculosis stricto sensu*, a cord-forming organism exhibiting rough colonies (2–4) while a few cordless isolates, referred as “smooth tubercle bacilli” (STB) were reported to form smooth colonies (5). The first three STB isolates made by Georges Canetti in 1968–1970 (6) were further named “*Mycobacterium canettii*” following the isolation of an additional STB isolate from a tuberculous lymph node in a Somali child (7). Then, a total of 93 STB have been isolated from patients exposed to tropical countries, mainly the Republic of Djibouti, which reports the highest prevalence and incidence of STB (5, 7–17). The reason for this geographical specificity is not really understood. Despite its rarity, STB deserve special attention due to their epidemiological, clinical, and microbiological characteristics, which are unique among the *M. tuberculosis* complex (MTBC).

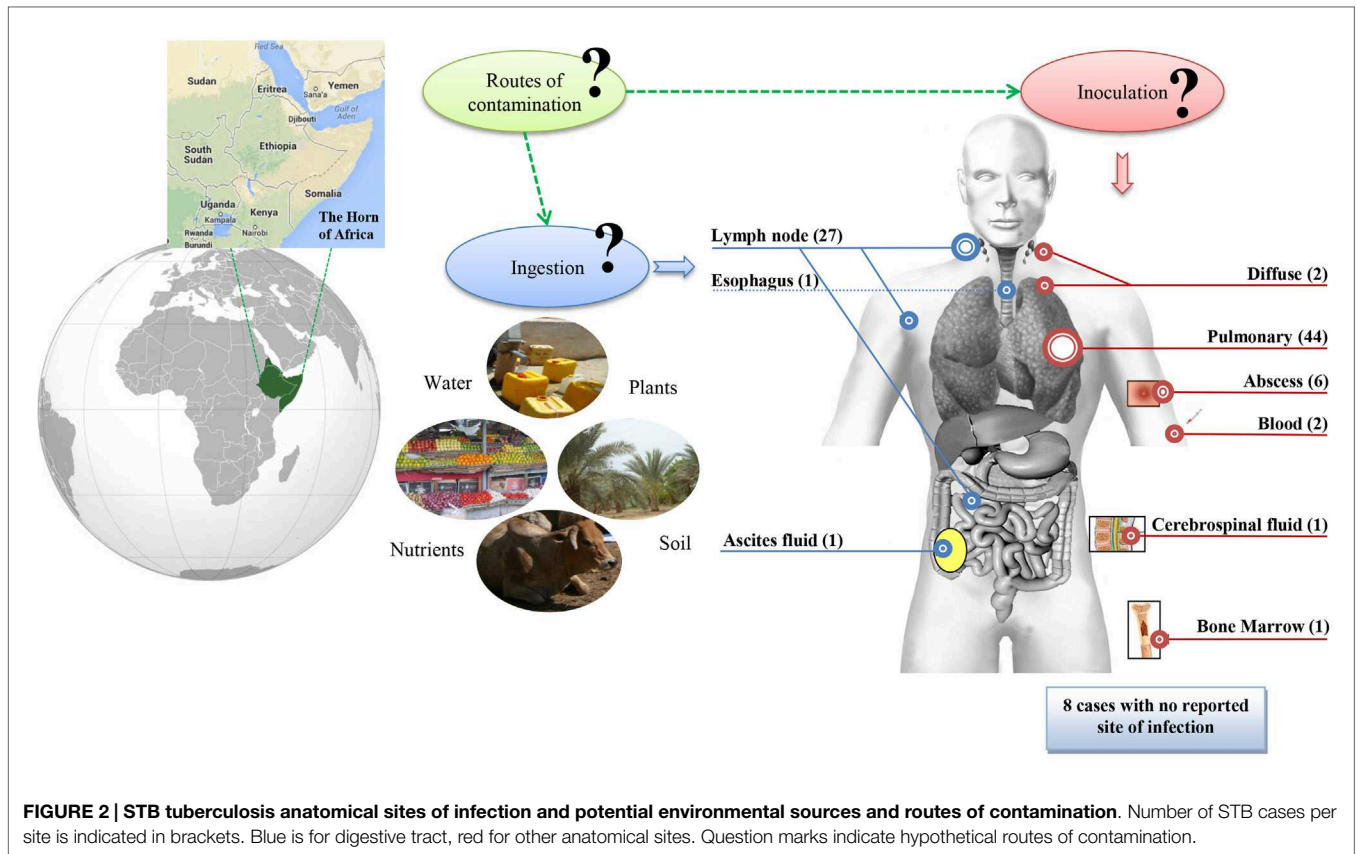
PARTICULARITIES OF THE STB INFECTION

No environmental or animal STB isolates have been identified, contrary to that of *M. tuberculosis* (18). Indeed, the three seminal STB isolates were not reported by Canetti himself, but were rather identified through two indirect sources (6, 19). Accordingly, the precise history of these seminal

isolates is poorly known, although it began prior to 1969, as deduced from a study on *M. tuberculosis* var. *hominis*, Canetti strain mycolic acids submitted for publication in 1968 (20). This first isolate was obtained from a 20-year-old French farmer suffering from pulmonary TB although he had apparently never left France (6, 19). Canetti obtained a second isolate from a 54-year-old farmer also suffering from pulmonary TB in Madagascar, then a third isolate from a man suffering tuberculous adenitis in Papeete, Tahiti (6, 19). Surprisingly, the first ever reported STB isolates were therefore from three patients with no reported contact with the Horn of Africa, where the vast majority of cases had been reported. In 1997, a fourth STB isolate (So93 strain) was reported as “*M. canettii*” (7). The more general term “STB” used here was quoted in a report on *M. tuberculosis* smooth variants in Djibouti (5). Since 1997, a survey of the literature found a total of 93 STB isolates, mainly obtained from patients exposed to tropical countries (Table S1 in Supplementary Material). Indeed, 82/93 (88%) isolates were obtained from patients exposed to the Republic of Djibouti, 2/93 (2%) from patients exposed to Uganda including one also exposed to Kenya, 2/93 (2%) from patients exposed to Somalia, 3 other patients exposed to France, French Polynesia, and Madagascar, and 4 cases with unknown geographical exposure (Figure 1A). With the notable exception of the three seminal isolates, all isolates were obtained between the 23° 26' 16" N and 23° 26' 16" S parallels in tropical countries with a coastline (Figure 1A). Following the description of the first cases in 1969 and 1970, few cases were reported between 1991 and 1997, although 29/93 cases were described from 1998 to 2000. A second peak in case reporting was observed between 2002 and 2003, with 17 cases

being described, and a third peak took place 8 years later with 10 new cases (Figure S1 in Supplementary Material). It should be noted that the number of published cases significantly correlates to the number of STB papers published over the same time period ($P = 1.208e - 13$, Pearson's correlation), suggesting a positive bias in reporting cases (Figure S1 in Supplementary Material). Interest in STB isolates gained ground around the 2000s, suggesting that efforts were concentrated where the main strains were collected, mainly in the Horn of Africa. Furthermore, the unusual macroscopic phenotype of the STB strains may delay their diagnosis and may even result in them being underreported. Clinical data available for 85/93 patients (5, 7, 8, 10, 11, 13–17) indicate 44/85 (52%) had the pulmonary form and 41/85 (48%) had the extra-pulmonary form, including lymph node involvement in 32% of cases (Figure 2). In Djibouti, no significant difference was found in the prevalence of the pulmonary form between STB [17/30 (56.6%)] and *M. tuberculosis stricto sensu* [2,188/3,772; (58%), $P = 0, 88 > 0, 1, X^2$ test] (*Plan National de Lutte Anti Tuberculeuse*, 1997). However, the prevalence of enlarged lymph nodes in STB (12/30; 40%) was significantly higher than in *M. tuberculosis stricto sensu* (717/3,772; 19%) ($P = 0.038, X^2$ test). In Djibouti, a recent epidemiological investigation found that all STB lymph nodes were diagnosed in children and that all STB children had lymph nodes which were infected (8). Indeed, the So93 strain was also obtained from lymphadenitis in a 2-year-old Somali child (7). Of note, the age of children with STB lymph nodes in the Horn of Africa shows a bimodal distribution with 7/14 children ≤ 4 years. This is the median age reported for *Mycobacterium avium hominissuis* lymph nodes (21). This observation suggests that young





children are infected by suction of contaminated fomites. These clinical observations suggest an oropharyngeal portal of entry for STB. Moreover, reports of STB-infected mesenteric lymph nodes (15) as well as one case of STB ascites (19) suggest a digestive tract route of infection in addition to the respiratory tract route. The establishment of an animal model using an oral route for STB infection could evaluate the possibility of STB infection through digestive tract route. Interestingly, in contrast to classical TB infection, there is no evidence of human-to-human transmission of STB infection, suggesting the existence of an as yet unknown environmental reservoir (5). Accordingly, “*M. canettii*” (CIPT140010059) was shown to survive in experimentally infected soil for a minimum of 12 months (22). Taken together, these observations suggest that soil may be a direct or indirect source of STB through drinking water and food, entering and replicating at the oropharyngeal portal of entry and spreading into the respiratory and digestive tracts (Figure 2).

PARTICULARITIES OF THE STB ORGANISMS

The generation time of STB is two to three times shorter than that of *M. tuberculosis* strains in both liquid media and solid media at 30°C and 37°C (3 and 8 days for STB and *M. tuberculosis* H37Rv, respectively, at 37°C as measured by BACTEC 460 System in numerical growth units), a feature also of *Mycobacterium microti*

(9). By definition, STB present smooth colonies, which are white to pale beige and glossy (Figure 1B) (5) correlating with the presence of a large amount of triglycosyl glycolipids (7, 23, 24). Through electron microscopy scanning, colonies were observed to vary from small, singular, flat and cone-shaped to larger compound colonies formed by a homogeneous distribution of bacilli in singlets or aggregated in small clumps instead of the cord-like aggregates usually seen with rough MTBC strains (7) (Figure 1B). Specific biochemical traits, including antibiotic susceptibility patterns, are reported in Table S2 in Supplementary Material. Matrix-Assisted Laser Desorption Ionization-Time-of-Flight Mass Spectrometry (MALDI-TOF-MS) fingerprinting (25) yields a distinctive peptide spectrum for “*M. canettii*” (Figure 1C). Five available whole STB genomes indicate a 4.4202–4.52595 Mb chromosome larger than that of the other MTBC members. This difference is reflected by a set of 890 predicted coding sequences (~20%) present in STB and absent in the other members of the MTBC (17). However, 14/890 (1.6%) genes only are common to all five genome-sequenced STB strains (Table S3 in Supplementary Material) (17). The rest of these genes are variably distributed between the different STB strains (17). Whereas the evolutionary of *M. tuberculosis* is mainly characterized by a genome size reduction linked to gene loss and host adaptation, STB still carry traces of interactions with donor organisms suggesting that STB are environmental organisms, which retain a broad spectrum adaptive capability (17). No phages have been observed, but a controversial 55-kb prophage was identified in STB-I (17,

26), nine spacers matching the *Mycobacterium marinum* strain M prophage, and two spacers matching the Thibault or Redi *Mycobacterium* phages. Three additional prophages, phiBN42_1, phiBN44_1, phiMCAN_1, have been described respectively as “*M. canettii*” CIPT 140070010, “*M. canettii*” CIPT 140060008 and “*M. canettii*” CIPT 140010059 (26). These prophages may play a major role in the evolution of STB, as previously reported for *M. abscessus* (27). Further study found that some STB isolates lacked the insertion element IS1081, while a new ISMycA1 (GenBank accession number AJ619854) was discovered in the “*M. canettii*” CIPT140010059 genome (12). ISMycA1 encodes a transposase which, surprisingly, shares 48% amino acid sequence identity with IS-encoded transposases of the *Mycobacterium ulcerans* plasmid (28). ISMycA1 is a distinctive characteristic of STB in comparison with the other MTBC members (12). Indeed, the original “*M. canettii*” strain (CIPT 140010059) and So93 are indistinguishable from the other MTBC members as a result of sequencing of 16S rRNA and housekeeping genes (*rpoB*, *katG*, *rpsL*, and *gyrA*) (7). Nevertheless, further analysis of six housekeeping genes yielded 14 (A-N) STB clonal groups (12, 17). The multiple locus variable number of tandem repeats analysis (MLVA) (10, 11) highlighted that ETR-A (allele 10), ETR-C (alleles 6 and 10), MIRU-02 (allele 3), MIRU-40 (allele 8), and Mtub29 (allele 5) were unique to STB strains (10). Compared to *M. tuberculosis* H37Rv, investigations showed the presence of an intact region of deletion RD9 and the *M. tuberculosis* specific deletion (TbD1) (11, 29, 30). Indeed, TbD1 region is present in 59 STB strains tested including the seminal isolate “*M. canettii*” CIPT140010059; along with 11 West African *M. africanum* isolates and 20 *Mycobacterium bovis* including two BCG strains. At the opposite, 40 of 46 tested *M. tuberculosis* strains were TbD1 deleted comprising representatives from major tuberculosis epidemics such as the Beijing, Haarlem, African *M. tuberculosis* clusters, and the seminal isolates made by Robert Kock in 1882 (11, 29). The region TbD1 contains two genes encoding two uncharacterized membrane proteins, *mmpS6* gene (Mycobacterium Membrane Protein Small) and *mmpL6* gene (Mycobacterium Membrane Protein Large). In *M. tuberculosis* H37Rv, *mmpS6* is absent and *mmpL6* is truncated.

Genomic analysis revealed that the precorrin gene *cobF*, preserved in many environmental mycobacteria, including *Mycobacterium kansasii* (31), is also present in all STB but is absent in all other MTBC members (8, 17). In STB, repetitive sequences of the PE-PGRS families are highly diverse; in particular, PE_PGRS62 is polymorphic and positively selected in STB, while it is highly preserved in MTBC (31). Indeed, STB strains show unprecedented high genetic heterogeneity with traces of intra-species horizontal gene transfer (HGT) compared to the worldwide population of MTBC strains, which represent one of the most extreme examples of a genetically homogeneous group (8, 12, 17). Recently, distributive conjugal transfer was found to be a predominant mechanism for lateral gene transfer among STB, supporting the high heterogeneity observed in this group (32, 33). This mechanism provides an incomparable means for generating rapidly remarkable genetic diversity in a single step, which makes each strain uniquely different from the others (32). Thus a few STB isolates from a geographically restricted region, the Horn of Africa, show a larger genetic diversity than the

world-wide population of MTBC strains. These observations led to a new evolutionary scenario for the emergence of pathogenic *M. tuberculosis* from an environmental organism, such as *M. kansasii*, through transitional “smooth” tubercle bacilli (34–36).

STB INFECTION MODELS

Only amoebas have been used as a cell model for “*M. canettii*” infection (37). In this model, 89% of “*M. canettii*” organisms, which were co-cultured with free-living *Acanthamoeba polyphaga* amoeba were ingested by trophozoites, a ratio which is significantly higher than for *M. tuberculosis*, *M. bovis*, and *M. avium* (37). This difference correlates with a 2.56 μm larger size for “*M. canettii*” and smoothness reflecting the specific presence of glycolipid containing triglycosyl. In a *M. marinum*–*Acanthamoeba* coculture model, it was shown that lipooligosaccharide modulates the phagocytosis of mycobacteria in *Acanthamoeba* (38). In contrast to *M. tuberculosis* and *M. bovis*, “*M. canettii*” survives into cytoplasmic vacuoles and escapes from encystment (37). This specific behavior could be related to the activation of cellulases Cel6, Cel12 and CBD2 to lyse the cellulose cell wall of the amoebal excyst (39, 40). In the absence of any known reservoir (5), further studies presenting animal models with contradictory results may not be relevant to natural human infection. A first model of guinea pigs, which were inoculated subcutaneously and intramuscularly with 1 mL 10^3 or 10^5 colony-forming units (CFU) of So93 or *M. tuberculosis* H37Rv did not show signs of clinical disease for 8 weeks (7). However, necropsy found overwhelming disseminated tuberculous lesions and severe loss of body fat deposits in guinea pigs inoculated with So93, in contrast to animals inoculated with *M. tuberculosis* H37Rv. In all animals, it has been found that the liver, spleen as well as the lungs were infected. Virulence, measured by microscopic and bacteriological examination and average root index of virulence calculation, was lower for *M. tuberculosis* H37Rv than for So93 (7). In a further study, BALB/c mice were infected intratracheally by 2×10^5 viable cells of “*M. canettii*” (strains CIPT 140010059 and So93) or *M. tuberculosis* H37Rv (41). Two and 3 weeks after infection, “*M. canettii*” induced larger perivascular infiltrates and significantly smaller areas of granuloma in the lung than *M. tuberculosis* H37Rv. Also, “*M. canettii*” CIPT 140010059 induced sustained TNF- α and iNOS expression in lungs combined with delayed and moderate IFN- γ expression. Four-week post-infection, “*M. canettii*” strains yielded almost 100% survivals significantly higher than 40–50% survivals in *M. tuberculosis*-infected animals. In addition, lung replication of “*M. canettii*” strains was significantly lower than that of *M. tuberculosis* H37Rv at all time points. At the final time point, pneumonic areas induced by the “*M. canettii*” CIPT 140010059 were significantly smaller than those produced by *M. tuberculosis* H37Rv (41). In a further model, BALB/c mice were infected intratracheally with 2.5×10^5 viable cells of “*M. canettii*” CIPT 140010059 or ten major genotypes of *M. tuberculosis* (H37Rv, Africa, Amsterdam, Beijing, Erdman, Haarlem, IS-in-Ori, Less-trans, Somalia, Zerocopy) (42). “*M. canettii*” and *M. tuberculosis* H37Rv did not induce lung pathology for 3 weeks, and “*M. canettii*” caused limited pneumonia with mild peribronchiolitis, perivascularitis and alveolitis in the absence of granuloma

formation at day 56 post-infection; at day 120 post-infection, “*M. canettii*” and *M. tuberculosis* H37Rv yielded a similar 10% death rate (42). Additional animal models were conducted by infecting BALB/c and C57BL/6 mice with 10^3 CFUs of STB-D, STB-L, STB-K, or STB-J, *M. tuberculosis* TbD1 positive or *M. tuberculosis* TbD1 negative by intranasal aerosol (17). The STB strains effectively multiplied in the lungs and disseminated to the spleen 3 weeks after inoculation, but consistently persisted for less time during the chronic infection phase (30 weeks), compared to both *M. tuberculosis* strains. Furthermore, 128 days after inoculation, histopathological analyses revealed less severe lung lesions and inflammation in STB-infected mice than in *M. tuberculosis* infected mice (17). The lower virulence and persistence of STB strains correlated to differences in both innate and adaptive immune responses (17). In infected SCID mice, recruitment of activate innate cells was observed in the lung parenchyma 3-week post-infection with STB to a lower extent compared to *M. tuberculosis* infection. In addition, 13-week post-infection lung recruitment of activated CD4⁺ and CD8⁺ lymphocytes was quantitatively lower in STB-infected mice compared to *M. tuberculosis*-infected mice (17).

CONCLUSION

With <100 reported cases, STB infection remains a neglected infectious disease in tropical countries in East Africa. Indeed, their unique morphological features, which are unusual among the MTBC, with smooth, shiny luxuriant, and rapidly growing colonies, may lower their presumptive identification as MTBC

REFERENCES

1. WHO (World Health Organization). *Global Tuberculosis Report*. (2014). Available from: http://apps.who.int/iris/bitstream/10665/137094/1/9789241564809_eng.pdf
2. Julian E, Roldan M, Sanchez-Chardi A, Astola O, Agusti G, Luquin M. Microscopic cords, a virulence-related characteristic of *Mycobacterium tuberculosis*, are also present in nonpathogenic mycobacteria. *J Bacteriol* (2010) **192**:1751–60. doi:10.1128/JB.01485-09
3. Middlebrook G, Dubos RJ, Pierce C. Virulence and morphological characteristics of mammalian tubercle bacilli. *J Exp Med* (1947) **86**:175–84. doi:10.1084/jem.86.2.175
4. Runyon EH. Identification of mycobacterial pathogens utilizing colony characteristics. *Am J Clin Pathol* (1970) **54**:578–86.
5. Koeck JL, Fabre M, Simon F, Daffe M, Garnotel E, Matan AB, et al. Clinical characteristics of the smooth tubercle bacilli ‘*Mycobacterium canettii*’ infection suggest the existence of an environmental reservoir. *Clin Microbiol Infect* (2011) **17**:1013–9. doi:10.1111/j.1469-0691.2010.03347.x
6. Goh KS, Legrand E, Sola C, Rastogi N. Rapid differentiation of “*Mycobacterium canettii*” from other *Mycobacterium tuberculosis* complex organisms by PCR-restriction analysis of the hsp65 gene. *J Clin Microbiol* (2001) **39**:3705–8. doi:10.1128/JCM.39.10.3705-3708.2001
7. van Soolingen D, Hoogenboezem T, de Haas PE, Hermans PW, Koedam MA, Teppema KS, et al. A novel pathogenic taxon of the *Mycobacterium tuberculosis* complex, Canetti: characterization of an exceptional isolate from Africa. *Int J Syst Bacteriol* (1997) **47**:1236–45. doi:10.1099/00207713-47-4-1236
8. Blouin Y, Cazajous G, Dehan C, Soler C, Vong R, Hassan MO, et al. Progenitor “*Mycobacterium canettii*” clone responsible for lymph node tuberculosis epidemic, Djibouti. *Emerg Infect Dis* (2014) **20**:21–8. doi:10.3201/eid2001.130652

members. Their cordless appearance observed after Ziehl–Neelsen staining further complicates first-line identification in endemic countries. The reservoirs and mode of transmission remain unknown but comparing clinical data with scarce experimental data suggests contaminated drinking water and food as potential sources, with local replication in the oropharynx and cervical lymph nodes and further dissemination in the respiratory and digestive tracts. In terms of this hypothesis, looking for STB in the stools of patients would be of interest, as it has been observed in patients with *M. tuberculosis* pulmonary tuberculosis (43, 44). Likewise, genetic and genomic data including large genome size and the abundance of phage sequences, suggest that STB form a heterogeneous group of tuberculosis organisms with intermediate features in between mammal-adapted *M. tuberculosis* organisms and environmental organisms such as *M. kansasii* (36). By means of conclusion, the data reviewed here could form the foundation of efforts toward elucidating the reservoirs and sources of STB, along with the development of laboratory tests aimed at a point-of-care diagnosis of STB infection (45).

ACKNOWLEDGMENTS

This study was financially supported by URMITE, IHU Méditerranée Infection, Marseille, France.

SUPPLEMENTARY MATERIAL

The Supplementary Material for this article can be found online at <http://journal.frontiersin.org/article/10.3389/fpubh.2015.00283>

9. Comas I, Chakravarti J, Small PM, Galagan J, Niemann S, Kremer K, et al. Human T cell epitopes of *Mycobacterium tuberculosis* are evolutionarily hyperconserved. *Nat Genet* (2010) **42**:498–503. doi:10.1038/ng.590
10. Fabre M, Koeck JL, Le Fleche P, Simon F, Herve V, Vergnaud G, et al. High genetic diversity revealed by variable-number tandem repeat genotyping and analysis of hsp65 gene polymorphism in a large collection of “*Mycobacterium canettii*” strains indicates that the *M. tuberculosis* complex is a recently emerged clone of “*M. canettii*”. *J Clin Microbiol* (2004) **42**:3248–55. doi:10.1128/JCM.42.7.3248-3255.2004
11. Fabre M, Hauck Y, Soler C, Koeck JL, van Ingen J, van Soolingen D, et al. Molecular characteristics of “*Mycobacterium canettii*” the smooth *Mycobacterium tuberculosis* bacilli. *Infect Genet Evol* (2010) **10**:1165–73. doi:10.1016/j.meegid.2010.07.016
12. Gutierrez MC, Brisse S, Brosch R, Fabre M, Omais B, Marmiesse M, et al. Ancient origin and gene mosaicism of the progenitor of *Mycobacterium tuberculosis*. *PLoS Pathog* (2005) **1**:e5. doi:10.1371/journal.ppat.0010005
13. Hugard L, Dubrous P, Massoure PL, Renoux E, Desemerie F. [*Mycobacterium canettii* in a tuberculous patient having stayed in Africa]. *Med Mal Infect* (2004) **34**(3):142–3. doi:10.1016/j.medmal.2003.12.005
14. Miltgen J, Morillon M, Koeck JL, Varnerot A, Briant JF, Nguyen G, et al. Two cases of pulmonary tuberculosis caused by *Mycobacterium tuberculosis* subsp canetti. *Emerg Infect Dis* (2002) **8**:1350–2. doi:10.3201/eid0811.020017
15. Pfyffer GE, Auckenthaler R, van Embden JD, van Soolingen D. *Mycobacterium canettii*, the smooth variant of *M. tuberculosis*, isolated from a Swiss patient exposed in Africa. *Emerg Infect Dis* (1998) **4**:631–4. doi:10.3201/eid0404.980414
16. Somoskovi A, Dormandy J, Mayrer AR, Carter M, Hooper N, Salfinger M. “*Mycobacterium canettii*” isolated from a human immunodeficiency virus-positive patient: first case recognized in the United States. *J Clin Microbiol* (2009) **47**:255–7. doi:10.1128/JCM.01268-08

17. Supply P, Marceau M, Mangenot S, Roche D, Rouanet C, Khanna V, et al. Genomic analysis of smooth tubercle bacilli provides insights into ancestry and pathoadaptation of *Mycobacterium tuberculosis*. *Nat Genet* (2013) **45**:172–9. doi:10.1038/ng.2517
18. Ghodbane R, Drancourt M. Non-human sources of *Mycobacterium tuberculosis*. *Tuberculosis* (2013) **93**:589–95. doi:10.1016/j.tube.2013.09.005
19. Bruno D. Tuberculoses à *Mycobacterium Canetti*. Epidémiologie, clinique, microbiologie et phylogénie. Medical Thesis, Bordeaux, France, 2006.
20. Asselineau C, Montrozier H, Prome JC. [Structure of alpha-mycolic acids isolated from the Canetti strain of *Mycobacterium tuberculosis*]. *Bull Soc Chim Fr* (1969) **2**:592–6.
21. Despierres L, Cohen-Bacrie S, Richet H, Drancourt M. Diversity of *Mycobacterium avium* subsp. *hominissuis* mycobacteria causing lymphadenitis, France. *Eur J Clin Microbiol Infect Dis* (2012) **31**:1373–9. doi:10.1007/s10096-011-1452-2
22. Ghodbane R, Mba Medie F, Lepidi H, Nappes C, Drancourt M. Long-term survival of tuberculosis complex mycobacteria in soil. *Microbiology* (2014) **160**:496–501. doi:10.1099/mic.0.073379-0
23. Daffe M, McNeil M, Brennan PJ. Novel type-specific lipooligosaccharides from *Mycobacterium tuberculosis*. *Biochemistry* (1991) **30**:378–88. doi:10.1021/bi00216a011
24. Daffe M, Lacave C, Laneelle MA, Laneelle G. Structure of the major triglycosyl phenol-phthiocerol of *Mycobacterium tuberculosis* (strain Canetti). *Eur J Biochem* (1987) **167**:155–60. doi:10.1111/j.1432-1033.1987.tb13317.x
25. El Khechine A, Couderc C, Flaudrops C, Raoult D, Drancourt M. Matrix-assisted laser desorption/ionization time-of-flight mass spectrometry identification of mycobacteria in routine clinical practice. *PLoS One* (2011) **6**:e24720. doi:10.1371/journal.pone.0024720
26. Fan X, Xie L, Li W, Xie J. Prophage-like elements present in *Mycobacterium* genomes. *BMC Genomics* (2014) **15**:243. doi:10.1186/1471-2164-15-243
27. Sassi M, Gouret P, Chabrol O, Pontarotti P, Drancourt M. Mycobacteriophage-derived diversification of *Mycobacterium abscessus*. *Biol Direct* (2014) **9**:19. doi:10.1186/1745-6150-9-19
28. Stinear TP, Pryor MJ, Porter JL, Cole ST. Functional analysis and annotation of the virulence plasmid pMUM001 from *Mycobacterium ulcerans*. *Microbiology* (2005) **151**:683–92. doi:10.1099/mic.0.27674-0
29. Brosch R, Gordon SV, Marmiesse M, Brodin P, Buchrieser C, Eiglmeier K, et al. A new evolutionary scenario for the *Mycobacterium tuberculosis* complex. *Proc Natl Acad Sci USA* (2002) **99**:3684–9. doi:10.1073/pnas.052548299
30. Marmiesse M, Brodin P, Buchrieser C, Gutierrez C, Simoes N, Vincent V, et al. Macro-array and bioinformatic analyses reveal mycobacterial 'core' genes, variation in the ESAT-6 gene family and new phylogenetic markers for the *Mycobacterium tuberculosis* complex. *Microbiology* (2004) **150**:483–96. doi:10.1099/mic.0.26662-0
31. Namouchi A, Karboul A, Fabre M, Gutierrez MC, Mardassi H. Evolution of smooth tubercle Bacilli PE and PE_PGRS genes: evidence for a prominent role of recombination and imprint of positive selection. *PLoS One* (2013) **8**:e64718. doi:10.1371/journal.pone.0064718
32. Gray TA, Krywy JA, Harold J, Palumbo MJ, Derbyshire KM. Distributive conjugal transfer in mycobacteria generates progeny with meiotic-like genome-wide mosaicism, allowing mapping of a mating identity locus. *PLoS Biol* (2013) **11**:e1001602. doi:10.1371/journal.pbio.1001602
33. Mortimer TD, Pepperell CS. Genomic signatures of distributive conjugal transfer among mycobacteria. *Genome Biol Evol* (2014) **6**(9):2489–500. doi:10.1093/gbe/evu175
34. Minnikin DE, Lee OY, Wu HH, Besra GS, Bhatt A, Nataraj V, et al. Ancient mycobacterial lipids: key reference biomarkers in charting the evolution of tuberculosis. *Tuberculosis* (2015) **95**(Suppl 1):S133–9. doi:10.1016/j.tube.2015.02.009
35. Wang J, Behr MA. Building a better bacillus: the emergence of *Mycobacterium tuberculosis*. *Front Microbiol* (2014) **5**:139. doi:10.3389/fmicb.2014.00139
36. Wang J, McIntosh F, Radomski N, Dewar K, Simeone R, Enninga J, et al. Insights on the emergence of *Mycobacterium tuberculosis* from the analysis of *Mycobacterium kansasii*. *Genome Biol Evol* (2015) **7**:856–70. doi:10.1093/gbe/evv035
37. Mba Medie F, Ben Salah I, Henrissat B, Raoult D, Drancourt M. *Mycobacterium tuberculosis* complex mycobacteria as amoeba-resistant organisms. *PLoS One* (2011) **6**:e20499. doi:10.1371/journal.pone.0020499
38. Alibaud L, Pawelczyk J, Gannoun-Zaki L, Singh VK, Rombouts Y, Drancourt M, et al. Increased phagocytosis of *Mycobacterium marinum* mutants defective in lipooligosaccharide production: a structure-activity relationship study. *J Biol Chem* (2014) **289**:215–28. doi:10.1074/jbc.M113.525550
39. Mba Medie F, Ben Salah I, Drancourt M, Henrissat B. Paradoxical conservation of a set of three cellulose-targeting genes in *Mycobacterium tuberculosis* complex organisms. *Microbiology* (2010) **156**:1468–75. doi:10.1099/mic.0.037812-0
40. Mba Medie F, Vincentelli R, Drancourt M, Henrissat B. *Mycobacterium tuberculosis* Rv1090 and Rv1987 encode functional beta-glucan-targeting proteins. *Protein Expr Purif* (2011) **75**:172–6. doi:10.1016/j.pep.2010.08.015
41. Lopez B, Aguilar D, Orozco H, Burger M, Espitia C, Ritacco V, et al. A marked difference in pathogenesis and immune response induced by different *Mycobacterium tuberculosis* genotypes. *Clin Exp Immunol* (2003) **133**:30–7. doi:10.1046/j.1365-2249.2003.02171.x
42. Dormans J, Burger M, Aguilar D, Hernandez-Pando R, Kremer K, Roholl P, et al. Correlation of virulence, lung pathology, bacterial load and delayed type hypersensitivity responses after infection with different *Mycobacterium tuberculosis* genotypes in a BALB/c mouse model. *Clin Exp Immunol* (2004) **137**:460–8. doi:10.1111/j.1365-2249.2004.02551.x
43. Bonnaville PE, Raoult D, Drancourt M. Gastric aspiration is not necessary for the diagnosis of pulmonary tuberculosis. *Eur J Clin Microbiol Infect Dis* (2013) **32**:569–71. doi:10.1007/s10096-012-1776-6
44. El Khechine A, Henry M, Raoult D, Drancourt M. Detection of *Mycobacterium tuberculosis* complex organisms in the stools of patients with pulmonary tuberculosis. *Microbiology* (2009) **155**:2384–9. doi:10.1099/mic.0.026484-0
45. Cohen-Bacrie S, Ninove L, Nougairde A, Charrel R, Richet H, Minodier P, et al. Revolutionizing clinical microbiology laboratory organization in hospitals with in situ point-of-care. *PLoS One* (2011) **6**:e22403. doi:10.1371/journal.pone.0022403
46. Wanger A, Mills K. Testing of *Mycobacterium tuberculosis* susceptibility to ethambutol, isoniazid, rifampin, and streptomycin by using Etest. *J Clin Microbiol* (1996) **34**:1672–6.
47. Feuerriegel S, Köser CU, Niemann S. *Mycobacterium canettii* is intrinsically resistant to both pyrazinamide and pyrazinoic acid. *J Antimicrob Chemother* (2003) **68**:1439–50. doi:10.1093/jac/dkt042

Conflict of Interest Statement: The authors declare that the research was conducted in the absence of any commercial or financial relationships that could be construed as a potential conflict of interest.

The reviewer Dr Gyanu Lamichhane and handling Editor Dr Ying Zhang declare their shared affiliation, and the handling Editor states that the process nevertheless met the standards of a fair and objective review.

Copyright © 2016 Aboubaker Osman, Bouzid, Canaan and Drancourt. This is an open-access article distributed under the terms of the Creative Commons Attribution License (CC BY). The use, distribution or reproduction in other forums is permitted, provided the original author(s) or licensor are credited and that the original publication in this journal is cited, in accordance with accepted academic practice. No use, distribution or reproduction is permitted which does not comply with these terms.

Supplementary Data

Supplementary Table 1: Informations on reported smooth tubercle bacilli strains

First Id	Alias	Collection Strain Code	TB site	Year isolation	Country of isolation	Patient nationality	Geographical exposure	Gender	Age	Genetic pattern	Principal reference
HB3177		CIPT140010059	Pulm	1968	FR	FR	FR	M	20	STB-A	[6]
HB3178		CIPT140010060	Pulm	1969	FR	FR	Madagascar	M	54	STB-A	[6]
HB3253		CIPT140010061	LN	1970	FR polynesia	FR	Papeete	M	NR	STB-A	[6]
CIPT140010062		CIPT140010062	NR	NR	NR	NR	NR	NR	NR	NR	[23]
910563			NR	1991	FR	NR	NR	NR	NR	NR	[6]
So93		So93	LN	1993	NLA	SOM	SOM	M	2	NR	[7]
NZM 217/94		NZM 217/94	LN	1993	Sw	Sw	Uganda and Kenya	M	56	STB-C	[15]
NR	19990160		Pulm	1998	FR	FR	DJ	M	36	STB-C	[14]
NR	19991574		Pulm	1999	FR	FR	DJ	M	55	STB-D	[14]
NR			Pulm	2002	FR	FR	DJ	M	21	NR	[13]
Percy3	19990516	CIPT140060008 Percy3	Pulm	1998	DJ	DJ	DJ	F	8	STB-D	[10]
Percy6	19990515	Percy6	Pulm	1998	DJ	FR	DJ	F	35	STB-D	[10]
Percy8	19990161	Percy8	LN	1998	DJ	FR	DJ	F	4	STB-C	[10]
Percy21a	19990160	Percy21a	Pulm	2000	DJ	FR	DJ	M	36	STB-C	[10]
Percy21b	20000342	Percy21b	NR	2000	DJ	DJ	DJ	F	NR	STB-D	[10]

Percy22		Percy22	Abs	2003	DJ	FR	DJ	NR	NR		[10]
Percy26	19991708	Percy26	LN	1999	DJ	DJ	DJ	F	18	STB-D	[10]
Percy29a	19990589	Percy29a	Pulm	1999	DJ	ETH	DJ	F	34	STB-D	[10]
Percy30		Percy30	NR	2003	DJ	DJ	DJ	NR	NR	NR	[10]
Percy31b		Percy31b	Blo	2003	DJ	ETH	DJ	NR	NR	NR	[10]
Percy50		Percy50	Pulm	1983	DJ	FR	DJ	NR	NR	NR	[10]
Percy58b		Percy58b	Pulm	2002	DJ	ETH	DJ	NR	NR	NR	[10]
Percy74	20010389	Percy74	Pulm	2001	DJ	DJ	DJ	M	NR	STB-D	[10]
Percy94b		Percy94b	Pulm	2002	DJ	DJ	DJ	NR	NR	NR	[10]
Percy99c	19991704	Percy99c	Pulm	1999	DJ	DJ	DJ	M	22	STB-D	[10]
Percy101		Percy101	Abs	2002	DJ	DJ	DJ	NR	NR	NR	[10]
Percy103		Percy103	BM	2002	DJ	DJ	DJ	NR	NR	NR	[10]
Percy106		Percy106	Pulm	2002	DJ	ETH	DJ	NR	NR	NR	[10]
Percy144		Percy144	LN	2002	DJ	FR	DJ	NR	NR	NR	[10]
Percy150	20001049	Percy150	Pulm	2000	DJ	DJ	DJ	M	NR	STB-D	[10]
Percy156	20010933	Percy156	LN	2001	DJ	DJ	DJ	M	27	STB-D	[10]
Percy189b	20001248	Percy189b	Pulm	2000	DJ	DJ	DJ	M	NR	STB-D	[10]
Percy197b		Percy197b	Pulm	2002	DJ	FR	DJ	NR	NR	NR	[10]
Percy199b	20001247	Percy199b	AF	2000	DJ	DJ	DJ	F	NR	STB-D	[10]
Percy205	20001246	Percy205	Pulm	2000	DJ	DJ	DJ	M	63	STB-D	[10]
Percy206	20001245	Percy206	Pulm	2000	DJ	DJ	DJ	M	NR	STB-D	[10]
Percy212	19981514	Percy212	LN	1998	DJ	DJ	DJ	M	32	STB-C	[10]
Percy229	19990645	Percy229	LN	1997	DJ	NR	DJ	NR	NR	STB-L	[10]
Percy245b	20010188	Percy245b	LN	2000	DJ	DJ	DJ	F	NR	STB-D	[10]
Percy246	20010390	Percy246	LN	2001	DJ	DJ	DJ	M	NR	STB-D	[10]
Percy257	19980862	Percy257	LN	1998	DJ	DJ	DJ	F	40	STB-D	[10]
Percy32	19990711	Percy32	LN	1999	DJ	DJ	DJ	M	13	STB-B	[10]

Percy79	20010391	Percy79	Pulm	2001	DJ	DJ	DJ	M	NR	STB-F	[10]
Percy26b		Percy26b	NR	2003	DJ	DJ	DJ	NR	NR	NR	[10]
Percy94	19991705	Percy94	Pulm	1999	DJ	DJ	DJ	M	42	STB-H	[10]
Percy213	19980864	Percy213	Pulm	1998	DJ	DJ	DJ	M	20	STB-H	[10]
Percy214	19980863	CIPT140070013 Percy214	Pulm	1998	DJ	DJ	DJ	F	27	STB-H	[10]
Percy258	19980865	Percy258	Pulm	1998	DJ	DJ	DJ	M	40	STB-H	[10]
Percy25	19991709	CIPT140070002 Percy25	LN	2000	DJ	DJ	DJ	M	7	STB-E	[10]
Percy65		CIPT140070017 Percy65	LN	1999	DJ	DJ	DJ	F	4	STB-J	[10]
Percy89	20000587	CIPT100070005 Percy89	LN	2000	DJ	ETH	DJ	F	NR	STB-G	[10]
Percy99b	20000473	CIPT140070007 Percy99b	Pulm	2000	DJ	DJ	DJ	M	NR	STB-I	[10]
Percy157	19991669	Percy157	Pulm	1999	DJ	DJ	DJ	M	NR	STB-N	[11, 17]
	19990263		Pulm	1997	FR	DJ	NR	NR	NR	STB-F	[12]
			CF	2005	USA	SUD	Uganda	F	30	NR	[16]
Percy300		Percy300	Blo	2003	DJ	DJ	DJ	NR	NR	NR	[11]
Percy329	20050642	Percy329	Pulm	2005	DJ	FR	DJ	NR	NR	STB-CD	[11, 17]
Percy358		Percy358	NR	2003	DJ	FR	DJ	NR	NR	NR	[11]
Percy516		Percy516	LN	2006	DJ	FR	DJ	NR	NR	NR	[11]
Percy673		Percy673	Abs	2007	DJ	DJ	DJ	NR	NR	NR	[11]
Percy756		Percy756	Pulm	2009	DJ	DJ	DJ	NR	NR	NR	[11]
NLA000200937		NLA000200937	Pulm	2002	NLA	ERI	DJ	NR	NR	NR	[11]
NLA000201000		NLA000201000	Pulm	2002	NLA	SOM	DJ	NR	NR	NR	[11]
NLA000400617		NLA000400617	Abs	2004	NLA	SOM	DJ	NR	NR	NR	[11]

Percy301		Percy301	LN	2003	DJ	DJ	DJ	NR	NR	NR	[11]
Percy525		Percy525	Pulm	2006	DJ	DJ	DJ	NR	NR	NR	[11]
Percy302		CIPT140070010 Percy302	Abs	2004	DJ	DJ	DJ	NR	NR	STB-K	[11]
Percy327		CIPT140070008 Percy327	Abs	1997	DJ	DJ	DJ	NR	NR	STB-L	[11]
NLA000701671		NLA000701671	Pulm	2007	NLA	SOM	DJ	NR	NR	NR	[11]
MTB_K116		MTB_K116	NR	NR	NR	NR	SOM	NR	NR	NR	[11]
3151/08			NR	NR	NR	GER*	NR	NR	NR	NR	[47]
NR	19990264		Pulm	1998	FR	NR	DJ	NR	NR	STB-F	[17]
NR	20040352		LN	2004	DJ	NR	DJ	NR	NR	STB-M	[17]
Percy976		Percy976	Pulm	2010	DJ	DJ	DJ	M	18	STB-A	[8]
Percy977		Percy977	Pulm	2010	DJ	DJ	DJ	F	22	STB-A	[8]
Percy979		Percy979	Pulm	2010	DJ	DJ	DJ	F	39	STB-A	[8]
Percy1004		Percy1004	LN	2010	DJ	DJ	DJ	M	14	NR	[8]
Percy1049		Percy1049	Pulm	2011	DJ	ETH	DJ	F	36	STB-A	[8]
Percy1060		Percy1060	Diffuse	2011	DJ	DJ	DJ	M	33	STB-A	[8]
Percy1062		Percy1062	Pulm	2011	DJ	FR	DJ	M	40	STB-C	[8]
Percy1064		Percy1064	Pulm	2011	DJ	DJ	DJ	M	55	STB-C	[8]
Percy1077		Percy1077	Esophagus	2011	DJ	FR	DJ	M	48	STB-A	[8]
Percy1078		Percy1078	LN	2011	DJ	FR	DJ	F	3	STB-A	[8]
Percy1079		Percy1079	LN	2011	DJ	FR	DJ	M	1	STB-A	[8]
Percy1084		Percy1084	LN	2011	DJ	FR	DJ	M	4	STB-A	[8]
Percy1085		Percy1085	LN	2011	DJ	FR	DJ	F	8	STB-A	[8]
Percy1086		Percy1086	Diffuse	2012	DJ	DJ	DJ	M	51	STB-A	[8]
Percy1101		Percy1101	Pulm	2011	DJ	DJ	DJ	F	26	STB-C	[8]
Percy1105		Percy1105	Pulm	2012	DJ	FR	DJ	M	44	STB-A	[8]

Percy1115		Percy1115	LN	2012	DJ	FR	DJ	M	3	STB-A	[8]
Percy1116		Percy1116	LN	2012	DJ	FR	DJ	M	12	STB-A	[8]
Percy1129		Percy1129	LN	2013	DJ	FR	DJ	F	11	STB-A	[8]
Percy1130		Percy1130	Pulm	2013	DJ	DJ	DJ	M	35	STB-A	[8]

LEGEND

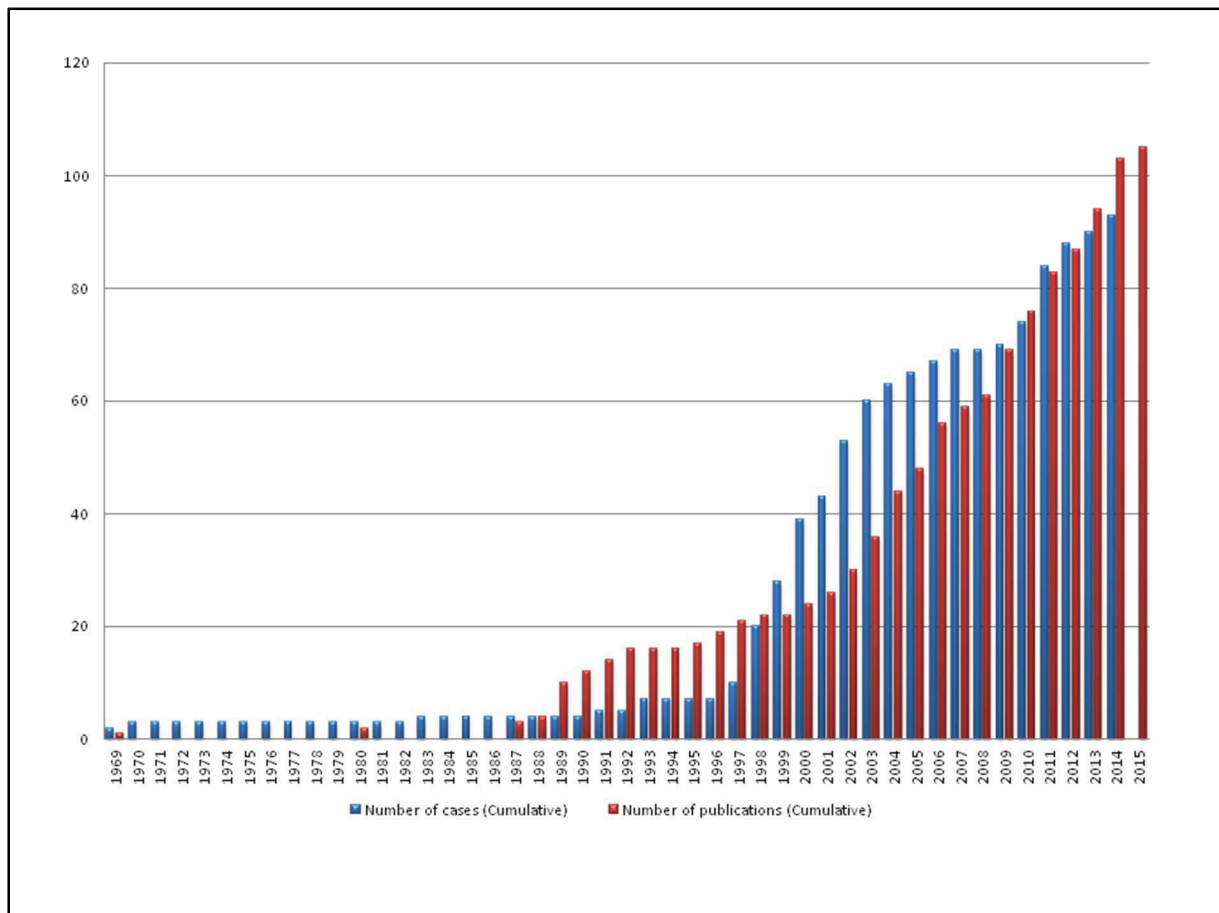
Pulm, pulmonary	DJ, Djibouti
LN, lymph node	FR, France
AF, ascites fluid	NLA, Netherlands
BM, bone marrow	Sw, Switzerland
Abs, abscess	ETH, Ethiopia
Blo, blood	SOM, Somalia
CF, cerebrospinal fluid	ERI, Eritrea
F: Female	SUD, Sudanese
M: Male	GER, Germany
NR, No Reported	

Yellow color: hallmarking of diagnosed cases out of Djibouti

Red color: alias and genetic pattern assigned by deduction

*Information obtained by correspondence with the author

Figure S1: The number of published cases of STB significantly correlates to the number of STB papers published over the same time period ($P = 1.208e - 13$, Pearson's correlation), suggesting a positive bias in reporting cases.



Supplementary Table 2: Classification of STB in comparison with *M. tuberculosis*

H37Rv.

Characteristics	STB	<i>M. tuberculosis</i> H37Rv	References
Morphological			
Colony appearance	Eugonic smooth	Eugonic rough	(5)
Depth of growth	Aerophilic	Micro-aerophilic	(22)
Doubling time in liquid Tween Albumin medium	17 hours	25 hours	(7)
Generation time			
- LJ medium	22 (16–25 days)	23 (18–25 days)	(5)(17)
- BACTEC 460 System	3 days	8 days	
Growth on minimum solid media (Trypticase-soy agar)	Positive	Negative	(5)
Biochemical			
Nitrate reductase	Present	Present	(5)
Niacin production	Absent	Present	(5)
Drug susceptibility			
Pyrazinamide (PZA) 100 mg/L	Resistant	Sensitive	(47)
<i>Thiophen-2-carboxylic acid hydrazine</i> (TCH) 2 mg/L	Resistant	Resistant	(15)
<i>Streptomycin</i> (SM)	2 – 10 µg/mL	0.25–1.0 µg/mL	(16)
Isoniazid (INH)	0.2–1 µg/mL	0.016–0.06 µg/mL	(46)
Rifampin (RIF)	0.2 µg/mL	0.06–0.25 µg/mL	
Ethambutol (EMB)	2.5 – 7.5 µg/mL	0.06–0.25 µg/mL	
Molecular			
Genome size (Mb)	4.29797 – 4.52595	4.4115	(17)
GC%	65.40 – 65.60	65.50	(17)
TbD1 region	Present	Absent	(29)

Supplementary Table 3. Orthologous genes common between the five genome-sequenced STB strains compared to *M. tuberculosis* H37Rv. Adapted from Supply et al, 2013.

<i>M. tuberculosis</i>	STB-K	STB-D	STB-J	STB-L	STB-A	Product
Strain H37Rv NC_000962	CIPT 140070010 FO203509	CIPT 140060008 FO203507	CIPT 140070017 FO203510	CIPT 140070008 FO203508	CIPT 140010059 HE572590	
–	<i>BN42_10093</i>	<i>BN44_10074</i>	<i>BN45_10072</i>	<i>BN43_10072</i>	<i>MYCCP_0071</i>	Conserved protein of unknown function
–	<i>BN42_10094</i>	<i>BN44_10075</i>	<i>BN45_10073</i>	<i>BN43_10073</i>	<i>MCAN_00631</i>	Transcriptional regulator, MerR family
–	<i>BN42_20253</i>	<i>BN44_10577</i>	<i>BN45_10579</i>	<i>BN43_10566</i>	<i>MCAN_05231</i>	Conserved exported protein of unknown function, probable WAG22-like antigen (part 1)

_	<i>BN42_20254</i>	<i>BN44_10577</i>	<i>BN45_10579</i>	<i>BN43_10566</i>	<i>MCAN_05231</i>	Conserved exported protein of unknown function, probable WAG22-like antigen (part 2)
_	<i>BN42_20255</i>	<i>BN44_10577</i>	<i>BN45_10579</i>	<i>BN43_10567</i>	<i>MCAN_05231</i>	Conserved exported protein of unknown function, probable WAG22-like antigen (part 3)
_	<i>BN42_20754</i>	<i>BN44_11037</i>	<i>BN45_20246</i>	<i>BN43_20415</i>	<i>MCAN_09441</i>	Conserved protein of unknown function
_	<i>BN42_20755</i>	<i>BN44_11038</i>	<i>BN45_20247</i>	<i>BN43_20416</i>	<i>MCAN_09451</i>	Precorrin-6A synthase [deacetylating]
_	<i>BN42_20756</i>	<i>BN44_11039</i>	<i>BN45_20248</i>	<i>BN43_20418</i>	<i>MCAN_09461</i>	Conserved protein of unknown function, uncharacterized PE-PGRS family protein PE_PGRS33 (part1)

_	<i>BN42_20756</i>	<i>BN44_11041</i>	<i>BN45_20248</i>	<i>BN43_20418</i>	<i>MCAN_09461</i>	Conserved protein of unknown function, uncharacterized PE-PGRS family protein PE_PGRS33 (part2)
_	<i>BN42_41322</i>	<i>BN44_70059</i>	<i>BN45_60303</i>	<i>BN43_60282</i>	<i>MCAN_32901</i>	Conserved protein of unknown function
_	<i>BN42_41323</i>	<i>BN44_70060</i>	<i>BN45_60304</i>	<i>BN43_60283</i>	<i>MCAN_32911</i>	Putative transposase fusion protein
_	<i>BN42_41325</i>	<i>BN44_70061</i>	<i>BN45_60306</i>	<i>BN43_60284</i>	<i>MCAN_32921</i>	Transposase (part 3)
_	<i>BN42_41326</i>	<i>BN44_70061</i>	<i>BN45_60306</i>	<i>BN43_60285</i>	<i>MCAN_32921</i>	Transposase (part 2)
_	<i>BN42_41327</i>	<i>BN44_70061</i>	<i>BN45_60307</i>	<i>BN43_60285</i>	<i>MCAN_32931</i>	Transposase (part 1)

CHAPITRE II

Étude microbiologique de la tuberculose pulmonaire à Djibouti

Extended spectrum of antibiotic susceptibility for tuberculosis, Djibouti.

Bouزيد F, Astier H, Osman DA, Javelle E, Hassan MO, Simon F, Garnotel E, Drancourt M.

Int J Antimicrob Agents. 2017. *In press.*

5. CHAPITRE II : Étude microbiologique de la tuberculose pulmonaire à Djibouti

5.1. Article 1 : Extended spectrum of antibiotic susceptibility for tuberculosis, Djibouti

Dans plusieurs pays à ressources limitées dont la République de Djibouti, le diagnostic de la tuberculose pulmonaire est essentiellement basé sur le tableau clinique des patients suspects de tuberculose et sur un examen microscopique direct des expectorations après coloration de Ziehl-Neelsen (Boyer-Cazajous et al., 2014). La culture des expectorations n'est pratiquée qu'en cas d'échec thérapeutique et le recours au GeneXpert (Cepheid, Sunnyvale, CA) (Zeka et al., 2011) est limité par le coût élevé et le manque de disponibilité des réactifs. Cependant, le seul examen microscopique des prélèvements respiratoires après coloration de Ziehl-Neelsen ne peut pas diagnostiquer la tuberculose pulmonaire car toutes les mycobactéries tuberculeuses ou non-tuberculeuses présentent les mêmes affinités tinctoriales (Koch and Cote, 1965).

De ce fait, ce mode de diagnostic laisse place à la possibilité que certains patients cliniquement diagnostiqués comme tuberculeux soient en réalité infectés par des mycobactéries non-tuberculeuses. Ce faux diagnostic serait la cause d'échec thérapeutique car les mycobactéries non-tuberculeuses sont peu sensibles aux antibiotiques utilisés pour le traitement anti-tuberculeux standard (Griffith et al., 2007). De plus, ces critères ne fournissent pas suffisamment d'informations pour discriminer entre les espèces du complexe *M. tuberculosis* qui causent la tuberculose. En particulier, la distinction des isolats de *M. canettii* parmi les autres membres du complexe *M. tuberculosis*, n'est possible qu'à travers l'observation du phénotype lisse des colonies avec confirmation par une technique moléculaire. L'absence de cette stratégie d'identification spécifique de l'agent pathogène suggère que le nombre de tuberculose à *M. canettii* peut être sous-évalué dans la corne de

l'Afrique. D'autre part, Djibouti présente une haute incidence de tuberculose de 378 cas sur 100 000 habitants en 2015 (WHO, 2016) potentiellement accentuée par la haute prévalence des souches MDR (Boyer-Cazajous et al., 2014) et le fait que les souches de *M. canettii* sont naturellement résistantes à la pyrazinamide et la streptomycine (Goh et al., 2001).

Afin d'actualiser les données microbiologiques sur la tuberculose pulmonaire à Djibouti y compris les infections à *M. canettii*, nous avons mené une étude épidémiologique prospective sur une période de 8 mois. Nous avons étendu notre objectif microbiologique à l'étude de sensibilité des isolats à des antibiotiques alternatifs aux antibiotiques anti-tuberculeux standards : la clofazimine, la micocycline, le chloramphénicol et la sulfadiazine. Ce projet a pu être mené à bien grâce à une collaboration étroite entre : (1) l'équipe de Hôpital pneumo-physiologie Chakib Saad Omar à Djibouti qui s'est chargée de la collecte des expectorations à partir de patients suspects de tuberculose pulmonaire et des informations relatives aux patients; (2) le laboratoire de biologie à l'Hôpital d'Instruction des Armées Alphonse Laveran à Marseille dirigé par le Pr. Eric Garnotel qui s'est chargé de la culture des expectorations; et (3) notre laboratoire (URMITE) où nous avons identifié les isolats au niveau de l'espèce et réalisé les tests de sensibilité aux antibiotiques. L'identification des isolats a été réalisée par la combinaison de plusieurs analyses : *i*) spectrométrie de masse couplant une source d'ionisation laser assistée par une matrice (MALDI-TOF-MS) (Zingue et al., 2016) ; *ii*) séquençage partiel des gènes *rpoB* et 16S ARNr (Drancourt et al., 2004; Adekambi et al., 2006) et *iii*) PCR multiplexe ciblant les régions de différence (Warren et al., 2006). Pour les tests de sensibilité aux antibiotiques, nous avons utilisé le système automatisé BACTEC™ MGIT™ 960 (Springer et al., 2009).

L'ensemble de ce travail nous a permis d'isoler 111 souches (94%) de *M. tuberculosis*, 5 souches (4%) de *M. canettii* et de manière inattendue deux mycobactéries non-tuberculeuses dont une souche de *Mycobacterium kansasii* et une souche de "*Mycobacterium simulans*" ;

pour la première fois isolées dans le contexte d'une infection pulmonaire à Djibouti. De manière intéressante, l'isolat de "*M. simulans* " constitue le second cas d'infection par cette mycobactérie à travers le monde (Tortoli et al., 2010). La prévalence de *M. canettii* obtenue (4%) était proche de celle rapportée précédemment (Koeck et al., 2002; Boyer-Cazajous et al., 2014).

Les tests de sensibilité aux antibiotiques antituberculeux ont permis de détecter 9 (12%) isolats de *M. tuberculosis* MDR. Cette prévalence est significativement moins importante que celles rapportées dans des études précédentes à savoir 72% (Millan-Lou et al., 2016) et 57% (Boyer-Cazajous et al., 2014). Notre travail nous a également permis d'obtenir 100% d'inhibition de tous les isolats testés avec la clofazimine (1.5 mg/L), la minocycline (4 mg/L), le chloramphénicol (5 mg/L) et 94% d'inhibition avec la sulfadiazine (20 mg/L).

En conclusion, nous avons actualisé les données microbiologiques de la tuberculose pulmonaire à Djibouti, initié la description formelle de "*M. simulans*" et proposé une nouvelle approche thérapeutique des patients tuberculeux en intégrant des antibiotiques anciens.

Accepted Manuscript

Title: Extended spectrum of antibiotic susceptibility for tuberculosis, djibouti

Author: Fériel Bouzid, Hélène Astier, Djaltou Aboubaker Osman, Emilie Javelle, Mohamed Osman Hassan, Fabrice Simon, Eric Garnotel, Michel Drancourt

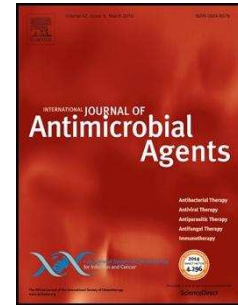
PII: S0924-8579(17)30282-0
DOI: <http://dx.doi.org/doi: 10.1016/j.ijantimicag.2017.07.007>
Reference: ANTAGE 5222

To appear in: International Journal of Antimicrobial Agents

Received date: 28-3-2017
Accepted date: 8-7-2017

Please cite this article as: Fériel Bouzid, Hélène Astier, Djaltou Aboubaker Osman, Emilie Javelle, Mohamed Osman Hassan, Fabrice Simon, Eric Garnotel, Michel Drancourt, Extended spectrum of antibiotic susceptibility for tuberculosis, djibouti, International Journal of Antimicrobial Agents (2017), <http://dx.doi.org/doi: 10.1016/j.ijantimicag.2017.07.007>.

This is a PDF file of an unedited manuscript that has been accepted for publication. As a service to our customers we are providing this early version of the manuscript. The manuscript will undergo copyediting, typesetting, and review of the resulting proof before it is published in its final form. Please note that during the production process errors may be discovered which could affect the content, and all legal disclaimers that apply to the journal pertain.



REVISED VERSION

1 Short communication

2

3 **Extended spectrum of antibiotic susceptibility for tuberculosis, Djibouti**

4

5 Fériel Bouzid^{a,b}, Hélène Astier^c, Djaltou Aboubaker Osman^d, Emilie Javelle^c, Mohamed
6 Osman Hassan^e, Fabrice Simon^f, Eric Garnotel^c, Michel Drancourt^{a*}

7

8 ^a Aix Marseille Université, URMITE, UMR CNRS 7278, IRD 198, INSERM 1095.

9 IHU Méditerranée Infection, Marseille 13005, France.

10 ^b Aix-Marseille Univ, CNRS, EIPL, Marseille, France

11 ^c Hôpital d'instruction des armées Alphonse Laveran, Marseille, France

12 ^d Centre d'Études et de Recherche de Djibouti (CERD), Institut de Recherche Médicinale
13 (IRM), Djibouti, Republic of Djibouti

14 ^e Hôpital pneumo-ptisiologie «Chakib Saad Omar», Republic of Djibouti

15 ^f Pôle Formation-Recherche, Hôpital d'instruction des armées Alphonse Laveran, Marseille,
16 France

17 *Corresponding author: Prof. Michel Drancourt, URMITE, UMR CNRS 7278, IRD 198,
18 INSERM U1095 IHU Méditerranée Infection, 19-21 Bd Jean Moulin 13005 Marseille,
19 France. Tel: +33 (0)4 13 73 24 01 fax: + 33 (0) 13 73 24 02

20 Email: michel.drancourt@univ-amu.fr

21

22 **Keywords:** Mycobacterium tuberculosis, Mycobacterium canettii, “Mycobacterium
23 simulans”, Mycobacterium kansasii, Horn of Africa

24

REVISED VERSION

25 Highlights

- 26 • An updated epidemiology of pulmonary tuberculosis in Djibouti is presented.
- 27 • *Mycobacterium canettii* is one mycobacterium responsible for pulmonary tuberculosis in
28 Djibouti.
- 29 • A second “*Mycobacterium simulans*” worldwide isolate was identified in Djibouti.
- 30 • Antileprosy, sulfamides and chloramphenicol drugs indicate no drug-resistant tuberculosis
31 in Djibouti.

32

33 Abstract

34 The Horn of Africa suffers from a high prevalence of tuberculosis which is reported to be
35 partly driven by multi-drug resistant (MDR) *Mycobacterium tuberculosis strictu sensu* strains.
36 We conducted a prospective study to investigate *M. tuberculosis* complex species causing
37 tuberculosis in Djibouti; along with their in vitro susceptibility to standard anti-tuberculous
38 antibiotics, in addition to clofazimine, minocycline, chloramphenicol and sulfadiazine.
39 Among the 118 mycobacteria isolates from 118 successive patients with suspected pulmonary
40 tuberculosis, 111 strains of *M. tuberculosis*, five *Mycobacterium canettii*, one
41 “*Mycobacterium simulans*” and one *Mycobacterium kansasii* were identified. Drug-
42 susceptibility tests performed on the first 78 isolates yielded nine MDR *M. tuberculosis*
43 isolates; all isolates being fully susceptible to clofazimine, minocycline, chloramphenicol and
44 75/78 susceptible to sulfadiazine. In the Horn of Africa, patients with confirmed pulmonary
45 tuberculosis caused by an in vitro susceptible strain may benefit from anti-leprosy drugs,
46 sulfamides and phenicol antibiotics.

47 **1. Introduction**

48 Tuberculosis remains a major deadly infectious disease worldwide, being
49 responsible for 10.4 million new cases and 1.4 million deaths in 2015 [1]. However, the
50 burden of tuberculosis greatly varies from one country to another, as illustrated by the ten-fold
51 variation in incidence, from 27/100,000 inhabitants in wealthy regions of America to an
52 average rate of 275/100,000 inhabitants in Africa [1]. The Horn of Africa, comprising
53 Djibouti, Ethiopia, Somalia and Eritrea, is a hotspot for tuberculosis with a high incidence of
54 378/100,000 inhabitants in Djibouti in 2015 [1] and 192/100,000 inhabitants in Ethiopia in
55 2015 [1]. In Djibouti, highly prevalent tuberculosis has been reported to be partly driven by
56 so-called multidrug-resistant (MDR) *Mycobacterium tuberculosis* isolates [2, 3] defined as
57 being resistant to at least isoniazid and rifampicin [4]. Moreover in Djibouti, tuberculosis has
58 been caused not only by *M. tuberculosis* isolates but also by *Mycobacterium canettii* in 3%
59 and up to 6% of cases [3, 5]. It should be noted that *M. canettii* organisms are naturally
60 resistant to pyrazinamide and streptomycin [6].

61 With a view to updating information on the microbiology of pulmonary
62 tuberculosis in Djibouti, we prospectively identified mycobacterial isolates from patients
63 presenting with clinically suspected pulmonary tuberculosis and extended in vitro drug
64 susceptibility tests for classic anti-tuberculous antibiotics to clofazimine [7], minocycline [8],
65 chloramphenicol [9] and sulfadiazine [10], all of which were shown to inhibit mycobacteria.

66

67 **2. Materials and methods**

68 **2.1. Patients and sample processing**

69 This study was approved by the IHU Méditerranée Infection, Ethics Committee Approval
70 n°2016-025, Marseille, France. The study was conducted in collaboration with the Hôpital
71 Pneumo-phtisiologie Chakib Saad Omar in Djibouti as part of their routine activity. All

REVISED VERSION

72 patients with suspected pulmonary tuberculosis who attended this hospital between May and
73 December 2016 were included in this study. Informed and consenting patients answered an
74 anonymized questionnaire containing personal information (age, gender, nationality, address,
75 job and travel out of Djibouti), HIV status, medical history and reported tuberculosis cases in
76 their family. Collected sputa were systematically examined by microscopy observation after
77 Ziehl-Neelsen staining. Samples were stored at 4°C before shipment. Every two weeks,
78 samples which tested positive for microscopic detection of acid-fast bacilli were shipped to
79 the biology laboratory in the Hôpital d'Instruction des Armées Alphonse Laveran, Marseille,
80 France, with an average transport time of eight days. Samples were then decontaminated
81 using the BD BBL™ MycoPrep™ Mycobacterial System Digestion/Decontamination Kit
82 (Becton Dickinson, Le Pont-de-Claix, France), and cultured on Coletsos medium (Bio-Rad,
83 Marnes-la-Coquette, France) and on egg-based Lowenstein-Jensen medium (Bio-Rad,
84 Marnes-la-Coquette, France), at 37°C for 60 days. Colonies of positive cultures were stained
85 with fluorescent auramine-O staining (Sigma, Saint-Quentin Fallavier, France). The presence
86 of mycobacteria was confirmed by detecting stained bacilli after fluorescence microscopy
87 examination.

88 2.2. Identification tests

89 Mycobacteria were identified by matrix-assisted laser desorption ionization time-of-flight
90 mass spectrometry (MALDI-TOF-MS) after direct deposit of the colonies [11]. Briefly,
91 colonies were spotted on a MALDI-TOF target plate and then covered with 1 µL matrix
92 solution. After drying, the target plate was introduced into the Microflex LT MALDI-TOF
93 mass spectrometer (Bruker Daltonics, Germany) for analysis. Generated spectra were
94 compared to the Bruker peptide profile database and identification was performed using the
95 pattern-matching process as previously described [11]. 16S rRNA and rpoB gene sequencing
96 [12, 13] were then performed to identify non-tuberculous mycobacteria. *M. tuberculosis*

REVISED VERSION

97 complex isolates were identified at the species level by specific multiplex PCR amplification
98 of regions of difference (RD) RD4, RD9 and RD12 [14] using *M. tuberculosis* H37Rv,
99 *Mycobacterium bovis* BCG Pasteur and *M. canettii* CIP 140010059^T as positive controls and
100 *Mycobacterium smegmatis* mc² 155 as a negative control. *M. canettii* identification was
101 confirmed by partial hsp65 gene sequencing [6] and quantitative real time PCR (qPCR)
102 targeting the cobF gene using cobF_Forward_5'-GCGACTGCTCGTTTCAGG-3',
103 cobF_Reverse_5'-GATGCGTGTCCCGACCTC-3' and cobF_Probe_5'-6FAM-
104 CCGGACACCCGAATCTGGTGG-3'. For all tuberculous isolates, real-time PCR targeting
105 *M. tuberculosis* specific deletion 1 (TbD1) was performed using TbD1_Forward 5'-
106 CAAAGGAACCGCGAAAGTTA-3', TbD1_Reverse 5'-ACCGTGATAAGCACCAGGAC-
107 3' and TbD1_Probe_5'-6FAM-TCGCGGTGATGTTGCTCTTCG-3'. All qPCR
108 experiments were conducted using the CFX96® qPCR, incorporating qPCR reagents
109 (Taqyon, Eurogentec, Liège, Belgium). The qPCR cycle was 50°C for two minutes, 95°C for
110 five minutes followed by 40 cycles of 95°C for one second and 60°C for 35 seconds and
111 finally 45°C for 30 seconds.

112 2.3. Drug susceptibility testing

113 Drug susceptibility tests for streptomycin, isoniazid, rifampicin, ethambutol and pyrazinamide
114 were performed in liquid medium by automated BACTEC™ MGIT™ 960 method using the
115 BACTEC™ MGIT™ 960 SIRE kit and the BACTEC™ MGIT™ 960 PZA kit (Becton
116 Dickinson). Final concentrations in MGIT tubes were 1 µg/mL for streptomycin, 0.10 µg/mL
117 for isoniazid, 1 µg/mL for rifampicin, 5 µg/mL for ethambutol and 100 µg/mL pyrazinamide
118 according to the manufacturer's recommendations (Becton Dickinson). *M. tuberculosis*
119 H37Rv was used as a control strain. Further susceptibility tests were performed by molecular
120 hybridization using the GenoType MTBDRplus kit (Hain LifeScience) to detect rifampicin
121 and isoniazid resistance. For the clofazimine, minocycline, chloramphenicol and sulfadiazine

REVISED VERSION

122 (CMCS) susceptibility test, mycobacterial liquid cultures were calibrated at a final
123 concentration of 10^5 colony-forming units /mL according to McFarland standards. Drug stock
124 solutions in dimethyl sulfoxide (Euromedex, Souffelweyersheim, France) were stored at -
125 20°C , except for sulfadiazine which was freshly prepared. The applied drug concentrations
126 were $1.5\ \mu\text{g/mL}$ for clofazimine, $4\ \mu\text{g/mL}$ for minocycline, $5\ \mu\text{g/mL}$ for chloramphenicol and
127 $20\ \mu\text{g/mL}$ for sulfadiazine, based on previous studies [7-10]. The CMCS susceptibility test
128 was performed by adapting the automated MGIT960 method. For each isolate tested, one
129 drug-free growth control tube and four additional drug-containing tubes were inoculated with
130 $0.5\ \text{mL}$ of mycobacterial suspension. An antimicrobial susceptibility testing set comprising
131 the five tubes was incubated into the Bactec MGIT 960 instrument (Becton Dickinson).
132 Results were analyzed by the Bactec MGIT 960 system within seven to ten days and
133 interpreted as previously described [15].

134

135 3. Results

136 Over an eight-month prospective study, 200 samples and questionnaires from 200
137 patients were sent to the laboratory. Seventy samples did not grow and 12 were contaminated.
138 Of the 118 mycobacteria isolated from 118 sputa, MALDI-TOF-MS identified 116 M.
139 tuberculosis complex isolates, one *M. kansasii* isolate and one unidentified isolate. Of 116 M.
140 tuberculosis complex isolates, the analysis of RDs by PCR multiplex yielded 111 M.
141 tuberculosis and five *M. canettii*. Molecular characterization showed that 51/111 (46%) M.
142 tuberculosis isolates were TbD1-positive. The five *M. canettii* isolates were firmly identified
143 by *cobF* gene-positivity, the presence of TbD1 region and a C to T transition in the *hsp65*
144 gene. One "*M. simulans*" and one *M. kansasii* isolates were firmly identified on the basis of a
145 16S rRNA and *rpoB* gene sequences with 99% sequence similarity with the references. For
146 the 110 M. tuberculosis-infected patients whose gender was known, 79 (71.8%) were men and

REVISED VERSION

147 31 (28.1%) were women, and the average age was 33 (13-73 years). Of the 108 patients
148 whose geographical origin was known, 92 patients (85%) were Djiboutian, 13 (12%) were
149 Ethiopian, two were Somalian and one patient was Yemenite. Only eight patients (7.2%)
150 reported a previous history of treatment for tuberculosis. Information on HIV status was
151 known for 88 of the *M. tuberculosis*-infected patients, of which three (3.4%) were HIV
152 positive. The five patients infected by *M. canettii* were all Djiboutian (three men and two
153 women, average age: 34 years) who originated from five different neighborhoods (Table 1).
154 These patients reported no tuberculosis history and were HIV negative. Three of these
155 patients reported a stay in Somaliland and one reported a stay in Ethiopia (Table 1). Travel to
156 Somaliland in 3/5 (60%) of *M. canettii*-infected patients was significantly higher than in
157 4/111 (3.6%) of *M. tuberculosis*-infected patients ($p = 0.001$, Fisher's exact test), but this was
158 not true for travel to Ethiopia ($p = 1$, Fisher's exact test). One "*M. simulans*" isolate with
159 uncertain pathogenicity was documented in a 40-year-old Djiboutian man living in Balbala, a
160 slightly urbanized suburb of Djibouti-town. This HIV-negative patient had been initially
161 diagnosed with cavitary pulmonary disease and had been unsuccessfully treated for non-
162 documented MDR tuberculosis. One *M. kansasii*-infected patient was a 46-year-old
163 Djiboutian man working as a painter and living in Quartier 7 of Djibouti. He reported a stay
164 of one year in Somaliland in 2012. The patient reported no tuberculosis history, was HIV
165 negative and had been previously diagnosed with non-documented MDR tuberculosis.

166 Drug susceptibility testing was performed for 78/118 (66%) isolates including 73 *M.*
167 tuberculosis, three *M. canettii*, one "*M. simulans*" and one *M. kansasii*. As for SIRE and PZA
168 susceptibility tests, 55/78 (70%) isolates were susceptible to all anti-tuberculosis drugs tested
169 (Table 2). The three *M. canettii* isolates were resistant to streptomycin and pyrazinamide. The
170 "*M. simulans*" isolate was resistant to rifampicin, isoniazid and pyrazinamide. The *M.*
171 *kansasii* isolate was resistant to the standard concentrations applied for the anti-tuberculous

REVISED VERSION

172 antibiotics. Nine MDR among the 73 *M. tuberculosis* were obtained by the BACTEC method
173 and confirmed by the molecular hybridization technique. HIV status was reported for seven
174 MDR-tuberculosis patients who were HIV negative. Past medical history of tuberculosis was
175 indicated in four of the nine cases of MDR *M. tuberculosis*. For the CMCS susceptibility test,
176 all 78 tested mycobacteria, including the nine MDR *M. tuberculosis* isolates were inhibited by
177 1.5 µg/mL clofazimine, 4 µg/mL minocycline, 5 µg/mL chloramphenicol and 20 µg/mL
178 sulfadiazine except for three *M. tuberculosis* isolates, including two MDR which were
179 resistant to sulfadiazine.

180 **4. Discussion**

181 In Djibouti, pulmonary tuberculosis is routinely diagnosed on the basis of clinical data
182 and positive microscopic observation of a sputum smear following Ziehl-Neelsen staining [3].
183 These criteria do not provide information on the mycobacterial species causing the
184 tuberculosis and leave scope for the possibility that some patients who are clinically
185 diagnosed with pulmonary tuberculosis are, in fact, infected by other mycobacteria.
186 Accordingly, our prospective study revealed *M. canettii* in some patients in Djibouti, in line
187 with observations previously reported in Djibouti [3, 5]. In addition, we recovered one strain
188 of *M. kansasii* and one strain of "*M. simulans*" which had not previously been reported in
189 Djibouti. However, the interpretation of these two isolates remains uncertain given the
190 absence of repeated sampling from these patients, and co-infection with tuberculous
191 mycobacteria cannot be excluded for the same reason [16]. Indeed, it is the second isolate of
192 "*M. simulans*" infection worldwide and, it should be noted, the index case reported a few
193 years ago was a Somali patient diagnosed with cavitary pulmonary disease mimicking MDR
194 tuberculosis [17]. The patient reported in this paper had a similar medical history, yet denied
195 having had any contact with Somalia. A few studies identified non-tuberculous mycobacteria

REVISED VERSION

196 as being responsible for pulmonary infection in Djibouti, including *Mycobacterium chelonae*,
197 *Mycobacterium fortuitum* and *Mycobacterium peregrinum* [3].

198 Our in vitro susceptibility data yielded a 9/73 (12.3%) frequency of MDR among M.
199 tuberculosis isolates, significantly lower than 72% (23/32) ($p=1.10^{-9}$, χ^2 test) and 57%
200 (51/88) ($p=2.10^{-9}$, χ^2 test) previously reported in Djibouti [2, 3]. The fact that previous
201 retrospective studies incorporated data from 2007-2011 [2, 3] and that tested samples had
202 been collected from hospitalized patients, may account for differences in estimations of the
203 actual MDR rate [2]. Moreover, because the present strain series is limited in terms of the
204 number of strains and the length of the collection, it may not be representative of the overall
205 current epidemiology of tuberculosis in Djibouti. Only larger and more long-term studies will
206 give a reasonable overview of the situation. We observed that one “*M. simulans*” isolate was
207 resistant to isoniazid and rifampicin, as previously reported [17], and was susceptible to
208 streptomycin and resistant to pyrazinamide, contrary to what had been reported for the first
209 strain [17]. Whether this observation indicates a natural heterogeneity of antibiotic
210 susceptibility pattern in “*M. simulans*” will depend on the observation of further isolates. *M.*
211 *kansasii* is naturally resistant to pyrazinamide [18] but higher inhibitory concentrations of
212 streptomycin, isoniazid, rifampicine and ethambutol than those applied in our study are
213 required [19].

214 In the absence of any standardized published protocol to test the in vitro susceptibility
215 of *M. tuberculosis* complex mycobacteria to anti-leprosy antibiotics, sulfadiazine and
216 chloramphenicol, we tested a single concentration in the upper limit of the inhibitory
217 concentrations previously reported in a few previous studies [7-10]. Bearing this limit in
218 mind, we observed that all *M. tuberculosis* complex isolates, including nine MDR isolates,
219 were in fact susceptible to clofazimine, minocycline and chloramphenicol, and 94% were
220 susceptible to sulfadiazine. In this paper, we report the antimicrobial activity of clofazimine,

REVISED VERSION

221 minocycline, chloramphenicol and sulfadiazine against “*M. simulans*” and *M. canettii*,
222 confirming previous observations [10, 17]. Moreover, the inhibition of *M. kansasii* by
223 chloramphenicol is herein demonstrated for the first time.

224 5. Conclusions

225 This study illustrates the impact of the accurate identification of mycobacteria
226 recovered from respiratory tract specimens to confirm and refine the diagnosis of tuberculosis
227 in countries with a high incidence rate of tuberculosis, where several *M. tuberculosis* complex
228 species are circulating. In Djibouti, mycobacteria responsible for suspected pulmonary
229 tuberculosis were susceptible in vitro to at least three different antibiotics from an extended
230 spectrum of anti-tuberculous, anti-leprosy, sulfamides and phenicol antibiotics. We propose
231 that such strains could be qualified as “multi-drug susceptible”, opposing the definition of
232 multi-drug resistant strains.

233 Anti-leprosy, sulfamides and phenicol antibiotics are all orally administered, may be
234 included in Directly Observed Treatment Short course strategy, and their potential toxicity is
235 well established, given the 30-50 years of prescription worldwide [20]. Data reported here
236 suggest that these antibiotics could be considered during the empirical treatment of patients
237 presenting with confirmed tuberculosis in the Horn of Africa.

238

239 Declarations

240 **Funding:** This study was financially supported by URMITE, IHU Méditerranée Infection,
241 Marseille, France.

242 **Competing Interests:** No conflict of interest

243 **Ethical Approval:** This study was approved by the IHU Méditerranée Infection, Ethics
244 Committee Approval n°2016-025, Marseille, France.

REVISED VERSION

245 **References**

- 246 [1] WHO (World Health Organization). Global tuberculosis report. 2016. Available from:
247 <http://apps.who.int/iris/bitstream/10665/250441/1/9789241565394-eng.pdf?ua=1>; 2016
248 [accessed 10/03/17]
- 249 [2] Millan-Lou MI, Olle-Goig JE, Tortola MT, Martin C, Samper S. Mycobacterial diversity
250 causing multi- and extensively drug-resistant tuberculosis in Djibouti, Horn of Africa. *Int J*
251 *Tuberc Lung Dis.* 2016;20:150-3.
- 252 [3] Boyer-Cazajous G, Martinaud C, Dehan C, Hassan MO, Gaas Y, Chenilleau-Vidal MC, et
253 al. High prevalence of multidrug resistant tuberculosis in Djibouti: a retrospective study. *J*
254 *Infect Dev Ctries.* 2014;8:233-6.
- 255 [4] Centers for Disease C, Prevention. Emergence of *Mycobacterium tuberculosis* with
256 extensive resistance to second-line drugs--worldwide, 2000-2004. *MMWR Morb Mortal*
257 *Wkly Rep.* 2006;55:301-5.
- 258 [5] Koeck JL, Bernatas JJ, Gerome P, Fabre M, Houmed A, Herve V, et al. [Epidemiology of
259 resistance to antituberculosis drugs in *Mycobacterium tuberculosis* complex strains isolated
260 from adenopathies in Djibouti. Prospective study carried out in 1999]. *Med Trop (Mars).*
261 2002;62:70-2.
- 262 [6] Goh KS, Legrand E, Sola C, Rastogi N. Rapid differentiation of "*Mycobacterium canettii*"
263 from other *Mycobacterium tuberculosis* complex organisms by PCR-restriction analysis of the
264 *hsp65* gene. *Journal of clinical microbiology.* 2001;39:3705-8.
- 265 [7] Jagannath C, Reddy MV, Kailasam S, O'Sullivan JF, Gangadharam PR. Chemotherapeutic
266 activity of clofazimine and its analogues against *Mycobacterium tuberculosis*. *In vitro,*
267 *intracellular, and in vivo studies.* *American journal of respiratory and critical care medicine.*
268 1995;151:1083-6.

REVISED VERSION

- 269 [8] Wallace RJ, Jr., Brown-Elliott BA, Crist CJ, Mann L, Wilson RW. Comparison of the in
270 vitro activity of the glycylicycline tigecycline (formerly GAR-936) with those of tetracycline,
271 minocycline, and doxycycline against isolates of nontuberculous mycobacteria. *Antimicrobial*
272 *agents and chemotherapy*. 2002;46:3164-7.
- 273 [9] Sohaskey CD. Enzymatic inactivation and reactivation of chloramphenicol by
274 *Mycobacterium tuberculosis* and *Mycobacterium bovis*. *FEMS Microbiol Lett*. 2004;240:187-
275 92.
- 276 [10] Ameen SM, Drancourt M. In vitro susceptibility of *Mycobacterium tuberculosis* to
277 trimethoprim and sulfonamides in France. *Antimicrobial agents and chemotherapy*.
278 2013;57:6370-1.
- 279 [11] Zingue D, Flaudrops C, Drancourt M. Direct matrix-assisted laser desorption ionisation
280 time-of-flight mass spectrometry identification of mycobacteria from colonies. *Eur J Clin*
281 *Microbiol Infect Dis*. 2016;35:1983-7.
- 282 [12] Adekambi T, Berger P, Raoult D, Drancourt M. *rpoB* gene sequence-based
283 characterization of emerging non-tuberculous mycobacteria with descriptions of
284 *Mycobacterium bolletii* sp. nov., *Mycobacterium phocaicum* sp. nov. and *Mycobacterium*
285 *aubagnense* sp. nov. *International journal of systematic and evolutionary microbiology*.
286 2006;56:133-43.
- 287 [13] Drancourt M, Bollet C, Carlioz A, Martelin R, Gayral JP, Raoult D. 16S ribosomal DNA
288 sequence analysis of a large collection of environmental and clinical unidentifiable bacterial
289 isolates. *Journal of clinical microbiology*. 2000;38:3623-30.
- 290 [14] Warren RM, Gey van Pittius NC, Barnard M, Hesselning A, Engelke E, de Kock M, et al.
291 Differentiation of *Mycobacterium tuberculosis* complex by PCR amplification of genomic
292 regions of difference. *Int J Tuberc Lung Dis*. 2006;10:818-22.

REVISED VERSION

- 293 [15] Springer B, Lucke K, Calligaris-Maibach R, Ritter C, Bottger EC. Quantitative drug
294 susceptibility testing of *Mycobacterium tuberculosis* by use of MGIT 960 and EpiCenter
295 instrumentation. *Journal of clinical microbiology*. 2009;47:1773-80.
- 296 [16] Griffith DE, Aksamit T, Brown-Elliott BA, Catanzaro A, Daley C, Gordin F, et al. An
297 official ATS/IDSA statement: diagnosis, treatment, and prevention of nontuberculous
298 mycobacterial diseases. *American journal of respiratory and critical care medicine*.
299 2007;175:367-416.
- 300 [17] Tortoli E, Rogasi PG, Fantoni E, Beltrami C, De Francisci A, Mariottini A. Infection due
301 to a novel mycobacterium, mimicking multidrug-resistant *Mycobacterium tuberculosis*. *Clin*
302 *Microbiol Infect*. 2010;16:1130-4.
- 303 [18] Sun Z, Zhang Y. Reduced pyrazinamidase activity and the natural resistance of
304 *Mycobacterium kansasii* to the antituberculosis drug pyrazinamide. *Antimicrobial agents and*
305 *chemotherapy*. 1999;43:537-42.
- 306 [19] da Silva Telles MA, Chimara E, Ferrazoli L, Riley LW. *Mycobacterium kansasii*:
307 antibiotic susceptibility and PCR-restriction analysis of clinical isolates. *J Med Microbiol*.
308 2005;54:975-9.
- 309 [20] Brouqui P, Quenard F, Drancourt M. Old antibiotics for emerging multidrug-
310 resistant/extensively drug-resistant tuberculosis (MDR/XDR-TB). *International journal of*
311 *antimicrobial agents*. 2017;49:554-7.

312

313

314

315

316

REVISED VERSION

317 **Table 1: Synopsis of five patients diagnosed with *M. canettii* pulmonary tuberculosis,**
 318 **Djibouti.**

Isolate	Gender	Age	Nationality	Job	Address in Djibouti	Travel outside Djibouti	HIV status
DJ 480	M	30	DJ	No occupation	Quartier 3	Somaliland 2015	No
DJ 514	F	41	DJ	No occupation	Quartier 7 bis	Somaliland 2014-2015	No
DJ 517	M	27	DJ	No occupation	Cité Poudrière	No	No
DJ 613	F	27	DJ	No occupation	Quartier 2	Somaliland 2012	No
DJ 734	M	47	DJ	Cooking	Quartier 7	Ethiopia 2015	No

319 M: men, F: women, DJ: Djiboutian

320

321

322

323

324

325

REVISED VERSION

326 **Table 2: In vitro drug susceptibility testing of mycobacteria isolated from patients**
 327 **suspected as having pulmonary tuberculosis, Djibouti.**

	Drugs					n/N Isolates
	STR (1 µg/mL)	INH (0.1 µg/mL)	RIF (1 µg/mL)	ETH (5 µg/mL)	PZA (100 µg/mL)	
Drug susceptibility profiles	S	S	S	S	S	55/73 M. tuberculosis
	S	S	S	S	R	1/73 M. tuberculosis
	S	R	S	S	R	1/73 M. tuberculosis
	R	S	S	S	S	7/73 M. tuberculosis
	R	S	S	S	R	3/3 M. canettii
	S	R	R	S	R	1/1 "M. simulans"
	R	R	R	S	R	4/73 M. tuberculosis
	R	R	R	R	R	5/73 M. tuberculosis 1/1 M. kansasii

328

329 STR: streptomycin, INH: isoniazid, RIF: rifampicin, ETH: ethambutol, PZA: pyrazinamide,

330 green square, S: susceptible; red square, R: resistant, n/N: number of obtained profiles / total

331 number of isolates

332

333

CHAPITRE II

Étude microbiologique de la tuberculose pulmonaire à Djibouti

Multi-drug resistant “*Mycobacterium occultatumposttuberculosis*” and *Mycobacterium tuberculosis* lung co-infection, the Horn of Africa.

Bouزيد F, Osman AD, Hassan MO, Ibrahim AW, Garnotel E, Drancourt M

In progress.

5.2. Article 2 : Multi-drug resistant “*Mycobacterium occultatumposttuberculosis*” and *Mycobacterium tuberculosis* lung co-infection, the Horn of Africa

Dans la Corne de l’Afrique, des rapports sporadiques ont montré des infections pulmonaires causées par des mycobactéries non-tuberculeuses (Tortoli et al., 2010; Firdessa et al., 2013; Boyer-Cazajous et al., 2014). Plus précisément, *Mycobacterium chelonae*, *Mycobacterium fortuitum* et *Mycobacterium peregrinum* ont été isolées à Djibouti (Boyer-Cazajous et al., 2014); *Mycobacterium intracellulare*, *Mycobacterium flavescens*, *Mycobacterium simiae* en Éthiopie (Firdessa et al., 2013) et “*Mycobacterium simulans*” en Somalie (Tortoli et al., 2010).

En étudiant les mycobactéries responsables de la tuberculose pulmonaire à Djibouti (Bouزيد et al., 2017a), nous avons isolé pour la première fois *Mycobacterium kansasii* et de manière inattendue une autre mycobactérie non-tuberculeuse identique à une mycobactérie qui n'a été rapporté qu'une fois sous la dénomination provisoire de “*M. simulans*” FI-09026 à partir d’un patient Somalien (Tortoli et al., 2010). Brièvement, cette souche a été isolée à partir d’un patient Djiboutien diagnostiqué avec une tuberculose pulmonaire résistante aux antibiotiques antituberculeux ayant des échecs thérapeutiques successifs. En analysant le dossier médical du patient et les données microbiologiques obtenues à Djibouti, nous avons démasqué une co-infection pulmonaire par *M. tuberculosis* et “*M. simulans*” et nous avons confirmé cette co-infection par l’identification d’un isolat obtenu à Djibouti comme *M. tuberculosis* et un autre comme étant “*M. simulans*”.

L’isolat index de “*M. simulans*” n’ayant été que partiellement décrit, nous avons alors procédé à la description phénotypique complète de cette espèce mycobactérienne. Au terme de cette étude, nous avons proposé de nommer cette nouvelle espèce “*Mycobacterium occultatumposttuberculosis*” signifiant « caché derrière la tuberculose ».

Ce travail se poursuivra par une description génomique de cette espèce.

Multi-drug resistant “*Mycobacterium occulta*posttuberculosis” and *Mycobacterium tuberculosis* lung co-infection, the Horn of Africa

Fériel Bouzid^{1,2}, Djaltou Aboubaker Osman³, Mohamed Osman Hassan⁵, Warsama Ibrahim Arreh⁵, Eric Garnotel⁴, Michel Drancourt^{1*}

¹Aix Marseille Université, URMITE, UMR CNRS 7278, IRD 198, INSERM 1095.

IHU Méditerranée Infection, Marseille 13005, France.

² Aix-Marseille Univ, CNRS, EIPL, Marseille, France

³Centre d'Études et de Recherche de Djibouti (CERD), Institut de Recherche Médicinale (IRM), Djibouti, Republic of Djibouti

⁴Hôpital d'instruction des armées Alphonse Laveran, Marseille, France

⁵Hôpital pneumo-phtisiologie «Chakib Saad Omar», Republic of Djibouti

*Corresponding author: Prof. Michel Drancourt michel.drancourt@univ-amu.fr

Keywords: “*Mycobacterium simulans*”, Djibouti, Horn of Africa

Abstract

In low-income countries in the Horn of Africa, pulmonary infections are usually considered as tuberculosis suspicions and their diagnosis rely only on clinical data and positive microscopic observation. This strategy promotes non-tuberculous mycobacteria to escape laboratory detection and facilitate their emergence in populations. A non-tuberculous mycobacterium strain FB-527 was unexpectedly cultured from sputum in a Djiboutian patient otherwise diagnosed with multi-drug resistant (MDR) tuberculosis. *RpoB* and 16S rRNA gene sequencing indicated that this isolate was identical to strain FI-09026 provisionally named “*Mycobacterium simulans*” reported only once from a Somali patient eight years before. Conventional phenotypic tests indicated that strain FB-527 mimicked *M. tuberculosis* on the basis of colony-morphology and positive enzymatic reactions using Zym Api strip. Strain FB-527 was *in vitro* resistant to rifampicin and isoniazid. Lung co-infection with two MDR mycobacteria has complicated the therapeutic evolution of this patient. After a complete description of strain FB-527 including genome sequencing, we propose to name this new species “*Mycobacterium occultatum posttuberculosis*” meaning “hidden behind tuberculosis”.

INTRODUCTION

Tuberculosis remains a major public health problem in several African countries with an average incidence of 275/100.000 inhabitants in the continent including 84% of cases presenting as pulmonary tuberculosis (WHO, 2016). In particular, the Republic of Djibouti located in the Horn of Africa, exhibits one of the highest incidence rates of tuberculosis worldwide with an estimated incidence of 378/100.000 inhabitants including 57% of cases presenting as pulmonary tuberculosis (WHO, 2016). Such high incidence rate is thought to be partially fueled by a high rate of antibiotic-resistant *Mycobacterium tuberculosis* strains (Boyer-Cazajous et al., 2014; Millan-Lou et al., 2016). However in the Republic of Djibouti, the diagnosis of pulmonary tuberculosis may not routinely rely upon the isolation of the causative pathogen agent but instead on the microscopic examination of sputum smear after Ziehl-Neelsen staining (Boyer-Cazajous et al., 2014). This approach to the diagnosis may leave uncertain the exact identification of the causative *M. tuberculosis* complex species as *Mycobacterium canettii* has been reported as being responsible for 3-6 % of the pulmonary tuberculosis in the Republic of Djibouti (Koeck et al., 2002; Boyer-Cazajous et al., 2014; Bouzid et al., 2017). Moreover, this culture-free diagnosis approach closes the door to the discovery of any additional mycobacterium diverting the current laboratory diagnosis strategy for pulmonary tuberculosis in developing countries.

Investigating mycobacteria responsible for pulmonary tuberculosis in the Republic of Djibouti by culturing sputum and accurately identifying colonies by a polyphasic approach, we unexpectedly isolated a non-tuberculous mycobacterium in one patient presenting with antibiotic-resistant pulmonary tuberculosis (Bouzid et al., 2017). The species was identical to a mycobacterium previously reported only once as being “*Mycobacterium simulans*” strain FI-09026 (Tortoli et al., 2010). In addition, according to the clinical and microbiological data

obtained in Djibouti and confirmed in France, co-infection with multidrug resistant *M. tuberculosis* has been revealed.

We report the case of this patient along with a complete polyphasic description of the non-tuberculosis isolate and its FI-09026 parent strain, allowing the description of a new *Mycobacterium* species that we propose to name “*Mycobacterium occultatumposttuberculosis*” (a mycobacterium hidden behind *M. tuberculosis*).

RESULTS

Case report

A 40-year-old Djiboutian man presented on February 2016 with a three-month cough at Chakib Saad Hospital, Djibouti, an hospital in charge of pulmonary pathologies. The patient was living in Balbala (Bouldhouqo) in Djibouti and working as a seller in clothing store. He reported no travel outside Djibouti, no medical, surgical or tuberculosis histories and was found to be HIV negative. A chest radiograph revealed a retractile opacity of the right upper lobe of the lung and a para-aortic opacity with micro nodules of the culmen (Figure 1). Direct microscopic examination of the sputum smear after Ziehl-Neelsen staining exhibited acid-fast bacilli but culture of the sputum was not performed. The patient was diagnosed as pulmonary tuberculosis and received first line anti-tuberculosis drugs. After three months of standard anti-tuberculosis treatment on May 2016, the patient returned to the hospital with persistent symptoms. A second direct examination of the sputum was positive and a rifampicin-resistant *M. tuberculosis* complex isolate was detected by GeneXpert® MTB/RIF lab test (Cepheid, Sunnyvale, CA). The patient was considered to be in failure for first-line treatment and was hospitalized and treated with multidrug resistant chemotherapy including daily kanamycine (1g), moxifloxacin (400mg), prothionamide (250mg), clofazimine (100mg), isoniazid (30 mg), ethionamide (250mg) and pyrazinamide (400 mg); with these dosages being adjusted to

the weight of the patient. On July 2016, a first positive MGIT (Becton Dickinson, Le Pont-de-Claix, France) culture obtained from sputum yielded a *M. tuberculosis* complex isolate (strain 5175) identified by SD BIOLINE TB Ag MPT64 Rapid test targeting the protein MPT64. In September 2016, improved clinical course contrasted with the positivity of sputum cultures in MGIT. The patient continued the treatment of the continuation phase. On November 2016, the patient was readmitted to the hospital. After the biochemical and microbiological assessment, the short phase was extended by another three months. Not responding to the treatment, the patient was declared in treatment failure in January 2017 and was placed on an intensive phase of antituberculosis therapy with kanamycine, levofloxacin, cycloserine, linezolid, para-aminosalicylic acid (PAS) and bedaquiline. This intensive phase of treatment was conditioned by a Directly Observed Treatment (DOT) follow-up for avoiding thus an interruption in the uptake of the medicines. Complementary microbiological investigations indicated co-infection with antibiotic-resistant *M. tuberculosis* and strain FB-527 as described below, as the final diagnosis.

Microbial Investigations

Further microbiological investigations were conducted in collaboration with “Hôpital d’instruction des armées Alphonse Laveran, Marseille, France” and “IHU Méditerranée Infection, Marseille, France”. The *M. tuberculosis* complex isolate strain 5175 obtained on July 2016 in Djibouti was sent to France on May 2017. Matrix-assisted laser desorption ionization-time of flight-mass spectrometry (MALDI-TOF-MS) identified a *M. tuberculosis* complex isolate. Analysis of regions of deletion by multiplex PCR yielded *M. tuberculosis* species (Warren et al., 2006). Rifampicin resistance was first detected on colonies by GeneXpert® MTB/RIF test. Drug susceptibility tests using ETEST® confirmed this isolate to be resistant to rifampicin (minimal inhibitory concentration (MIC) > 32 mg/L), streptomycin

(MIC > 1,024 mg/L) and ethambutol (MIC > 256 mg/L). On drug-supplemented solid media, *M. tuberculosis* strain 5175 was susceptible chloramphenicol (20 mg/L) and clofazimine (1.5 mg/L) but resistant to pyrazinamide (MIC, 100 mg/L) and minocycline (MIC, 4 mg/L).

By the end of September 2016, one sputum specimen was received in Marseille and was cultured on Coletsos medium (Bio-Rad, Marnes-la-Coquette, France) at 37°. After two-month incubation, only one rough colony was observed by the naked eye and microscopic examination after auramine-O staining was positive, the strain was referred as strain FB-527. Sub-cultures of this colony on BACTEC MGIT medium (Becton-Dickinson) and Middlebrook 7H10 (Becton-Dickinson) were positive within 7 days and 10 days respectively. A MALDI-TOF-MS profile obtained by direct deposit of colony did not match any entry of the Bruker database (version December, 2015). Then, *rpoB* and 16S rRNA partial gene sequencing identified this isolate FB-527 as "*M. simulans*" (Bouزيد et al., 2017). Colonies were tested negative for the GeneXpert® MTB/RIF test.

Phenotypic characterization of strain FB-527

Strain FB-527 displayed rough and non-pigmented colonies growing at a temperature range of 25°C to 37°C after 10-day incubation on egg-based Coletsos medium. Colonies morphology resembled that of *M. tuberculosis* H37Rv (Figure 2A). Optimal growth was obtained at 37°C under micro-aerophilic atmosphere as well as in presence of 5% CO₂. Growth occurred up to up to only 1% NaCl. Ziehl-Neelsen staining showed dispersed pink bacilli and clumps (Figure 2B). Further observation of colonies by electron microscopy showed rod-shaped bacilli measuring $1.33 \pm 0.17 \mu\text{m}$ long and $0.62 \pm 0.06 \mu\text{m}$ large (Figure 1C). A reproducible MALDI-TOF-MS profile was generated which was easily distinguishable from that of *M. tuberculosis* H37Rv (Figure 3). The catalase test was positive at room temperature, niacin production and Tween 80 hydrolysis tests were negative. Alkaline

phosphatase, esterase (C4), lipase esterase (C8), lipase (C14), leucine arylamidase, acid phosphatase and phosphoamidase were positive for both strains FB-527 and FI-09026as detected with the API ZYM strip (bioMérieux, Craaponne, France) and yielded a pattern undistinguishable from *M. tuberculosis* H37Rv used as a positive control (Supplementary table 1). However, inoculation of the API CORYNE strip (bioMérieux) indicated that strain FB-527 was positive for nitrate reductase, phosphatase alcaline, β -glucosidase and fermentation of D-glucose, D-maltose and D-saccharose while strain FI-09026 was positive for pyrazinamidase, phosphatase alcaline and ribose fermentation and *M. tuberculosis* H37Rv was positive for alkaline phosphataseonly (Supplementary table 1). Antibiotic susceptibility pattern tested using *E*TEST® showed that the isolate FB-527 was *in vitro* susceptible to streptomycine (MIC <0.064mg/L), amikacin (MIC, 3 mg/L), clarithromycin (MIC, 0.032 mg/L), ethambutol (MIC, 0.5 mg/L), linezolid (MIC, 0.125 mg/L) and trimethoprim-sulfamethoxazole (MIC <0.002 mg/L); intermediate toazithromycin (MIC, 8 mg/L), levofloxacin (MIC, 2 mg/L) and rifampicin (MIC, 2 mg/L); and resistant todoxycycline (MIC > 12 mg/L), imipenem (MIC > 32 mg/L), meropenem (MIC > 32 mg/L) and isoniazide (MIC > 256 mg/L) (Table 1). StrainFB-572 was also susceptible to chloramphenicol (20 mg/L), clofazimine (1.5 mg/L) and minocycline (MIC, 4 mg/L) (Bouزيد et al., 2017). Drug susceptibility profile of strain FI-09026 was also completed (Tortoli et al., 2010) and showed that this strain is susceptible to chloramphenicol (20 mg/L), azithromycine (MIC < 0.19 mg/L) and doxycycline (MIC, 0.25 mg/L); and resistant to levofloxacin (MIC, 12 mg/L), clofazimine (1.5 mg/L) and minocycline (4 mg/L) (Table 1).

Genetic characterization

The 16S rRNA gene sequence's highest similarity was of 99.6% with "*Mycobacterium simulans*" strain FI-09026 (FJ786255). Phylogenetic tree based on the 16S rRNA gene sequences highlighted the position of "*M. occultatum*post*tuberculosis*" strain FB-527 as a

member of the *Mycobacterium szulgai* complex closely related to *Mycobacterium riyadhense* (Figure 4). We also sequenced a 733-bp *rpoB* gene fragment in FB-527 strain (Adekambi et al., 2006). This sequence's highest similarity was of 99.3% with "*Mycobacterium simulans*" strain FI-09026 (FJ786254) which enforced the identity of strain FB-527 and strain FI-09026 at the level species.

DISCUSSION

We unexpectedly diagnosed a Djiboutian patient as having seemingly antibiotic-resistant pulmonary tuberculosis due to co-infection with "*M. occultatumposttuberculosis*" and *M. tuberculosis*.

The identification of "*M. occultatumposttuberculosis*" strain FB-527 isolate was firmly established by *rpoB* and 16S rRNA gene sequencing (Bouزيد et al., 2017). This isolate is the second one to be reported worldwide as the index case led to the partial description of this non-tuberculous *Mycobacterium* species (Tortoli et al., 2010). The first case of infection by "*M. occultatumposttuberculosis*" strain FI-09026 had been made from the sputum of a Somali patient with severe cavitary pulmonary disease who had been firstly diagnosed as MDR tuberculosis (Tortoli et al., 2010). Medical history of this patient included pulmonary tuberculosis diagnosed four years before with interrupted therapy (Tortoli et al., 2010). The two only patients reported to be infected with "*M. occultatumposttuberculosis*" were not immune-compromised and were originated from the same geographical area, the Horn of Africa (Somalia and the Republic of Djibouti) which otherwise remains an endemic area of tuberculosis (WHO, 2016).

The case herein reported gave us the opportunity to completely describe this emerging species now comprising two isolates strain FB-527 and strain FI-09026 with phenotypic and genetic data. We propose to name this species as "*Mycobacterium*

occultatumposttuberculosis” meaning a mycobacterium hidden behind *M. tuberculosis* with strain FB-527 as the type strain. Strain FB-527^T has been deposited in the CSUR collection under number P4791 and in the DSMZ collection (in progress). Our investigations confirmed “*M. occultatumposttuberculosis*” as a member of the *Mycobacterium szulgai* complex closely related to *Mycobacterium riyadhense* (Tortoli et al., 2010), another non-tuberculous *Mycobacterium* species phenotypically mimicking *M. tuberculosis* (van Ingen et al., 2009).

This case report adds to the list of *Mycobacterium* species responsible for pulmonary infection in patients exposed to the Horn of Africa (Table 2). Indeed, in addition to *M. tuberculosis* complex members, sporadic reports showed pulmonary infections due to non-tuberculous mycobacteria with *M. tuberculosis* co-infection for three cases (Tortoli et al., 2010; Firdessa et al., 2013; Boyer-Cazajous et al., 2014; Bouzid et al., 2017). Therefore, there is a necessity for an accurate documentation of cases as the antibiotic-susceptibility pattern of these eight different species is not the same, thus impeding the antibiotic treatment of patients. Even within the same species, we showed that the profile of drug susceptibility differs between strain FB-527 and strain FI-09026 (Table 1).

Moreover, this case indicates that an accurate identification of *Mycobacterium* species responsible for pulmonary infection should rely on culturing sputum specimens in order to isolate colonies to be identified, rather than bypassing culture by direct examination after Ziehl-Neelsen staining or some diagnostic assays based on non-specific DNA tests. The index “*M. occultatumposttuberculosis*” FI-09026 isolate was misidentified as a member of the *M. tuberculosis* complex by using the GenoType© *Mycobacterium* CM test. In addition, confusing results were obtained after reverse hybridization test (GenoType MTBC) and GenoType MTBDRplus test (Tortoli et al., 2010). Comparing “*M. occultatumposttuberculosis*” FB-527 and *M. tuberculosis* H37Rv phenotypes, we have also shown that characterization based on colony morphology or the profile of enzymatic reactions

can lead to misidentification. However, MALDI-TOF-MS (Zingue et al., 2016) and *rpoB* gene sequencing (Adekambi et al., 2006) gave an accurate identification. We urge for further research in culturing *Mycobacterium* species and the implementation of effective culture facilities in emerging countries instead of the sole development of PCR amplification-based approach to the diagnosis of pulmonary tuberculosis and related syndromes (Asmar and Drancourt, 2015).

Methods

Strain isolation and identification

Isolation and identification procedure of “*M. occultaumposttuberculosis*” strain FB-527 was described previously (Bouزيد et al., 2017). Culture was maintained on egg-based Coletsos (Bio-Rad, Marnes-la-Coquette, France), Middlebrook 7H10 (Becton Dickinson, Le Pont de Claix, France) supplemented with 10% oleic acid-albumin-dextrose-catalase (OADC) (Becton Dickinson). This strain was deposited in CSUR collection under the number the P4791 and in DSMZ (in progress).

“*M. simulans*” FI-09026 was purchased from DSMZ collection under the number DSM 45395. Freeze-dried colonies were cultured on Coletsos (Bio-Rad), Middlebrook 7H10 supplemented with 10% OADC (Becton Dickinson) and in mycobacteria Growth Indicator Tube (MGIT) liquid medium (BACTEC™ MGIT™ 960, Becton Dickinson). Identification was confirmed by partial sequencing of *rpoB* gene and 16S rRNA (Drancourt et al., 2004; Adekambi et al., 2006). This stain was further deposited in the CSUR collection under the number the P4792. Conserved *M. tuberculosis* strain 5175 in Djibouti was cultured in France on the three media detailed above. Identification was performed first by MALDI-TOF- MS (Zingue et al., 2016). The species level has been specified by specific multiplex PCR

amplification of regions of difference (RD) RD4, RD9 and RD12 (Warren et al., 2004).

Rifampicin resistance was assessed by GeneXpert® MTB/RIF lab test (Cepheid, Sunnyvale, CA). Drug susceptibility testing to rifampicin, streptomycin and ethambutol were performed using *ETEST*® (bioMérieux). In addition, susceptibility to chloramphenicol (20 mg/L), clofazimine (1.5 mg/L), minocycline (4 mg/L) and pyrazinamide (100 mg/L) were performed in 6-well plates including two drug-free wells and four drug-supplemented wells on solid media by inoculating 10⁶ colony-forming units (CFUs) onto MOD9 solid medium (Asmar et al., 2015) incorporating the tested antibiotic.

Phenotypic characterization

“*M. occultaumposttuberculosis*” strain FB-527 strain was cultured in egg-based Coletsos medium (Bio-Rad) or Middlebrook 7H10 (Becton Dickinson) supplemented with 10% oleic acid-albumin-dextrose-catalase (OADC) (Becton Dickinson) at 25-42 °C for four weeks. Inoculated plates were inspected daily by naked eyes to determine the growth time. Colonies were microscopically examined after Ziehl-Neelsen staining (RAL diagnostics, Martillac, France). The size of the microorganisms was determined by transmission electron microscopy after negative staining of bacteria. After overnight fixation with 2.5% glutaraldehyde at 4°C, bacterial suspension was applied to the top of a formvar carbon 400 mesh nickel grid (FCF400-Ni, EMS) and stained with 1 % ammonium molybdate (1-800-ACROS, USA). Electron micrographs were acquired on a Tecnai G20 transmission electron microscope (FEI) operated at 200 Kev. MALDI-TOF- MS protein analysis was carried out after direct colony-deposit as previously described (Zingue et al., 2016). Salt tolerance was tested by supplementing the Middlebrook 7H10 solid medium with 0–5% NaCl as previously described (Asmar et al., 2016). Niacin production was detected using BBL™ Taxo™ TB Niacin test

strips (Becton Dickinson) as described by the manufacturer. Tween 80 hydrolysis test was performed as previously described (Phelippeau et al., 2017).

Enzyme activities were determined for “*M. occultaumposttuberculosis*” strain FB-527 and strain FI-09026 by inoculating a API® ZYM and API® Coryne (bioMérieux) as indicated by the manufacturer using *M. tuberculosis* H37Rv as positive control. The minimal inhibitory concentration (MIC) of the major antimycobacterial agents was determined using ETEST® (bioMérieux). Further, susceptibility to 1.5 mg/L clofazimine, 4 mg/L minocycline and 5 mg/L chloramphenicol was tested by using 6-well plates including two drug-free wells and four drug-supplemented wells on solid media by inoculating 10⁶ colony-forming units (CFUs) onto MOD9 solid medium (Asmar et al., 2015) incorporating the tested antibiotic.

Phylogenetic analysis

Phylogenetic tree based on 16S rRNA sequences was constructed using the Clustal W and MEGA5 software programs. The evolutionary history was inferred by using the Maximum Likelihood method based on the Hasegawa-Kishino-Yano model.

Acknowledgements

This study was financially supported by URMITE, IHU Méditerranée Infection, Marseille, France; and by the A*MIDEX project (n° ANR-11-IDEX-0001-02) funded by the «Investissements d’Avenir» French Government program, managed by the French National Research Agency (ANR). FB benefits from a PhD grant by IHU Méditerranée Infection, Marseille, France. FB benefits from a PhD grant by IHU Méditerranée Infection, Marseille, France.

Competing Financial Interests

The authors declare that they have no competing interests.

Funding

This study was funded by the Méditerranée-Infection Foundation.

Author contributions statement

Performed the experiments: F.B, C.R, Di P.F and H.A. Performed bioinformatics: B.E.

Medical staff in Djibouti: D.A.O, W.I.A, M.O.H. Reviewed data: E.G and M.D

References

- Aboubaker Osman, D., Bouzid, F., Canaan, S., and Drancourt, M. (2015). Smooth Tubercle Bacilli: Neglected Opportunistic Tropical Pathogens. *Frontiers in public health* 3, 283. doi: 10.3389/fpubh.2015.00283.
- Adekambi, T., Berger, P., Raoult, D., and Drancourt, M. (2006). rpoB gene sequence-based characterization of emerging non-tuberculous mycobacteria with descriptions of *Mycobacterium bolletii* sp. nov., *Mycobacterium phocaicum* sp. nov. and *Mycobacterium aubagnense* sp. nov. *Int J Syst Evol Microbiol* 56(Pt 1), 133-143. doi: 10.1099/ijms.0.63969-0.
- Asmar, S., Chatellier, S., Mirande, C., van Belkum, A., Canard, I., Raoult, D., et al. (2015). A Novel Solid Medium for Culturing *Mycobacterium tuberculosis* Isolates from Clinical Specimens. *J Clin Microbiol* 53(8), 2566-2569. doi: 10.1128/JCM.01149-15.
- Asmar, S., and Drancourt, M. (2015). Rapid culture-based diagnosis of pulmonary tuberculosis in developed and developing countries. *Front Microbiol* 6, 1184. doi: 10.3389/fmicb.2015.01184.
- Asmar, S., Sassi, M., Phelippeau, M., and Drancourt, M. (2016). Inverse correlation between salt tolerance and host-adaptation in mycobacteria. *BMC Res Notes* 9, 249. doi: 10.1186/s13104-016-2054-y.
- Blouin, Y., Hauck, Y., Soler, C., Fabre, M., Vong, R., Dehan, C., et al. (2012). Significance of the identification in the Horn of Africa of an exceptionally deep branching *Mycobacterium tuberculosis* clade. *PLoS One* 7(12), e52841. doi: 10.1371/journal.pone.0052841.
- Bouzid, F., Astier, H., Osman, D.A., Javelle, E., Hassan, M.O., Simon, F., et al. (2017). Extended spectrum of antibiotic susceptibility for tuberculosis, djibouti. *Int J Antimicrob Agents*. doi: 10.1016/j.ijantimicag.2017.07.007.

- Boyer-Cazajous, G., Martinaud, C., Dehan, C., Hassan, M.O., Gaas, Y., Chenilleau-Vidal, M.C., et al. (2014). High prevalence of multidrug resistant tuberculosis in Djibouti: a retrospective study. *J Infect Dev Ctries* 8(2), 233-236. doi: 10.3855/jidc.3837.
- Drancourt, M., Berger, P., and Raoult, D. (2004). Systematic 16S rRNA gene sequencing of atypical clinical isolates identified 27 new bacterial species associated with humans. *J Clin Microbiol* 42(5), 2197-2202.
- Firdessa, R., Berg, S., Hailu, E., Schelling, E., Gumi, B., Erenso, G., et al. (2013). Mycobacterial lineages causing pulmonary and extrapulmonary tuberculosis, Ethiopia. *Emerg Infect Dis* 19(3), 460-463. doi: 10.3201/eid1903.120256.
- Ghebremariam, M.K., Michel, A.L., Nielen, M., Vernooij, J.C., and Rutten, V.P. (2017). Farm-level risk factors associated with bovine tuberculosis in the dairy sector in Eritrea. *Transbound Emerg Dis*. doi: 10.1111/tbed.12622.
- Koeck, J.L., Bernatas, J.J., Gerome, P., Fabre, M., Houmed, A., Herve, V., et al. (2002). [Epidemiology of resistance to antituberculosis drugs in Mycobacterium tuberculosis complex strains isolated from adenopathies in Djibouti. Prospective study carried out in 1999]. *Med Trop (Mars)* 62(1), 70-72.
- Millan-Lou, M.I., Olle-Goig, J.E., Tortola, M.T., Martin, C., and Samper, S. (2016). Mycobacterial diversity causing multi- and extensively drug-resistant tuberculosis in Djibouti, Horn of Africa. *Int J Tuberc Lung Dis* 20(2), 150-153. doi: 10.5588/ijtld.15.0268.
- Phelippeau, M., Asmar, S., Osman, D.A., Sassi, M., Robert, C., Michelle, C., et al. (2017). "Mycobacterium massilipolynesiensis" sp. nov., a rapidly-growing mycobacterium of medical interest related to Mycobacterium phlei. *Sci Rep* 7, 40443. doi: 10.1038/srep40443.

- Sindani, I., Fitzpatrick, C., Falzon, D., Suleiman, B., Arube, P., Adam, I., et al. (2013). Multidrug-resistant tuberculosis, Somalia, 2010-2011. *Emerg Infect Dis* 19(3), 478-480. doi: 10.3201/eid1903.121287.
- Tortoli, E., Rogasi, P.G., Fantoni, E., Beltrami, C., De Francisci, A., and Mariottini, A. (2010). Infection due to a novel mycobacterium, mimicking multidrug-resistant *Mycobacterium tuberculosis*. *Clin Microbiol Infect* 16(8), 1130-1134. doi: 10.1111/j.1469-0691.2009.03063.x.
- van Ingen, J., Al-Hajj, S.A., Boeree, M., Al-Rabiah, F., Enaimi, M., de Zwaan, R., et al. (2009). *Mycobacterium riyadhense* sp. nov., a non-tuberculous species identified as *Mycobacterium tuberculosis* complex by a commercial line-probe assay. *Int J Syst Evol Microbiol* 59(Pt 5), 1049-1053. doi: 10.1099/ijs.0.005629-0.
- Warren, R.M., Gey van Pittius, N.C., Barnard, M., Hesselning, A., Engelke, E., de Kock, M., et al. (2006). Differentiation of *Mycobacterium tuberculosis* complex by PCR amplification of genomic regions of difference. *Int J Tuberc Lung Dis* 10(7), 818-822.
- WHO (World Health Organization). Global tuberculosis report. 2016. Available from: <http://apps.who.int/iris/bitstream/10665/250441/1/9789241565394-eng.pdf?ua=1>; 2016
- Zingue, D., Flaudrops, C., and Drancourt, M. (2016). Direct matrix-assisted laser desorption ionisation time-of-flight mass spectrometry identification of mycobacteria from colonies. *Eur.J.Clin.Microbiol.Infect.Dis.* 35(12), 1983-1987. doi: 10.1007/s10096-016-2750-5 [doi];10.1007/s10096-016-2750-5 [pii].

Figures legends

Figure 1: Initial chest radiograph done during the first diagnosis. It revealed a retractile opacity of the right upper lobe of the lung and a para-aortic opacity with micro nodules of the culmen.

Figure 2: Morphological characteristics of “*M. occultatumposttuberculosis*” strain FB-527.

A) Colony aspect of “*M. occultatumposttuberculosis*” strain FB-527 cultured on coletsos medium compare to *M. tuberculosis* H37Rv. The two mycobacteria display rough colonies.

B) Ziehl-Neelsen staining showed pink bacilli with dispersed or clumped mycobacteria.

C) Transmission electron microscopy of “*M. occultatumposttuberculosis*” strain FB-527. The scale bar represents 500 nm.

Figure 3: MALDI-TOF-MS spectra of “*M. occultatumposttuberculosis*” strain FB-527 in comparison with that of *M. tuberculosis* H37Rv.

Figure 4: Phylogenetic tree based on the 16S rRNA gene sequence bootstrapped 1,000 times indicating the phylogenetic position of “*M. occultatumposttuberculosis*” strain FB-527 and strain FI-09026 here referred as “*M. simulans*”. The tree was constructed using the ClustalW and MEGA5 software programs. Bootstrap values $\geq 90\%$ are indicated at nodes. Bar: 0.002 substitutions per nucleotide position.

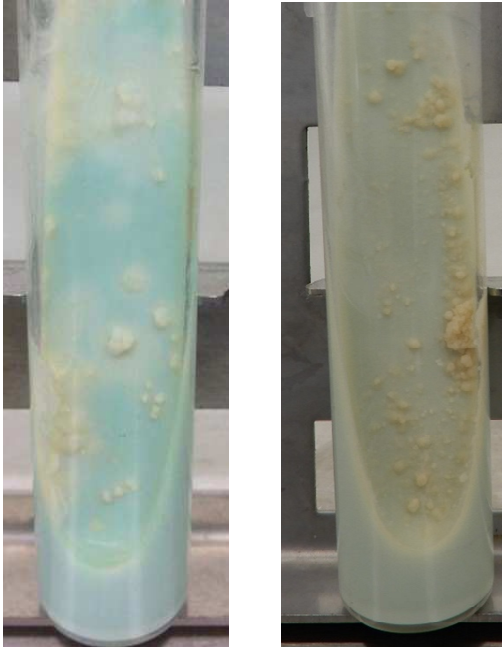
Figure 1



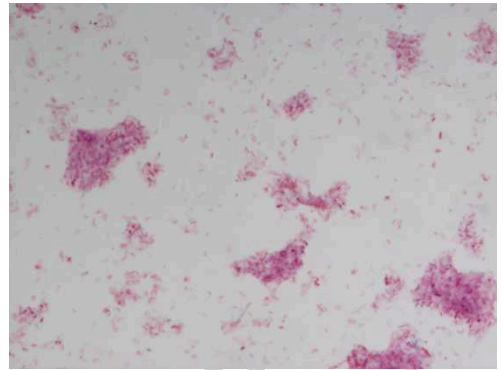
In progress

Figure 2

A



B



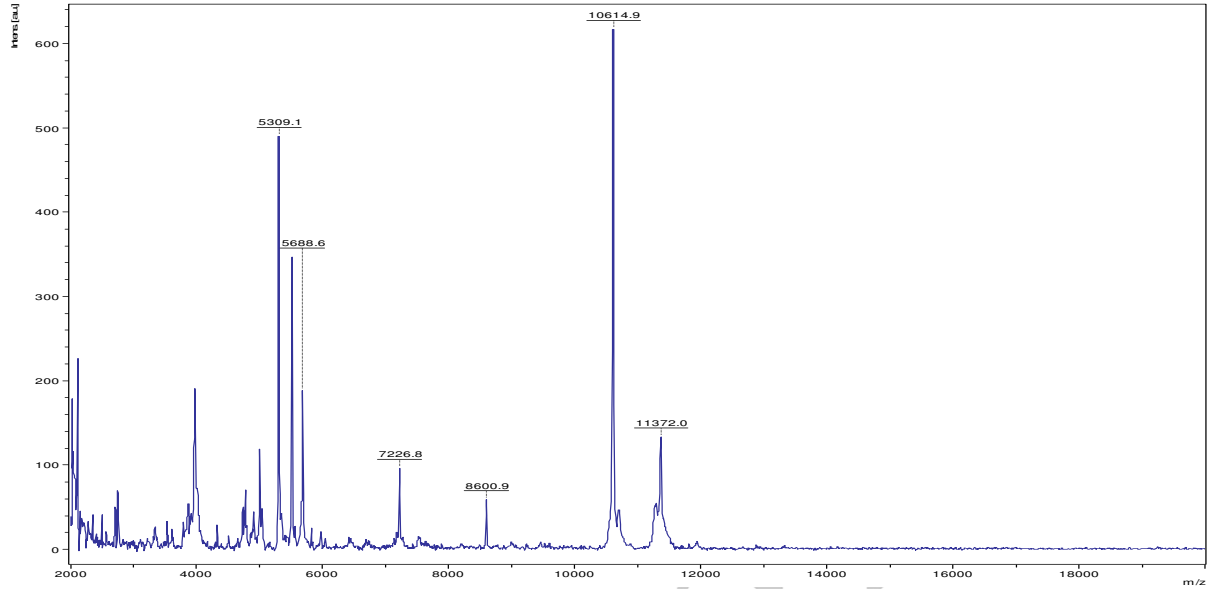
C



"M. occultaumposttuberculosis" M. tuberculosis H37Rv
FB-527

Figure 3

"M. occultatum posttuberculosis" FB-527



M. tuberculosis H37Rv

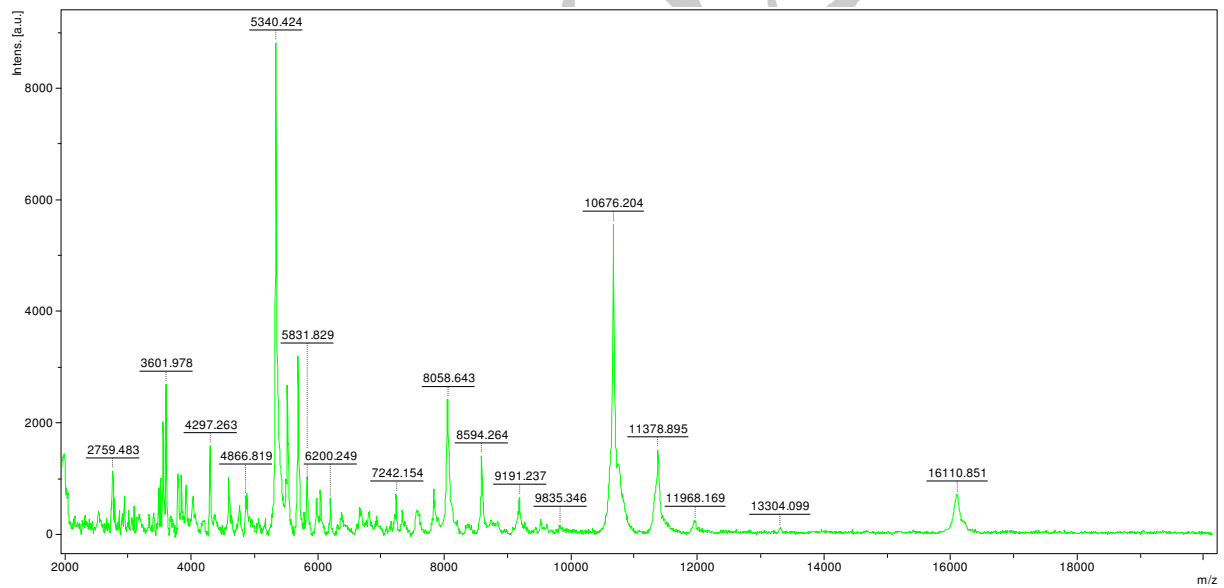


Figure 4

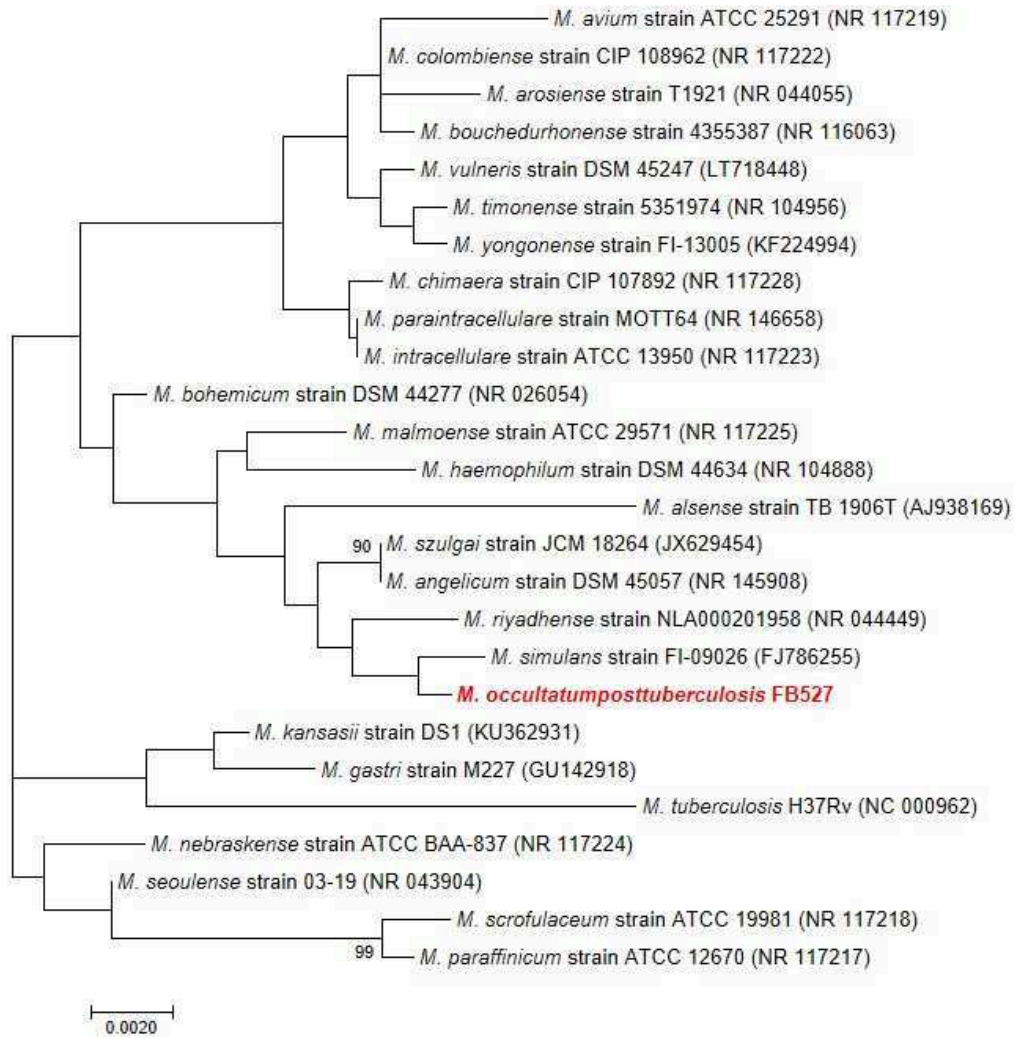


Table 1 : Minimum inhibitory concentration (MIC) of selected antibiotics against “*M. occulta*posttuberculosis”. MIC values are given in g/L.

Drug	MIC (Interpretation ^a)	
	Strain FB-527	Strain FI-09026
Amikacin	3 (S)	8 (S) ^b
Clarithromycin	0.032 (S)	0.5 (S) ^b
Linezolid	0.125(S)	0.5 (S) ^b
Ethambutol	0.50 (S)	4 (I) ^b
Azithromycin	8 (I)	0.125-0.19 (S)
Streptomycine	<0.064(S)	>64 (R) ^b
TRIM/SULFA	<0.002 (S)	4–76 (R) ^b
Doxycycline	12-16 (R)	0.25 (S)
Rifampicin	1-2 (I)	4 (I) ^b
Levofloxacin	2 (I)	12 (R)
Isoniazide	>256 (R)	(R) ^b
Imipenem	>32 (R)	>32 (R)
Meropenem	>32 (R)	>32 (R)
Clofazimine (1.5 mg/L)	S ^c	R
Minocycline (4 mg/L)	S ^c	R
Chloramphenicol (4 mg/L)	S ^c	S

^a I, intermediate; S, susceptible; R, resistant

^bResults according to Tortoli et al., 2010

^cResults according to Bouzid et al., 2017

Table 2: *Mycobacterium* species responsible for pulmonary infection in patients exposed to the Horn of Africa.

Mycobacterium	Country of isolation	Reference
<i>M. tuberculosis</i>	Djibouti Ethiopia Somalia Eritrea	(Bouzig et al., 2017) (Firdessa et al., 2013) (Sindani et al., 2013) (WHO, 2016)
<i>M. canettii</i>	Djibouti Ethiopia Somalia	(Aboubaker Osman et al., 2015)
<i>M. bovis</i>	Djibouti Ethiopia Eritrea	(Blouin et al., 2012) (Firdessa et al., 2013) (Ghebremariam et al., 2017)
<i>M. africanum</i>	Djibouti	(Blouin et al., 2012)
<i>M. chelonae</i>	Djibouti	(Boyer-Cazajous et al., 2014)
<i>M. fortuitum</i>		
<i>M. peregrinum</i>		
<i>M. intracellulare</i>	Ethiopia	(Firdessa et al., 2013)
<i>M. flavescens</i>		
<i>M. simiae</i>		
<i>M. kansasii</i>	Djibouti	(Bouzig et al., 2017)
“ <i>M. occultatum</i> posttuberculosis”	Somalia	(Tortoli et al., 2010)
	Djibouti	Our study

Supplementary Data

Supplementary table 1: Enzyme activities for “*M. occultaumposttuberculosis*” strain FB-527 and strain FI-09026 determined by inoculating a API® ZYM and API® Coryne strips

API ZYM				
	Reactions/enzymes	" <i>M. occultaumpost tuberculosis</i> " FB-527	" <i>M. occultaumpost tuberculosis</i> " FI-09026	<i>M. tuberculosis</i> H37Rv
2	Alkaline phosphatase	+	+	+
3	Esterase (C4)	+	+	+
4	Lipase esterase (C8)	+	+	+
5	Lipase (C14)	+	+	+
6	Leucine arylamidase	+	+	+
7	Valine arylamidase	-	-	-
8	Cystine arylamidase	-	-	-
9	Trypsin	-	-	-
10	Chymotrypsin	-	-	-
11	Acid phosphatase	+	+	+
12	Phosphoamidase	+	+	+
13	α-Galactosidase	-	-	-
14	β-Galactosidase	-	-	-
15	β-Glucuronidase	-	-	-
16	α-Glucosidase	-	-	-
17	β-Glucosidase	-	-	-
18	N-Acetyl-β-glucosaminidase	-	-	-
19	α-Mannosidase	-	-	-
20	α-Fucosidase	-	-	-

API Coryne			
Reactions/Enzymes	" <i>M. occulta</i> post <i>tuberculosis</i> " FB527	" <i>M.</i> <i>occulta</i> post <i>tuberculosis</i> " FI- 09026	<i>M. tuberculosis</i> H37Rv
Nitrate reductase	+	-	-
Pyrazinamidase	-	+	-
Pyrrolidonyl Arylamidase	-	-	-
Phosphatase Alcaline	+	+	+
β -Glucuronidase	-	-	-
β -Galactosidase	-	-	-
D-Glucosidase	-	-	-
N-Acetyl- β - Glucosaminidase	-	-	-
β -glucosidase (ESculine)	+	-	-
Urease	-	-	-
Hydrolyse (GELatine)	-	-	-
Fermentation 0	-	-	-
Fermentation (GLUcose)	+	-	-
Fermentation (RIBose)	-	+	-
Fermentation (XYLose)	-	-	-
Fermentation (MANnitrol)	-	-	-
Fermentation (MALtose)	+	-	-
Fermentation (LACtose)	-	-	-
Fermentation (SACcharose)	+	-	-
Fermentation (GLYcoGène)	-	-	-
Catalase	+	+	+

CHAPITRE III

Modèle murin d'infection à *Mycobacterium canettii* par voie digestive

Ready experimental translocation of *Mycobacterium canettii* yields pulmonary tuberculosis.

Bouزيد F, Brégeon F, Lepidi H, Donoghue HD, Minnikin DE, Drancourt M.

Infect Immun. 2017. *In press.*

6. CHAPITRE III : Modèle murin d'infection à *Mycobacterium canettii* par voie digestive

Dans la littérature, moins de 100 cas d'infection à *M. canettii* ont été rapportés (Aboubaker Osman et al., 2015); une infection limitée géographiquement à la Corne de l'Afrique et notre travail épidémiologique prospectif à Djibouti nous a permis d'estimer une prévalence d'infections pulmonaires à *M. canettii* de 4% (Bouزيد et al., 2017a). Cette rareté semble être corrélée à l'absence de transmission inter-humaine des infections à *M. canettii* (Koeck et al., 2011) mais mérite d'être confirmée par des études épidémiologiques plus longues et plus complètes. De plus, un réservoir environnemental de *M. canettii* dans la Corne de l'Afrique avait été suggéré (Koeck et al., 2011).

Notre travail bibliographique (Aboubaker Osman et al., 2015) a montré qu'il n'y a pas de différence significative entre la prévalence des cas d'infection pulmonaire causés par *M. canettii* à celle causés par *M. tuberculosis*. En revanche, la prévalence des adénopathies causées par *M. canettii* était significativement plus élevée que celle obtenues par *M. tuberculosis* ($P < 0.05$). De plus, des cas d'infection à *M. canettii* ont été rapportés au niveau de l'œsophage (Blouin et al., 2014), des ganglions mésentériques (Pfyffer et al., 1998) et des ascites fluides (Fabre et al., 2004). Par ailleurs, il a été suggéré que la faible hydrophobicité de *M. canettii* comparée à celle de *M. tuberculosis* pourrait entraîner un faible pouvoir de transmission par aérosols (Jankute et al., 2017). Par conséquent, l'ensemble de ces données laisse penser que la porte d'entrée digestive pourrait être une voie d'infection préférentielle de *M. canettii*.

Dans ce contexte, nous avons développé un modèle d'infection à *M. canettii* par voie digestive. Le gavage des souris a été réalisé par l'introduction d'une sonde qui atteint directement l'estomac de la souris. L'expérience a été réalisée avec un groupe de 28 souris

infectées inoculées avec 10^6 *M. canettii* qui a été comparé à un groupe de 10 souris inoculées avec une solution saline. La dissémination de la mycobactérie a été suivie à des intervalles de temps différents (J1, J3, J7, J17 et J28 post-infection (p.i.) par culture et PCR des homogénats des organes et par des analyses anatomo-pathologiques sur des organes fixés.

Dans les temps précoces (J1 et J3 p.i.), nous avons clairement mis en évidence la dissémination de *M. canettii* essentiellement vers les poumons (8/16). Cette dissémination s'explique par la translocation rapide de *M. canettii* du tube digestif vers la circulation lymphatique et qui a été confirmée par la détection de *M. canettii* dans les ganglions mésentériques, les ganglions oeso-trachéaux et les ganglions cervicaux à J1 et J3 p.i. De plus, une dissémination secondaire de *M. canettii* dans la circulation sanguine a été observée par les cultures positives réalisées au niveau de la rate, du foie et du sang. À partir du 7^{ème} jour et jusqu'au 28^{ème} jour p.i., une installation de *M. canettii* a été observée dans 11/12 poumons. Le bacille a été également retrouvé dans 8/12 ganglions cervicaux, 8/12 rates et moins fréquemment dans les ganglions oeso-trachéaux et axillaires, la graisse brune, le foie, les reins et le sang. Les analyses anatomo-pathologiques ont révélé des lésions inflammatoires avec formation de granulomes au niveau de tous les poumons analysés à J14 et J28 p.i. Un foie sur quatre a présenté trois petits granulomes à J28 p.i. Cependant, nous n'avons pas observé de lésions dans les ganglions cervicaux et axillaires, les rates, les reins et les graisses. Toutefois, nous avons constaté que la présence de lésion était corrélée avec la charge bacillaire dans le tissu.

Ce modèle expérimental nous a permis de démontrer clairement que *M. canettii* est infectieuse par voie digestive et que les poumons étaient la cible primaire de *M. canettii*. La dissémination vers les sites ganglionnaires reste aussi prédominante en particulier dans les temps tardifs. Ce mode d'infection serait proche de celui de *Mycobacterium bovis* qui infecte les individus essentiellement par voie digestive après la consommation de lait contaminé.

Ces données apportent des connaissances nouvelles pour une meilleure compréhension de l'épidémiologie des infections à *M. canettii* dans la Corne de l'Afrique et nous renseigne sur la possibilité d'infection des populations par *M. canettii* à travers une source alimentaire contaminée. Toutefois des investigations sur le terrain sont encore nécessaires pour rechercher et déterminer le réservoir environnemental de *M. canettii*.

Ce projet de recherche a reçu la médaille du meilleur poster lors de la Journée Scientifique de la Fondation Méditerranée Infection, à Marseille le 1^{er} Juillet 2016.

REVISED VERSION

1 **Ready experimental translocation of *Mycobacterium canettii* yields pulmonary**
2 **tuberculosis**

3 Running title: *M. canettii* translocation to lung

4 Fériel Bouzid^{a,b}, Fabienne Brégeon^a, Hubert Lepidi^a, Helen D. Donoghue^c,

5 David E. Minnikin^d, Michel Drancourt^{a*}

6
7 ^aAix Marseille Univ, URMITE, UMR CNRS 7278, IRD 198, INSERM 1095, IHU
8 Méditerranée Infection, 13005 Marseille, France.

9 ^bAix-Marseille Univ, CNRS, EIPL IMM FR3479, Marseille, France

10 ^cCentre for Clinical Microbiology, Royal Free Campus, University College London, London
11 NW3 2PF, UK

12 ^dInstitute of Microbiology and Infection, School of Biosciences, University of Birmingham,
13 Edgbaston, Birmingham B15 2TT, UK

14
15 ^{*}Correspondance author: Pr. Michel Drancourt, URMITE, IHU Méditerranée Infection, 19-21
16 Bd Jean Moulin 13005 Marseille, France. Tel: +33 (0)4 13 73 24 01 fax: + 33 (0) 13 73 24 02

17 Email: Michel.Drancourt@univ-amu.fr

18

19 **ABSTRACT**

20 *Mycobacterium canettii*, with smooth colony morphology, is the tuberculous organism
21 retaining most genetic traits from the putative last common ancestor of the rough morphology
22 *Mycobacterium tuberculosis* complex. To explore whether *M. canettii* can infect individuals
23 by the oral route, mice were fed with phosphate buffered saline or 10^6 *M. canettii* and were
24 sacrificed over a 28-day experiment. While no *M. canettii* was detected in negative controls,
25 *M. canettii*-infected mice yielded granuloma-like lesions in 4/4 lungs at days 14 and 28 post-
26 inoculation (p.i.), positive PCR detection of *M. canettii* in 5/8 mesenteric lymph nodes at days
27 1 and 3 p.i., also in 5/6 pooled stools collected from day 1 to day 28 p.i. Smooth *M. canettii*-
28 colonies grew from 68% of lungs and 36% of spleens and cervical lymph nodes but in less
29 than 20% of axillary lymph nodes, liver, brown fat, kidney or blood throughout the 28-day
30 experiment. Ready murine translocation after digestive tract challenge demonstrates the
31 potential of ingested *M. canettii* to relocate to distant organs and lungs. The demonstration of
32 this relocation supports the possibility that populations could be infected by environmental *M.*
33 *canettii*.

34

35 **Keywords:** *Mycobacterium canettii*, tuberculosis, animal model, oral infection,
36 *Mycobacterium tuberculosis* complex

37 **INTRODUCTION**

38 *Mycobacterium canettii* is a rare member of the *Mycobacterium tuberculosis* complex
39 (MTBC), responsible for fewer than one hundred reported cases of tuberculosis in patients
40 exposed to the Horn of Africa, with a few exceptions (1). In the MTBC, *M. canettii* is most
41 closely related to the vanished ancestor (1–5). *M. canettii* is uniquely characterized by a large
42 4.48 ± 0.05 Mb and mosaic genome with traces of intra-species horizontal gene transfer
43 (HGT) (3, 5, 6), including *M. tuberculosis* specific deletion 1 (TbD1) that is deleted in
44 “modern” *M. tuberculosis* lineages (7). In culture, *M. canettii* appears as large and cordless
45 mycobacteria, with smooth colonies (3, 8, 9). Previous studies have suggested that smooth *M.*
46 *canettii* may be less well transmitted in aerosols than rough *M. tuberculosis* (9, 10).
47 Preliminary investigations indicated that cultured *M. canettii* was less hydrophobic than *M.*
48 *tuberculosis* (11, 12). Since higher hydrophobicity was linked to enhanced aerosol
49 performance in non-tuberculous mycobacteria (13), it was suggested that the relatively low
50 hydrophobicity of *M. canettii* could be responsible for its lack of aerosol transmission (11).
51 *M. canettii*-infected patients present with pulmonary and lymphatic tuberculosis (1). The
52 absence of properly designed study limits interpreting the current lack of evidence for inter-
53 human transmission (9). This supports the existence of an unknown environmental or animal
54 reservoir and suggests that *M. canettii* is poorly adapted to any specific host, behaving as an
55 opportunist rather than an obligate pathogen (9). Published cases indicate that in Djibouti,
56 cervical lymphadenitis was significantly more prevalent during *M. canettii* infection than
57 during *M. tuberculosis* infection (1). Also, *M. canettii* was reported to cause esophageal
58 tuberculosis (14), mesenteric lymph nodes tuberculosis (15) and ascites (16) and several
59 isolates have been cultured in gastric fluid (14). These clinical observations led to our
60 hypothesis that the digestive tract was a possible portal of entry of *M. canettii* (1). We

REVISED VERSION

61 developed a murine model to explore this hypothesis in an etiological perspective contributing
62 to a better understanding of *M. canettii* infections.

63 **RESULTS**

64 **Clinical outcome of challenged mice**

65 In a first step, we observed that the *M. canettii* strain CIP 140010059^T (STB-A) (5) here
66 investigated resisted a two-hour exposure to pH of 2 to 5 chosen to mimic the low pH
67 encountered in murine stomach and intestines (17). CFUs obtained following acid exposure
68 ($3.11 \times 10^4 \pm 7.85 \times 10^3$ CFUs) were not statistically different compare to those obtained with
69 mycobacterial suspension in PBS ($3.76 \times 10^4 \pm 3.94 \times 10^3$ CFUs) ($p = 0.19$). Mice challenged
70 with *M. canettii* by oro-gastric inoculation exhibited no spontaneous death or symptoms of
71 discomfort through the 28-day experiment. There was no difference in mean body weight at
72 baseline between infected animals (20.98 ± 2.93 g) or controls (21.46 ± 3.30 g) ($P = 0.1$). We
73 observed a significant gain in body weight from the first week until the end of the experiment
74 in controls ($P = 0.04$) and infected mice ($P = 0.006$).

75 ***M. canettii* disseminates after digestive tract challenge**

76 To follow the dissemination of *M. canettii*, organs and peritoneum from *M. canettii*-
77 challenged mice and control mice were cultured. Obtained colonies were identified by matrix-
78 assisted laser desorption ionization time-of-flight mass spectrometry (MALDI-TOF-MS) and
79 real-time PCR targeting *M. canettii* TbD1 region in the presence of negative controls. Culture
80 of samples from negative control mice remained negative for *M. canettii*. Furthermore,
81 cultures of eight collected lungs from *M. canettii*-infected mice euthanized immediately after
82 inoculation remained negative. Considering both series of experiments, twenty-five of 28
83 infected mice (89%) had at least one organ with viable *M. canettii*, corresponding to 64/294
84 (22 %) culture-positive samples (Table 1). Mouse gender was not significantly associated

REVISED VERSION

85 with the number of infected mice or culture-positive samples (14/16 males versus 11/12
86 females; 33/174 samples in males versus 31/120 in females; $P = 0.15$). At day 1 p.i., 2/4
87 animals from the first series of experiments had culture-positive organs (animal # 1, positive
88 lungs and blood; animal # 3, positive spleen and liver). In the second series, three animals #
89 2b, 3b and 4b had culture-positive lungs and one animal #1b had a culture-positive spleen.
90 Oeso-tracheal lymph nodes examined in the second series revealed positive cultures in all
91 cases (Table 1). In the first series, *M. canettii* cultures were obtained at day 3 p.i. in 4/4
92 animals including 3/4 lung samples (mice #5, #7 and #8), 1/4 brown fat (mouse #6) and 1/4
93 liver (mouse #7). In the second series, positive culture of lungs (1/4) and cervical lymph
94 nodes (2/4) were observed in animals #5b, #6b and #8b respectively. On day 7 p.i. and day 14
95 p.i., 8/8 lungs were culture-positive, associated with a culture-positive spleen (5/8), cervical
96 lymph nodes (4/8), axillary lymph nodes (2/8) and 1/8 each of liver, kidney and blood. During
97 the dissection of the lungs from mouse #15, we observed macroscopically hypertrophic oeso-
98 tracheal lymph nodes. After this observation, sampling of this tissue was performed. Oeso-
99 tracheal lymph nodes yielded positive cultures in 2/2 sampled animals at day 14 p.i. (mice #15
100 and #16). At day 28 p.i., culture was positive in 4/4 cervical lymph nodes; 3/4 lungs, spleens
101 and tracheal lymph nodes; 2/4 axillary lymph nodes; and 1/4 liver, brown fat, blood and
102 kidney. All cultured *M. canettii* isolates retained smooth colony morphology. Throughout the
103 28-day experiment, culture was negative for all white fat and peritoneum samples from *M.*
104 *canettii*-challenged mice (Table 1). Microbial contamination prevented any isolation of *M.*
105 *canettii* from mesenteric lymph nodes and stools.

106 **Quantification of *M. canettii* organisms in culture-positive tissues**

107 In order to quantify the *M. canettii* load in infected tissues, quantitative real-time PCR was
108 performed for homogenates of culture-positive tissues, all lungs, mesenteric lymph nodes and
109 pooled stools. While the negative controls and nine culture-negative lungs remained negative,

REVISED VERSION

110 the *M. canettii* TbD1 region was detected in 30/64 (47%) culture-positive tissues including
111 16/19 (84%) lungs, 5/9 (44%) oeso-tracheal lymph nodes, 4/10 (40%) cervical lymph nodes,
112 4/10 (40%) spleens and 1/4 (25%) livers (Figure 1 and Supplementary Table 1). For
113 mesenteric lymph nodes, the *M. canettii* TbD1 region was detected in 5/8 (62%) samples from
114 3/4 and 2/4 challenged mice at day 1 and 3 p.i. respectively (Supplementary Table 1).
115 Quantification of the number of mycobacteria normalized per 10^6 mice cells by qPCR showed
116 that mesenteric lymph nodes represent the most loaded site early in the experiment, with $93 \pm$
117 121 mycobacteria / 10^6 cells at day 1 p.i. and 360 ± 199 mycobacteria / 10^6 cells at day 3 p.i.
118 For the same periods, the mycobacterial burden was lower in the lungs with 108 ± 187
119 mycobacteria / 10^6 cells at day 1 p.i. and 50 ± 86 mycobacteria / 10^6 cells at day 3 p.i. Oeso-
120 tracheal nodes and spleen had a respective load of 43 and 12.5 mycobacteria / 10^6 cells at day
121 1 p.i. However, at day 28 p.i., the oeso-tracheal nodes and lungs were the most loaded sites
122 with a respective burden of $2.68 \times 10^3 \pm 1.68 \times 10^3$ mycobacteria / 10^6 cells and $1 \times 10^3 \pm 9.34$
123 $\times 10^2$ mycobacteria / 10^6 cells against a lower load on cervical lymph nodes 94 ± 108
124 mycobacteria / 10^6 cells, spleen 47 ± 32 mycobacteria / 10^6 cells and liver 45 mycobacteria /
125 10^6 cells. Throughout the 28-day experiment, a statistically significant increase in bacterial
126 load in infected lungs was noted ($P = 0.009$ day 1 versus day 28; $p = 0.02$ day 3 vs day 28 and
127 $p = 0.03$ day 14 vs day 28) (Figure 1B). In infected spleen, the bacterial load between day 1
128 and day 28 p.i. was relatively stable (around 12 to 82 mycobacteria / 10^6 cells). For cervical
129 lymph nodes, a low load of 4 mycobacteria per 10^6 cells was detected in one positive sample
130 at day 7 p.i. The mycobacterial burden in this tissue was relatively more important later, with
131 a bacterial load of 514/ 10^6 cells at day 14 p.i. in one positive sample and a mean of 94 ± 108
132 mycobacteria / 10^6 cells from two positive samples at day 28 p.i. The detection of *M. canettii*
133 in stool appeared early (10 mycobacteria/100 mg at day 1 and 2 p.i.) and persisted throughout

REVISED VERSION

134 the experiment, with a tendency to increase at day 28 with 33 mycobacteria /100 mg stools
135 (Supplementary Table 2).

136 **Translocated *M. canettii* induce lung pathology**

137 The spleen weight remained stable throughout the experiments without any significant
138 differences between infected animals (0.085 ± 0.01 g) and controls (0.083 ± 0.008 g) ($P =$
139 0.63). No lesions were observed in any tissues sampled in controls. In contrast, in *M. canettii*-
140 challenged mice, there was clear pathology in the lungs from day 7 p.i until day 28 p.i. In
141 these animals, gross pathology indicated bilateral and globally symmetric congestion of the
142 lungs, dominant in the posterior and upper areas, with patchy dark red zones. Pathological
143 examination was performed in organs sampled in the first series of the experiment. While
144 control mice lungs remain normal until day 28 p.i., microscopic examination of infected mice
145 lungs showed a normal aspect at day 1 p.i., light inflammatory infiltrates at day 7 p.i. and
146 major lesions in 4/4 lungs sampled at day 14 p.i. and 28 p.i. Lesions were characterized by
147 peribronchiolitis, perivascularitis with alveolitis and granuloma-like lesions – defined as a
148 limited area of nodular inflammatory lesions comprised of lymphocytes and macrophages
149 (Figure 2A). In diseased lungs and in granuloma-like lesions, Ziehl-Neelsen staining disclosed
150 a multi-bacillary status with numerous organisms within cells with macrophage morphology
151 (Figure 2A). In addition to lungs, moderate lesions were observed in one liver dedicated to the
152 histology at day 28 p.i. from *M. canettii*-challenged mice (Figure 2B). Microscopic
153 examination showed three small granuloma-like lesions on the same sample while liver in
154 control mice remain normal. No lesions were observed in axillary and cervical lymph nodes,
155 spleens, kidneys or the white and brown fat throughout the 28-day experiment. In the
156 analyzed histological sections, no acid-fast bacilli were detected by Ziehl-Neelsen staining.
157 Pathology and microbial load data obtained at day 14 and day 28 p.i. are summarized in Table
158 2.

REVISED VERSION

159 **DISCUSSION**

160 Mice challenged with ingested *M. canettii* organisms that resist the low pH
161 encountered in murine stomach and intestines (17) develop lung tuberculosis. This
162 observation, authenticated by the negative controls in each experiment and the firm
163 identification of growing organisms, was reproduced in both males and females eliminating
164 any potential sex-related bias. A few previously published models for *M. canettii* infection
165 have relied on subcutaneous and intramuscular inoculation of Guinea pigs (18) and intra-
166 tracheal or intranasal aerosol inoculation of mice (5, 19, 20). However, these models did not
167 mimic clinical situations, as there is no epidemiological or clinical evidence for patients
168 becoming infected via the parenteral or respiratory route. Accordingly, the limited number of
169 *M. canettii*-infection cases in endemic regions of the Horn of Africa and the absence of
170 reported human-to-human transmission do not favor the hypothesis of a widespread
171 respiratory disease (1, 9). Scarce epidemiological and clinical observations may suggest
172 contaminated drinking water and food as potential sources with an oral route of entry (1). On
173 these bases, the present study aimed to explore for the first time the hypothesis of digestive
174 tract infection by *M. canettii*.

175 In this model positivity of lungs at day 1-3 p.i. was interpreted as resulting from the
176 rapid dissemination of *M. canettii* from the digestive tract via a lymphatic route. This is
177 supported by the detection of *M. canettii* in the mesenteric, oeso-tracheal and cervical lymph
178 nodes soon afterwards. The gavage procedure was performed in awakened animals and no
179 cough or dyspnea event was observed. Accordingly, lung collected from mice euthanized
180 immediately after inoculation remained sterile. Procedure-induced lung contamination is
181 therefore improbable. Further culture-positivity of liver and spleen suggest a secondary blood
182 dissemination of *M. canettii*. Microscopic observation of pathological lesions including
183 granuloma-like lesions in infected lungs correlating with high burden of mycobacteria,

REVISED VERSION

184 supports the installation of *M. canettii* in this organ and suggests that lungs are primary targets
185 of *M. canettii*. At the opposite, the absence of detectable inflammatory response in spleens,
186 lymphoid organs, fats and kidneys correlates with the fact that mycobacteria were not
187 detected or detected at low burden in these organs.

188 The dissemination of bacteria from the intestines has been extensively described and
189 defined as translocation (21). We propose that *M. canettii* strain STB-A should be designated
190 as an additional pathogen that can translocate within the patient. However, the other smooth
191 tubercle bacilli clonal groups from STB-B to STB-M (3, 5) might behave differently when
192 infecting individuals by the oral route; and data here reported cannot be extrapolated for the
193 other members of the MTBC. Indeed, the specificity of the results here reported will have to
194 be assessed in further experiments. The observations that rodents infected by the digestive
195 route with either *M. canettii* or *M. bovis* (22) all develop pulmonary tuberculosis, indicates
196 that this route of infection could be a common feature. *M. bovis* infection gives an example of
197 human tuberculosis contracted through the oral route by consuming cattle products;
198 unpasteurized contaminated milk in particular (23). The ease of humans contracting
199 tuberculosis from hunted animals is also illustrated by the case of a 1,000-year-old Pre-
200 Colombian South American population being infected with *Mycobacterium pinnipedii* from
201 sea mammals (24). Currently, it is not known if *M. pinnipedii* is transmissible between
202 humans. However, digestive tract infection by *M. tuberculosis* remains unclear since previous
203 gavage experiments yielded contradictory results (25, 26). Therefore in the absence of definite
204 results, *M. tuberculosis* could not be used as a control in our study strictly focusing on *M.*
205 *canettii*. Moreover, developing an experimental model of digestive tract infection by *M.*
206 *tuberculosis* has no acknowledged epidemiological and clinical basis: it is well established
207 that *M. tuberculosis* infection is an air-borne disease in the vast majority of cases (27) with

REVISED VERSION

208 few cases of inoculation tuberculosis (28) and no reported case of digestive tract infection by
209 *M. tuberculosis*.

210 It would be of great interest to know how the limited number of human cases have
211 been infected by *M. canettii* in East Africa. In order to determine the origins of *M. canettii*
212 infections in the Horn of Africa and elsewhere, intensive investigations of environmental and
213 animal sources are mandatory. The type of reservoir harbouring *M. canettii* in the Horn of
214 Africa remains unclear, with perhaps unspecified animals maintaining an equilibrium with an
215 environmental source. Recently, it was shown that *M. canettii* was able to persist in soil much
216 longer than *M. tuberculosis* (29), so ongoing exchanges between the environment and animals
217 are possibly favoured. In addition, thermal inactivation experiments showed that *M. canettii*
218 survives up to a temperature of 45°C which is compatible with an environmental reservoir in
219 the Horn of Africa but suggests that cooked drinks and foods are unlikely sources of
220 contamination (30).

221 *M. canettii* is the earliest recognizable associate member of the MTBC and this
222 taxon plays a pivotal role (2–5, 11). Indeed, given the likely evolutionary pathway from
223 environmental *Mycobacterium kansasii* to *M. canettii* (4, 11, 31–33), a vital step in the
224 mammalian evolution of modern virulent members of the MTBC from environmental
225 mycobacteria, is the dissemination of a potential ancestral intestinal pathogen, such as *M.*
226 *canettii*, to other organs, particularly lungs. The present results show, for the first time, that *M.*
227 *canettii* is efficiently transferred from intestine to lung in mice. Although the experimental
228 data herein reported obviously cannot be directly extrapolated to human disease, they
229 nevertheless support further clinical investigations to assess the potential role of digestive
230 route of contamination with *M. canettii* in exposed populations.

231

REVISED VERSION

232 **MATERIALS AND METHODS**233 **Ethic statement**

234 The experimental protocol, registered by the “Ministère de l’Enseignement Supérieur et de la
235 Recherche” under reference n° 2015092415474605 was approved by the Institutional Animal
236 Care and Use Committee of Aix-Marseille University “C2EA-14”, France. Mice were
237 handled according to the rules of Décret N° 2013–118, Février 7, 2013, France. All
238 procedures on animals were performed in accordance with the European law and agreed with
239 'Animal Research: Reporting In Vivo Experiments' (ARRIVE Guidelines
240 <http://www.nc3rs.org.uk>). Animals were euthanized using blood sampling via intra-cardiac
241 puncture under deep volatile anesthesia (sevoflurane) followed by cervical dislocation. All
242 these experiments were performed in a biosafety level 3 laboratory of the Faculté de
243 Médecine, Aix-Marseille Université.

244 **Strains, culture conditions and preparation of inocula**

245 *M. canettii* strain CIP 140010059^T (STB-A) (5) was cultured in Middlebrook 7H10 (Becton
246 Dickinson, Le Pont de Claix, France) supplemented with 10% oleic acid-albumin-dextrose-
247 catalase (OADC) (Becton Dickinson). Prior to infection, mycobacteria were re-suspended in
248 phosphate buffered saline (PBS), vortexed for 10 minutes with sterile glass balls and
249 centrifuged for 1 min at 300 g to remove clumps. The supernatant was dispersed by expelling
250 the suspension 10 times through a sterile 25-Gauge needle attached to a 1-mL syringe.
251 Calibration was performed according to McFarland standards and confirmed by counting
252 mycobacteria after Ziehl-Neelsen staining. We then assayed the in vitro resistance of *M.*
253 *canettii* to low pH. A 100- μ L *M. canettii* suspension containing 10^6 mycobacteria was mixed
254 with 900 μ L of pH-modified PBS solutions at pH of 2 to 5. Acid challenge was carried out for
255 two hours at 37°C. Next, PBS (pH 6.8) was added up to 10 fold. Samples were serially diluted

REVISED VERSION

256 and plated onto Middlebrook 7H10 supplemented with 10% OADC (Becton Dickinson) to
257 assess viability during challenge by scoring colony-forming units (CFUs).

258 **General procedures and mice challenge**

259 A total of 46 eight-week old Balb/cByj mice (25 males, 21 females) (Charles River
260 Laboratories, L'Arbresle, Lyon, France) were housed in individual plastic cages (two to three
261 animals per cage) placed in an isolator with free access to water and standard diet food. Mice
262 were randomly allocated to the control group (five males and five females) and the M.
263 canettii-infected group (20 males, 16 females). For each mouse, 200 μ L of sterile PBS or
264 mycobacterial suspension adjusted to 10^6 M. canettii in PBS were administered by gavage
265 using a sterile steel 20-gauge feeding needle for rodents with ball-tips (Instech Laboratories,
266 Inc., Philadelphia, USA) to ensure soft placement. To assess any possibility of procedure-
267 induced lung contamination, eight M. canettii-infected mice were euthanized immediately
268 after inoculation and the lungs were collected and cultured. After one-month incubation,
269 cultures remained negative. For the remaining mice, animals were transferred back in their
270 cages after challenge and housed in a safety cabinet with food and water ad libitum. All mice
271 were observed daily for signs of discomfort and respiratory distress.

272 **Clinical outcome**

273 Each animal was weighed before challenge, the first day post-infection (p.i.) and then every
274 two days. In a first series of experiments aimed to document dissemination of M. canettii, 30
275 mice were challenged at different time intervals: four infected mice (two males and two
276 females) and two control mice (one male and one female) were euthanized at 1, 3, 7, 14 and
277 28 days p.i. Blood sampling was performed by trans-parietal intra-cardiac puncture and
278 aliquoted for culture and PCR. Stools as well as miscellaneous organs were sampled including
279 cervical, axillaries and oeso-tracheal lymph nodes, lungs, spleen, liver, kidneys, brown and
280 white fats. The peritoneum was swabbed. Stools from mice challenged the same day were

REVISED VERSION

281 pooled. Spleens were immediately weighed to account for spleen weight loss or gain. All
282 organs were stored at -80°C for microbial load experiments. Two animals of each group were
283 randomly assigned to have a part of the organs fixed in 4% formalin for Ziehl Neelsen
284 staining and histopathology. The one to two collected oeso-tracheal lymph nodes were too
285 small to be divided; only culture and PCR were performed. In a second series of experiments,
286 8 additional mice (six males and two females) were challenged under the same conditions.
287 This second series aimed to precisely determine the translocation of the bacteria from the
288 digestive tract during the early periods. In order to do this, four animals were euthanized at
289 day 1 p.i. (two males and two females) and day 3 p.i. (four males). In addition to series one
290 sampling, oeso-tracheal and mesenteric lymph nodes were sampled at early times.

291 **Mycobacterial culture**

292 Stored organs were thawed and ground in sterile PBS then cultured in Middlebrook 7H10 -
293 OADC (Becton Dickinson). Inoculated media were examined weekly by the naked eye for
294 mycobacterial colonies for up to four weeks. Colonies were confirmed by MALDI-TOF-MS
295 (34) and by a real-time PCR system targeting *M. canettii* TbD1 region.

296 **PCR-based experiments**

297 Molecular detection was used to confirm the identification of cultured colonies and to
298 quantify the *M. canettii* mycobacteria load in tissues. For positive cultures, colonies were
299 inactivated in 200 μL PBS by one-hour incubation at 56°C with 200 μL G2 buffer and 20 μL
300 proteinase K (20 mg/mL), then broken with glass powder using a FastPrep instrument (MP
301 Biomedical Europe, Illkirch, France) at a speed of 6.5 m/s for 90 s. DNA was extracted using
302 EZ1 DNA Tissue Kit (Qiagen, Hilden, Germany). Quantitative real-time PCR (qPCR) was
303 performed using the CFX96® qPCR and incorporating qPCR reagents (Takyon, Eurogentec,
304 Liege, Belgium). Specific primers of *M. canettii* targeting TbD1 region were designed:

REVISED VERSION

305 TbD1_ Forward 5'-CAAAGGAACCGCGAAAGTTA-3', TbD1_ Reverse 5'-
306 ACCGTGATAAGCACCAGGAC-3' and TbD1_Probe 5'-6FAM-
307 TCGCGGTGATGTTGCTCTTCG-3'. Colonies were identified using TbD1 PCR in the
308 presence of negative controls. For quantification, all lungs, mesenteric lymph nodes, stools as
309 well as homogenates of tissues growing *M. canettii*, were tested. Aliquots of 150 μ L were
310 incubated overnight at 56°C with 150 μ L of G2 buffer mixed with 15 μ L proteinase K (20
311 mg/mL). After two cycles of mechanical lysis (45s), total DNA was then extracted using the
312 EZ1 DNA Tissue Kit. DNA extraction from stools was performed using QIAamp® DNA
313 Stool Kit (Qiagen, Hilden, Germany). Two qPCR were performed targeting *M. canettii* TbD1
314 and the housekeeping mouse hydroxyl-methylbilane synthase gene (HMBS) for normalization
315 as previously described (35). For both systems, the qPCR cycle was 50°C for 2 minutes, 95°C
316 for 5 minutes followed by 40 cycles of 95°C for 1 second and 60°C for 35 seconds; and
317 finally 45°C for 30 seconds. Negative controls consisted of DNA extracted from organs and
318 stools from PBS-challenged mice. In addition, a standard curve of *M. canettii* TbD1 qPCR
319 was generated using extracted DNA from 10-fold serial dilution of *M. canettii* suspensions
320 (10^7 CFUs/mL to 1 CFU/mL). Simultaneously, L929 mice cells were calibrated from 10^6 cells
321 to one cell per 200 μ L then suspensions were extracted and quantified using qPCR targeting
322 the HMBS gene to generate a calibration curve. The density of mycobacteria (expressed in
323 mycobacteria/cell) was tabulated by dividing the number of mycobacteria DNA copies by the
324 number of mouse cell DNA copies (Supplementary Table 3).

325 **Pathological examination**

326 Organs were fixed with 4% buffered formalin and embedded in paraffin. Serial sections (3-
327 μ m) of these specimens were obtained for routine hematoxylin-eosin-saffron and Ziehl-
328 Neelsen staining. In all pathological examinations, tissues collected from PBS-challenged
329 mice were used as negative controls.

REVISED VERSION

330 **Statistical analyses**

331 Statistics were performed using Sigmat plot 13, Systat Software Inc. The data were expressed
332 as the means \pm standard deviation (SD). Student's t-test or the Mann-Whitney rank-sum test
333 was used for inter-group comparisons with $P < 0.05$ being regarded as significant.

334 **ACKNOWLEDGEMENTS**

335 This study was financially supported by URMITE, IHU Méditerranée Infection, Marseille,
336 France; and by the A*MIDEX project (n° ANR-11-IDEX-0001-02) funded by the
337 «Investissements d'Avenir» French Government program, managed by the French National
338 Research Agency (ANR).

339

340 **Conflict of interests**

341 The authors declare that they have no competing interests.

342

REVISED VERSION

343 **References**

- 344 1. Aboubaker Osman D, Bouzid F, Canaan S, Drancourt M. 2015. Smooth Tubercle
345 Bacilli: Neglected Opportunistic Tropical Pathogens. *Front public Heal* 3:283.
- 346 2. Boritsch EC, Supply P, Honore N, Seemann T, Stinear TP, Brosch R. 2014. A glimpse
347 into the past and predictions for the future: the molecular evolution of the tuberculosis
348 agent. *Mol Microbiol* 93:835–852.
- 349 3. Gutierrez MC, Brisse S, Brosch R, Fabre M, Omais B, Marmiesse M, Supply P,
350 Vincent V. 2005. Ancient origin and gene mosaicism of the progenitor of
351 *Mycobacterium tuberculosis*. *PLoS Pathog* 1:e5.
- 352 4. Minnikin DE, Lee OY, Wu HH, Besra GS, Bhatt A, Nataraj V, Rothschild BM,
353 Spigelman M, Donoghue HD. 2015. Ancient mycobacterial lipids: Key reference
354 biomarkers in charting the evolution of tuberculosis. *Tuberculosis* 95 Suppl 1, S133-
355 S139.
- 356 5. Supply P, Marceau M, Mangenot S, Roche D, Rouanet C, Khanna V, Majlessi L,
357 Criscuolo A, Tap J, Pawlik A, Fiette L, Orgeur M, Fabre M, Parmentier C, Frigui W,
358 Simeone R, Boritsch EC, Debie AS, Willery E, Walker D, Quail MA, Ma L, Bouchier
359 C, Salvignol G, Sayes F, Cascioferro A, Seemann T, Barbe V, Locht C, Gutierrez MC,
360 Leclerc C, Bentley SD, Stinear TP, Brisse S, Medigue C, Parkhill J, Cruveiller S,
361 Brosch R. 2013. Genomic analysis of smooth tubercle bacilli provides insights into
362 ancestry and pathoadaptation of *Mycobacterium tuberculosis*. *Nat Genet* 45:172–179.
- 363 6. Boritsch EC, Khanna V, Pawlik A, Honore N, Navas VH, Ma L, Bouchier C, Seemann
364 T, Supply P, Stinear TP, Brosch R. 2016. Key experimental evidence of chromosomal
365 DNA transfer among selected tuberculosis-causing mycobacteria. *Proc Natl Acad Sci*
366 *U S A* 113:9876–9881.
- 367 7. Brosch R, Gordon S V, Marmiesse M, Brodin P, Buchrieser C, Eiglmeier K, Garnier T,

REVISED VERSION

- 368 Gutierrez C, Hewinson G, Kremer K, Parsons LM, Pym AS, Samper S, van Soolingen
369 D, Cole ST. 2002. A new evolutionary scenario for the *Mycobacterium tuberculosis*
370 complex. *Proc Natl Acad Sci U S A* 99:3684–3689.
- 371 8. Boritsch EC, Frigui W, Cascioferro A, Malaga W, Etienne G, Laval F, Pawlik A, Le
372 Chevalier F, Orgeur M, Ma L, Bouchier C, Stinear TP, Supply P, Majlessi L, Daffe M,
373 Guilhot C, Brosch R. 2016. pks5-recombination-mediated surface remodelling in
374 *Mycobacterium tuberculosis* emergence. *Nat Microbiol* 1:15019.
- 375 9. Koeck JL, Fabre M, Simon F, Daffe M, Garnotel E, Matan AB, Gerome P, Bernatas JJ,
376 Buisson Y, Pourcel C. 2011. Clinical characteristics of the smooth tubercle bacilli
377 “*Mycobacterium canettii*” infection suggest the existence of an environmental
378 reservoir. *Clin Microbiol Infect* 17:1013–1019.
- 379 10. Fabre M, Hauck Y, Soler C, Koeck JL, van Igen J, van Soolingen D, Vergnaud G,
380 Pourcel C. 2010. Molecular characteristics of “*Mycobacterium canettii*” the smooth
381 *Mycobacterium tuberculosis* bacilli. *InfectGenetEvol* 10:1165–1173.
- 382 11. Minnikin DE, Lee OY, Wu HH, Nataraj V, Donoghue HD, M. ridell, M. watanabe,
383 alderwick L, Bhatt A, Besra GS. 2015. Pathophysiological Implications of Cell
384 Envelope Structure in *Mycobacterium tuberculosis* and Related Taxa, p 145-175. In
385 Ribón W (ed), *Tuberculosis - Expanding Knowledge*, Croatia.
- 386 12. Jankute M, Nataraj V, Lee OY, Wu HHT, Ridell M, Garton NJ, Barer MR, Minnikin
387 DE, Bhatt A, Besra GS. 2017. The role of hydrophobicity in tuberculosis evolution and
388 pathogenicity. *Sci Rep* 7:1315.
- 389 13. Falkinham III JO. 2003. Mycobacterial aerosols and respiratory disease. *Emerg Infect*
390 *Dis* 9:763–767.
- 391 14. Blouin Y, Cazajous G, Dehan C, Soler C, Vong R, Hassan MO, Hauck Y, Boulais C,
392 Andriamanantena D, Martinaud C, Martin E, Pourcel C, Vergnaud G. 2014. Progenitor

REVISED VERSION

- 393 “Mycobacterium canettii” clone responsible for lymph node tuberculosis epidemic,
394 Djibouti. *Emerg Infect Dis* 20:21–28.
- 395 15. Pfyffer GE, Auckenthaler R, van Embden JD, van Soolingen D. 1998. *Mycobacterium*
396 *canettii*, the smooth variant of *M. tuberculosis*, isolated from a Swiss patient exposed in
397 Africa. *Emerg Infect Dis* 4:631–634.
- 398 16. Fabre M, Koeck JL, Le FP, Simon F, Herve V, Vergnaud G, Pourcel C. 2004. High
399 genetic diversity revealed by variable-number tandem repeat genotyping and analysis
400 of *hsp65* gene polymorphism in a large collection of “*Mycobacterium canettii*” strains
401 indicates that the *M. tuberculosis* complex is a recently emerged clone of “*M. canettii*”.
402 *J Clin Microbiol* 42:3248–3255.
- 403 17. McConnell EL, Basit AW, Murdan S. 2008. Measurements of rat and mouse
404 gastrointestinal pH, fluid and lymphoid tissue, and implications for in-vivo
405 experiments. *J Pharm Pharmacol* 60:63–70.
- 406 18. van Soolingen D, Hoogenboezem T, de Haas PE, Hermans PW, Koedam MA,
407 Teppema KS, Brennan PJ, Besra GS, Portaels F, Top J, Schouls LM, van Embden JD.
408 1997. A novel pathogenic taxon of the *Mycobacterium tuberculosis* complex, *Canetti*:
409 characterization of an exceptional isolate from Africa. *Int J Syst Bacteriol* 47:1236–
410 1245.
- 411 19. Lopez B, Aguilar D, Orozco H, Burger M, Espitia C, Ritacco V, Barrera L, Kremer K,
412 Hernandez-Pando R, Huygen K, van Soolingen D. 2003. A marked difference in
413 pathogenesis and immune response induced by different *Mycobacterium tuberculosis*
414 genotypes. *Clin Exp Immunol* 133:30–37.
- 415 20. Dormans J, Burger M, Aguilar D, Hernandez-Pando R, Kremer K, Roholl P, Arend
416 SM, van Soolingen D. 2004. Correlation of virulence, lung pathology, bacterial load
417 and delayed type hypersensitivity responses after infection with different

REVISED VERSION

- 418 Mycobacterium tuberculosis genotypes in a BALB/c mouse model. *Clin Exp Immunol*
419 137:460–468.
- 420 21. Schweinburg FB, Seligman AM, Fine J. 1950. Transmural migration of intestinal
421 bacteria; a study based on the use of radioactive *Escherichia coli*. *N Engl J Med*
422 242:747–751.
- 423 22. Clarke KA, Fitzgerald SD, Zwick LS, Church S V, Kaneene JB, Wismer AR, Bolin
424 CA, Hattey JA, Yuzbasiyan-Gurkan V. 2007. Experimental inoculation of meadow
425 voles (*Microtus pennsylvanicus*), house mice (*Mus musculus*), and Norway rats (*Rattus*
426 *norvegicus*) with *Mycobacterium bovis*. *J Wildl Dis* 43:353–365.
- 427 23. Smith RM, Drobniewski F, Gibson A, Montague JD, Logan MN, Hunt D, Hewinson G,
428 Salmon RL, O’Neill B. 2004. *Mycobacterium bovis* infection, United Kingdom. *Emerg*
429 *Infect Dis* 10:539–541.
- 430 24. Bos KI, Harkins KM, Herbig A, Coscolla M, Weber N, Comas I, Forrest SA, Bryant
431 JM, Harris SR, Schuenemann VJ, Campbell TJ, Majander K, Wilbur AK, Guichon RA,
432 Wolfe Steadman DL, Cook DC, Niemann S, Behr MA, Zumarraga M, Bastida R,
433 Huson D, Nieselt K, Young D, Parkhill J, Buikstra JE, Gagneux S, Stone AC, Krause J.
434 2014. Pre-Columbian mycobacterial genomes reveal seals as a source of New World
435 human tuberculosis. *Nature* 514:494–497.
- 436 25. Pierce C, Dubos RJ, Middlebrook G. 1947. Infection of mice with mammalian tubercle
437 bacilli grown in tween-albumin liquid medium. *J Exp Med* 86:159–174.
- 438 26. Lefford MJ. 1984. Diseases in mice and rats, p 947-977. In Kubica GP and Wayne LG
439 (ed), *The mycobacteria*, New York.
- 440 27. Fogel N. 2015. Tuberculosis: A disease without boundaries. *Tuberculosis* 95:527–531.
- 441 28. Frankel A, Penrose C, Emer J. 2009. Cutaneous tuberculosis: a practical case report
442 and review for the dermatologist. *J Clin Aesthet Dermatol* 2:19–27.

REVISED VERSION

- 443 29. Ghodbane R, Mba Medie F, Lepidi H, Nappez C, Drancourt M. 2014. Long-term
444 survival of tuberculosis complex mycobacteria in soil. *Microbiology* 160:496–501.
- 445 30. Aboubaker Osman D, Garnotel E, Drancourt M. 2017. Dry-heat inactivation
446 of "Mycobacterium canettii" *BMC Res Notes* 10:201.
- 447 31. Veyrier FJ, Dufort A, Behr MA. 2011. The rise and fall of the Mycobacterium
448 tuberculosis genome. *Trends Microbiol* 19:156–161.
- 449 32. Veyrier F, Pletzer D, Turenne C, Behr MA. 2009. Phylogenetic detection of horizontal
450 gene transfer during the step-wise genesis of Mycobacterium tuberculosis. *BMC Evol*
451 *Biol* 9:196.
- 452 33. Wang J, McIntosh F, Radomski N, Dewar K, Simeone R, Enninga J, Brosch R, Rocha
453 EP, Veyrier FJ, Behr MA. 2015. Insights on the emergence of Mycobacterium
454 tuberculosis from the analysis of Mycobacterium kansasii. *Genome Biol Evol* 7:856–
455 870.
- 456 34. Zingue D, Flaudrops C, Drancourt M. 2016. Direct matrix-assisted laser desorption
457 ionisation time-of-flight mass spectrometry identification of mycobacteria from
458 colonies. *Eur J Clin Microbiol Infect Dis* 35:1983–1987.
- 459 35. Ding S, Chi MM, Scull BP, Rigby R, Schwerbrock NM, Magness S, Jobin C, Lund
460 PK. 2010. High-fat diet: bacteria interactions promote intestinal inflammation which
461 precedes and correlates with obesity and insulin resistance in mouse. *PLoSOne*
462 5:e12191.
- 463
- 464
- 465
- 466
- 467

REVISED VERSION

468 **Table 1:** Culture results of samples from mice challenged with *M. canettii*.

Mice Ref	Sex	Day p.i.	Samples											
			OT LN	AX LN	CV LN	B Fat	W Fat	Lung	Liver	Spleen	Kidney	Blood	P swab	
First series														
#1	M		...	-	-	-	-	-	+	-	-	-	+	-
#2	M		...	-	-	-	-	-	-	-	-	-	-	-
#3	F		...	-	-	-	-	-	-	+	+	-	-	-
#4	F	1	...	-	-	-	-	-	-	-	-	-	-	-
Second series														
#1b	F		+	-	-	-	-	-	-	-	+	-	-	-
#2b	F		+	-	-	-	-	-	+	-	-	-	-	-
#3b	M		+	-	-	-	-	-	+	-	-	-	-	-
#4b	M		+	-	-	-	-	-	+	-	-	-	-	-
First series														
#5	M		...	-	-	-	-	-	+	-	-	-	-	-
#6	M		...	-	-	-	+	-	-	-	-	-	-	-
#7	F		...	-	-	-	-	-	+	+	-	-	-	-
#8	F	3	...	-	-	-	-	-	+	-	-	-	-	-
Second series														
#5b	M		-	-	-	-	-	-	+	-	-	-	-	-
#6b	M		-	-	+	-	-	-	-	-	-	-	-	-
#7b	M		-	-	-	-	-	-	-	-	-	-	-	-
#8b	M		-	-	+	-	-	-	-	-	-	-	-	-
First series														
#9	M		...	-	-	-	-	-	+	-	-	-	-	-
#10	M	7	...	-	+	-	-	-	+	+	-	-	-	-

REVISED VERSION

#11	F		...	-	-	-	-	+	-	+	-	-	-
#12	F		...	-	-	-	-	+	-	-	+	-	-
#13	M		...	+	-	-	-	+	-	+	-	-	-
#14	M	14	...	-	+	-	-	+	-	+	-	-	-
#15	F		+	+	+	-	-	+	-	+	-	-	-
#16	F		+	-	+	-	-	+	-	+	-	+	-
#17	M		+	-	+	+	-	+	+	+	+	+	-
#18	M	28	-	-	+	-	-	-	-	-	-	-	-
#19	F		+	+	+	-	-	+	+	+	-	-	-
#20	F		+	+	+	-	-	+	-	+	-	-	-

469

470 Abbreviations: M: Male; F: Female; LN: Lymph nodes; Ax: axillary; CV: cervical; OT: oeso-

471 tracheal; B: brown; W: white; P: peritoneal; ... : not sampled

472

473

474

475

476

477

478

479

480

481

482

483 **Table 2: Merged pathology and microbial load data.**

		Day 14 p.i.			Day 28 p.i.				
Mice	Organ	culture	qPCR	pathology	Mice	Organ	culture	qPCR	pathology
#14	Lung	+	4.39/10 ⁴	yes	#19	Lung	+	1.08/10 ³	yes
#15		+	-	yes	#20		+	2.56/10 ⁴	yes
#14	Spleen	+	-	no	#19	Spleen	+	8.3/10 ⁵	no
#15		+	-	no	#20		+	3.3/10 ⁵	no
#14	Liver	-	\	no	#19	Liver	+	-	yes
#15		-	\	no	#20		-	\	no
#14	Kidneys	-	\	no	#19	Kidneys	-	\	no
#15		-	\	no	#20		-	\	no
#14	Brown Fat	-	\	no	#19	Brown Fat	-	\	no
#15		-	\	no	#20		-	\	no
#14	Axillary	-	\	no	#19	Axillary	+	-	no
#15	LN	+	-	no	#20	LN	+	-	no
#14	Cervical	+	-	no	#19	Cervical	+	-	no
#15	LN	+	-	no	#20	LN	+	1.8/10 ⁵	no

484

485

REVISED VERSION

486 **Figure legends:**

487 **Figure 1. Dot-plot representation of the burden of *M. canettii* organisms (number of**
488 **mycobacteria divided by the number of cells) in tissues growing *M. canettii*, as**
489 **extrapolated from real-time PCR calibration curves.**

490 **(A)** Results obtained in lymphoid tissues in *M. canettii*-challenged mice **(B)** Results of the
491 nonparametric Mann-Whitney rank-sum test to compare *M. canettii* burden in the lungs of
492 inoculated mice, through the 28-day experiment. A statistically significant increase in
493 bacterial load in infected lungs was noted throughout the 28-day experiment. Asterisk (*)
494 indicates statistical significance (* $P \leq 0.05$; ** $P \leq 0.01$).

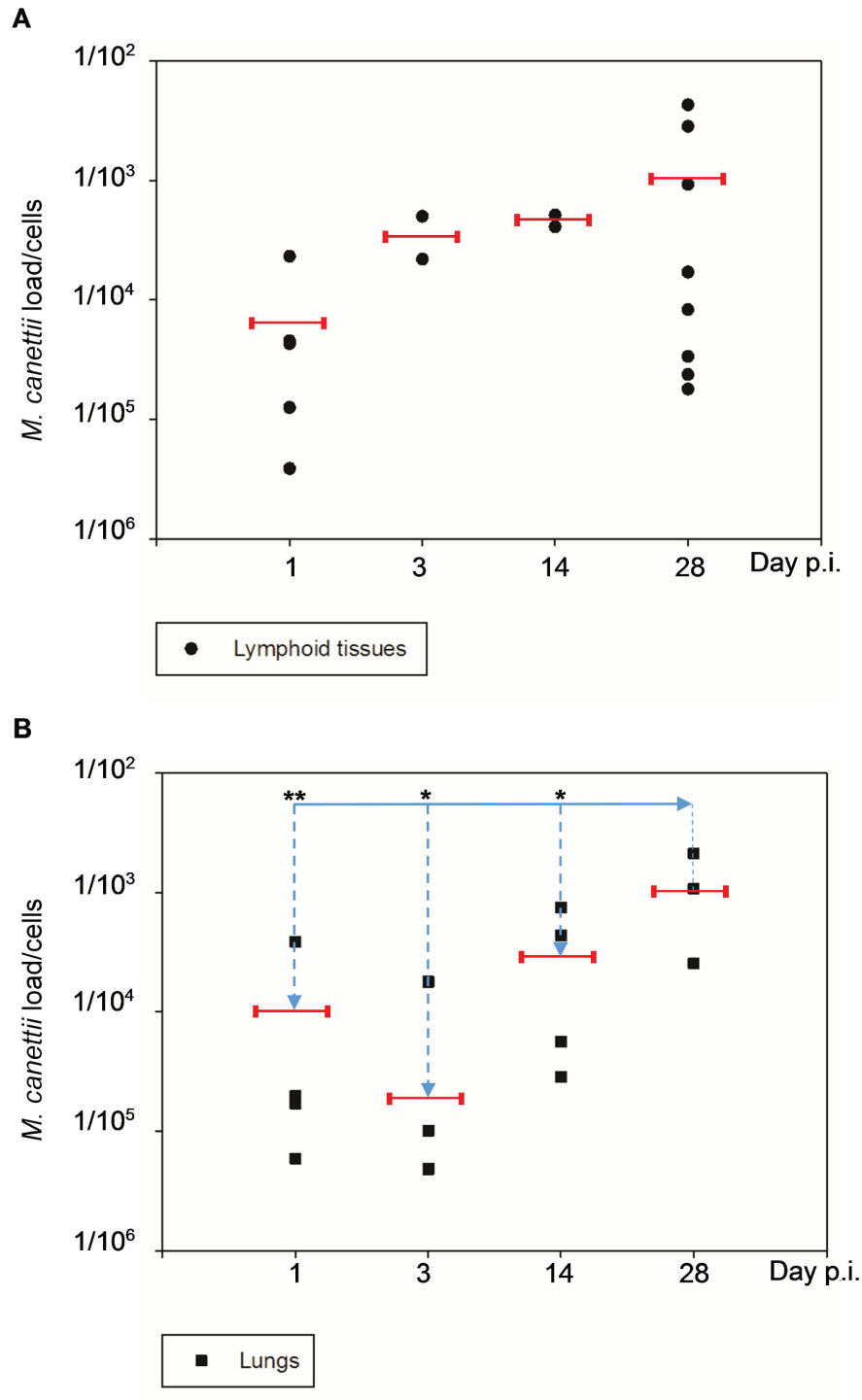
495 **Figure 2. Representative pathological findings from lungs and liver of *M. canettii*-**
496 **infected mice challenged at day 28 post-inoculation**

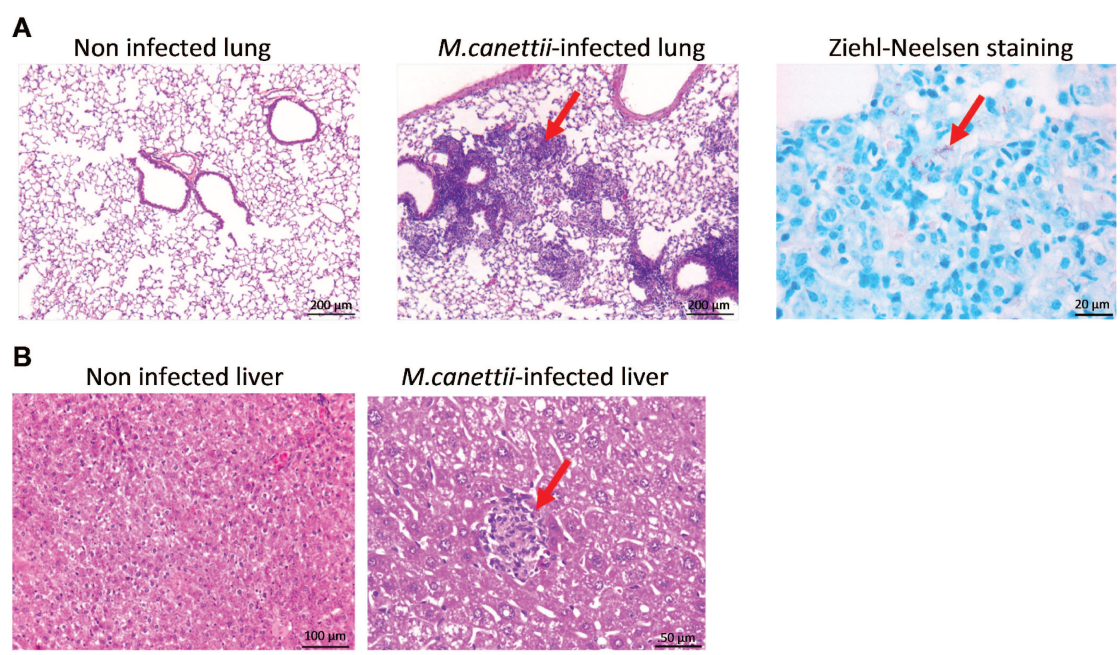
497 **A)** Photomicrographs after hematoxylin eosin staining of normal lungs from uninfected
498 mouse and *M. canettii*-infected lungs with clear alveolitis and granuloma-like lesions. Ziehl-
499 Neelsen staining showed a multibacillary status with intracellular organisms within cells with
500 macrophage morphology.

501 **B)** Photomicrographs of liver from *M. canettii*-infected mouse showed small granuloma-like
502 lesions while no lesions were observed in liver of control mice.

503

504





Supplementary Data

Supplementary Table 1: *M. canettii* load per cells

Sample	Day p.i.	<i>M. canettii</i> DNA copy	cells DNA copy	<i>M. canettii</i> load per cells	<i>M. canettii</i> load normalized per 10 ⁶ cells
MESENTERIC LYMPH NODES					
#1b	J1	4,64E+00	2,01E+04	2,31E-04	2,31E+02
#2b	J1	3,55E+00	9,20E+05	3,86E-06	3,86E+00
#3b	J1	2,46E+01	5,45E+05	4,51E-05	4,51E+01
#7b	J3	3,39E+00	6,77E+03	5,01E-04	5,01E+02
#8b	J3	6,61E+01	3,02E+05	2,19E-04	2,19E+02
LUNGS					
#1	J1	3,00E+02	7,70E+05	3,90E-04	3,90E+02
#2b	J1	1,69E+01	9,90E+05	1,71E-05	1,71E+01
#3b	J1	8,34E+00	1,41E+06	5,91E-06	5,91E+00
#4b	J1	1,61E+01	8,13E+05	1,98E-05	1,98E+01
#5	J3	1,54E+01	1,52E+06	1,01E-05	1,00E+01
#7	J3	1,46E+01	2,99E+06	4,88E-06	4,88E+00
#8	J3	1,47E+02	8,23E+05	1,79E-04	1,79E+02
#5b	J3	5,39E+00	1,12E+06	4,81E-06	4,81E+00
#11	J7	7,72E+02	7,51E+05	1,03E-03	1,03E+03
#13	J14	5,70E+02	7,60E+05	7,50E-04	7,50E+02
#15	J14	1,15E+03	2,62E+06	4,39E-04	4,39E+02
#16	J14	4,48E+01	7,94E+05	5,64E-05	5,64E+01
#14	J14	3,33E+01	1,16E+06	2,87E-05	2,87E+01
#17	J28	1,63E+03	7,70E+05	2,12E-03	2,12E+03
#19	J28	1,42E+03	1,32E+06	1,08E-03	1,08E+03
#20	J28	2,41E+02	9,43E+05	2,56E-04	2,56E+02
OESO-TRACHEAL LYMPH NODES					
#2b	J1	2,23E+01	5,19E+05	4,30E-05	4,30E+01
#14	J14	3,02E+02	7,36E+05	4,10E-04	4,10E+02
#17	J28	3,87E+03	9,03E+05	4,29E-03	4,29E+03
#19	J28	6,04E+02	6,52E+05	9,26E-04	9,26E+02
#20	J28	2,01E+03	7,10E+05	2,83E-03	2,83E+03
SPLEENS					
#3	J1	1,03E+01	8,23E+05	1,25E-05	1,25E+01
#17	J28	2,41E+01	1,02E+06	2,36E-05	2,36E+01
#19	J28	9,17E+01	1,11E+06	8,26E-05	8,26E+01

#20	J28	2,64E+01	7,89E+05	3,35E-05	3,35E+01
CERVICAL LYMPH NODES					
#10	J7	1	2,45E+05	4,08E-06	4,08E+00
#16	J14	4,54E+01	8,84E+04	5,14E-04	5,14E+02
#17	J28	4,48E+00	2,63E+04	1,70E-04	1,70E+02
#20	J28	1,51E+00	8,47E+04	1,78E-05	1,78E+01
LIVER					
#17	J28	1,31E+01	2,90E+05	4,52E-05	4,52E+01

Supplementary Table 2: Quantitative real-time PCR using *M. canettii* TbD1 system for pooled stools of *M. canettii* challenged mice

Stools (mg)	Day post-inoculation	<i>M. canettii</i> /100 mg stool
100	0	0
220	1	11
127	2	5.75
196	3	0
103	7	2.65
127	14	2.28
100	28	33

Supplementary Table 3: Quantitative real-time PCR using *M. canettii* TbD1 and HMBS gene systems to generate calibration curves

<i>M. canettii</i> DNA copy	Ct (TbD1)
10 ⁶	15.18 ± 0.18
10 ⁵	18,34 ± 0.23
10 ⁴	22,74 ± 0.13
10 ³	27,97 ± 0.4
10 ²	32,4 ± 0.16
10 ¹	35,25 ± 1.63
10 ⁰	37.01 ± 2.59

Mouse cell L929 DNA copy	Ct (HMBS)
10 ⁶	20,41 ± 0.04
10 ⁵	22,27 ± 0.3
10 ⁴	25,96 ± 0.33
10 ³	29,37 ± 1.02
10 ²	34,26 ± 0.54
10 ¹	38,36 ± 0.69
10 ⁰	0

CHAPITRE IV

Infection des tissus adipeux par *Mycobacterium canettii*

***Mycobacterium canettii* Infection of Adipose Tissues.**

Bouزيد F, Brégeon F, Poncin I, Weber P, Drancourt
M, Canaan S.

Front Cell Infect Microbiol. 2017.

7. CHAPITRE IV : Infection des tissus adipeux par *Mycobacterium canettii*

Bien que *M. tuberculosis* ait un tropisme particulier pour le poumon où il persiste dans les macrophages, il a été démontré que le tissu adipeux blanc pouvait être un réservoir permettant à *M. tuberculosis* de persister sous forme quiescente à l'intérieur des adipocytes matures (Neyrolles et al., 2006; Agarwal et al., 2014; Agarwal et al., 2016; Rastogi et al., 2016). Il existe chez les mammifères, deux types de tissus adipeux: le tissu adipeux blanc (WAT) et le tissu adipeux brun (BAT) qui diffèrent par leurs fonctions physiologiques, la morphologie des adipocytes les constituant et la distribution tissulaire (Gomez-Hernandez et al., 2016). Le WAT constitue la principale réserve d'énergie de l'organisme, tandis que le BAT assure la thermogénèse chez les animaux hibernant et les nouveau-nés (Cannon and Nedergaard, 2004; Gomez-Hernandez et al., 2016) et reste métaboliquement actif chez les adultes (Nedergaard et al., 2007).

Une seule étude a fait la part des deux types tissulaires et a démontré l'atteinte du WAT et BAT par *M. bovis* injecté par voie intraveineuse chez la souris (Mauss and Levy, 1972). De plus, il a été démontré que les dépôts de *M. bovis* surviennent dans le BAT avant le WAT (Mauss and Levy, 1972). Comme indiqué dans le chapitre précédent, nous avons été les premiers à explorer la dissémination de *M. canettii* après une inoculation oro-gastrique de souris (Bouzid et al., 2017b). Dans ce cadre, nous avons également montré la dissémination de *M. canettii* uniquement dans le tissu adipeux brun chez deux souris sacrifiées à J3 et J28 p.i. (Bouzid et al., 2017b). Afin de mieux comprendre les interactions de *M. canettii* avec les tissus adipeux naturels, nous avons développé des modèles cellulaires expérimentaux basés sur l'extraction et la culture primaire des pré-adipocytes blancs et bruns à partir de tissus adipeux murins. Et pour compléter notre travail, nous avons étudié les interactions de *M. canettii* vs *M. tuberculosis* avec les pré-adipocytes et adipocytes matures de la lignée

cellulaire murine 3T3-L1 ainsi que leur capacité à accumuler des lipides à partir de l'hôte et à survivre dans cet environnement.

Brièvement, les cellules ont été infectées pendant 4 heures avec soit *M. canetti* soit *M. tuberculosis*. Les mycobactéries extracellulaires ont été éliminées par des lavages intensifs et/ou traitement par l'amikacine. Un suivi du comportement intracellulaire des mycobactéries a alors été réalisé par différentes observations microscopiques (microscopie confocale et microscopie électronique) et par la détermination des unités formant des colonies (UFCs). Dans les pré-adipocytes primaires, les deux mycobactéries ont pu infecter 18 à 22% de cellules et ont présenté une réplication continue au sein de ces cellules pendant 7 jours d'expérimentation. L'analyse des données microscopiques ne révèle aucune différence significative entre le ratio d'infection des pré-adipocytes blancs ou bruns par les deux mycobactéries ($P = 0.47$ pour *M. Canettii* et $P = 0.33$ pour *M. tuberculosis*). En revanche, le nombre de mycobactéries intracellulaires était significativement supérieur dans les pré-adipocytes bruns comparé aux pré-adipocytes blancs ($P = 0.02$ pour *M. canettii* et $P = 0.03$ pour *M. tuberculosis*).

Les adipocytes matures 3T3-L1 ont été infectés par des souches fluorescentes de *M. canettii* CIPT 140010059 ; souche sauvage que nous avons transformée par un vecteur d'expression constitutif contenant un gène codant pour le fluorophore mCherry et qui a été déposée dans la collection de souches CSUR (n°P3621). Cette souche nous a permis de confirmer la localisation intracellulaire de *M. canettii*. Au cours de ces expériences, nous avons également constaté que 30% des mycobactéries intracellulaires étaient en contact avec les corps lipidiques des adipocytes matures. Ces mêmes observations ont été confirmées par microscopie électronique et ont permis de montrer pour la première fois que *M. canettii* était capable d'accumuler des lipides sous formes d'inclusions lipidiques intra-cytosoliques. Cependant, *M. canettii* était capable d'infecter seulement 9% des adipocytes matures vs

17% avec *M. tuberculosis* ($p = 0,001$). De manière intéressante, nous avons mis en évidence un comportement intracellulaire différentiel entre *M. canettii* et *M. tuberculosis* : *M. canettii* continue à se répliquer dans ces cellules jusqu'au jour 12 p.i. alors que *M. tuberculosis* arrête sa réplication à partir du jour 3 p.i. Nous avons également démontré pour la première fois que *M. canettii* avait la capacité d'accumuler des lipides sous forme d'inclusions lipidiques intracytosoliques à partir des adipocytes matures, sans pour autant présenter de signes de persistance ou de dormance comme dans le cas de *M. tuberculosis*.

En conclusion, ces résultats indiquent que les pré-adipocytes bruns pourraient constituer une cible potentielle des mycobactéries du complexe *M. tuberculosis* ; ils illustrent un comportement différentiel entre *M. canettii* et *M. tuberculosis* dans le même contexte d'infection cellulaire et guident les investigations sur le réservoir de *M. canettii* dans le tissu adipeux brun des mammifères.



Mycobacterium canettii Infection of Adipose Tissues

Fériel Bouzid^{1,2}, Fabienne Brégeon^{2,3}, Isabelle Poncin¹, Pascal Weber², Michel Drancourt² and Stéphane Canaan^{1*}

¹ Aix-Marseille Université, CNRS, EPL IMM FR3479, Marseille, France, ² Aix Marseille Université, URMITE, UMR CNRS 7278, IRD 198, INSERM 1095, IHU Méditerranée Infection, Marseille, France, ³ Service des Explorations Fonctionnelles Respiratoires, Centre Hospitalo-Universitaire Nord, Pôle Cardio-Vasculaire et Thoracique, Assistance Publique Hôpitaux de Marseille, Marseille, France

Adipose tissues were shown to host *Mycobacterium tuberculosis* which is persisting inside mature adipocytes. It remains unknown whether this holds true for *Mycobacterium canettii*, a rare representative of the *M. tuberculosis* complex responsible for lymphatic and pulmonary tuberculosis. Here, we infected primary murine white and brown pre-adipocytes and murine 3T3-L1 pre-adipocytes and mature adipocytes with *M. canettii* and *M. tuberculosis* as a positive control. Both mycobacteria were able to infect 18–22% of challenged primary murine pre-adipocytes; and to replicate within these cells during a 7-day experiment with the intracellular inoculums being significantly higher in brown than in white pre-adipocytes for *M. canettii* ($p = 0.02$) and *M. tuberculosis* ($p = 0.03$). Further *in-vitro* infection of 3T3-L1 mature adipocytes yielded 9% of infected cells by *M. canettii* and 17% of infected cells by *M. tuberculosis* ($p = 0.001$). Interestingly, *M. canettii* replicated and accumulated intra-cytosolic lipid inclusions within mature adipocytes over a 12-day experiment; while *M. tuberculosis* stopped replicating at day 3 post-infection. These results indicate that brown pre-adipocytes could be one of the potential targets for *M. tuberculosis* complex mycobacteria; and illustrate differential outcome of *M. tuberculosis* complex mycobacteria into adipose tissues. While white adipose tissue is an unlikely sanctuary for *M. canettii*, it is still an open question whether *M. canettii* and *M. tuberculosis* could persist in brown adipose tissues.

Keywords: tuberculosis, *Mycobacterium canettii*, *Mycobacterium tuberculosis*, adipose tissues, adipocyte

OPEN ACCESS

Edited by:

Anthony Baughn,
University of Minnesota, United States

Reviewed by:

Siouxie Wiles,
University of Auckland, New Zealand
Brian Weinrick,
Albert Einstein College of Medicine,
United States

Murugesan V. S. Rajaram,
Ohio State University at Columbus,
United States

*Correspondence:

Stéphane Canaan
stephane.canaan@imm.cnrs.fr

Received: 23 February 2017

Accepted: 02 May 2017

Published: 17 May 2017

Citation:

Bouzid F, Brégeon F, Poncin I, Weber P, Drancourt M and Canaan S (2017) *Mycobacterium canettii* Infection of Adipose Tissues. *Front. Cell. Infect. Microbiol.* 7:189. doi: 10.3389/fcimb.2017.00189

INTRODUCTION

In mammals, brown adipose tissue (BAT) and white adipose tissue (WAT) are mainly composed of mature adipocytes, pre-adipocytes and immune cells (Ouchi et al., 2011). WAT and BAT differ in cell morphology, tissue distribution and physiological functions (Gomez-Hernandez et al., 2016): WAT constitutes the main energy reserve of the organism while BAT ensures thermogenesis in hibernating animals and newborns (Cannon and Nedergaard, 2004; Gomez-Hernandez et al., 2016) and remains metabolically active in adults (Nedergaard et al., 2007).

Adipose tissues have been previously supposed to act as long-term sanctuaries sheltering *Mycobacterium tuberculosis*, the major agent of human tuberculosis worldwide (Neyrolles et al., 2006; Kim et al., 2011; Agarwal et al., 2014, 2016; Rastogi et al., 2016). *In vitro* experiments were conducted using murine 3T3-L1 mature adipocytes (Neyrolles et al., 2006; Kim et al., 2011; Rastogi et al., 2016), and 3T3-L1 pre-adipocytes (Neyrolles et al., 2006), but also with murine

primary pre-adipocytes and mature adipocytes obtained from WAT (Agarwal et al., 2014). In immune-competent mice, intravenously and intra-nasally inoculated *M. tuberculosis* disseminates in WAT of visceral, subcutaneous, peri-renal and mesenteric adipose depots (Agarwal et al., 2014, 2016). In these models, the burden of *M. tuberculosis* in WAT depots stagnated or decreased with time (Agarwal et al., 2014). Indeed, compelling data show that *M. tuberculosis* adopts in mature adipocytes and WAT a non-replicating, dormant state characterized by an arrest of multiplication, accumulation of intra-cytosolic lipid inclusions (ILIs), resistance to anti-mycobacterial drugs (Neyrolles et al., 2006; Agarwal et al., 2014) and up-regulation of *dosR* and *icl* genes (Rastogi et al., 2016). The infection of mature adipocytes was therefore proposed as a suitable model to study the accumulation of neutral lipids into ILIs within mycobacteria (Santucci et al., 2016).

Among the *M. tuberculosis* complex (MTBC), *Mycobacterium canettii* is a peculiar member specifically diagnosed in dozens of tuberculosis patients with reported contacts to the Horn of Africa (Aboubaker Osman et al., 2015). *M. canettii* differs from the other members of the MTBC by possessing a larger 4.48 ± 0.05 Mb mosaic genome and producing cordless and smooth-looking mycobacteria (Gutierrez et al., 2005; Koeck et al., 2011; Supply et al., 2013; Boritsch et al., 2016a) with an ability of intra-species horizontal gene transfer (Boritsch et al., 2016b). *M. canettii* infection mainly presents as lymph node and pulmonary tuberculosis (Koeck et al., 2011; Aboubaker Osman et al., 2015). However, *M. canettii* pulmonary tuberculosis is unique in being seemingly non-contagious (Koeck et al., 2011).

In order to further examine the *in-vitro* interactions of *M. canettii* with natural adipose tissues, we developed *in-vitro* experimental models using primary murine white and brown pre-adipocytes; and further investigated the interactions between *M. canettii* and murine 3T3-L1 pre-adipocytes and mature adipocytes using *M. tuberculosis* H37Rv as a positive control.

MATERIALS AND METHODS

Mycobacteria

M. tuberculosis H37Rv and *M. canettii* CIPT 140010059 were used in this study. Mycobacteria were cultivated in Middelbrook 7H10 (Becton Dickinson, Le Pont de Claix, France) supplemented with 10% oleic acid-albumin-dextrose-catalase (OADC) (Becton Dickinson). Fluorescent *M. canettii* CIPT 140010059 mCherry (CSURP3621) was constructed by transforming the pMV261 mCherry vector (gift from L. Kremer, CPBS, Montpellier, France) into the *M. canettii* strain (Alibaud et al., 2011). Fluorescent strains were cultured in Middlebrook 7H10 broth supplemented with 10% OADC and 50 $\mu\text{g}/\text{mL}$ kanamycin (Sigma). Prior to infection, mycobacteria were resuspended in phosphate buffered saline (PBS), shaken on a vortex mixer for 10 min with glass ball to disperse clumps and centrifuged for 1 min at 300 g to remove residual clumps. The supernatant was then dispersed by expelling the suspension 10 times through a sterile 25-gauge needle attached to a 1-mL syringe. Calibration was then performed according to McFarland standard confirmed

by counting mycobacteria after Ziehl-Neelsen staining (RAL diagnostics, Martillac, France). All experiments using these mycobacteria were performed in a biosafety level 3 laboratory of the Faculté de Médecine, Aix-Marseille Université, France.

Primary Murine Pre-adipocyte Culture

The experiments conducted on mice was approved by the Institutional Animal Care and Use Committee of Aix-Marseille University "C2EA-14," France and registered by the "Ministère de l'Enseignement Supérieur et de la Recherche" under reference n° 2015092415474605. Mice were handled according to the rules of Décret N° 2013-118, Février 7, 2013, France. Inguinal WAT and inter-scapular BAT were collected from ten 6-week-old Balb/cByj mice. Pre-adipocytes cells were isolated from tissues as described elsewhere (Aune et al., 2013) and then cultured in complete culture medium Dulbecco's Modified Eagle Medium DMEM/F12 (Invitrogen, France) supplemented with 10% heat-inactivated fetal bovine serum (FBS) and were plated at a concentration of 5×10^4 cells/ml/well in 12-well plates and incubated at 37°C under a 5% CO₂ atmosphere.

3T3-L1 Cell Lines

Murine embryonic fibroblasts 3T3-L1 (ATCC, lot 62158491) were cultured in DMEM (Invitrogen, France) supplemented with 10% heat-inactivated FBS at 37°C under a 5% CO₂ atmosphere. Prior to confluence, cells were plated at 5×10^4 cells/well in a 12-well sterile plates and incubated as described above. Six days after plating, pre-adipocytes reach confluency and stop dividing. Adipocyte differentiation was initiated upon confluency by adding 1 $\mu\text{g}/\text{mL}$ insulin (Sigma), 0.5 mM isobutyl-methylxanthine (Sigma), and 1 μM dexamethasone (sigma) into the culture medium. After 48 h of induction, the medium was replaced by DMEM-10% FBS containing 1 $\mu\text{g}/\text{mL}$ of insulin and maintained each 2 days in order to achieve a full differentiation as previously described (Neyrolles et al., 2006). Adipocyte differentiation was checked by BODIPY 493/503 staining (Sigma) of lipid droplets over the 2-week experiments.

Infection

Pre-adipocytes and mature adipocytes were infected with a multiplicity of infection (MOI) of 1 per cell at day 6 after plating and at day 10 post-induction respectively. Accordingly, 1×10^5 cells per well were infected with 1×10^5 mycobacteria. After 4-h incubation, cells were washed 3 times with serum-free DMEM to remove all extracellular bacteria. Only mature adipocytes were then incubated with 200 $\mu\text{g}/\text{mL}$ amikacin for 2 h and then washed thrice. The last wash was plated to validate the correct elimination of extracellular mycobacteria. The inoculated cultures were incubated with fresh complete medium up to 7 days for primary cultures and 12 days for 3T3-L1 cell lines at 37°C under a 5% CO₂ atmosphere. At various time points, infected cells were lysed in PBS containing 0.1% Triton X-100 and the lysate was plated at 10-fold dilutions from 10^{-1} to 10^{-4} onto Middlebrook 7H10 agar plates incubated at 37°C under a 5% CO₂ atmosphere. The

number of colonies enumerated after 20-day of incubation was used to estimate the number of colony-forming units (CFUs) per 10^5 cells. All experiments were conducted in triplicate: three independent plates the same day for primary cell infection experiments and three replicates at different days with different bacterial cultures for 3T3-L1 cells infection experiments.

Intracellular Localization of Mycobacteria

Ziehl-Neelsen staining (RAL diagnostics, Martillac, France) was performed on infected cells (MOI 1:1 and 5:1) at day 3 p.i. Observations were acquired using the slide scanner Axio Scan.Z1 (Zeiss) (Magnification 20X) with a color Hitachi tri-CCD (1,800 × 1,200 pixels) camera. The number of intracellular mycobacteria per one cell was recorded on image acquisition by ImageJ software.

M. canettii mCherry was used to localize intracellular bacteria using confocal microscopy. Infected adipocytes (MOI 10) were fixed using 4% formaldehyde at day 3 p.i. Lipid droplets were stained with BODIPY 493/503 (Sigma). The images were acquired using a confocal microscope (Zeiss, Spinning disk with a Yokogawa head and an emCCD camera 512 × 512 pixels) at magnification 63X/1.4 oil objective.

Processing for Electron Microscopy

Cells were fixed at room temperature with 2.5% glutaraldehyde in Na-cacodylate buffer 0.1 M (pH 7.2) containing 0.1 M sucrose, 5 mM CaCl_2 , and MgCl_2 5 mM, washed with complete cacodylate buffer and postfixed for 1 h at room temperature with 1% osmium tetroxide in the same buffer without sucrose (de Chastellier, 2008). They were washed with buffer, scratched gently, concentrated in agar up to 2% with cacodylate buffer and processed for 1 h at room temperature with 1% uranyl acetate in maleate buffer. The samples were dehydrated in a graded series of ethanol solutions and gradually incorporated in Spurr resin. Thin sections (80 nm thick) were stained with 1% uranyl acetate in distilled water and then with lead citrate before being observed by electron microscopy.

Nile Red Staining

Adipocytes were infected with *M. canettii* at MOI 5:1 on 12-well plate. At day 7 p.i. all wells were lysed in 500 μL water containing 0.1% Triton X-100. The pooled lysate was sonicated and centrifuged at 9,000 g for 25 min. The *M. canettii* cells were washed thrice with 0.1% Triton X-100 and the pellet was resuspended in 500 μL of PBS containing 0.05% Tween 80. Nile red staining was performed as previously described (Christensen et al., 1999). The stained smears were subjected to high resolution confocal (Zeiss AiryScan head, magnification 63X, Numerical aperture = 1.4), with higher resolution (1.6X) than conventional confocal.

Lactate Dehydrogenase (LDH) Assay

LDH, a soluble cytoplasmic enzyme released into extracellular space when the cell membrane is damaged, was used as an estimator of cell lysis (Korzeniewski and Callewaert, 1983). Culture supernatants of uninfected or infected mature adipocytes

with *M. canettii* or *M. tuberculosis* (MOI 1) were collected at day 3, 7, and 12 post-inoculation. The release of LDH from negative controls and infected cells was measured spectrophotometrically at 340 nm on a Cobas 8000 (Roche, Meylan, France).

Statistical Analyses

Statistics were performed using the SigmaPlot13 software. The distribution of the variables was assessed statistically with the Shapiro-Wilk test. The equality of the variance was checked using the Brown-Forsythe test. All data were normally distributed and were expressed using means \pm standard deviation. The statistical significance was performed using the Student *T*-test. The Chi-square test was used to compare rates and proportions with Yates correction. A $p < 0.05$ was regarded as significant.

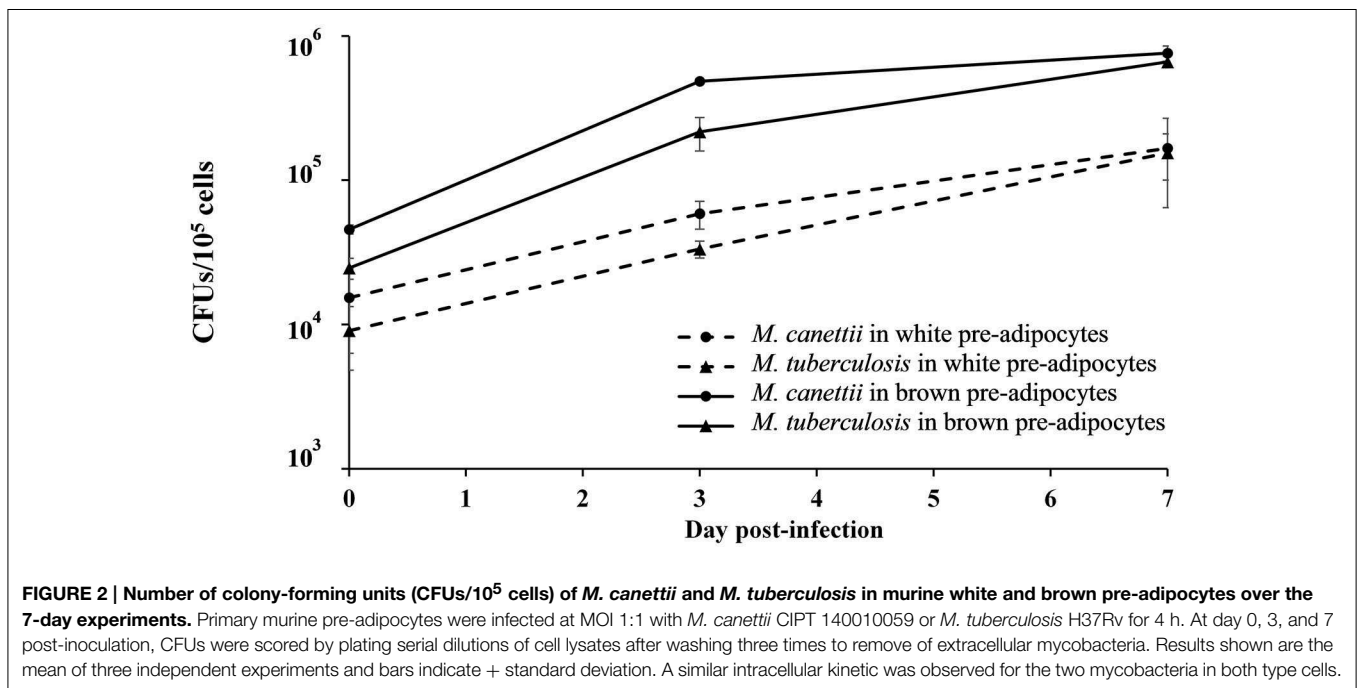
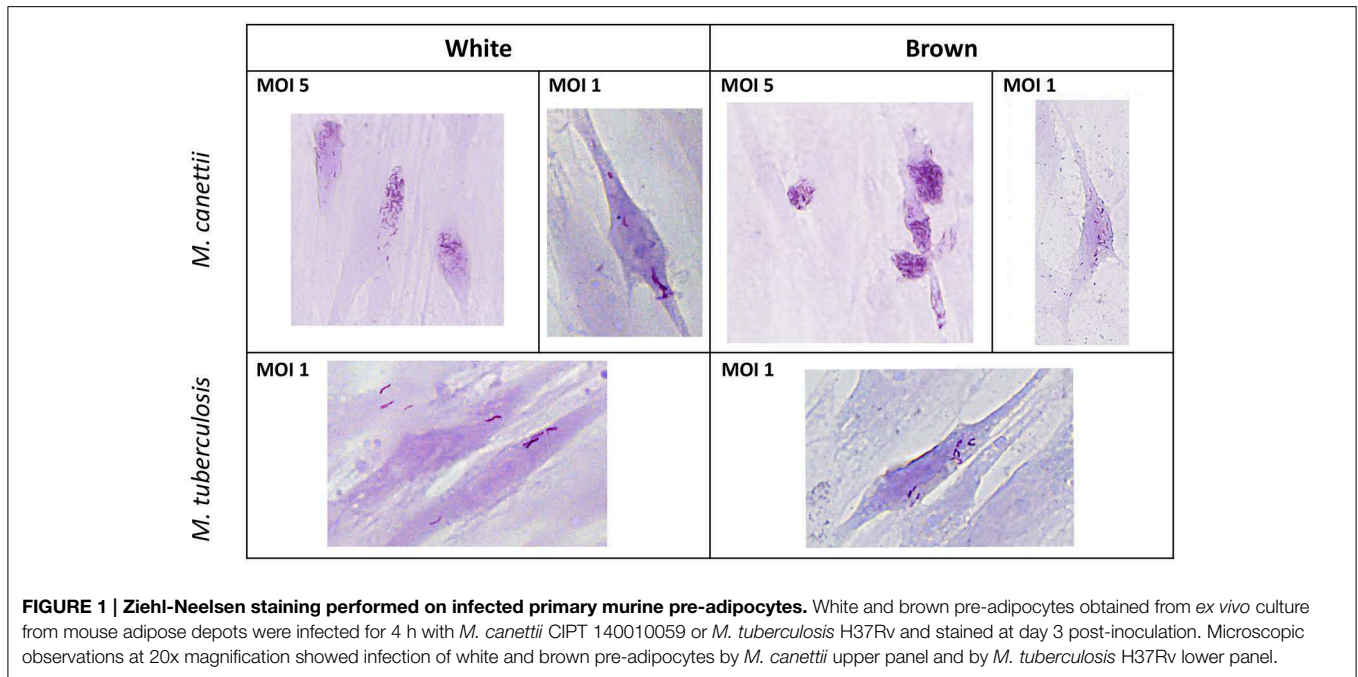
RESULTS

M. canettii and *M. tuberculosis* within Primary Murine Pre-adipocytes

Pre-adipocytes purified from murine inguinal WAT and interscapular BAT were *ex vivo* inoculated with *M. canettii* or *M. tuberculosis* for 4 h p.i. For all experiments, extracellular mycobacteria were removed by extensive washing with serum-free medium, 4 h p.i. At day 3 p.i. Ziehl-Neelsen staining was performed to assess the ability of mycobacteria to infect primary murine pre-adipocytes. While negative control cells remained free of detectable mycobacteria, microscopic observations clearly showed intracellular *M. canettii* and *M. tuberculosis* in white and brown pre-adipocytes (Figure 1).

The ratio of infected cells relative to the total number of observed cells as well as the average number of intracellular bacilli per one cell were measured on a random selection of 10 microscope fields on stained infected cells at day 3 p.i. (see Supplementary Data S1). White pre-adipocytes infected at MOI 1:1 yielded 19% and 18% of infected cells with 9 ± 6 *M. canettii* bacilli per cell and 7 ± 5 *M. tuberculosis* organisms per cell, respectively. Likewise, 22 and 19% of brown pre-adipocytes were infected with 16 ± 7 *M. canettii* organisms/cell and 11 ± 4 *M. tuberculosis* organisms/cell, respectively. The ratio of infection did not significantly differ between brown and white pre-adipocytes ($p = 0.7$ for *M. canettii* and $p = 0.8$ for *M. tuberculosis*, χ^2 test) but the number of bacilli in brown pre-adipocytes was significantly higher than in white pre-adipocytes ($p = 0.02$ for *M. canettii* and $p = 0.03$ for *M. tuberculosis*).

In order to confirm these observations and to study the viability of bacilli into the infected cells, the number of intracellular mycobacteria was quantified by scoring CFUs/ 10^5 cells after plating infected cell lysates with *M. canettii* or *M. tuberculosis* at MOI 1:1 at different time intervals (Figure 2) (see Supplementary Data S1). At day 0, white pre-adipocytes had internalized 15% ($1.5 \times 10^4 \pm 9 \times 10^3$ CFUs) and 10% ($9 \times 10^3 \pm 4 \times 10^3$ CFUs) of the initial 1×10^5 inoculum of *M. canettii* and *M. tuberculosis*, respectively. As for brown pre-adipocytes, 45% ($4.5 \times 10^4 \pm 2.3 \times 10^3$ CFUs) of the *M. canettii* inoculum and 25% ($2.47 \times 10^4 \pm 4 \times 10^3$ CFUs) of the *M. tuberculosis* inoculum was phagocytized. By scoring



CFUs, intracellular *M. canettii* and *M. tuberculosis* organisms were more abundant in primary brown pre-adipocytes than in white pre-adipocytes ($p = 0.01$ for *M. canettii* and $p = 0.008$ for *M. tuberculosis*) which is consistent with our microscopic observations.

A similar intracellular behavior was observed for *M. canettii* and *M. tuberculosis* during the 7-day experiment in primary white and brown pre-adipocytes: both mycobacteria survived and multiplied with approximately one log gain.

Interactions between *M. canettii* and 3T3-L1 Pre-adipocytes and Mature Adipocytes

M. canettii Is Internalized into 3T3-L1 Pre-adipocytes and Mature Adipocytes

To explore *M. canettii* interactions with 3T3-L1 pre-adipocytes and mature adipocytes compare to *M. tuberculosis* (Neyrolles et al., 2006; Kim et al., 2011), the quantification of the ratio

of infected cells/total cells and the number of intracellular bacilli/cell were performed on a random selection of 10 microscope fields after Ziehl-Neelsen staining of infected cells at day 3 p.i. (see Supplementary Data S1). For pre-adipocytes, 20% of cells were infected with 7 ± 5 *M. canettii* organisms/cell while 40% of cells were infected with 12 ± 6 *M. tuberculosis* organisms/cell which is significantly higher compared to *M. canettii* infection ($p < 0.001$, χ^2 test). Under the same conditions, only 9% and 17% of adipocytes were infected with *M. canettii* and *M. tuberculosis*, respectively. The ratio of infected cells was significantly higher for pre-adipocytes compared to mature adipocytes ($p = 0.002$ for *M. canettii* and $p < 0.001$ for *M. tuberculosis*, χ^2 test).

To confirm the intracellular location of *M. canettii* within 3T3-L1 mature adipocytes, cells were inoculated with *M. canettii* CIPT 140010059 mCherry (CSURP3621) at MOI = 10. Three days p.i. infected cells were treated with BODIPY 493/503 stain and fixed. Confocal microscopy observations showed the presence of 15 ± 6 intracellular *M. canettii* inside adipocytes, as compared to negative controls which remained free of detectable mCherry-fluorescence (Figure 3A). We noticed that approximately 30% of intracellular *M. canettii* organisms were localized in close contacts with cytoplasmic lipid bodies (LBs) in 100% of the observed adipocytes (Figure 3A white squares).

Further electron microscopy observation of adipocytes infected at a MOI 5:1 for 3 days demonstrated the presence of *M. canettii* within adipocytes in close contact with adipocyte LBs, corroborating observations performed by confocal microscopy (Figure 3B, upper panel). Intracellular *M. canettii* bacilli were loaded with small electron-dense vesicles resembling ILIs (Figure 3B, upper panel). We also found that some pre-adipocytes that failed to reach full differentiation were infected by *M. canettii* which had weakly accumulated ILIs (Figure 3B, lower panel).

Intracellular Outcome of Internalized *M. canettii*

Using the 3T3-L1 continuous cell line which is more robust and easier to manipulate than primary cells, it was possible to compare the successive steps of infection over 12 days in three independent experiments conducted at different days, comparing pre-adipocytes and mature adipocytes. After thorough dispersal of the mycobacterial aggregate, cells were infected with *M. tuberculosis*, used as positive control, or *M. canettii* at a MOI 1:1 for 4 h followed by extensive elimination of extracellular mycobacteria. All results were compared with non-infected cells manipulated in parallel, which remained negative in culture during the 12-day experiment. At various time points 0, 3, 7, and 12 days p.i. cells were lysed and viable bacterial content was measured by plating cell lysates onto Middelbrook agar 7H10 and scoring CFUs/ 10^5 cells (Figure 4) (see Supplementary Data S1).

As for internalization, at day 0, pre-adipocytes contained 25% of the initial *M. canettii* inoculum ($2.5 \times 10^4 \pm 5 \times 10^3$ CFUs) and 50% of the initial *M. tuberculosis* inoculum ($5 \times 10^4 \pm 8 \times 10^3$ CFUs). In mature adipocyte infection experiments, 12% ($1.2 \times 10^4 \pm 4 \times 10^3$ CFUs) of the infecting *M. canettii* inoculum and 37% of the infecting *M. tuberculosis* inoculum ($3.7 \times 10^4 \pm 4 \times 10^3$ CFUs) was internalized. Initial infection of mature adipocytes

was significantly lower with *M. canettii* ($p = 0.001$) than with *M. tuberculosis*, as observed with infected pre-adipocytes ($p = 0.006$), but numbers of intracellular mycobacteria from day 0 were significantly higher in pre-adipocytes than in mature adipocytes ($p = 0.01$ for *M. canettii* and $p = 0.03$ for *M. tuberculosis*).

As for intracellular behavior, both mycobacteria continuously replicated into pre-adipocytes during the 12-day experiment and gained two logs between day 0 and day 12 (Figure 4). In mature adipocytes, *M. tuberculosis* and *M. canettii* showed two different kinetics: intracellular *M. tuberculosis* inoculum stabilized between day 3 and 12 p.i. (4 ± 3.66 CFUs gain), whereas *M. canettii* replicated with a $2 \times 10^1 \pm 2.5 \times 10^1$ CFUs gain between day 3 and 12 p.i. which is significantly higher than *M. tuberculosis* ($p = 0.01$) (Figure 4) but this load remains lower than in pre-adipocytes (Figure 4).

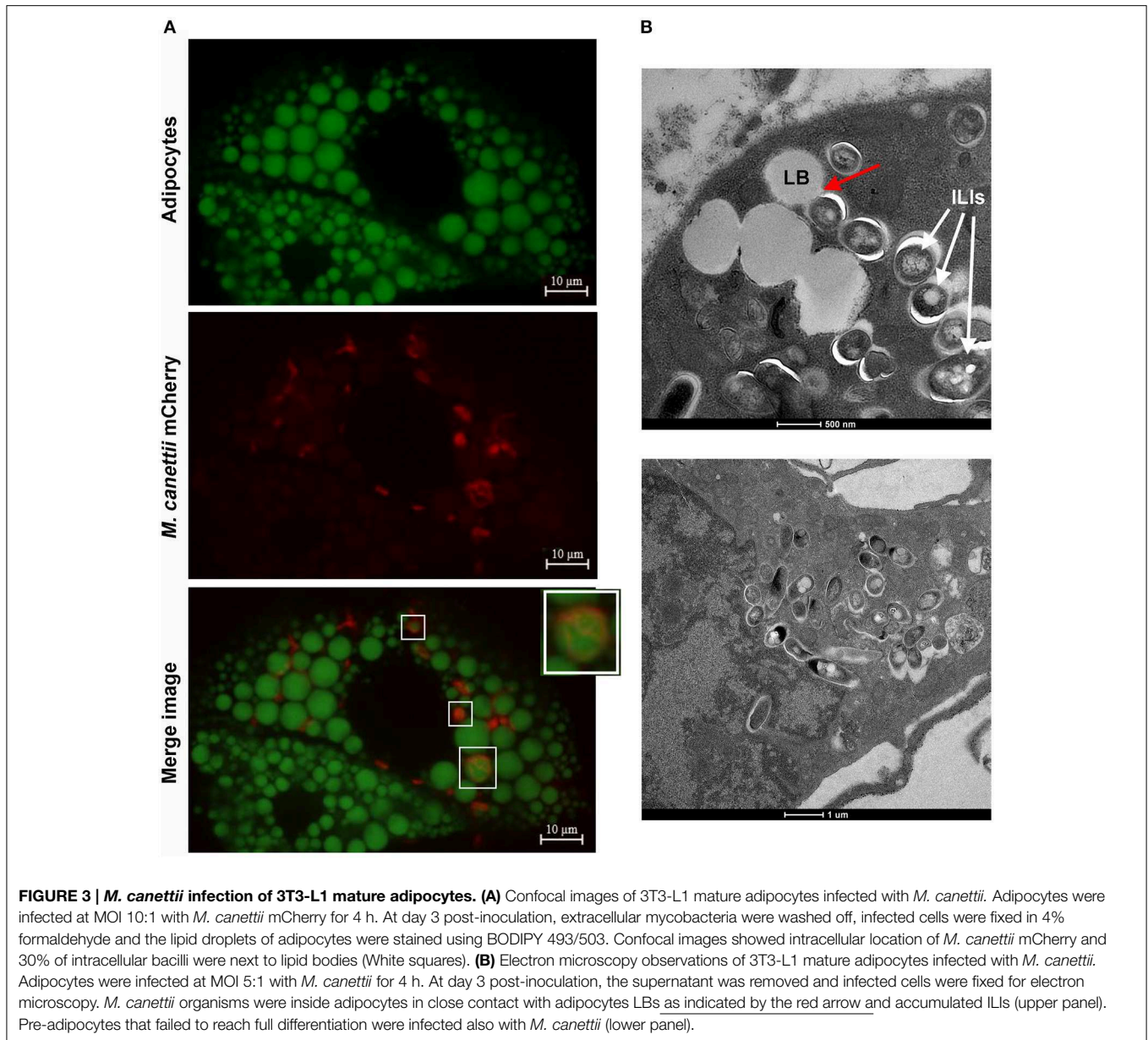
The arrest of *M. tuberculosis*'s replication inside adipocytes has been correlated with a heavy accumulation of ILIs leading to a dormant state (Neyrolles et al., 2006; Kim et al., 2011; Agarwal et al., 2014). To investigate whether this holds true for *M. canettii*, intra-adipocyte bacilli were extracted at day 7 p.i. after Triton X-100 cell lysis and sonication. While Middlebrook 7H10 agar-grown *M. canettii* were free of detectable ILIs, Nile-red staining showed that intracellular *M. canettii* yielded ILIs (Figure 5). Intracellular *M. canettii* presented variable numbers of small ILIs corresponding to 60% ILI⁺¹ and 40% ILI⁺² profiles which were previously described (Caire-Brandli et al., 2014).

Intracellular *M. canettii* Induce Mature Adipocyte Cytolysis

Microscopic examination indicated that *M. canettii* infection yielded no cytolysis on mature 3T3-L1 adipocytes up to day 7 p.i. but cellular debris were observed at day 12 p.i. while a smaller amount of cellular debris was observed in uninfected control cells. Microscopic observation of *M. tuberculosis*-infected cells clearly showed cellular debris at day 7 p.i. A cytolytic effect of mycobacteria was further investigated by measuring the lactate-dehydrogenase (LDH) in the supernatant of infected and non-infected control adipocytes (see Supplementary Data S1). We observed a progressive increase of the LDH concentration in the three culture supernatants. However, the increase of LDH concentration was significantly higher in *M. canettii*-infected adipocytes than in negative control adipocytes at day 3 p.i. ($p = 0.002$) and day 12 p.i. ($p < 0.001$) (Figure 6). In *M. tuberculosis*-infected cells, high rates of LDH concentration measured throughout the 12-day experiment were significantly higher compared to uninfected cells and *M. canettii* infected cells at each time point (Figure 6). Positive and high correlation was noted between the rates of LDH release and the count of CFUs in the case of *M. canettii* and *M. tuberculosis* infection ($r = 0.90$ for *M. canettii* and $r = 0.88$ for *M. tuberculosis*).

DISCUSSION

Data here reported indicate that *M. canettii* is able to infect, survive and replicate in primary murine white and brown pre-adipocytes which are constantly detected in adipose tissues



(Cawthorn et al., 2012) and 3T3-L1 pre-adipocytes and mature adipocytes after *in-vitro* and *ex-vivo* experimental infection. Differentiation of 3T3-L1 cells was induced so as to obtain *in vitro* model of mature white adipocytes (Morrison and McGee, 2015). Data were authenticated by their reproducibility over a triplicate experiment in the presence of negative controls. All experiments with *M. tuberculosis*, here used as a positive control, were in agreement with those previously reported (Neyrolles et al., 2006; Kim et al., 2011; Agarwal et al., 2014). We extended for the first time these observations to brown pre-adipocytes.

Mature adipocytes were infected by *M. canettii* at a lower infectivity than *M. tuberculosis* (Neyrolles et al., 2006; Kim et al., 2011). *M. tuberculosis* binds to adipocytes through scavenger receptors (Neyrolles et al., 2006) but assessing whether this also

holds true for *M. canettii* was beyond the scope of our study. Further, *M. tuberculosis* stopped replicating in mature adipocytes in agreement with its previously demonstrated dormant state inside mature adipocytes (Neyrolles et al., 2006; Kim et al., 2011; Agarwal et al., 2014; Rastogi et al., 2016). Unexpectedly, *M. canettii* continuously replicated and accumulated small ILIs. ILIs, previously reported in *M. tuberculosis* (McKinney et al., 2000; Daniel et al., 2004; Deb et al., 2006; Peyron et al., 2008; Russell et al., 2009), *M. bovis* BCG (Low et al., 2009, 2010), *M. leprae* (Mattos et al., 2010, 2011) and *M. smegmatis* (Garton et al., 2002; Dhoubib et al., 2011) are here observed for the first time in *M. canettii*. Accordingly, the ILI⁺/ILI²⁺ and not ILI³⁺ profiles of intracellular *M. canettii* agree with its replicating-state (Caire-Brandli et al., 2014). However, the experimental model used here

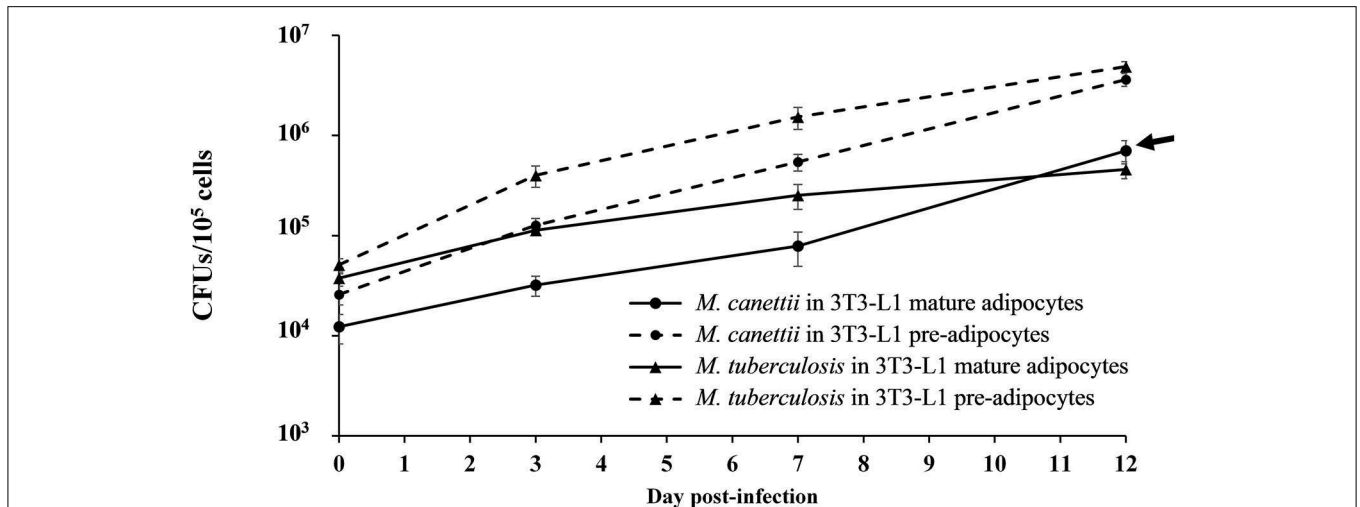


FIGURE 4 | Intracellular kinetic of *M. canettii* CIPT 140010059 and *M. tuberculosis* H37Rv in 3T3-L1 pre-adipocytes and adipocytes during 12-day experiments. Cells were infected at MOI 1:1 with *M. canettii* or *M. tuberculosis* for 4 h. The number of bacterial colony forming units (CFU) was determined at the indicated time points (0, 3, 7, and 12 day p.i.). A similar intracellular kinetic was observed for *M. canettii* and *M. tuberculosis* inside pre-adipocytes. However, in mature adipocytes *M. tuberculosis* stopped its replication between day 3 and 12 day p.i. while *M. canettii* continued to replicate (arrow). Data shown are the mean \pm standard deviation of three independent experiments.

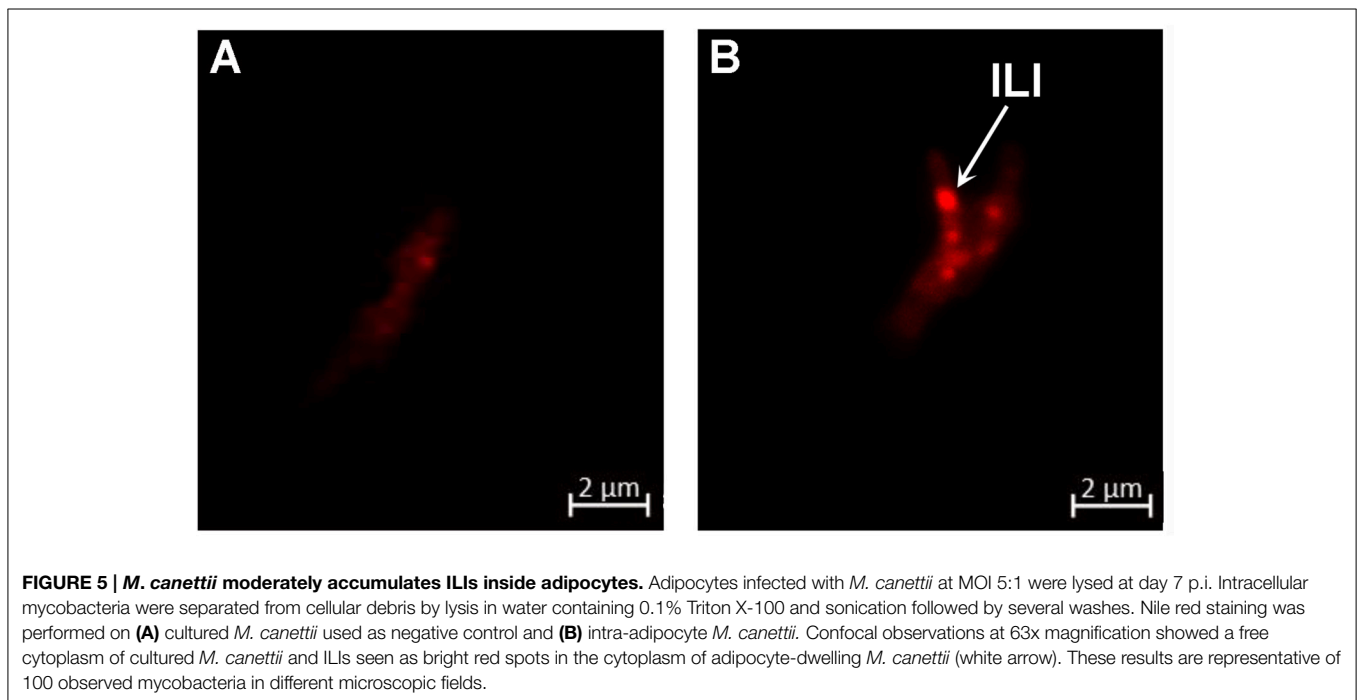
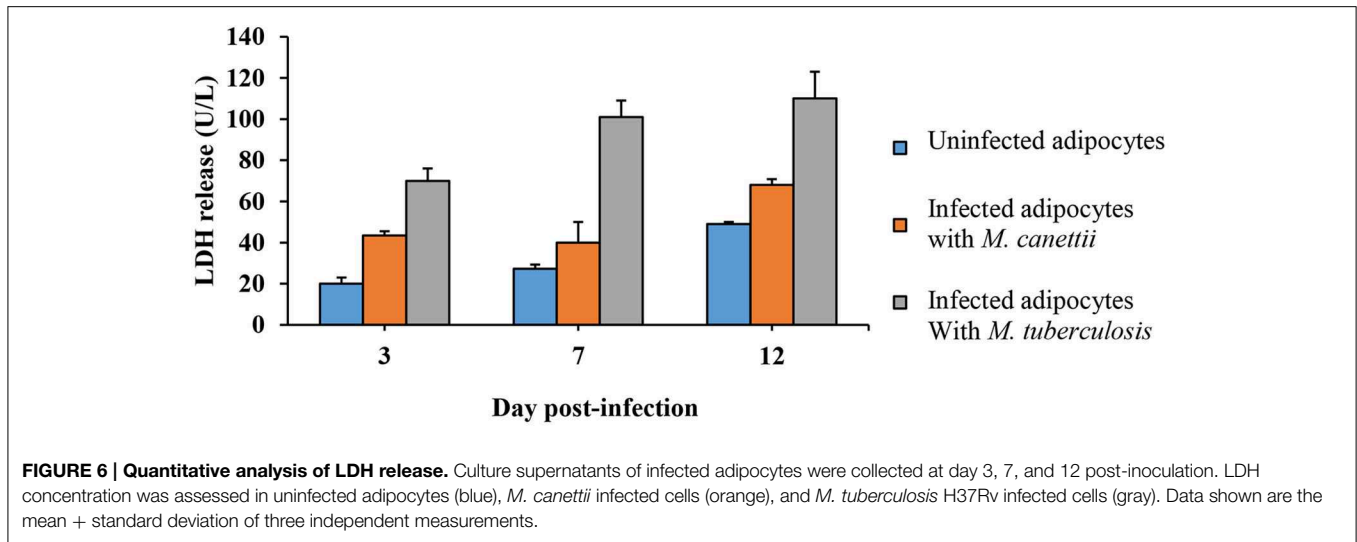


FIGURE 5 | *M. canettii* moderately accumulates ILIs inside adipocytes. Adipocytes infected with *M. canettii* at MOI 5:1 were lysed at day 7 p.i. Intracellular mycobacteria were separated from cellular debris by lysis in water containing 0.1% Triton X-100 and sonication followed by several washes. Nile red staining was performed on (A) cultured *M. canettii* used as negative control and (B) intra-adipocyte *M. canettii*. Confocal observations at 63x magnification showed a free cytoplasm of cultured *M. canettii* and ILIs seen as bright red spots in the cytoplasm of adipocyte-dwelling *M. canettii* (white arrow). These results are representative of 100 observed mycobacteria in different microscopic fields.

did not enable us to observe potential long-term dormancy of *M. canettii* in mature adipocytes.

The primary and 3T3-L1 pre-adipocytes also phagocytized *M. canettii* and *M. tuberculosis* as previously shown with other particles (Cousin et al., 1999). More precisely, the amount of intracellular mycobacteria was significantly higher in brown than in white pre-adipocytes, corroborating previous observation of the earlier deposition of *M. bovis* in the BAT after intravenous

administration in mice (Mauss and Levy, 1972). *In vivo*, the rich vascular network of BAT (Shimizu et al., 2014) could facilitate the tissue infection by *M. canettii*. Furthermore, the burden of intracellular mycobacteria was higher in pre-adipocytes than in mature adipocytes. Pre-adipocytes are fibroblast-like cells lacking cytoplasmic lipid droplets thus capable of rapidly phagocytosing (Hoffman and Dow, 2016); while mature adipocytes have lost this phagocytic activity (Cousin et al.,



1999). Likewise, foamy macrophages loaded with LBs lost the ability to phagocytize mycobacteria compared to undifferentiated non-foamy macrophages (Peyron et al., 2008). These data indicate that pre-adipocytes are preferential targets for MTBC mycobacteria.

In conclusion, our results offer new pieces of information regarding the subtle interplay between MTBC mycobacteria and their hosts: infection of pre-adipocytes and adipocytes is a probable common feature of the MTBC at large, being shared by distantly related *M. tuberculosis* and *M. canettii* (Gutierrez et al., 2005), nevertheless, the intracellular outcome depends on the mycobacteria. While WAT is an unlikely sanctuary for *M. canettii*, the question remains open as for BAT. In the current quest for a yet unknown animal reservoir for *M. canettii*, our observations suggest that any mammal harboring BAT is a candidate reservoir, suggesting new field of investigations.

AUTHOR CONTRIBUTIONS

SC and MD, conceived and supervised the experiments; Fé.B, performed the experiments; Fa.B, conducted the mice experiment; IP, conducted the electron microscopic observations; PW, was helpful for all confocal observations; SC and MD, and

Fé.B analyzed the data and drafted the manuscript. All authors reviewed and approved the manuscript.

FUNDING

This study was financially supported by URMITE, IHU Méditerranée Infection, Marseille, France; CNRS and by the A*MIDEX project (n°ANR-11-IDEX-0001-02) funded by the “Investissements d’Avenir” French Government program, managed by the French National Research Agency (ANR).

ACKNOWLEDGMENTS

We thank the Biochemistry Laboratory–(Hospital of la Timone, Marseille, France) directed by Prof. Régis GUIEU for the LDH assay. The authors acknowledge Pablo Gluschkof who contributed to review the manuscript and Farid Soltani who contributed to analyze the slide scans of stained cells.

SUPPLEMENTARY MATERIAL

The Supplementary Material for this article can be found online at: <http://journal.frontiersin.org/article/10.3389/fcimb.2017.00189/full#supplementary-material>

REFERENCES

- Aboubaker Osman, D., Bouzid, F., Cnaan, S., and Drancourt, M. (2015). Smooth tubercle bacilli: neglected opportunistic tropical pathogens. *Front. Public Health* 3:283. doi: 10.3389/fpubh.2015.00283
- Agarwal, P., Khan, S. R., Verma, S. C., Beg, M., Singh, K., Mitra, K., et al. (2014). *Mycobacterium tuberculosis* persistence in various adipose depots of infected mice and the effect of anti-tubercular therapy. *Microbes Infect.* 16, 571–580. doi: 10.1016/j.micinf.2014.04.006
- Agarwal, P., Pandey, P., Sarkar, J., and Krishnan, M. Y. (2016). *Mycobacterium tuberculosis* can gain access to adipose depots of mice infected via the intra-nasal route and to lungs of mice with an infected subcutaneous fat implant. *Microb. Pathog.* 93, 32–37. doi: 10.1016/j.micpath.2016.01.004
- Alibaud, L., Rombouts, Y., Trivelli, X., Burguiere, A., Cirillo, S. L., Cirillo, J. D., et al. (2011). A *Mycobacterium marinum* TesA mutant defective for major cell wall-associated lipids is highly attenuated in *Dictyostelium discoideum* and zebrafish embryos. *Mol. Microbiol.* 80, 919–934. doi: 10.1111/j.1365-2958.2011.07618.x
- Aune, U. L., Ruiz, L., and Kajimura, S. (2013). Isolation and differentiation of stromal vascular cells to beige/brite cells. *J. Vis. Exp.* 73:50191. doi: 10.3791/50191
- Boritsch, E. C., Frigui, W., Cascioferro, A., Malaga, W., Etienne, G., Laval, F., et al. (2016a). pks5-recombination-mediated surface remodelling

- in *Mycobacterium tuberculosis* emergence. *Nat. Microbiol.* 1:15019. doi: 10.1038/nmicrobiol.2015.19
- Boritsch, E. C., Khanna, V., Pawlik, A., Honore, N., Navas, V. H., Ma, L., et al. (2016b). Key experimental evidence of chromosomal DNA transfer among selected tuberculosis-causing mycobacteria. *Proc. Natl. Acad. Sci. U.S.A.* 113, 9876–9881. doi: 10.1073/pnas.1604921113
- Caire-Brandli, I., Papadopoulos, A., Malaga, W., Marais, D., Canaan, S., Thilo, L., et al. (2014). Reversible lipid accumulation and associated division arrest of *Mycobacterium avium* in lipoprotein-induced foamy macrophages may resemble key events during latency and reactivation of tuberculosis. *Infect. Immun.* 82, 476–490. doi: 10.1128/IAI.01196-13
- Cannon, B., and Nedergaard, J. (2004). Brown adipose tissue: function and physiological significance. *Physiol. Rev.* 84, 277–359. doi: 10.1152/physrev.00015.2003
- Cawthorn, W. P., Scheller, E. L., and MacDougald, O. A. (2012). Adipose tissue stem cells meet preadipocyte commitment: going back to the future. *J. Lipid Res.* 53, 227–246. doi: 10.1194/jlr.R021089
- Christensen, H., Garton, N., Horobin, R., Minnikin, D., and Barer, M. (1999). Lipid domains of mycobacteria studied with fluorescent molecular probes. *Mol. Microbiol.* 31, 1561–1572. doi: 10.1046/j.1365-2958.1999.01304.x
- Cousin, B., Munoz, O., Andre, M., Fontanilles, A. M., Dani, C., Cousin, J. L., et al. (1999). A role for preadipocytes as macrophage-like cells. *FASEB J.* 13, 305–312.
- Daniel, J., Deb, C., Dubey, V. S., Sirakova, T. D., Abomoelak, B., Morbidoni, H. R., et al. (2004). Induction of a novel class of diacylglycerol acyltransferases and triacylglycerol accumulation in *Mycobacterium tuberculosis* as it goes into a dormancy-like state in culture. *J. Bacteriol.* 186, 5017–5030. doi: 10.1128/JB.186.15.5017-5030.2004
- Deb, C., Daniel, J., Sirakova, T. D., Abomoelak, B., Dubey, V. S., and Kolattukudy, P. E. (2006). A novel lipase belonging to the hormone-sensitive lipase family induced under starvation to utilize stored triacylglycerol in *Mycobacterium tuberculosis*. *J. Biol. Chem.* 281, 3866–3875. doi: 10.1074/jbc.M505556200
- de Chastellier, C. (2008). EM analysis of phagosomes. *Methods Mol. Biol.* 445, 261–285. doi: 10.1007/978-1-59745-157-4_17
- Dhouib, R., Ducret, A., Hubert, P., Carriere, F., Dukan, S., and Canaan, S. (2011). Watching intracellular lipolysis in mycobacteria using time lapse fluorescence microscopy. *Biochim. Biophys. Acta* 1811, 234–241. doi: 10.1016/j.bbali.2011.01.001
- Garton, N., Christensen, H., Minnikin, D., Adegbola, R., and Barer, M. (2002). Intracellular lipophilic inclusions of mycobacteria *in vitro* and in sputum. *Microbiology* 148, 2951–2958. doi: 10.1099/00221287-148-10-2951
- Gomez-Hernandez, A., Beneit, N., Diaz-Castroverde, S., and Escribano, O. (2016). Differential role of adipose tissues in obesity and related metabolic and vascular complications. *Int. J. Endocrinol.* 2016:1216783. doi: 10.1155/2016/1216783
- Gutierrez, M. C., Brisse, S., Brosch, R., Fabre, M., Omais, B., Marmiesse, M., et al. (2005). Ancient origin and gene mosaicism of the progenitor of *Mycobacterium tuberculosis*. *PLoS Pathog.* 1:e5. doi: 10.1371/journal.ppat.0010005
- Hoffman, A. M., and Dow, S. W. (2016). Concise review: stem cell trials using companion animal disease models. *Stem Cells* 34, 1709–1729. doi: 10.1002/stem.2377
- Kim, J. S., Ryu, M. J., Byun, E. H., Kim, W. S., Whang, J., Min, K. N., et al. (2011). Differential immune response of adipocytes to virulent and attenuated *Mycobacterium tuberculosis*. *Microbes Infect.* 13, 1242–1251. doi: 10.1016/j.micinf.2011.07.002
- Koeck, J. L., Fabre, M., Simon, F., Daffe, M., Garnotel, E., Matan, A. B., et al. (2011). Clinical characteristics of the smooth tubercle bacilli '*Mycobacterium canettii*' infection suggest the existence of an environmental reservoir. *Clin. Microbiol. Infect.* 17, 1013–1019. doi: 10.1111/j.1469-0691.2010.03347.x
- Korzeniewski, C., and Callewaert, D. M. (1983). An enzyme-release assay for natural cytotoxicity. *J. Immunol. Methods* 64, 313–320. doi: 10.1016/0022-1759(83)90438-6
- Low, K. L., Rao, P. S., Shui, G., Bendt, A. K., Pethe, K., Dick, T., et al. (2009). Triacylglycerol utilization is required for regrowth of *in vitro* hypoxic nonreplicating *Mycobacterium bovis* bacillus Calmette-Guerin. *J. Bacteriol.* 191, 5037–5043. doi: 10.1128/JB.00530-09
- Low, K. L., Shui, G., Natter, K., Yeo, W. K., Kohlwein, S. D., Dick, T., et al. (2010). Lipid droplet-associated proteins are involved in the biosynthesis and hydrolysis of triacylglycerol in *Mycobacterium bovis* bacillus Calmette-Guerin. *J. Biol. Chem.* 285, 21662–21670. doi: 10.1074/jbc.M110.135731
- Mattos, K. A., D'Avila, H., Rodrigues, L. S., Oliveira, V. G., Sarno, E. N., Atella, G. C., et al. (2010). Lipid droplet formation in leprosy: toll-like receptor-regulated organelles involved in eicosanoid formation and *Mycobacterium leprae* pathogenesis. *J. Leukoc. Biol.* 87, 371–384. doi: 10.1189/jlb.0609433
- Mattos, K. A., Lara, F. A., Oliveira, V. G., Rodrigues, L. S., D'Avila, H., Melo, R. C., et al. (2011). Modulation of lipid droplets by *Mycobacterium leprae* in Schwann cells: a putative mechanism for host lipid acquisition and bacterial survival in phagosomes. *Cell. Microbiol.* 13, 259–273. doi: 10.1111/j.1462-5822.2010.01533.x
- Mauss, H., and Levy, F. M. (1972). Involvement of adipose tissue in experimental tuberculosis of the mouse. *Pathol. Microbiol.* 38, 333–345.
- McKinney, J. D., Honer zu Bentrup, K., Munoz-Elias, E. J., Miczak, A., Chen, B., Chan, W. T., et al. (2000). Persistence of *Mycobacterium tuberculosis* in macrophages and mice requires the glyoxylate shunt enzyme isocitrate lyase. *Nature* 406, 735–738. doi: 10.1038/35021074
- Morrison, S., and McGee, S. L. (2015). 3T3-L1 adipocytes display phenotypic characteristics of multiple adipocyte lineages. *Adipocyte* 4, 295–302. doi: 10.1080/21623945.2015.1040612
- Nedergaard, J., Bengtsson, T., and Cannon, B. (2007). Unexpected evidence for active brown adipose tissue in adult humans. *Am. J. Physiol. Endocrinol. Metab.* 293, E444–E452. doi: 10.1152/ajpendo.00691.2006
- Neyrolles, O., Hernandez-Pando, R., Pietri-Rouxel, F., Fornes, P., Tailleux, L., Payan, J. A., et al. (2006). Is adipose tissue a place for *Mycobacterium tuberculosis* persistence? *PLoS ONE* 1:e43. doi: 10.1371/journal.pone.0000043
- Ouchi, N., Parker, J. L., Lugus, J. J., and Walsh, K. (2011). Adipokines in inflammation and metabolic disease. *Nat. Rev. Immunol.* 11, 85–97. doi: 10.1038/nri2921
- Peyron, P., Vaubourgeix, J., Poquet, Y., Levillain, F., Botanch, C., Bardou, F., et al. (2008). Foamy macrophages from tuberculous patients' granulomas constitute a nutrient-rich reservoir for *M. tuberculosis* persistence. *PLoS Pathog.* 4:e1000204. doi: 10.1371/journal.ppat.1000204
- Rastogi, S., Agarwal, P., and Krishnan, M. Y. (2016). Use of an adipocyte model to study the transcriptional adaptation of *Mycobacterium tuberculosis* to store and degrade host fat. *Int. J. Mycobacteriol.* 5, 92–98. doi: 10.1016/j.ijmyco.2015.10.003
- Russell, D. G., Cardona, P. J., Kim, M. J., Allain, S., and Altare, F. (2009). Foamy macrophages and the progression of the human tuberculosis granuloma. *Nat. Immunol.* 10, 943–948. doi: 10.1038/ni.1781
- Santucci, P., Bouzid, F., Smichi, N., Poncin, I., Kremer, L., De Chastellier, C., et al. (2016). Experimental models of foamy macrophages and approaches for dissecting the mechanisms of lipid accumulation and consumption during dormancy and reactivation of Tuberculosis. *Front. Cell. Infect. Microbiol.* 6:122. doi: 10.3389/fcimb.2016.00122
- Shimizu, I., Aprahamian, T., Kikuchi, R., Shimizu, A., Papanicolaou, K. N., MacLauchlan, S., et al. (2014). Vascular rarefaction mediates whitening of brown fat in obesity. *J. Clin. Invest.* 124, 2099–2112. doi: 10.1172/JCI71643
- Supply, P., Marceau, M., Mangenot, S., Roche, D., Rouanet, C., Khanna, V., et al. (2013). Genomic analysis of smooth tubercle bacilli provides insights into ancestry and pathoadaptation of *Mycobacterium tuberculosis*. *Nat. Genet.* 45, 172–179. doi: 10.1038/ng.2517

Conflict of Interest Statement: The authors declare that the research was conducted in the absence of any commercial or financial relationships that could be construed as a potential conflict of interest.

Copyright © 2017 Bouzid, Brégeon, Poncin, Weber, Drancourt and Canaan. This is an open-access article distributed under the terms of the Creative Commons Attribution License (CC BY). The use, distribution or reproduction in other forums is permitted, provided the original author(s) or licensor are credited and that the original publication in this journal is cited, in accordance with accepted academic practice. No use, distribution or reproduction is permitted which does not comply with these terms.

Supplementary Data

Ratio of infection

Cell type	<i>M. canettii</i>		<i>M. tuberculosis</i>	
	Total number of cells per microscopic field	Number of infected cells per microscopic field	Total number of cells per microscopic field	Number of infected cells per microscopic field
white pre-adipocytes	27	4	25	6
	15	2	46	10
	21	5	25	8
	14	4	29	4
	17	4	35	3
	23	5	22	4
	20	4	26	6
	17	2	27	3
	24	3	30	4
	28	6	15	2
TOTAL	206	39	280	50

Brown pre-adipocytes	33	12	16	4
	12	3	8	1
	15	4	11	3
	17	3	15	4
	12	1	15	2
	19	3	19	5
	25	4	23	4
	15	2	18	3
	16	3	19	3
	13	2	17	2
TOTAL	177	37	161	31

3T3-L1 pre-adipocytes	30	10	30	11
	27	3	23	12
	12	2	14	7
	27	4	22	9
	20	7	27	8
	28	4	29	12
	18	3	28	11
	11	1	17	8
	13	2	23	9
	21	6	19	7
TOTAL	207	42	232	94

3T3-L1 mature adipocytes	26	3	20	3
	25	2	20	2
	16	2	15	2
	13	1	21	5
	23	2	25	5
	24	0	24	6
	25	2	17	2
	28	3	24	3
	35	4	40	6
	12	2	22	4
TOTAL	227	21	228	38

Number of intracellular bacilli

		Number of intracellular bacilli per one cell obtained by microscopy	
		<i>M. canettii</i>	<i>M. tuberculosis</i>
white pre-adipocytes	Cell type		
		22	8
		9	2
		1	7
		9	4
		3	5
		9	3
		5	8
		14	6
		11	11
	10	19	

Brown pre-adipocytes		23	11
		18	9
		17	18
		23	12
		6	8
		4	13
		19	6
		21	16
		19	12
		7	6

3T3-L1 pre-adipocytes		3	23
		6	6
		2	10
		15	13
		13	22
		3	4
		16	8
		5	11
		8	12
		2	14

Scoring CFUs

Cell type	Day p.i.	CFUs/10 ⁵ cells	
		<i>M. canettii</i>	<i>M. tuberculosis</i>
White pre-adipocytes	day 0		
	well 1	24000	8400
	well 2	6000	5200
	well 2	16000	13600
	day 3		
	well 1	67600	28800
	well 2	44000	37600
	well 2	64400	33600
	day 7		
	well 1	160000	216000
	well 2	272000	136000
	well 2	68000	112000

Brown pre-adipocytes	day 0		
	well 1	42800	27600
	well 2	44800	19200
	well 2	30800	31200
	day 3		
	well 1	500000	276000
	well 2	288000	200000
	well 2	484000	156000
	day 7		
	well 1	672000	728000
	well 2	752000	608000
	well 2	856000	652000

3T3-L1 pre-adipocytes	day 0		
	well 1	31200	51200
	well 2	20400	58800
	well 2	25600	43000
	day 3		
	well 1	148000	432000
	well 2	104000	292000
	well 2	128000	476000
	day 7		
	well 1	432000	1160000
	well 2	636000	1920000
	well 2	568000	1520000
	J12		
	well 1	3360000	5000000
	well 2	4240000	4240000
well 2	3280000	5400000	

3T3-L1 mature adipocytes	day 0		
	well 1	10800	42000
	well 2	9200	34400
	well 2	16800	36400
	day 3		
	well 1	39600	113600
	well 2	31200	110400
	well 2	25200	115200
	day 7		
	well 1	112000	288000
	well 2	56000	172000
	well 2	68000	300000
	J12		
	well 1	896000	520000
	well 2	528000	356000
well 2	688000	500000	

LDH measurments

LDH measurments			
Day p.i.	Uninfected mature adipocytes	Infected cells with <i>M. canettii</i>	Infected cells with <i>M. tuberculosis</i>
Day 3			
well 1	17	45	64
well 2	20	42	69
well 2	23	43	77
Day 7			
well 1	25	33	108
well 2	28	47	92
well 2	29	39	104
Day 12			
well 1	50	69	125
well 2	48	67	101
well 2	49	68	104

CHAPITRE V

Approches expérimentales pour l'étude du métabolisme des lipides des bacilles tuberculeux

Experimental models of foamy macrophages and approaches for dissecting the mechanisms of lipid accumulation and consumption during dormancy and reactivation of tuberculosis.

Santucci P, Bouzid F, Smichi N, Poncin I, Kremer L, De Chastellier C, Drancourt M, Canaan S.

Front Cell Infect Microbiol. 2016. Review.

8. CHAPITRE V : Approches expérimentales pour l'étude du métabolisme des lipides des bacilles tuberculeux: revue de la littérature

Le succès de *M. tuberculosis* en tant que pathogène majeur de l'homme s'explique en partie par sa capacité à rentrer dans un état de dormance qui lui permet d'échapper à l'éradication par le système immunitaire et le protège contre les molécules thérapeutiques testées à ce jour (Russell et al., 2009). En effet, au cours de la primo-infection par *M. tuberculosis*, les cellules immunitaires s'agrègent autour des tissus infectés conduisant à la formation de granulomes organisés (Peyron et al., 2008; Russell et al., 2009). Dans le granulome, les macrophages infectés se différencient en macrophages spumeux ou « foamy » (FMs) replets de corps lipidiques (LBs) (Peyron et al., 2008). Les bacilles de *M. tuberculosis* phagocytés adaptent leurs voies métaboliques pour rentrer dans un état de dormance caractérisé par l'accumulation d'inclusions lipidiques intracytosoliques (ILIs) importés à partir des cellules hôtes ou synthétisés de novo (Daniel et al., 2011). Les ILIs constituent une source d'énergie pour la persistance des mycobactéries, en particulier de *M. tuberculosis* et semblent participer à sa réactivation (Daniel et al., 2011; Caire-Brandli et al., 2014). Les mécanismes moléculaires par lesquels les mycobactéries intra-phagosomiques interagissent avec les LBs de l'hôte, assimilent les lipides et les consomment, sont encore mal compris. Au cours des dernières années, plusieurs modèles animaux et cellulaires ont été développés visant à disséquer ces processus complexes.

Notre travail bibliographique a eu pour objectifs de présenter les modèles *in vitro* et *in vivo* les plus pertinents qui permettent d'induire le phénotype spumeux des macrophages et de provoquer l'accumulation et la consommation des ILIs par *M. tuberculosis*. Ces modèles permettent d'apporter des éléments pour la compréhension des mécanismes de réalisation de ses phénotypes. Nous avons également discuté les avantages et les limites de chaque modèle

pour faciliter le choix du modèle le plus adapté à la question posée (Santucci et al., 2016). Entre autres, le modèle d'infection des adipocytes matures a été rapporté. Ces cellules sont naturellement riches en lipides mimant ainsi les conditions des macrophages spumeux. Ce modèle a été adapté pour induire la dormance de *M. tuberculosis* caractérisée par l'accumulation d'ILIs, la résistance aux antibiotiques antituberculeux et la régulation positive des gènes *dosR* and *icl* (Neyrolles et al., 2006; Agarwal et al., 2014; Agarwal et al., 2016; Rastogi et al., 2016). En utilisant ce modèle, nous avons réussi à induire l'accumulation modérée d'ILIs dans *M. canettii* mais la mycobactérie n'a pas présenté un stade de dormance contrairement à *M. tuberculosis* et a continué sa réplication durant les 12 jours d'expérimentation (Bouزيد et al., 2017c). L'ensemble de cette revue bibliographique présente un excellent outil de travail pour les chercheurs travaillant sur le métabolisme des lipides chez les mycobactéries.



Experimental Models of Foamy Macrophages and Approaches for Dissecting the Mechanisms of Lipid Accumulation and Consumption during Dormancy and Reactivation of Tuberculosis

Pierre Santucci^{1†}, Ferial Bouzid^{1,2†}, Nabil Smichi^{1,3}, Isabelle Poncin¹, Laurent Kremer^{3,4}, Chantal De Chastellier¹, Michel Drancourt² and Stéphane Canaan^{1*}

¹ Aix-Marseille Université, Centre National de la Recherche Scientifique, EPL, Marseille, France, ² Aix-Marseille Université, Institut National de la Santé et de la Recherche Médicale, Centre National de la Recherche Scientifique, Institut de Recherche pour le Développement, URMITE, Marseille, France, ³ Centre d'études d'agents Pathogènes et Biotechnologies pour la Santé, Centre National de la Recherche Scientifique FRE3689, Université de Montpellier, Montpellier, France, ⁴ Centre d'études d'agents Pathogènes et Biotechnologies pour la Santé, Institut National de la Santé et de la Recherche Médicale, Montpellier, France

OPEN ACCESS

Edited by:

Lisa A. Morici,
Tulane University School of Medicine,
USA

Reviewed by:

Jianping Xie,
Southwest University, China
Robert B. Abramovitch,
Michigan State University, USA

*Correspondence:

Stephane Canaan
stephane.canaan@imm.cnrs.fr

[†]These authors have contributed
equally to this work.

Received: 03 August 2016

Accepted: 22 September 2016

Published: 07 October 2016

Citation:

Santucci P, Bouzid F, Smichi N,
Poncin I, Kremer L, De Chastellier C,
Drancourt M and Canaan S (2016)
Experimental Models of Foamy
Macrophages and Approaches for
Dissecting the Mechanisms of Lipid
Accumulation and Consumption
during Dormancy and Reactivation of
Tuberculosis.
Front. Cell. Infect. Microbiol. 6:122.
doi: 10.3389/fcimb.2016.00122

Despite a slight decline since 2014, tuberculosis (TB) remains the major deadly infectious disease worldwide with about 1.5 million deaths each year and with about one-third of the population being latently infected with *Mycobacterium tuberculosis*, the etiologic agent of TB. During primo-infection, the recruitment of immune cells leads to the formation of highly organized granulomas. Among the different cells, one outstanding subpopulation is the foamy macrophage (FM), characterized by the abundance of triacylglycerol-rich lipid bodies (LB). *M. tuberculosis* can reside in FM, where it acquires, from host LB, the neutral lipids which are subsequently processed and stored by the bacilli in the form of intracytosolic lipid inclusions (ILI). Although host LB can be viewed as a reservoir of nutrients for the pathogen during latency, the molecular mechanisms whereby intraphagosomal mycobacteria interact with LB and assimilate the LB-derived lipids are only beginning to be understood. Past studies have emphasized that these physiological processes are critical to the *M. tuberculosis* infectious-life cycle, for propagation of the infection, establishment of the dormancy state and reactivation of the disease. In recent years, several animal and cellular models have been developed with the aim of dissecting these complex processes and of determining the nature and contribution of their key players. Herein, we review some of the *in vitro* and *in vivo* models which allowed to gain significant insight into lipid accumulation and consumption in *M. tuberculosis*, two important events that are directly linked to pathogenicity, granuloma formation/maintenance and survival of the tubercle bacillus under non-replicative conditions. We also discuss the advantages and limitations of each model, hoping that this will serve as a guide for future investigations dedicated to persistence and innovative therapeutic approaches against TB.

Keywords: granuloma, adipocyte, amoeba, mycobacteria, pathogenesis, lipid body

INTRODUCTION

With 9.6 million new cases and 1.5 million deaths in 2014, tuberculosis (TB) ranks alongside with HIV as the major cause of deadly infectious diseases (WHO, 2015). It is estimated that about one-third of the world population is infected with the etiological agent of TB, *Mycobacterium tuberculosis*, but only 5 to 10% of the infected individuals are at risk of developing active disease within a few years. Most individuals remain asymptomatic after the primary infection. In such individuals, bacilli do not divide but may persist for decades in a dormant state until reactivation of bacilli leads to active disease (WHO, 2015).

Infection with *M. tuberculosis* follows a relatively well-defined sequence of events (Russell, 2001; Russell et al., 2009a). After inhalation of contaminated aerosols, *M. tuberculosis* reaches the lungs, where the bacilli are phagocytosed by alveolar macrophages. Prognosis of the disease, viz, active or dormant, will depend on the host's ability to contain the bacilli at the site of infection. In most cases, the bacilli induce a local pro-inflammatory response which leads to the recruitment of other immune cells (macrophages, dendritic cells and lymphocytes) from neighboring blood vessels. The latter accumulate around the alveolar macrophages, at the site of infection, to form a granuloma which is the hallmark of TB (Russell, 2007; Peyron et al., 2008; Gideon and Flynn, 2011; Galagan, 2014).

The tuberculous granuloma is a highly elaborate host protective structure, which represents an essential immune mechanism for containing the bacilli inside the lungs without fully eradicating them (Kaufmann, 2001; Russell, 2001). The formation process, the composition and maintenance of this well-organized system have been extensively investigated and reviewed over the last decade (Russell et al., 2009a; Ramakrishnan, 2012; Guirado and Schlesinger, 2013). Briefly, macrophages differentiate into epithelioid cells or become highly vacuolated or even fuse to form multi-nucleated giant cells (Puissegur et al., 2007; Russell et al., 2009a; Feng et al., 2014). Other macrophages, which are the focus of intense research, differentiate into foam cells characterized by the intracytosolic accumulation of neutral lipids in the form of lipid bodies (LB) also known as lipid droplets or lipid vacuoles (Daniel et al., 2004; Deb et al., 2006; Russell et al., 2009a). These specific foamy macrophages (FM) are found in the interface region flanking the central necrotic center of the granuloma (Peyron et al., 2008).

Traditionally, FM were qualified as passive organelles involved in lipid storage. More recently, it became clear that these organelles play a central role in several inflammatory diseases, such as atherosclerosis, or in chronic infectious diseases (Russell et al., 2009b). Different myeloid cell types have been used to generate lipid-loaded foam cells and to provide insights into their contribution in chronic inflammatory conditions. In the context of TB, pathologists have described the presence of FM within granulomatous structures in both experimentally-infected animals and patients (Ridley and Ridley, 1987; Cardona et al., 2000), especially in individuals developing secondary TB (Pagel, 1925; Florey, 1958; Hunter et al., 2007), thereby suggesting that FM may play a central role in mycobacterial persistence and reactivation.

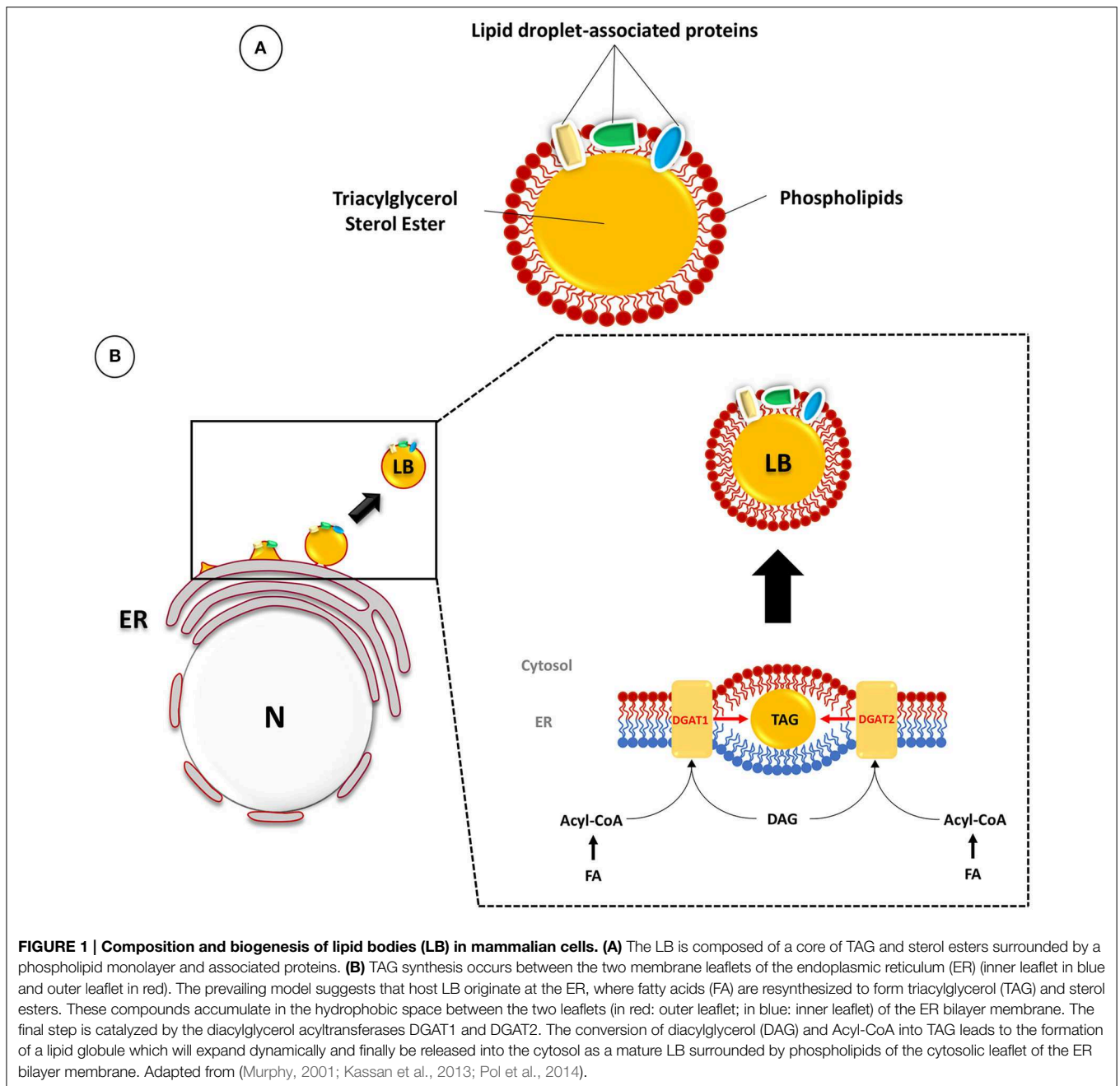
Since *M. tuberculosis* is facing important physiological changes as TB progresses toward containment of the bacilli within granulomas, it is assumed that this involves adaptive requirements that are distinct from those encountered during the initial phase of infection (Hingley-Wilson et al., 2003; McKinney and Gomez, 2003; Sasseti and Rubin, 2003). Among these, accumulation of neutral lipids, essentially triacylglycerol (TAG), within intracytosolic lipid inclusions (ILI) (Dhouib et al., 2011), has been proposed to serve as a source of carbon and energy, and represents a hallmark of persistent and non-dividing mycobacteria (Garton et al., 2002; Daniel et al., 2011). Therefore, residing within specialized lipid-rich cells, rather than in conventional macrophages, would be beneficial and even promote *M. tuberculosis* persistence within granulomatous lesions. This also implies that bacilli must produce lipolytic enzymes and/or activate host hydrolytic enzymes in order to degrade the host neutral lipids into free fatty acids (FFA) and then re-synthesize TAG for subsequent ILI formation. Clearly, the abundance of genes encoding enzymes involved in lipid metabolism (Cole et al., 1998) strongly suggests that *M. tuberculosis* uses host-derived lipids while persisting *in vivo* (Höner Zu Bentrup and Russell, 2001).

The purpose of the present review is firstly to recall how host cells become foamy, by accumulating neutral lipids in the form of LB and, second, to describe and compare different foam cell models and approaches that have served to delineate lipid accumulation and consumption processes developed by *M. tuberculosis* and other mycobacteria within their host cells. Advantages and drawbacks of each model are also discussed.

LIPID BODIES IN FOAM CELLS: A RESERVOIR OF LIPIDS FOR PERSISTENT *M. tuberculosis*

The presence of neutral lipid storage organelles in the cytoplasm of most eukaryotes (named LB) and prokaryotes (named ILI) has been known for a long time. In all cases, these ubiquitous structures are composed of a core of neutral lipids, such as sterol esters and TAG, surrounded by a monolayer of phospholipids, in which cholesterol ester and proteins are inserted (Figure 1A; Murphy, 2001; Martin and Parton, 2005; Pol et al., 2014). A large number of associated proteins have been discovered in recent studies devoted to the composition and dynamics of LB formation (Brasaemle et al., 2004; Yang et al., 2012). Furthermore, it is now clear that, beyond neutral lipid storage, the functions of LB are multiple, and this knowledge has given rise to new hypotheses concerning the role of these organelles in several physiological processes (Saka and Valdivia, 2012).

The current models of LB biogenesis have been reviewed extensively (Murphy and Vance, 1999; Ohsaki et al., 2009; Saka and Valdivia, 2012). The prevailing model suggests that host LB originate at the endoplasmic reticulum (ER), where fatty acids are used to re-synthesize TAG and sterol esters. The *de novo* anabolic process leading to TAG synthesis relies on multiple enzymatic steps, the final one being catalyzed by diacylglycerol acyltransferases (DGAT) (Harris et al., 2011; Pol et al., 2014).



Among these, DGAT1 and DGAT2 are located in the ER where they can synthesize TAG from diacylglycerol (DAG) and acyl-CoA. TAG and sterol esters then accumulate in the hydrophobic space between the leaflets of the ER bilayer membrane, where they are subsequently engulfed by phospholipids of the cytosolic leaflet and pinched off the ER membrane into the cytosol (Figure 1B; Murphy, 2001; Kassan et al., 2013; Pol et al., 2014).

Over one decade ago, Garton et al. established that *M. tuberculosis* could accumulate neutral lipids in the form of ILI *in vitro* and in sputum of TB patients (Garton et al., 2002). Since then, ILI formation has been extensively described and analyzed

in several mycobacterial species, including *M. tuberculosis* (McKinney et al., 2000; Daniel et al., 2004, 2011; Deb et al., 2006), *M. bovis* BCG (Low et al., 2009, 2010), *M. leprae* (Mattos et al., 2010, 2011), *M. abscessus* (Viljoen et al., 2016), and *M. smegmatis* (Dhouib et al., 2011). It has been proposed, but not yet proven, that storage of fatty acids in the form of TAG within ILI could serve as a source of carbon and energy during dormancy and reactivation of *M. tuberculosis* (Peyron et al., 2008; Low et al., 2009; Daniel et al., 2011; Dhouib et al., 2011).

Currently, almost nothing is known concerning the biological mechanism by which the storage of fatty acids may promote

mycobacterial intracellular survival. Several hypotheses have been raised over the years, suggesting that ILI do not only serve as carbon source during infection, but could also reduce a wide range of oxido-reductive and metabolic stress (Kumar et al., 2011; Lee et al., 2013). It has also been proposed that the TAG accumulation can function in metabolic coupling to balance changes in metabolism of other *M. tuberculosis* lipids (Jain et al., 2007).

Accumulation of neutral lipids in the form of ILI has also been demonstrated *in vitro* or *in vivo* for a wide range of microorganisms including *Rhodococcus*, Hepatitis C, and Dengue viruses, or *Chlamydia* (Saka and Valdivia, 2012; Alvarez, 2016) where they may serve other purposes.

Stimulated by these observations, several investigators have focused their activity on the search of external stimuli that may promote the accumulation of LB in macrophages and in other cells, with the aim of addressing the following key questions: (i) How do mycobacteria gain access to lipids from FM? (ii) How do they translocate the cellular lipids into their own cytoplasm? (iii) How are ILI formed and what is their composition? (iv) What are the lipolytic enzymes (from the host and mycobacteria) involved in these mechanisms? and (v) Is the arrest/resumption of mycobacterial division occurring during persistence and reactivation, respectively, linked to LB and ILI formation/consumption? At least some of these questions have been addressed thanks to the recent development of a panel of experimental models.

EXPERIMENTAL MODELS AND APPROACHES FOR STUDYING MYCOBACTERIAL LIPID METABOLISM DURING THE DORMANCY AND REACTIVATION STAGES OF TB

Several stimuli were tested for designing foam cell models that rest upon the following observations. Firstly, the granuloma is considered to be a hypoxic environment. The high cell density and poor vascularization seems to be responsible for this low oxygen content which has been shown to promote foam cell formation (Bostrom et al., 2006; Cardoso et al., 2015; Datta et al., 2016). Secondly, most FM are localized in the close vicinity of the caseous center (Cáceres et al., 2009) where decaying cells may provide neutral lipids or phospholipids (Kim et al., 2010). Such external nutrients are known to play a major role on macrophage lipid metabolism (Shashkin et al., 2005) and may lead to a foamy phenotype *in vivo*. Finally, specific cell wall-associated components, such as mycolic acids from pathogenic mycobacteria, might be involved in the formation of lipid-loaded cells inside the granuloma (Peyron et al., 2008; Russell et al., 2009a).

Animal Models

Several models have been developed in mice to analyze different aspects of granuloma formation and the interactions between *M. tuberculosis* and the granulomatous environment. Karakousis et al. (2004) induced artificial granuloma formation in mice in

order to mimic the caseous granuloma by physical containment of extracellular *M. tuberculosis*. This was achieved by inoculating liquid cultures of *M. tuberculosis* into the lumen of polyvinylidene fluoride (PVDF) hollow fibers with a syringe and a 20 gauge needle. The ends of the fibers were heat-sealed and individual fibers were prepared by heat-sealing at 2 cm intervals. Mice were anesthetized and the dorsal skin surface was sterilized with 70% ethanol. A small incision was made at the nape of the neck, and one fiber was deposited into the subcutaneous space of each flank. Incisions were closed with a surgical clip. The PVDF fibers have a molecular mass cut-off of 500 kDa, which allows diffusion of small soluble molecules but prevents the entry of host immune cells and the exit of bacilli. This model is particularly suitable for studying the behavior of extracellular *M. tuberculosis* within the host. Granulomatous lesions developed around the hollow fibers. In this micro-environment, the bacilli demonstrated an altered physiological state reminiscent of that of persistent bacilli which are characterized by stationary-state CFU counts, decreased metabolic activity and antimicrobial susceptibility. The accumulation of neutral lipids in the form of ILI within these bacilli was, however, not analyzed.

Another mouse model was developed by Geisel et al. (2005) and Rhoades et al. (2005) based on polystyrene beads coated with trehalose dimycolate (TDM) from *M. tuberculosis*. Following subcutaneous injection in mice of the TDM-loaded beads in a Matrigel matrix, the murine cells started to invade the matrix and remodeled the site under the influence of the mycobacterial lipid. Histological examination of the tissue sections revealed the abundance of adipophilin (ADRP or Plin2)-expressing foam cells around the inoculated beads and cryosections of TDM-induced granulomas showed an abundance of LB in foam cells (Kim et al., 2010).

One of the hallmarks of human TB is the development of granulomatous inflammatory lesions with central caseous necrosis and encapsulation of lesions by a fibrous connective tissue. In order to study interactions that occurs into granulomatous lesions, infection mouse models have been established allowing researchers to obtain crucial information concerning macrophages immune status, such as polarization, proliferation but also focusing onto cells differentiation during mycobacterial infection (Ordway et al., 2005, 2006). Based on that, few signaling networks have been proven to be associated to pathogen recognition response, macrophages immune and metabolic reprogramming, such as lipid metabolism and foamy appearance (Ordway et al., 2005; Schaale et al., 2013).

However, most commonly used mouse strains, such as BALB/c and C57BL/6, fail to develop well-organized granulomas with central necrosis (Kramnik et al., 2000; Keller et al., 2004). This prompted Kramnik and collaborators to develop another mouse strain, C3HeB/FeJ, referred to as the “Kramnik mouse model” (Kramnik et al., 1998) which, following infection with *M. tuberculosis*, develops highly organized and encapsulated necrotic lesions in the lungs resembling human pulmonary lesions (Pichugin et al., 2009). C3HeB/FeJ mice are highly susceptible to *M. tuberculosis* infection but possess an otherwise intact and functional immune system. By combining immunohistochemical staining approaches with advanced

imaging techniques, Driver et al. were able to follow disease progression in real time and localize bacilli and responsiveness to monotherapy within several days after exposure to low dose aerosol (Driver et al., 2012). More recently, Irwin et al. identified three distinct lesion types, arbitrarily called type I, II, and III, that vary in cell composition and organization in the granulomas resulting from aerosol infection (Irwin et al., 2015). Type I lesions most closely resembled classical human TB granulomas in that they are solid, encapsulated and caseous necrotic. They contain also large amounts of FM, of major interest for studying lipid accumulation and consumption during the persistence and reactivation phases of TB. However, to our knowledge, the “Kramnik mouse model” has not been used yet for such studies.

This model presents major advantages over other mouse models as the lesions, upon aerosol infection with *M. tuberculosis*, most closely resemble classical human TB granulomas. This model is a real asset for studying the progress of infection because the lesions contain all the immune cells involved in granuloma formation. In this context, *in situ* EM analysis of granulomas during the differentiation of infected macrophages into FM would be quite informative in terms of transfer to and accumulation of host cell neutral lipids in the form of ILI within the bacilli. These animal models are certainly attractive tools for *in vivo* drug assessments and monitoring the effect of drugs that can penetrate *M. tuberculosis*-containing granulomas. However, the complexity of the granulomatous lesions causes some experimental limitations. For instance, it is difficult to obtain homogenous preparations of pure FM or to isolate, in sufficient amounts, either FM or persistent bacilli confined within these cells, to undertake thorough studies to monitor physiological events, including lipid accumulation/consumption.

In vitro Model of Human Mycobacterial Granulomas

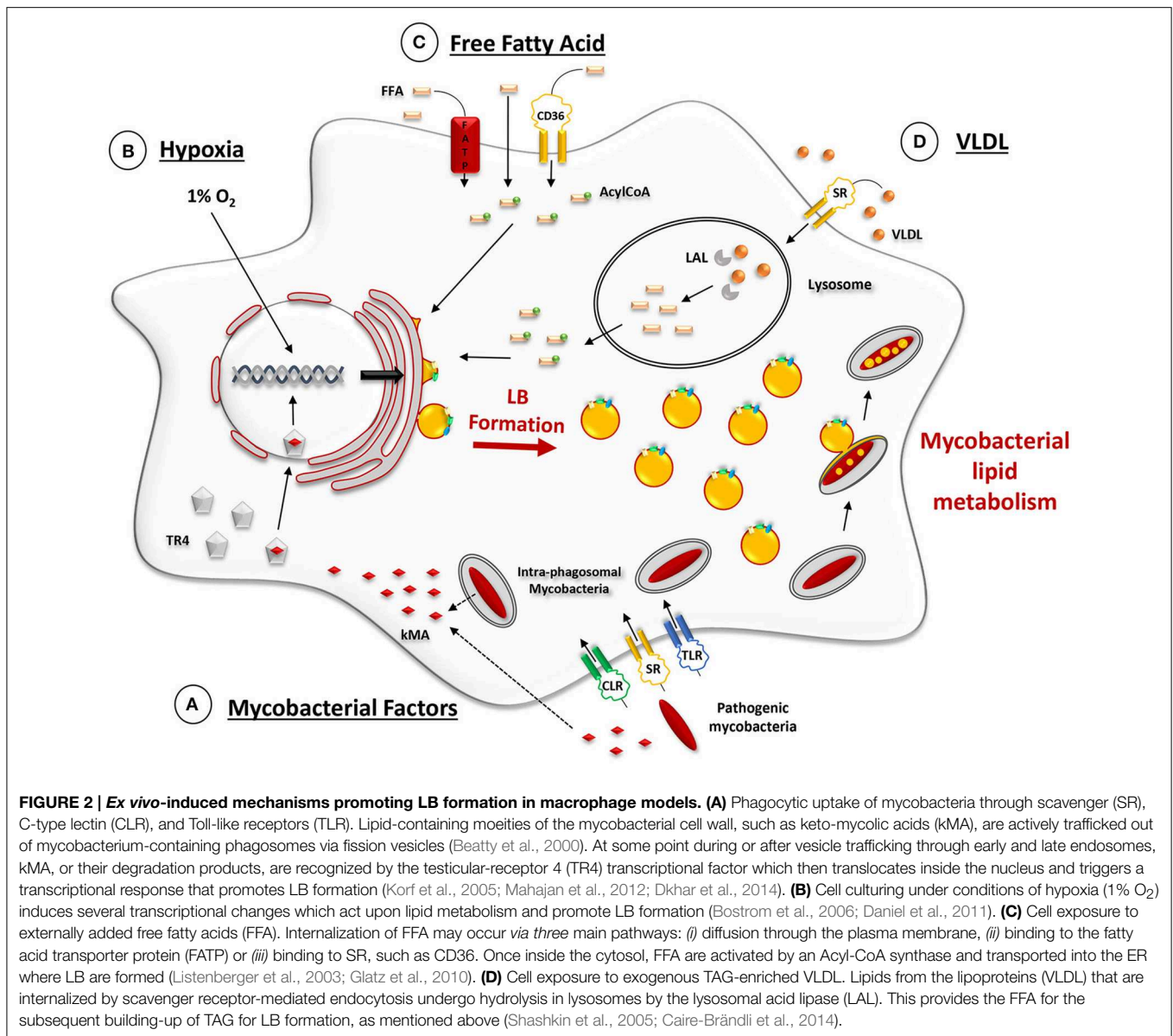
This model was first developed by Puissegur et al. to decipher the cellular and molecular events corresponding to the very first steps of granuloma formation in the *M. tuberculosis*-infected host (Puissegur et al., 2004). Peripheral blood mononuclear cells (PBMC), isolated from the blood of healthy donors, were exposed to either live *M. bovis* BCG or to mycobacterial antigen-coated sepharose beads within a cell culture dish. This led to the progressive recruitment of macrophages around the live bacilli or coated beads which were then phagocytosed by macrophages. This event was followed by the differentiation of macrophages into multi-nucleated giant cells and epithelioid cells and finally, the recruitment of a ring of activated lymphocytes around the newly-formed structure. All in all, the formation and spatial organization of this *in vitro*-grown structure mimicked that of natural mycobacterial granulomas found in *M. tuberculosis*-infected patients.

This model was subsequently used by Peyron et al. to analyze the formation of FM and to study their interaction with *M. tuberculosis* or *M. smegmatis* (Peyron et al., 2008). In this context, 1×10^6 PBMC freshly isolated from healthy donors were purified by Ficoll density gradient separation and exposed to very low concentrations of viable *M. tuberculosis* (1×10^4) or

M. smegmatis (1×10^3). The culture medium was RPMI-1640 + Glutamax containing 7.5% human AB serum. Three different imaging approaches were used to study LB formation. Briefly, for light microscopy studies, granuloma cells were collected and plated onto glass coverslips with a cytospin, fixed and stained with Oil red-O. After counterstaining with haematoxylin, cells were observed under an inverted microscope. For fluorescence analyses, granuloma cells were collected in PBS and LB were stained with Nile Red and observed under a confocal microscope. For electron microscopy (EM) studies, whole granulomas were fixed and processed for EM. Thin sections were prepared at different depths through the granulomas. The combination of these approaches at selected time points during granuloma formation allowed to visualize the morphological appearance of the different cell types, the presence or absence of bacilli within the different cells and the interaction between the bacilli and LB within FM. Of major interest was the differentiation of about 50% of the population of macrophages into FM within the *in vitro* granulomas obtained by exposure to *M. tuberculosis* but not to *M. smegmatis*. Within FM, as opposed to non-FM, bacilli were unable to divide. EM analyses of FM showed that LB, initially distributed randomly throughout the host cytosol, migrated toward *M. tuberculosis*-containing phagosomes with which they progressively made contact. Ultimately, the bacilli were enclosed in a compartment filled with lipids in which they accumulated, in turn, host cell lipids in the form of ILI (Peyron et al., 2008). These results showed, for the first time, that bacilli could use host-derived TAG as a potential source of nutrients to persist within granuloma FM. The process by which LB interacted with, and delivered their contents to, phagosomes remained, however, unclear until the advent of other models (see section Cells Exposed to Lipoproteins below).

Interestingly, this model allowed to identify mycobacterial factors involved in the differentiation of macrophages into FM within tuberculous granulomas (Figure 2A). Past work by Korf et al. had shown that mycolic acid (MA), a major lipid component of the cell wall of *M. tuberculosis*, administered to the peritoneal cavity or to the airways of mice could induce a unique macrophage morphotype, similar to the FM observed in human tuberculous granulomas (Korf et al., 2005). Following the above discovery, Peyron et al. compared FM formation in model granulomas obtained by exposure of PBMC either to *M. tuberculosis*, which synthesizes keto MA (kMA) or to *M. smegmatis*, which is devoid of kMA because the *hma* gene (Rv0642c, *mmaA4*) required for the production of oxygenated mycolic acid in pathogenic species, is not present in the non-pathogenic strain, *M. smegmatis*. FM were found only in granulomas prepared with *M. tuberculosis* or with recombinant strains of *M. smegmatis* over-expressing the *hma* gene product (Peyron et al., 2008).

Two recent studies confirmed that *in vitro*-grown human granulomas could be obtained by exposing PBMC to *M. tuberculosis* (Kapoor et al., 2013; Guirado et al., 2015). Using fluorescence microscopy approaches, Kapoor et al. confirmed that *M. tuberculosis* could accumulate lipids in the form of ILI within macrophages of the granulomatous structure. In addition, *M. tuberculosis* acquired other characteristics of



dormant bacilli, such as loss of acid-fastness and tolerance to rifampicin (Kapoor et al., 2013). Treatment of such granulomas with monoclonal antibodies raised against tumor necrosis factor- α (TNF α), lead to resuscitation of bacilli and concurrent IL1 consumption, suggestive of events resembling reactivation of TB. Guirado et al. identified the FM by staining the structures with Nile red (Guirado et al., 2015). They also showed that the amount of LB within FM was significantly higher when the PBMC used to construct the artificial human granulomas had been isolated from the blood of individuals with latent TB as opposed to that of healthy donors, thereby suggesting that differentiation of macrophages into FM is dependent on the host's immune status (Guirado et al., 2015).

A major advantage of the *in vitro*-grown human granuloma model, over *in vivo* animal models or *ex vivo* human biopsies, is the availability of live granuloma cells for analysis of their

specific features and interactions with *M. tuberculosis* during persistence and reactivation. However, its complexity further restricts the panel of experimentations. For example, it is difficult to obtain preparations of either pure FM or of pure non-foamy macrophages and to undertake detailed kinetic studies of cellular events during transition from one to the other. In addition, this type of model adds limited clues with respect to lipid accumulation/consumption in mycobacteria, thus prompting several investigators to develop simpler, better defined and easier-to-handle foam cell models.

Foam Cell Models

Cells Cultured under Conditions of Hypoxia

In recent work, Daniel et al. (2011) analyzed the acquisition of dormancy characteristics by *M. tuberculosis* residing in cells cultured under conditions of hypoxia (Figure 2B). Their model

was based on several observations among which: (i) caseous granulomas in the lungs of humans with untreated pulmonary TB contain lipid-loaded FM which harbor acid-fast bacilli (Hunter et al., 2007); (ii) such FM, which are found inside the hypoxic environment of TB granulomas, contain abundant stores of TAG and are thought to provide a lipid-rich environment for *M. tuberculosis* (Russell, 2007; Peyron et al., 2008); (iii) human macrophages cultured under conditions of hypoxia (1% O₂) accumulate TAG in LB (Bostrom et al., 2006); and (iv) tuberculous granulomas in guinea pigs, rabbits and non-human primates are hypoxic (Via et al., 2008).

Two different types of macrophages were used in their study. In the first case, THP-1 monocytes were cultured in RPMI-1640 containing 10% fetal calf serum in a 5% CO₂ incubator atmosphere at 37°C and differentiated into THP-M (THP-1 Macrophages), a frequently used macrophage-like cell line, obtained by stimulation with 100 nM phorbol 12-myristate 13-acetate (PMA) for 3 days. In the second case, the buffy coat obtained from Blood Centers after separation of other blood components was used for isolation of PBMC by density gradient centrifugation on Ficoll-Paque PLUS. PBMC were resuspended in RPMI-1640 and allowed to adhere onto plastic Petri dishes. Two hours later, non-adherent cells were removed and the adherent cells (mostly monocytes) were allowed to differentiate into macrophages over a period of 7 days under a 21% O₂, 5% CO₂ atmosphere in RPMI-1640 containing 10% human serum AB and 10 ng/ml granulocyte-macrophage colony stimulating factor (GM-CSF). Both types of macrophages were then infected with *M. tuberculosis* H37Rv at a MOI of either 0.1 or 5 bacilli per cell, and then incubated under hypoxia (1% O₂, 5% CO₂) for up to 5 days. Identical cells cultured in a normal environment (21% O₂, 5% CO₂) served as a control.

Under hypoxia conditions, both types of infected macrophages became foamy as shown by the accumulation of TAG-rich Oil-Red O-stained lipid droplets (Daniel et al., 2011). Inside such hypoxic FM, about half of the *M. tuberculosis* population developed tolerance to isoniazid, lost acid-fast staining and accumulated ILI. Moreover by disrupting the *Tgs1* gene, which is involved in TAG synthesis (Daniel et al., 2004; Sirakova et al., 2006; Viljoen et al., 2016), ILI formation and tolerance against antibiotics are reduced, suggesting that the lipid accumulation and drug tolerance are closely related (Baek et al., 2011). Subsequently, radioisotope and fluorescent fatty acid labeling of host TAG provided evidence for the utilization of the fatty acids from host TAG for lipid metabolism inside *M. tuberculosis*. Furthermore, reverse transcription PCR measurement revealed that several genes, known to be associated with dormancy and lipid metabolism, were upregulated in *M. tuberculosis* within the hypoxic lipid-loaded macrophages. Finally, *M. tuberculosis* was shown to replicate more slowly, thereby suggesting that the accumulation of TAG in mycobacterial ILI may be involved in mycobacterial growth. This latter result should, however, be interpreted with caution since at least 30% of the THP-M cells were no longer adherent by day 3 post-infection.

Cell growth under conditions of hypoxia represents an interesting approach for obtaining FM that closely resemble

those formed under the hypoxic environment found in human tuberculous granulomas. However, to the extent that *in vitro* culturing of cells, and more especially of cell lines, such as THP-M, with or without hypoxia, may lead to cell death and the resulting release of fatty acids, the latter may serve as a source for TAG in both cellular LB and mycobacterial ILI rather than hypoxia itself. Likewise, *M. tuberculosis*, mostly in human macrophages, perturbs cellular lipid homeostasis, which results in the accumulation of LB in macrophages (Kim et al., 2010; Singh et al., 2012; Podinovskaia et al., 2013).

Cells Exposed to Fatty Acids

Murine bone marrow-derived macrophages (BMDM) exposed to oleic acid

Several teams have shown that *M. tuberculosis* infection can lead to the retention of lipids and the maintenance of a foamy phenotype, notably when the host cell is a human monocyte-derived macrophages (HMDM) fed with human serum AB during culturing or within human *in vitro*-grown granulomas (Peyron et al., 2008).

The FM phenotype can also be induced by feeding BMDM with exogenous fatty acids, such as oleic acid. In this experimental model (Lee et al., 2013; Podinovskaia et al., 2013) BMDM were incubated for 24 h in medium containing 400 μM oleate, complexed with BSA (Figure 2C). Cells were then infected with *M. tuberculosis* and the retention of the sequestered lipids was monitored for several days. The neutral lipids within LB were stained with the hydrophobic dye BODIPY 493/503 and observed by confocal microscopy. Comparable levels of fluorescent intensity were observed in both uninfected and infected macrophages after 24 h of exposure to oleate. Uninfected cells rapidly lost their LB content upon further culturing while those infected with *M. tuberculosis* retained the lipids within the LB, presumably due to reduced phagosomal lipolysis albeit many other factors may also be responsible for the decreased degradation/turnover of lipids in the infected cells.

Using the same model system, lipids in the form of ILI were also seen within *M. tuberculosis*, as reported previously (Peyron et al., 2008). To determine whether *M. tuberculosis* could have access to the host cell-derived lipids, cells were first infected with *M. tuberculosis* and incubated for 4 days to allow for the establishment of the infection. Cells were then exposed to oleate overnight and then pulsed with BODIPY FL-C16. This fluorescent dye was incorporated into both the host LB and the ILI within *M. tuberculosis*, thereby demonstrating that *M. tuberculosis* has access to lipids initially sequestered in host cell LB. However, how mycobacteria gain access to host lipids remained obscure.

Dictyostelium discoideum exposed to palmitic acid

The amoeba, *Dictyostelium discoideum*, widely used to characterize a variety of cellular processes, has been used recently to characterize the intracellular lipid metabolism and identify new proteins involved in lipid storage (Du et al., 2013).

In order to induce the accumulation of lipid droplets in *D. discoideum*, the axenic growth medium was supplemented with 200 μM non-esterified palmitic acid C16 prepared from a

100 mM stock solution stored at -20°C . After 3 h of incubation in the presence of free-fatty acid (FFA), cells were re-incubated in fat-free medium. At selected time points thereafter, LB formation/degradation was monitored with Nile red, that serves to stain neutral lipids within LB, and further analyzed by thin layer chromatography (Du et al., 2013). Following exposure to palmitic acid for 3 h, the cells contained large amounts of LB and the TAG concentration had increased approximately 23-fold (Figure 3A; Du et al., 2013).

Based on these observations, Barisch et al. made use of this new foam cell model to characterize both the host and mycobacterial lipid metabolism upon *M. marinum* infection (Barisch et al., 2015). *D. discoideum* was first grown in axenic medium supplemented with $200\ \mu\text{M}$ palmitic acid for 3 h. In some cases, BODIPY 558/568 C12 was added at a final concentration of $2\ \mu\text{M}$ to label host TAG. After re-incubation in medium devoid of FFA, the cells were infected with *M. marinum*. Interactions between host LB and the *M. marinum*-containing vacuole were monitored by fluorescence microscopy and electron microscopy and time-lapse movies taken with a spinning disc confocal system. Strikingly, and within only 10 min post-infection, BODIPY-labeled LB, initially scattered in the host cell cytosol, started to cluster around *M. marinum*-containing vacuoles, and this process continued until significant depletion of LB in the host cell cytosol (Figure 3B; Barisch et al., 2015).

When similar experiments were performed with amikacin-killed bacteria, LB were not recruited to the *M. marinum*-containing vacuoles (Figure 3C). That lipid droplets accumulate in the close vicinity of vacuoles containing live, but not dead, mycobacteria suggests an active recruitment of the LB. Mycobacterial factors secreted into the host cytosol may participate in this process. The authors reported that the amount of LB-associated BODIPY fluorescence in the cytoplasm of cells exposed to amikacin-killed *M. marinum* was not significantly different from that observed in uninfected cells (Barisch et al., 2015). Therefore, the absence of visible lipid droplets in the close vicinity of vacuoles containing dead bacilli could be related to the induction of a lower number of lipid droplets.

At 3 h post-infection, an accumulation of BODIPY-stained neutral lipids was observed in the lumen of the bacterium-containing vacuole (Figures 3D,E). EM analysis revealed also the presence of lipid and membrane-related structures within the *M. marinum*-containing vacuoles and, at later stages, ILI could be visualized inside the bacilli. These data suggest that the neutral lipids contained in host LB are delivered into the bacilli-containing vacuole from where they are transferred to mycobacteria where they accumulate in the form of ILI. In *D. discoideum* infected with *M. marinum*, it appears that the TAG-rich LB are engulfed by phagocytic vacuoles via a process that is reminiscent of autophagy (Peyron et al., 2008) rather

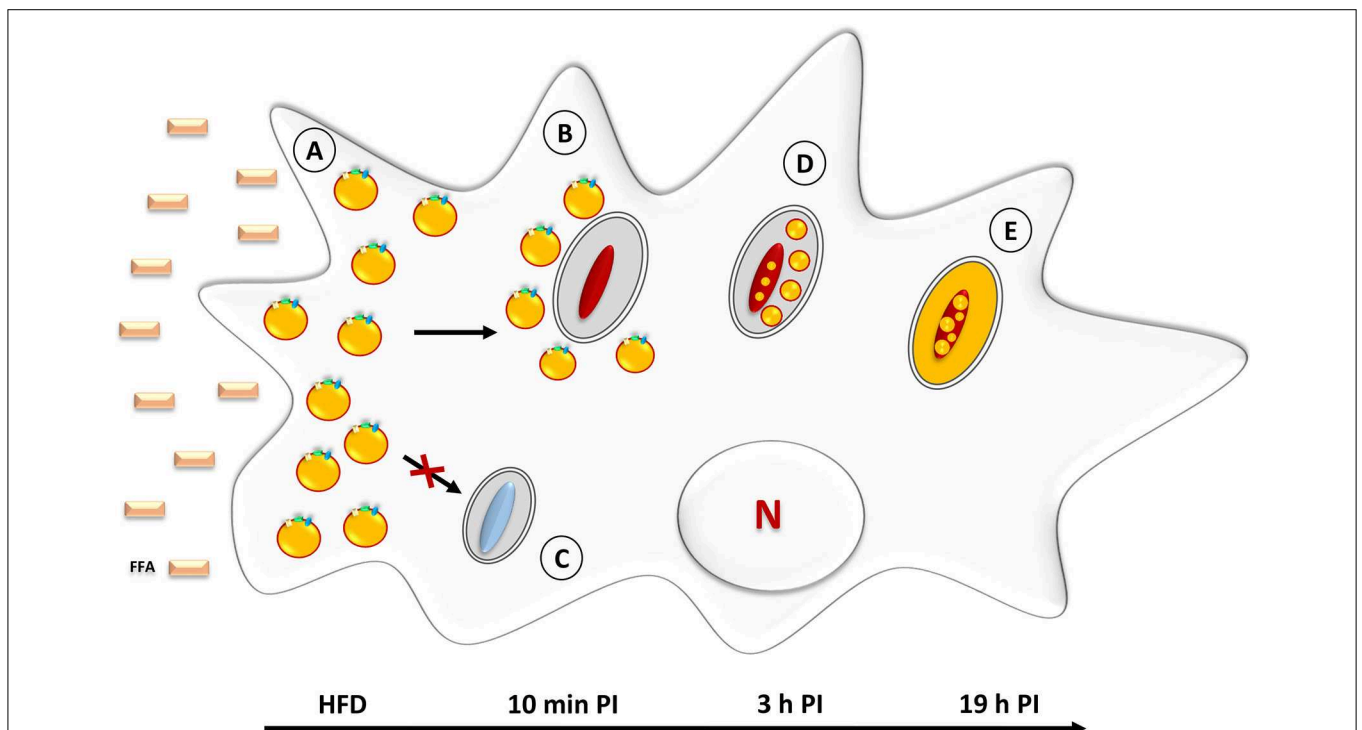


FIGURE 3 | Neutral lipid accumulation in *Mycobacterium marinum*-infected *D. discoideum*. (A) Prior to infection, amoebae are incubated with palmitic acid, corresponding to the High Fat Diet (HFD). This triggers the rapid formation of LB which leads to a foamy appearance. (B) Within 10 min post-infection with *M. marinum*, LB are gathered around the mycobacteria-containing vacuoles. (C) Infection with amikacin-killed mycobacteria fails to induce LB movement/relocation to the mycobacteria-containing vacuoles. (D) At 3 h post-infection, intact LB are found within the lumen of *M. marinum*-containing vacuoles. At this stage, a few ILI are already detectable inside the bacteria. (E) At later stages (19 h post-infection), neutral lipids are homogeneously distributed inside the mycobacterial cytosol where they accumulate in the form of large ILI.

than by direct fusion of LB with mycobacterium-containing phagosomes. The latter mechanism has been proven by EM approaches in another foam cell model (Caire-Brändli et al., 2014), described under section Cells Exposed to Lipoproteins.

Although the well-established model *D. discoideum* presents major assets for studying host-pathogen interplay, its main limitations reside in its growth conditions which are clearly different from those used to grow pathogenic mycobacteria. Whereas amoeba are grown at 22°C, *M. tuberculosis* has an optimal growth temperature of 37°C. Therefore, infections in *Dictyostelium* can only be performed with mycobacterial species growing at low temperatures, such as *M. marinum*, a species genetically related to *M. tuberculosis* and causing TB-like diseases in frogs and fish.

Cells Exposed to Lipoproteins

It has been suggested that the use of lipoprotein, rather than FFA, as an external source of lipids allows a lower lipid diffusion rate inside the host cell, a critical step for studying lipid metabolism of intracellular mycobacteria (Figure 2C; Dhouib et al., 2011; Caire-Brändli et al., 2014). Several investigators have, therefore, opted to expose mycobacterium-infected macrophages to lipoproteins, a choice guided by the fact that lipoproteins would provide lipids for the development of FM located close to the necrotic center of the granulomas (Peyron et al., 2008) where the caseum contains large amounts of cholesterol esters, cholesterol, TAG, and phospholipids from damaged/decaying cells (Kim et al., 2010). Lipids in lipoproteins that are internalized by scavenger receptor-mediated endocytosis undergo hydrolysis in lysosomes and provide the fatty acids for the subsequent biosynthesis of TAG in LB (Figure 2D).

It is well known that when mycobacteria reside in phagosomes of foam cells, both the LB that give the cells their foamy appearance and the ILI accumulating in persistent bacilli, contain TAG as the major lipid component (Christensen et al., 1999; Tauchi-Sato et al., 2002; Wältermann and Steinbüchel, 2005). For this reason, a new experimental model of FM was developed (Caire-Brändli et al., 2014). In this model VLDL was preferred to low-density lipoprotein (LDL) or high-density lipoprotein (HDL) as an external source of lipid, because of its high TAG content (Mori et al., 2001). In contrast, LDL has a high sterol content and a low TAG content and HDL has a low content of both TAG and sterol. The experimental set-up consisted in first infecting BMDM with *M. avium* and, after active replication for 6 days, exposing the cells to VLDL as a lipid source (Caire-Brändli et al., 2014). Quantitative analysis of detailed EM observations combined with scoring of the number of CFU showed the following results: (i) macrophages became foamy (Figure 4A), and mycobacteria formed ILI (Figure 4C), for which host TAG, rather than cholesterol, was essential; (ii) host lipid transfer occurred *via* mycobacterium-induced fusion between LB and phagosomes (Figure 4B); (iii) mycobacteria displayed a thinned cell wall and became elongated but mycobacterial division was arrested; (iv) upon removal of VLDL, both the macrophage LB and the mycobacterial ILI declined within hours, and simultaneous resumption of mycobacterial division restored the number of bacteria to the same level as that found in untreated

control macrophages (Caire-Brändli et al., 2014). From these data, the authors proposed that VLDL-driven FM constitute a well-defined cellular system in which to study changed metabolic states of intracellular mycobacteria that may relate to persistence and reactivation of TB.

The strength of this experimental system resides in its ability to generate defined conditions for triggering the formation or removal of LB, which induces ILI formation or consumption, respectively, and, in turn, leads to the reversible arrest of mycobacterial division without affecting bacterial growth. Furthermore, the use of EM approaches has allowed to studying major events at the subcellular level that cannot be observed by confocal microscopy, such as fusion of LB with mycobacterium-containing phagosomes or the alteration of the mycobacterial cell wall by thinning out of the electron-translucent outermost layer. The latter might result from an altered mycolic acid synthesis that might be responsible for loss of acid fastness and resistance to antibiotics (Bhatt et al., 2007; Vilch ze et al., 2014). Moreover, this approach allowed the authors to qualitatively demonstrate (i) incremental stages of ILI formation and, (ii) the presence or absence of septum formation in elongated cells. Importantly, these observations were sufficiently reliable and reproducible for quantitative analysis that allowed the authors to characterize the relationship between fluctuations of the ILI status and the arrest of mycobacterial division.

One may argue that under physiological conditions, neither monocytes nor lipoproteins will be found in the interstitium where a granuloma develops. Monocyte recruitment at such an inflammatory site may, however, be accompanied by an increased vascular permeability that would allow lipoproteins to leave the intravascular compartment, whereafter chemical modification enhances their uptake through scavenger receptors on macrophages.

In any case, this experimental model could be extremely beneficial for delineating the molecular mechanism responsible for the fusion of host LB with mycobacterium-containing phagosomes which leads to the translocation of host lipids to mycobacterium-containing phagosomes and for identifying the mycobacterial lipases involved in TAG accumulation and consumption during persistence and reactivation of TB.

Adipocytes

About 15% of the reactivation cases of TB occur at extrapulmonary sites without an apparent pathology in the lungs (Wares et al., 2005; WHO, 2015). Many different organs and tissues are likely to host persistent *M. tuberculosis* during latency. Infection of non-immune cells with *M. tuberculosis* was, therefore, explored (Neyrolles et al., 2006; Randall et al., 2015). The adipose tissue, which is broadly distributed throughout the body, was likely to be a haven of choice for *M. tuberculosis* firstly because adipocytes display macrophage-like properties, such as the ability to phagocytose inert particles or living microorganisms, and, more especially because they could provide a natural lipid-rich environment for persistent bacilli (Cousin et al., 1999; Charri re et al., 2003; Neyrolles et al., 2006; Agarwal et al., 2014; Rastogi et al., 2016).

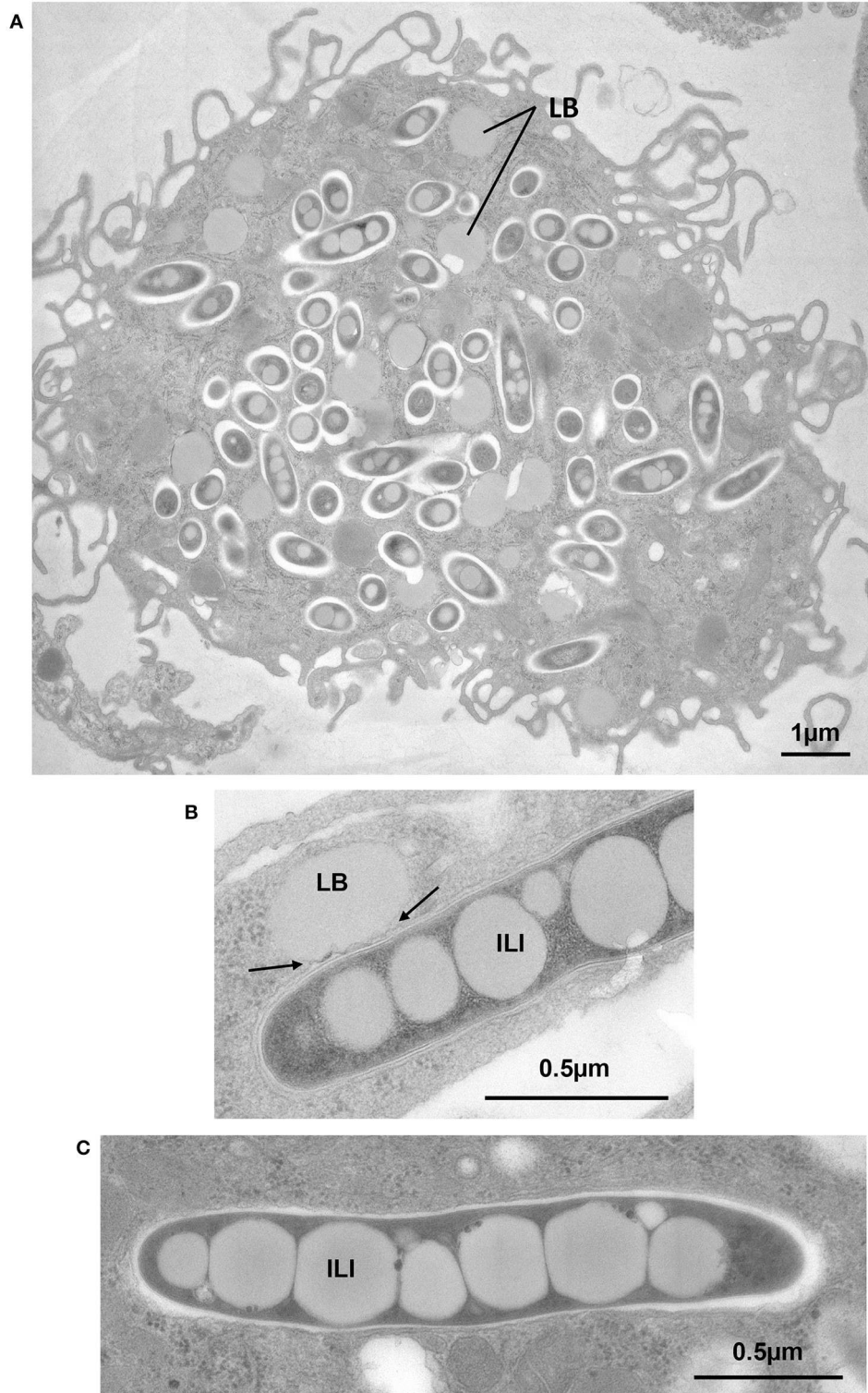


FIGURE 4 | Exposure of BMDM to VLDL induces foam cell formation, transfer of host TAG to mycobacterium-containing phagosomes by fusion of LB with phagosomes and accumulation of TAG in the form of ILI. BMDM were infected with *M. avium* or *M. bovis* BCG. At day 6 post-infection., cells were exposed to VLDL for 24 h, fixed and processed for EM. **(A)** *M. avium*-infected cell displaying large amounts of LB, typical of FM. **(B)** BCG-containing phagosome in direct contact with an LB showing deformation of the phagosome membrane (arrows). **(C)** Intraphagosomal *M. avium* displaying several large ILI, 0.4 to 0.5 μm in width, and extending across the full width of the *M. avium* cytoplasm.

In this context, both the 3T3-L1 murine adipose cell line and human primary adipocytes were used as models to investigate interactions with *M. tuberculosis*. The immortalized 3T3-L1 murine cell line, derived from embryonic fibroblasts, has been widely used to obtain mature adipocytes by a chemically-induced differentiation process (Agarwal et al., 2014). The differentiation process of 3T3-L1 cells leads to the increased synthesis and huge accumulation of TAG in the form of LB (Figure 5A). Likewise, primary human adipocytes extracted from plastic surgery wastes can also be differentiated *in vitro* (Agarwal et al., 2014). During the infection process, *M. tuberculosis* is taken up by adipocytes of murine or human origin, after binding to scavenger receptors, and persists in a non-replicating state (Neyrolles et al., 2006). EM observations performed at 24 h post-infection, showed intracellular bacilli within membrane-bound vacuoles. A few bacilli were observed inside vacuoles whose electron translucent lumen was similar to that of LB. This observation added to the fact that the membrane of such vacuoles stained positively for perilipin, a specific surface marker of lipid droplets in adipocytes (Blanchette-Mackie et al., 1995), suggests that they most likely resulted from the fusion of adipocyte

lipid droplets with the *M. tuberculosis*-containing vacuoles. Strikingly, bacilli within these vacuoles were heavily loaded with intracytosolic electron-translucent lipid inclusions, suggestive of a possible persistent phenotype (Figure 5B; Neyrolles et al., 2006). In agreement with these results, a more recent study proved that both *M. tuberculosis* H37Rv and H37Ra strains persist in a non-replicating state within adipocytes for up to 10 days post-infection (Kim et al., 2011). Interestingly, in this work observations of infected cells by confocal microscopy clearly showed intracellular bacilli in the close vicinity of LB, as demonstrated before with EM approaches (Neyrolles et al., 2006).

Finally, experimental infection of mature adipocytes directly isolated from the inguinal foot pads of mice or differentiated *ex vivo* from murine stromal vascular cells confirmed that *M. tuberculosis* infects natural murine adipocytes and pre-adipocytes (Agarwal et al., 2014). The fact that intra-adipocyte bacilli accumulate ILI starting from the third day post-infection, as assessed by a Nile red staining of neutral lipids (Agarwal et al., 2014), strengthens the validity of the 3T3-L1 murine cell model for studying lipid accumulation mechanisms leading to the persistence of *M. tuberculosis* outside the lungs. They also present

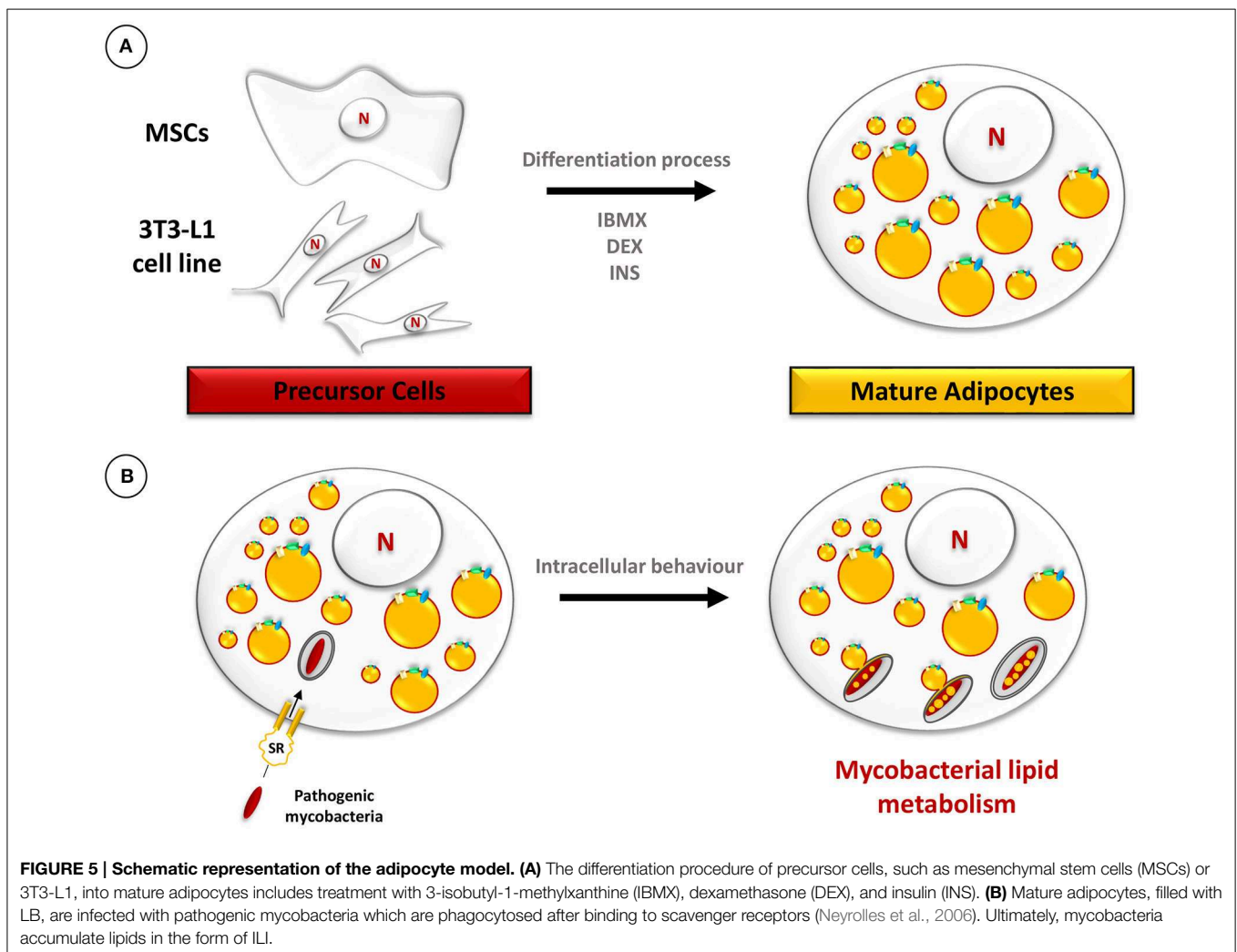


FIGURE 5 | Schematic representation of the adipocyte model. (A) The differentiation procedure of precursor cells, such as mesenchymal stem cells (MSCs) or 3T3-L1, into mature adipocytes includes treatment with 3-isobutyl-1-methylxanthine (IBMX), dexamethasone (DEX), and insulin (INS). **(B)** Mature adipocytes, filled with LB, are infected with pathogenic mycobacteria which are phagocytosed after binding to scavenger receptors (Neyrolles et al., 2006). Ultimately, mycobacteria accumulate lipids in the form of ILI.

the technical advantage of physiologically storing fat, thereby providing a natural lipid-rich environment, without additional induction steps to provide a foamy phenotype. However, once differentiated into mature adipocytes, filled with LB, the cells cannot revert back to a non-foamy phenotype. Therefore, this model is suitable for studying the accumulation of mycobacterial lipids but the fact that the cellular lipid-rich environment is non-reversible make this system inappropriate for investigating lipid consumption within mycobacteria.

CONCLUDING REMARKS AND FUTURE PROSPECTS

The different models presented in the present review have allowed to obtain relevant information on lipid metabolism in the context of *M. tuberculosis* persistence and reactivation. The use of animal models and *ex vivo* experimental systems have led to breakthrough information regarding cellular and molecular aspects related to (i) the acquisition of a foam cell phenotype where cells can be induced to store fat within LB under specific stimuli; (ii) the transfer of host LB contents to the lumen of the mycobacterium-containing phagosome following fusion events between LB and phagosomes, and (iii) the accumulation of neutral lipids in the form of ILI within mycobacteria.

Indeed, this large number of well-established host-pathogens systems, has allowed, recently the identification of a wide range of macrophages genes which are directly involved into pro-inflammatory response, energetic metabolism, such as glucose and lipid anabolism/catabolism leading to a foamy phenotype (Singh et al., 2015; Bhagyaraj et al., 2016; Holla et al., 2016).

In addition to those host factors, several mycobacterial proteins are likely to be involved in these various processes and identified (Deb et al., 2006; Kim et al., 2010; Low et al., 2010; Daniel et al., 2016).

As pointed out by Höner Zu Bentrup and Russell (2001), many genes of the *M. tuberculosis* genome encode enzymes involved in lipid metabolism (Cole et al., 1998). Among these, several might play important roles in the above-mentioned processes, particularly in the fusion events between LB and mycobacterium-containing phagosomes and the release of host lipids. As proposed by Caire-Brändli et al. (2014), these events can be viewed as the reverse steps involved in the transfer of lipids from the ER into the cytosol in the form of LB. The phospholipid monolayer leaflet covering the entire LB could merge with the outer leaflet of the phagosome membrane bilayer. This would leave the lipid contents between the two leaflets of the phagosomal membrane bilayer, where they remain separated from the mycobacterial surface by the inner leaflet. Because this remaining phospholipid barrier would present a different molecular arrangement than the otherwise intact phagosome membrane bilayer, it might be more vulnerable to the attack by mycobacterial lipolytic enzymes. Several mycobacteria, like *M. avium*, *M. tuberculosis*, and *M. bovis* BCG, seem to use essentially the neutral lipids contained within LB as a source of carbon during persistence, by secreting their own lipolytic enzymes and by activating host lipolytic enzymes (Daniel et al.,

2011; Singh et al., 2012). In this context, *M. tuberculosis* genes encoding lipid/ester hydrolases, with a wide range of hydrolytic activities (Dedieu et al., 2013), deserve special attention. These enzymes display specific properties, such as the ability to be secreted and the capacity to hydrolyze phospholipid membrane layers. Cytotoxic effects have also been associated with some of these enzymes (Bakala N'goma et al., 2010; Schué et al., 2010). We propose that these enzymes attack the inner leaflet of the phagosome membrane bilayer. As a consequence, the LB content is released inside the phagosomal lumen, in the immediate vicinity of the mycobacterial surface. EM analyses also revealed that TAG from LB are rapidly re-used to form ILI, indicating that these molecules are first hydrolyzed to produce FFA and then imported inside the bacterial cytosol (Caire-Brändli et al., 2014). This implies the contribution of mycobacterial lipases exposed at the cell wall surface. The *HSL*-homologue LipY (Rv3097c), which hydrolyses long fatty acyl chains, is secreted by a type VII secretion system (ESX-5). LipY remains one of the most studied lipase of *M. tuberculosis* (Deb et al., 2006; Mishra et al., 2008; Delorme et al., 2012). Deletion of the *lipY* gene is accompanied by a significant decrease in the amount of ILI, indicating that LipY participates in TAG hydrolysis (Deb et al., 2006), although additional lipolytic activities are likely to be involved (Côtes et al., 2007; Dhouib et al., 2010; Schué et al., 2010). Recent transcriptomic studies in adipocytes infected with *M. tuberculosis* also favored the potential involvement of various *M. tuberculosis* lipases, cutinases, and esterases in lipid accumulation/consumption processes (Rastogi et al., 2016).

How the major lipolysis products derived from host TAG (DAG, MAG, and FFA) are formed and how they gain access to the mycobacterial cytosol is not fully understood. Over the past few years, several membrane proteins have been identified as potential actors of nutrient uptake and/or lipid mobilization in mycobacteria (Daniel et al., 2014; Ates et al., 2015; Martinot et al., 2016). Interestingly, a specific class of fatty acid transporter proteins (FATP), conserved in mycobacteria and humans, has been identified as a potential actor in the mobilization and activation of FFA (Hirsch et al., 1998; Daniel et al., 2014) leading to TAG synthesis by bacterial di and triacylglycerol synthases (Daniel et al., 2004; Sirakova et al., 2006; Viljoen et al., 2016).

We anticipate that the use of these various and complementary models and approaches described in the present review will undoubtedly facilitate the discovery of new cellular events and/or mycobacterial factors that will help to further delineate the intricate mechanisms involved in mycobacterial lipid acquisition and assimilation during the intracellular lifestyle of *M. tuberculosis*.

AUTHOR CONTRIBUTIONS

PS participated in the drafting of the section on lipid accumulation in macrophages, FB on adipocytes and NS on Dictyostelium parts. The introduction section was written by PS and FB. The figures were drawn by PS and electron microscopy pictures were provided by CD and IP. MD was helpful for correcting the manuscript. LK, CD, and SC completed and

revised the entire manuscript. All of this work was proposed and supervised by SC.

ACKNOWLEDGMENTS

PS. received financial support for his PhD fellowship from the Ministère de l'Enseignement Supérieur et de la Recherche, France; FB and NS received financial support from the IHU Méditerranée Infection, Marseille, France. We are also grateful for the support from the Centre National de la Recherche Scientifique (CNRS), the Université d'Aix-Marseille (AMU),

the Institut National de la Santé et de la Recherche Médicale (INSERM), the Fondation pour la Recherche Médicale (FRM) (DEQ20150331719) and the Assistance Publique Hôpitaux de Marseille (APHM). The EM observations were performed in the PiCSL EM core facility (Institut de Biologie du Développement/Aix Marseille Université, Marseille, France), a member of the France-BioImaging research infrastructure. CD and SC would like to acknowledge the expertise of Lutz Thilo (University of Cape Town, South Africa) who contributed to setting up the experimental model of VLDL-driven foamy macrophages.

REFERENCES

- Agarwal, P., Khan, S. R., Verma, S. C., Beg, M., Singh, K., Mitra, K., et al. (2014). *Mycobacterium tuberculosis* persistence in various adipose depots of infected mice and the effect of anti-tubercular therapy. *Microbes Infect.* 16, 571–580. doi: 10.1016/j.micinf.2014.04.006
- Alvarez, H. M. (2016). Triacylglycerol and wax ester-accumulating machinery in prokaryotes. *Biochimie* 120, 28–39. doi: 10.1016/j.biochi.2015.08.016
- Ates, L. S., Ummels, R., Commandeur, S., Van De Weerd, R., Sparrius, M., Weerdenburg, E., et al. (2015). Essential role of the ESX-5 secretion system in outer membrane permeability of pathogenic *Mycobacteria*. *PLoS Genet.* 11:e1005190. doi: 10.1371/journal.pgen.1005190
- Baek, S. H., Li, A. H., and Sasseti, C. M. (2011). Metabolic regulation of mycobacterial growth and antibiotic sensitivity. *PLoS Biol.* 9:e1001065. doi: 10.1371/journal.pbio.1001065
- Bakala N'goma, J. C., Schué, M., Carrière, F., Geerlof, A., and Canaan, S. (2010). Evidence for the cytotoxic effects of *Mycobacterium tuberculosis* phospholipase C towards macrophages. *Biochim. Biophys. Acta* 1801, 1305–1313. doi: 10.1016/j.bbali.2010.08.007
- Barisch, C., Paschke, P., Hagedorn, M., Maniak, M., and Soldati, T. (2015). Lipid droplet dynamics at early stages of *Mycobacterium marinum* infection in Dictyostelium. *Cell. Microbiol.* 17, 1332–1349. doi: 10.1111/cmi.12437
- Beatty, W. L., Rhoades, E. R., Ullrich, H. J., Chatterjee, D., Heuser, J. E., and Russell, D. G. (2000). Trafficking and release of mycobacterial lipids from infected macrophages. *Traffic* 1, 235–247. doi: 10.1034/j.1600-0854.2000.010306.x
- Bhagyaraj, E., Nanduri, R., Saini, A., Dkhar, H. K., Ahuja, N., Chandra, V., et al. (2016). Human Xenobiotic Nuclear Receptor PXR augments *Mycobacterium tuberculosis* survival. *J. Immunol.* 197, 244–255. doi: 10.4049/jimmunol.1600203
- Bhatt, A., Fujiwara, N., Bhatt, K., Gurcha, S. S., Kremer, L., Chen, B., et al. (2007). Deletion of kasB in *Mycobacterium tuberculosis* causes loss of acid-fastness and subclinical latent tuberculosis in immunocompetent mice. *Proc. Natl. Acad. Sci. U.S.A.* 104, 5157–5162. doi: 10.1073/pnas.0608654104
- Blanchette-Mackie, E. J., Dwyer, N. K., Barber, T., Coxey, R. A., Takeda, T., Rondinone, C. M., et al. (1995). Perilipin is located on the surface layer of intracellular lipid droplets in adipocytes. *J. Lipid Res.* 36, 1211–1226.
- Bostrom, P., Magnusson, B., Svensson, P. A., Wiklund, O., Borén, J., Carlsson, L. M., et al. (2006). Hypoxia converts human macrophages into triglyceride-loaded foam cells. *Arterioscler. Thromb. Vasc. Biol.* 26, 1871–1876. doi: 10.1161/01.ATV.0000229665.78997.0b
- Brasaemle, D. L., Dolios, G., Shapiro, L., and Wang, R. (2004). Proteomic analysis of proteins associated with lipid droplets of basal and lipolytically stimulated 3T3-L1 adipocytes. *J. Biol. Chem.* 279, 46835–46842. doi: 10.1074/jbc.M409340200
- Cáceres, N., Tapia, G., Ojanguren, I., Altare, F., Gil, O., Pinto, S., et al. (2009). Evolution of foamy macrophages in the pulmonary granulomas of experimental tuberculosis models. *Tuberculosis (Edinb.)* 89, 175–182. doi: 10.1016/j.tube.2008.11.001
- Caire-Brändli, I., Papadopoulos, A., Malaga, W., Marais, D., Canaan, S., Thilo, L., et al. (2014). Reversible lipid accumulation and associated division arrest of *Mycobacterium avium* in lipoprotein-induced foamy macrophages may resemble key events during latency and reactivation of tuberculosis. *Infect. Immun.* 82, 476–490. doi: 10.1128/IAI.01196-13
- Cardona, P. J., Llatjós, R., Gordillo, S., Díaz, J., Ojanguren, I., Ariza, A., et al. (2000). Evolution of granulomas in lungs of mice infected aerogenically with *Mycobacterium tuberculosis*. *Scand. J. Immunol.* 52, 156–163. doi: 10.1046/j.1365-3083.2000.00763.x
- Cardoso, M. S., Silva, T. M., Resende, M., Appelberg, R., and Borges, M. (2015). Lack of the transcription factor hypoxia-inducible factor 1alpha (HIF-1alpha) in macrophages accelerates the necrosis of *Mycobacterium avium*-induced granulomas. *Infect. Immun.* 83, 3534–3544. doi: 10.1128/IAI.00144-15
- Charrière, G., Cousin, B., Arnaud, E., André, M., Bacou, F., Penicaud, L., et al. (2003). Preadipocyte conversion to macrophage. Evidence of plasticity. *J. Biol. Chem.* 278, 9850–9855. doi: 10.1074/jbc.M210811200
- Christensen, H., Garton, N. J., Horobin, R. W., Minnikin, D. E., and Barer, M. R. (1999). Lipid domains of mycobacteria studied with fluorescent molecular probes. *Mol. Microbiol.* 31, 1561–1572. doi: 10.1046/j.1365-2958.1999.01304.x
- Cole, S. T., Brosch, R., Parkhill, J., Garnier, T., Churcher, C., Harris, D., et al. (1998). Deciphering the biology of *Mycobacterium tuberculosis* from the complete genome sequence. *Nature* 393, 537–544. doi: 10.1038/31159
- Côtes, K., Dhouib, R., Douchet, I., Chahinian, H., De Caro, A., Carrière, F., et al. (2007). Characterization of an exported monoglyceride lipase from *Mycobacterium tuberculosis* possibly involved in the metabolism of host cell membrane lipids. *Biochem. J.* 408, 417–427. doi: 10.1042/BJ20070745
- Cousin, B., Munoz, O., Andre, M., Fontanilles, A. M., Dani, C., Cousin, J. L., et al. (1999). A role for preadipocytes as macrophage-like cells. *FASEB J.* 13, 305–312.
- Daniel, J., Deb, C., Dubey, V. S., Sirakova, T. D., Abomoelak, B., Morbidoni, H. R., et al. (2004). Induction of a novel class of diacylglycerol acyltransferases and triacylglycerol accumulation in *Mycobacterium tuberculosis* as it goes into a dormancy-like state in culture. *J. Bacteriol.* 186, 5017–5030. doi: 10.1128/JB.186.15.5017-5030.2004
- Daniel, J., Kapoor, N., Sirakova, T., Sinha, R., and Kolattukudy, P. (2016). The perilipin-like PPE15 protein in *Mycobacterium tuberculosis* is required for triacylglycerol accumulation under dormancy-inducing conditions. *Mol. Microbiol.* 101, 784–794. doi: 10.1111/mmi.13422
- Daniel, J., Maamar, H., Deb, C., Sirakova, T. D., and Kolattukudy, P. E. (2011). *Mycobacterium tuberculosis* uses host triacylglycerol to accumulate lipid droplets and acquires a dormancy-like phenotype in lipid-loaded macrophages. *PLoS Pathog.* 7:e1002093. doi: 10.1371/journal.ppat.1002093
- Daniel, J., Sirakova, T., and Kolattukudy, P. (2014). An acyl-CoA synthetase in *Mycobacterium tuberculosis* involved in triacylglycerol accumulation during dormancy. *PLoS ONE* 9:e114877. doi: 10.1371/journal.pone.0114877
- Datta, M., Via, L. E., Chen, W., Baish, J. W., Xu, L., Barry, C. E. III, et al. (2016). Mathematical model of oxygen transport in tuberculosis granulomas. *Ann. Biomed. Eng.* 44, 863–872. doi: 10.1007/s10439-015-1415-3
- Deb, C., Daniel, J., Sirakova, T. D., Abomoelak, B., Dubey, V. S., and Kolattukudy, P. E. (2006). A novel lipase belonging to the hormone-sensitive lipase family induced under starvation to utilize stored triacylglycerol in *Mycobacterium tuberculosis*. *J. Biol. Chem.* 281, 3866–3875. doi: 10.1074/jbc.M505556200
- Dedieu, L., Serveau-Avesque, C., Kremer, L., and Canaan, S. (2013). Mycobacterial lipolytic enzymes: a gold mine for tuberculosis research. *Biochimie* 95, 66–73. doi: 10.1016/j.biochi.2012.07.008

- Delorme, V., Diomandé, S. V., Dedieu, L., Cavalier, J. F., Carrière, F., Kremer, L., et al. (2012). MmPPOX Inhibits *Mycobacterium tuberculosis* lipolytic enzymes belonging to the hormone-sensitive lipase family and alters mycobacterial growth. *PLoS ONE* 7:e46493. doi: 10.1371/journal.pone.0046493
- Dhouib, R., Ducret, A., Hubert, P., Carrière, F., Dukan, S., and Canaan, S. (2011). Watching intracellular lipolysis in mycobacteria using time lapse fluorescence microscopy. *Biochim. Biophys. Acta* 1811, 234–241. doi: 10.1016/j.bbali.2011.01.001
- Dhouib, R., Laval, F., Carrière, F., Daffe, M., and Canaan, S. (2010). A monoacylglycerol lipase from *Mycobacterium smegmatis* Involved in bacterial cell interaction. *J. Bacteriol.* 192, 4776–4785. doi: 10.1128/JB.00261-10
- Dkhar, H. K., Nanduri, R., Mahajan, S., Dave, S., Saini, A., Somavarapu, A. K., et al. (2014). *Mycobacterium tuberculosis* keto-mycolic acid and macrophage nuclear receptor TR4 modulate foamy biogenesis in granulomas: a case of a heterologous and noncanonical ligand-receptor pair. *J. Immunol.* 193, 295–305. doi: 10.4049/jimmunol.1400092
- Driver, E. R., Ryan, G. J., Hoff, D. R., Irwin, S. M., Basaraba, R. J., Kramnik, I., et al. (2012). Evaluation of a mouse model of necrotic granuloma formation using C3HeB/FeJ mice for testing of drugs against *Mycobacterium tuberculosis*. *Antimicrobial Agents Chemother.* 56, 3181–3195. doi: 10.1128/AAC.00217-12
- Du, X., Barisch, C., Paschke, P., Herrfurth, C., Bertinetti, O., Pawolleck, N., et al. (2013). Dictyostelium lipid droplets host novel proteins. *Eukaryot. Cell* 12, 1517–1529. doi: 10.1128/EC.00182-13
- Feng, Y., Dorhoi, A., Mollenkopf, H. J., Yin, H., Dong, Z., Mao, L., et al. (2014). Platelets direct monocyte differentiation into epithelioid-like multinucleated giant foam cells with suppressive capacity upon mycobacterial stimulation. *J. Infect. Dis.* 210, 1700–1710. doi: 10.1093/infdis/jiu355
- Florey, H. (1958). "Tuberculosis," in *General Pathology Based on Lectures Delivered at the Sir William Dunn School of Pathology*, ed W. B. Saunders (Oxford: University of Oxford), 829–870.
- Galagan, J. E. (2014). Genomic insights into tuberculosis. *Nat. Rev. Genet.* 15, 307–320. doi: 10.1038/nrg3664
- Garton, N. J., Christensen, H., Minnikin, D. E., Adegbola, R. A., and Barer, M. R. (2002). Intracellular lipophilic inclusions of mycobacteria *in vitro* and in sputum. *Microbiology* 148, 2951–2958. doi: 10.1099/00221287-148-10-2951
- Geisel, R. E., Sakamoto, K., Russell, D. G., and Rhoades, E. R. (2005). *In vivo* activity of released cell wall lipids of *Mycobacterium bovis* bacillus Calmette-Guerin is due principally to trehalose mycolates. *J. Immunol.* 174, 5007–5015. doi: 10.4049/jimmunol.174.8.5007
- Gideon, H. P., and Flynn, J. L. (2011). Latent tuberculosis: what the host "sees"? *Immunol. Res.* 50, 202–212. doi: 10.1007/s12026-011-8229-7
- Glatz, J. F., Luiken, J. J., and Bonen, A. (2010). Membrane fatty acid transporters as regulators of lipid metabolism: implications for metabolic disease. *Physiol. Rev.* 90, 367–417. doi: 10.1152/physrev.00003.2009
- Guirado, E., Mbawuike, U., Keiser, T. L., Arcos, J., Azad, A. K., Wang, S. H., et al. (2015). Characterization of host and microbial determinants in individuals with latent tuberculosis infection using a human granuloma model. *MBio* 6, e02537–e02514. doi: 10.1128/mBio.02537-14
- Guirado, E., and Schlesinger, L. S. (2013). Modeling the *Mycobacterium tuberculosis* granuloma - the critical battlefield in host immunity and disease. *Front. Immunol.* 4:98. doi: 10.3389/fimmu.2013.00098
- Harris, C. A., Haas, J. T., Streeper, R. S., Stone, S. J., Kumari, M., Yang, K., et al. (2011). DGAT enzymes are required for triacylglycerol synthesis and lipid droplets in adipocytes. *J. Lipid Res.* 52, 657–667. doi: 10.1194/jlr.M013003
- Hingley-Wilson, S. M., Sambandamurthy, V. K., and Jacobs, W. R. Jr. (2003). Survival perspectives from the world's most successful pathogen, *Mycobacterium tuberculosis*. *Nat. Immunol.* 4, 949–955. doi: 10.1038/ni981
- Hirsch, D., Stahl, A., and Lodish, H. F. (1998). A family of fatty acid transporters conserved from *mycobacterium* to man. *Proc. Natl. Acad. Sci. U.S.A.* 95, 8625–8629. doi: 10.1073/pnas.95.15.8625
- Holla, S., Prakhar, P., Singh, V., Karnam, A., Mukherjee, T., Mahadik, K., et al. (2016). MUSASHI-mediated expression of JMJD3, a H3K27me3 demethylase, is involved in foamy macrophage generation during mycobacterial infection. *PLoS Pathog.* 12:e1005814. doi: 10.1371/journal.ppat.1005814
- Höner Zu Bentrup, K., and Russell, D. G. (2001). Mycobacterial persistence: adaptation to a changing environment. *Trends Microbiol.* 9, 597–605. doi: 10.1016/S0966-842X(01)02238-7
- Hunter, R. L., Jagannath, C., and Actor, J. K. (2007). Pathology of postprimary tuberculosis in humans and mice: contradiction of long-held beliefs. *Tuberculosis (Edinb).* 87, 267–278. doi: 10.1016/j.tube.2006.11.003
- Irwin, S. M., Driver, E., Lyon, E., Schrupp, C., Ryan, G., Gonzalez-Juarrero, M., et al. (2015). Presence of multiple lesion types with vastly different microenvironments in C3HeB/FeJ mice following aerosol infection with *Mycobacterium tuberculosis*. *Dis. Model. Mech.* 8, 591–602. doi: 10.1242/dmm.019570
- Jain, M., Petzold, C. J., Schelle, M. W., Leavell, M. D., Mougous, J. D., Bertozzi, C. R., et al. (2007). Lipidomics reveals control of *Mycobacterium tuberculosis* virulence lipids via metabolic coupling. *Proc. Natl. Acad. Sci. U.S.A.* 104, 5133–5138. doi: 10.1073/pnas.0610634104
- Kapoor, N., Pawar, S., Sirakova, T. D., Deb, C., Warren, W. L., and Kolattukudy, P. E. (2013). Human granuloma *in vitro* model, for TB dormancy and resuscitation. *PLoS ONE* 8:e53657. doi: 10.1371/journal.pone.0053657
- Karakousis, P. C., Yoshimatsu, T., Lamichhane, G., Woolwine, S. C., Nuermberger, E. L., Grosset, J., et al. (2004). Dormancy phenotype displayed by extracellular *Mycobacterium tuberculosis* within artificial granulomas in mice. *J. Exp. Med.* 200, 647–657. doi: 10.1084/jem.20040646
- Kassan, A., Herms, A., Fernández-Vidal, A., Bosch, M., Schieber, N. L., Reddy, B. J., et al. (2013). Acyl-CoA synthetase 3 promotes lipid droplet biogenesis in ER microdomains. *J. Cell Biol.* 203, 985–1001. doi: 10.1083/jcb.201305142
- Kaufmann, S. H. (2001). How can immunology contribute to the control of tuberculosis? *Nat. Rev. Immunol.* 1, 20–30. doi: 10.1038/35095558
- Keller, C., Lauber, J., Blumenthal, A., Buer, J., and Ehlers, S. (2004). Resistance and susceptibility to tuberculosis analysed at the transcriptome level: lessons from mouse macrophages. *Tuberculosis* 84, 144–158. doi: 10.1016/j.tube.2003.12.003
- Kim, J. S., Ryu, M. J., Byun, E. H., Kim, W. S., Whang, J., Min, K. N., et al. (2011). Differential immune response of adipocytes to virulent and attenuated *Mycobacterium tuberculosis*. *Microbes Infect.* 13, 1242–1251. doi: 10.1016/j.micinf.2011.07.002
- Kim, M. J., Wainwright, H. C., Locketz, M., Bekker, L. G., Walther, G. B., Dittrich, C., et al. (2010). Caseation of human tuberculosis granulomas correlates with elevated host lipid metabolism. *EMBO Mol. Med.* 2, 258–274. doi: 10.1002/emmm.201000079
- Korf, J., Stoltz, A., Verschoor, J., De Baetselier, P., and Grooten, J. (2005). The *Mycobacterium tuberculosis* cell wall component mycolic acid elicits pathogen-associated host innate immune responses. *Eur. J. Immunol.* 35, 890–900. doi: 10.1002/eji.200425332
- Kramnik, I., Demant, P., and Bloom, B. B. (1998). Susceptibility to tuberculosis as a complex genetic trait: analysis using recombinant congenic strains of mice. *Novartis Found. Symp.* 217, 120–131; discussion 132–127.
- Kramnik, I., Dietrich, W. F., Demant, P., and Bloom, B. R. (2000). Genetic control of resistance to experimental infection with virulent *Mycobacterium tuberculosis*. *Proc. Natl. Acad. Sci. U.S.A.* 97, 8560–8565. doi: 10.1073/pnas.150227197
- Kumar, A., Farhana, A., Guidry, L., Saini, V., Hondalus, M., and Steyn, A. J. (2011). Redox homeostasis in mycobacteria: the key to tuberculosis control? *Expert Rev. Mol. Med.* 13, e39. doi: 10.1017/S1462399411002079
- Lee, W., Vanderven, B. C., Fahey, R. J., and Russell, D. G. (2013). Intracellular *Mycobacterium tuberculosis* exploits host-derived fatty acids to limit metabolic stress. *J. Biol. Chem.* 288, 6788–6800. doi: 10.1074/jbc.M112.445056
- Listenberger, L. L., Han, X., Lewis, S. E., Cases, S., Farese, R. V. Jr., Ory, D. S., et al. (2003). Triglyceride accumulation protects against fatty acid-induced lipotoxicity. *Proc. Natl. Acad. Sci. U.S.A.* 100, 3077–3082. doi: 10.1073/pnas.0630588100
- Low, K. L., Rao, P. S., Shui, G., Bendt, A. K., Pethe, K., Dick, T., et al. (2009). Triacylglycerol utilization is required for regrowth of *in vitro* hypoxic non-replicating *Mycobacterium bovis* bacillus Calmette-Guerin. *J. Bacteriol.* 191, 5037–5043. doi: 10.1128/JB.00530-09
- Low, K. L., Shui, G., Natter, K., Yeo, W. K., Kohlwein, S. D., Dick, T., et al. (2010). Lipid droplet-associated proteins are involved in the biosynthesis and hydrolysis of triacylglycerol in *Mycobacterium bovis* bacillus Calmette-Guerin. *J. Biol. Chem.* 285, 21662–21670. doi: 10.1074/jbc.M110.135731
- Mahajan, S., Dkhar, H. K., Chandra, V., Dave, S., Nanduri, R., Janmeja, A. K., et al. (2012). *Mycobacterium tuberculosis* modulates macrophage lipid-sensing nuclear receptors PPARgamma and TR4 for survival. *J. Immunol.* 188, 5593–5603. doi: 10.4049/jimmunol.1103038

- Martin, S., and Parton, R. G. (2005). Caveolin, cholesterol, and lipid bodies. *Semin. Cell Dev. Biol.* 16, 163–174. doi: 10.1016/j.semcdb.2005.01.007
- Martinot, A. J., Farrow, M., Bai, L., Layre, E., Cheng, T. Y., Tsai, J. H., et al. (2016). Mycobacterial metabolic syndrome: LprG and Rv1410 regulate triacylglyceride levels, growth rate and virulence in *Mycobacterium tuberculosis*. *PLoS Pathog.* 12:e1005351. doi: 10.1371/journal.ppat.1005351
- Mattos, K. A., D'Avila, H., Rodrigues, L. S., Oliveira, V. G., Sarno, E. N., Atella, G. C., et al. (2010). Lipid droplet formation in leprosy: toll-like receptor-regulated organelles involved in eicosanoid formation and *Mycobacterium leprae* pathogenesis. *J. Leukoc. Biol.* 87, 371–384. doi: 10.1189/jlb.0609433
- Mattos, K. A., Lara, F. A., Oliveira, V. G., Rodrigues, L. S., D'Avila, H., Melo, R. C., et al. (2011). Modulation of lipid droplets by *Mycobacterium leprae* in Schwann cells: a putative mechanism for host lipid acquisition and bacterial survival in phagosomes. *Cell. Microbiol.* 13, 259–273. doi: 10.1111/j.1462-5822.2010.01533.x
- Mckinney, J. D., and Gomez, J. E. (2003). Life on the inside for *Mycobacterium tuberculosis*. *Nat. Med.* 9, 1356–1357. doi: 10.1038/nm1103-1356
- Mckinney, J. D., Höner Zu Bentrup, K., Muñoz-Elías, E. J., Miczak, A., Chen, B., Chan, W. T., et al. (2000). Persistence of *Mycobacterium tuberculosis* in macrophages and mice requires the glyoxylate shunt enzyme isocitrate lyase. *Nature* 406, 735–738. doi: 10.1038/35021074
- Mishra, K. C., De Chastellier, C., Narayana, Y., Bifani, P., Brown, A. K., Besra, G. S., et al. (2008). Functional role of the PE domain and immunogenicity of the *Mycobacterium tuberculosis* triacylglycerol hydrolase LipY. *Infect. Immun.* 76, 127–140. doi: 10.1128/IAI.00410-07
- Mori, M., Itabe, H., Higashi, Y., Fujimoto, Y., Shiomi, M., Yoshizumi, M., et al. (2001). Foam cell formation containing lipid droplets enriched with free cholesterol by hyperlipidemic serum. *J. Lipid Res.* 42, 1771–1781.
- Murphy, D. J. (2001). The biogenesis and functions of lipid bodies in animals, plants and microorganisms. *Prog. Lipid Res.* 40, 325–438. doi: 10.1016/S0163-7827(01)00013-3
- Murphy, D. J., and Vance, J. (1999). Mechanisms of lipid-body formation. *Trends Biochem. Sci.* 24, 109–115. doi: 10.1016/S0968-0004(98)01349-8
- Neyrolles, O., Hernández-Pando, R., Pietri-Rouxel, F., Fornes, P., Tailleux, L., Payan, J. A., et al. (2006). Is adipose tissue a place for *Mycobacterium tuberculosis* persistence? *PLoS ONE* 1:e43. doi: 10.1371/journal.pone.0000043
- Ohsaki, Y., Cheng, J., Suzuki, M., Shinohara, Y., Fujita, A., and Fujimoto, T. (2009). Biogenesis of cytoplasmic lipid droplets: from the lipid ester globule in the membrane to the visible structure. *Biochim. Biophys. Acta* 1791, 399–407. doi: 10.1016/j.bbailip.2008.10.002
- Ordway, D., Harton, M., Henao-Tamayo, M., Montoya, R., Orme, I. M., and Gonzalez-Juarrero, M. (2006). Enhanced macrophage activity in granulomatous lesions of immune mice challenged with *Mycobacterium tuberculosis*. *J. Immunol.* 176, 4931–4939. doi: 10.4049/jimmunol.176.8.4931
- Ordway, D., Henao-Tamayo, M., Orme, I. M., and Gonzalez-Juarrero, M. (2005). Foamy macrophages within lung granulomas of mice infected with *Mycobacterium tuberculosis* express molecules characteristic of dendritic cells and antiapoptotic markers of the TNF receptor-associated factor family. *J. Immunol.* 175, 3873–3881. doi: 10.4049/jimmunol.175.6.3873
- Pagel, W. (1925). Fat and lipid content to tuberculous tissue: Histochemical investigation. *Virchows Arch. Path. Anat.* 256, 629–640. doi: 10.1007/BF01891650
- Peyron, P., Vaubourgeix, J., Poquet, Y., Levillain, F., Botanch, C., Bardou, F., et al. (2008). Foamy macrophages from tuberculous patients' granulomas constitute a nutrient-rich reservoir for *M. tuberculosis* persistence. *PLoS Pathog.* 4:e1000204. doi: 10.1371/journal.ppat.1000204
- Pichugin, A. V., Yan, B. S., Sloutsky, A., Kobzik, L., and Kramnik, I. (2009). Dominant role of the *sst1* locus in pathogenesis of necrotizing lung granulomas during chronic tuberculosis infection and reactivation in genetically resistant hosts. *Am. J. Pathol.* 174, 2190–2201. doi: 10.2353/ajpath.2009.081075
- Podinovsky, M., Lee, W., Caldwell, S., and Russell, D. G. (2013). Infection of macrophages with *Mycobacterium tuberculosis* induces global modifications to phagosomal function. *Cell. Microbiol.* 15, 843–859. doi: 10.1111/cmi.12092
- Pol, A., Gross, S. P., and Parton, R. G. (2014). Review: biogenesis of the multifunctional lipid droplet: lipids, proteins, and sites. *J. Cell Biol.* 204, 635–646. doi: 10.1083/jcb.201311051
- Puissegur, M. P., Botanch, C., Duteyrat, J. L., Delsol, G., Caratero, C., and Altare, F. (2004). An *in vitro* dual model of mycobacterial granulomas to investigate the molecular interactions between mycobacteria and human host cells. *Cell. Microbiol.* 6, 423–433. doi: 10.1111/j.1462-5822.2004.00371.x
- Puissegur, M. P., Lay, G., Gilleron, M., Botella, L., Nigou, J., Marrakchi, H., et al. (2007). Mycobacterial lipomannan induces granuloma macrophage fusion via a TLR2-dependent, ADAM9- and beta1 integrin-mediated pathway. *J. Immunol.* 178, 3161–3169. doi: 10.4049/jimmunol.178.5.3161
- Ramakrishnan, L. (2012). Revisiting the role of the granuloma in tuberculosis. *Nat. Rev. Immunol.* 12, 352–366. doi: 10.1038/nri3211
- Randall, P. J., Hsu, N. J., Quesniaux, V., Ryffel, B., and Jacobs, M. (2015). *Mycobacterium tuberculosis* infection of the 'non-classical immune cell'. *Immunol. Cell Biol.* 93, 789–795. doi: 10.1038/icb.2015.43
- Rastogi, S., Agarwal, P., and Krishnan, M. Y. (2016). Use of an adipocyte model to study the transcriptional adaptation of *Mycobacterium tuberculosis* to store and degrade host fat. *Int. J. Mycobacteriol.* 5, 92–98. doi: 10.1016/j.ijmyco.2015.10.003
- Rhoades, E. R., Geisel, R. E., Butcher, B. A., McDonough, S., and Russell, D. G. (2005). Cell wall lipids from *Mycobacterium bovis* BCG are inflammatory when inoculated within a gel matrix: characterization of a new model of the granulomatous response to mycobacterial components. *Tuberculosis* 85, 159–176. doi: 10.1016/j.tube.2004.10.001
- Ridley, D. S., and Ridley, M. J. (1987). Rationale for the histological spectrum of tuberculosis. A basis for classification. *Pathology* 19, 186–192. doi: 10.3109/00313028709077132
- Russell, D. G. (2001). *Mycobacterium tuberculosis*: here today, and here tomorrow. *Nat. Rev. Mol. Cell Biol.* 2, 569–577. doi: 10.1038/35085034
- Russell, D. G. (2007). Who puts the tubercle in tuberculosis? *Nat. Rev. Microbiol.* 5, 39–47. doi: 10.1038/nrmicro1538
- Russell, D. G., Cardona, P. J., Kim, M. J., Allain, S., and Altare, F. (2009a). Foamy macrophages and the progression of the human tuberculosis granuloma. *Nat. Immunol.* 10, 943–948. doi: 10.1038/ni.1781
- Russell, D. G., Vanderven, B. C., Glennie, S., Mwandumba, H., and Heyderman, R. S. (2009b). The macrophage marches on its phagosome: dynamic assays of phagosome function. *Nat. Rev. Immunol.* 9, 594–600. doi: 10.1038/nri2591
- Saka, H. A., and Valdivia, R. (2012). Emerging roles for lipid droplets in immunity and host-pathogen interactions. *Annu. Rev. Cell Dev. Biol.* 28, 411–437. doi: 10.1146/annurev-cellbio-092910-153958
- Sassetti, C. M., and Rubin, E. J. (2003). Genetic requirements for mycobacterial survival during infection. *Proc. Natl. Acad. Sci. U.S.A.* 100, 12989–12994. doi: 10.1073/pnas.2134250100
- Schaale, K., Brandenburg, J., Kispert, A., Leitges, M., Ehlers, S., and Reiling, N. (2013). Wnt6 is expressed in granulomatous lesions of *Mycobacterium tuberculosis*-infected mice and is involved in macrophage differentiation and proliferation. *J. Immunol.* 191, 5182–5195. doi: 10.4049/jimmunol.12.01819
- Schué, M., Maurin, D., Dhoub, R., N'goma, J. C., Delorme, V., Lambeau, G., et al. (2010). Two cutinase-like proteins secreted by *Mycobacterium tuberculosis* show very different lipolytic activities reflecting their physiological function. *FASEB J.* 24, 1893–1903. doi: 10.1096/fj.09-144766
- Shashkin, P., Dragulev, B., and Ley, K. (2005). Macrophage differentiation to foam cells. *Curr. Pharm. Des.* 11, 3061–3072. doi: 10.2174/1381612054865064
- Singh, V., Jamwal, S., Jain, R., Verma, P., Gokhale, R., and Rao, K. V. (2012). *Mycobacterium tuberculosis*-driven targeted recalibration of macrophage lipid homeostasis promotes the foamy phenotype. *Cell Host Microbe* 12, 669–681. doi: 10.1016/j.chom.2012.09.012
- Singh, V., Kaur, C., Chaudhary, V. K., Rao, K. V., and Chatterjee, S. (2015). *M. tuberculosis* secretory protein ESAT-6 induces metabolic flux perturbations to drive foamy macrophage differentiation. *Sci. Rep.* 5:12906. doi: 10.1038/srep12906
- Sirakova, T. D., Dubey, V. S., Deb, C., Daniel, J., Korotkova, T. A., Abomoelak, B., et al. (2006). Identification of a diacylglycerol acyltransferase gene involved in accumulation of triacylglycerol in *Mycobacterium tuberculosis* under stress. *Microbiology* 152, 2717–2725. doi: 10.1099/mic.0.28993-0
- Tauchi-Sato, K., Ozeki, S., Houjou, T., Taguchi, R., and Fujimoto, T. (2002). The surface of lipid droplets is a phospholipid monolayer with a unique Fatty Acid composition. *J. Biol. Chem.* 277, 44507–44512. doi: 10.1074/jbc.M207712200
- Via, L. E., Lin, P. L., Ray, S. M., Carrillo, J., Allen, S. S., Eum, S. Y., et al. (2008). Tuberculous granulomas are hypoxic in guinea pigs, rabbits, and nonhuman primates. *Infect. Immun.* 76, 2333–2340. doi: 10.1128/IAI.01515-07

- Vilchèze, C., Molle, V., Carrere-Kremer, S., Leiba, J., Mourey, L., Shenai, S., et al. (2014). Phosphorylation of KasB regulates virulence and acid-fastness in *Mycobacterium tuberculosis*. *PLoS Pathog.* 10:e1004115. doi: 10.1371/journal.ppat.1004115
- Viljoen, A., Blaise, M., de Chastellier, C., and Kremer, L. (2016). MAB_3551c encodes the primary triacylglycerol synthase involved in lipid accumulation in *Mycobacterium abscessus*. *Mol. Microbiol.* doi: 10.1111/mmi.13482. [Epub ahead of print].
- Wältermann, M., and Steinbüchel, A. (2005). Neutral lipid bodies in prokaryotes: recent insights into structure, formation, and relationship to eukaryotic lipid depots. *J. Bacteriol.* 187, 3607–3619. doi: 10.1128/JB.187.11.3607-3619.2005
- Wares, F., Balasubramanian, R., Mohan, A., and Sharma, S. K. (2005). “Tuberculosis control in India. New Delhi: Directorate General of Health Services. Ministry of Health and Family Welfare,” in *Extrapulmonary Tuberculosis: Management and Control*, eds S. P. Agarwal and L. S. Chauhan (Publisher Ministry of Health), 95–114.
- WHO (2015). *Global Tuberculosis Report*. Available online at: http://www.who.int/tb/publications/global_report/en/
- Yang, H., Galea, A., Sytnyk, V., and Crossley, M. (2012). Controlling the size of lipid droplets: lipid and protein factors. *Curr. Opin. Cell Biol.* 24, 509–516. doi: 10.1016/j.ceb.2012.05.012

Conflict of Interest Statement: The authors declare that the research was conducted in the absence of any commercial or financial relationships that could be construed as a potential conflict of interest.

Copyright © 2016 Santucci, Bouzid, Smichi, Poncin, Kremer, De Chastellier, Drancourt and Canaan. This is an open-access article distributed under the terms of the Creative Commons Attribution License (CC BY). The use, distribution or reproduction in other forums is permitted, provided the original author(s) or licensor are credited and that the original publication in this journal is cited, in accordance with accepted academic practice. No use, distribution or reproduction is permitted which does not comply with these terms.



CONCLUSIONS & PERSPECTIVES

9. Conclusions et perspectives

Les infections à *M. canettii* sont relativement rares mais suscitent constamment de nouvelles questions scientifiques. Notre travail de thèse nous a permis de dégager des observations intéressantes, d'avancer de nouvelles hypothèses et d'apporter certains éléments de réponse offrant ainsi de nouvelles perspectives épidémiologiques, cliniques et également mécanistiques. L'ensemble de nos contributions nous a également amené à reconsidérer la nosologie de cette infection. Nous proposons de qualifier les infections à *M. canettii* de « canettose », une entité nosologique étroitement liée, mais clairement distincte de la tuberculose classique. Pour soutenir cette distinction nosologique, les aspects épidémiologiques, cliniques et microbiologiques de l'infection à *M. canettii* ont été détaillés et comparés avec ceux de *M. tuberculosis* (**Tableaux 1 et 2**).

De point de vue épidémiologique, notre travail sur la microbiologie de la tuberculose pulmonaire à Djibouti nous a permis d'isoler cinq nouvelles souches de *M. canettii* montrant qu'elle est activement circulante à Djibouti et supportant son caractère endémique à la Corne de l'Afrique. Cette localisation géographique spécifique de *M. canettii* la distingue des infections à *M. tuberculosis* qui sont distribuées sur le monde entier ([WHO, 2016](#)). Bien que notre étude ait révélé une prévalence d'infections pulmonaires par *M. canettii* à Djibouti de 4% vs 94% pour *M. tuberculosis*, une étude prospective sur les atteintes extra-pulmonaires et ganglionnaires à Djibouti actuellement en cours est nécessaire pour compléter la prévalence exacte de *M. canettii*. Jusqu'à lors, 106 cas microbiologiquement confirmés d'infection à *M. canettii* ont été rapportés dans la littérature ([Aboubaker Osman et al., 2015](#); [Briquet, 2015](#); [Bouzid et al., 2017a](#)). Malgré les éventuelles sous-estimations, la prévalence de *M. canettii* reste faible comparée à celle de *M. tuberculosis* qui a touché plus de 10 millions de personnes en 2015 ([WHO, 2016](#)). Dans la Corne de l'Afrique, l'implantation d'une stratégie d'identification plus fine à l'échelle de l'espèce et notamment la distinction de *M. canettii*

serait requise. Ceci permettrait de collecter des données épidémiologiques exactes et de faciliter le traitement des patients infectés par *M. canettii* pour lesquels la prescription de la pyrazinamide et la streptomycine est inefficace contrairement aux patients infectés par *M. tuberculosis* (**Tableau 2**).

Ce même travail nous a également permis d'isoler deux mycobactéries non-tuberculeuses à partir de patients suspects de tuberculose : *Mycobacterium kansasii* et "*Mycobacterium occulta*posttuberculosis". Encore une fois, nous avons observé la nécessité d'implanter une approche polyphasique pour l'identification des mycobactéries en passant par le MALDI-TOF-MS, la PCR standard multiplexe et le séquençage pour affiner l'identification à l'échelle de l'espèce. Ceci permet d'éviter les échecs thérapeutiques et d'adapter le traitement des patients suivant le type d'infection contractée. La stratégie d'identification que nous avons développée dans ce travail a été transférée dans l'activité de routine du laboratoire diagnostic de l'IHU permettant de rendre un résultat précis. Cette stratégie pourrait être encore simplifiée par le développement de systèmes d'une PCR multiplexe en temps réel pour avoir le résultat plus rapidement. Par ailleurs, nous avons testé un nouveau panel d'antibiotiques incluant la clofazimine, la minocycline, le chloramphénicol et la sulfadiazine et démontré leur efficacité pour inhiber les mycobactéries y compris les souches multi-résistantes. Nous avons proposé d'inclure ces antibiotiques dans le traitement de la tuberculose pulmonaire. Cependant, des études systématiques de sensibilité avec différentes espèces de mycobactéries seraient intéressantes pour compléter le spectre d'inhibition de ces molécules.

De point de vue clinique, le mode d'infection et de transmission de *M. canettii* restent inconnus. D'une part les infections à *M. canettii* sont non transmissibles entre individus et d'autre part elles provoquent près de 45% de formes extra-pulmonaires, y compris 30% d'adénopathies avec possibilité d'atteindre l'œsophage, les ganglions mésentériques et les ascites fluides (**Tableau 1**). Par contre, seul 15% de cas d'infection à *M. tuberculosis* sont

extra-pulmonaires (WHO, 2016). Sur cette base, nous avons proposé que la voie digestive serait une voie de contamination possible pour *M. canettii*. À travers un modèle animal, nous avons montré la translocation de *M. canettii* à partir du tube digestif et sa dissémination dans différents organes du corps dont les poumons et les ganglions cervicaux. Cette capacité rappelle celle de *Mycobacterium bovis* qui affecte les humains essentiellement par voie digestive. Cependant, ce modèle animal reste préliminaire et pour mieux comprendre la physiopathologie de ce phénomène, un modèle animal plus poussé doit être développé en prolongeant la période de suivi et en organisant des analyses anatomopathologiques sur un plus grand nombre de souris. Dans tous les cas, nos résultats suggèrent que les sources d'eau saumâtre, les produits animaux crus, le lait et les produits laitiers peuvent constituer des sources potentielles de *M. canettii* dans la Corne de l'Afrique et vont par conséquent être explorées au cours des prochains mois. En effet, des recherches intensives sur le terrain sont prochainement programmées par le Professeur Didier Raoult et le Docteur Bernard Davoust.

Un troisième volet de notre thèse a permis de mettre en évidence un comportement intracellulaire différentiel entre *M. canettii* et *M. tuberculosis* dans les adipocytes matures. Dans une étude antérieure, la co-culture des amibes *Acanthamoeba polyphaga* avec *M. canettii* a également révélé un comportement particulier de cette mycobactérie (**Tableau 2**). Dans ce modèle, *M. canettii* ingérée par les trophozoïtes survie dans des vacuoles cytoplasmiques mais échappe à leur enkystement contrairement à *M. tuberculosis* (Mba Medie et al., 2011). Dans cette partie, nous avons démontré que le tissu adipeux brun pourrait constituer une des cibles potentielles de *M. canettii* voire même un réservoir. Ce résultat propose alors un réservoir candidat qui doit être considéré lors des investigations sur le terrain. Ce travail ouvre également les perspectives de nouveaux modèles cellulaires et/ou animaux pour comprendre le mécanisme d'infection de *M. canettii*.

En conclusion, l'ensemble des résultats générés au cours de cette thèse montrent que l'infection à *M. canettii* est différente de celle à *M. tuberculosis* et qu'elle représente une entité nosologique différente de la tuberculose. Ce travail de recherche a reçu la médaille d'argent lors de la Journée Scientifique de la Fondation Méditerranée Infection, à Marseille le 07 Juillet 2017.

Tableau 1 : Tableau comparatif entre la tuberculose et la canettose. Les différences sont indiquées en orange.

	TUBERCULOSE	CANETTOSE
Épidémiologie		
Prévalence	10.4 million en 2015	106 au total
Distribution géographique	Monde entier	Corne de l'Afrique
Statut immunitaire		
Immunocompétent	+	+
Immunodéprimé	+	+
Site d'infection		
Pulmonaire	+++ (85%)	49 (54,4%)
Ganglionnaire	++	27 (30%)
Disséminé	++	5 (5,6%)
Gastro-Intestinal	+	2 (2,2%)
Système nerveux central	+ (1%)	1 (1,1%)
Abcès variés	+	6 (6,7%)
Cutané	+	0
Génito-urinaire	+	0
Oculaire	+	0
Musculo-squelettique	+	0
Transmission		
Aérosols	+++	?
Inoculation	+	?
Digestive	+/-	++
Entre humains	+++	?

Tableau 2 : Tableau comparatif entre *M. tuberculosis* H37Rv et *M. canettii* CIPT

140010059. Les différences sont indiquées en orange.

	<i>M. tuberculosis</i> H37Rv	<i>M. canettii</i> CIPT140010059
Microbiologie		
Gram	+	+
Aspect de la colonie	Rugueux	Lisse
Couleur de la colonie	Blanc-ivoire	Beige-pâle
Forme de la bactérie	Bacille	Bacille
Arrangement	Agrégats cordés	Singletons ou petits agrégats
Tolérance à l'oxygène	Micro-aérophilie	Aérophilie
Temps de dédoublement sur milieu liquide	25 heures	17 heures
Température de culture	37°C	37°C
Acido-alcool-résistance	+	+
Mobilité	Non	Non
Sporulation	Non	Non
Taille	1.7±0.3 µm	2.56±0.5 µm

Caractères biochimiques		
Nitrate reductase	+	+
Production de Niacin	+	-
Catalase 22°C	+	+
Catalase 68°C	-	-
Uréase	+	+
Hydrolyse du Tween 80	+	+
Présence de la β-glucosidase	+	-

Sensibilité aux antibiotiques		
Rifampicine (1 µg/mL)	S	S
Isoniazide (0.2 µg/mL)	S	S
Ethambutol (1 µg/mL)	S	S
Streptomycine (> 32 µg/mL)	S	R
Pyrazinamide (> 32 µg/mL)	S	R
Ofloxacin (1 µg/mL)	S	S
Kanamycine (1 µg/mL)	S	S
Amikacine (4 µg/mL)	S	S
Clofazimine (1 µg/mL)	S	S

Rifabutine (1 µg/mL)	S	S
Ciprofloxacine (1,5 µg/mL)	S	S

Caractères moléculaires		
Taille du génome (Mb)	4.4115	4.48206
GC%	65.50	65.60
Plasmide	0	0
Gènes	4008	4293
Protéines	3906	4064
Gènes uniques	-	14
rRNA (opéron)	3	3
tRNA	45	45

Comportement intra-amibien		
% mycobactéries phagocytées	12.4±0.3%	89±0.6%
% amibes infectées	26±1%	32±2%
Survie dans les trophozoïtes	+	+
Multiplication dans les trophozoïtes	-	-
Enkystement	Survie dans les kystes	Échappe à l'enkystement



REFERENCES

10. Références

- Aboubaker Osman, D., Bouzid, F., Canaan, S., and Drancourt, M. (2015). Smooth Tubercle Bacilli: Neglected Opportunistic Tropical Pathogens. *Frontiers in public health* 3, 283. doi: 10.3389/fpubh.2015.00283.
- Aboubaker Osman, D., Garnotel, E., and Drancourt, M. (2017). Dry-heat inactivation of "*Mycobacterium canettii*". *BMC Res Notes* 10(1), 201. doi: 10.1186/s13104-017-2522-z.
- Adekambi, T., Berger, P., Raoult, D., and Drancourt, M. (2006). rpoB gene sequence-based characterization of emerging non-tuberculous mycobacteria with descriptions of *Mycobacterium bolletii* sp. nov., *Mycobacterium phocaicum* sp. nov. and *Mycobacterium aubagnense* sp. nov. *Int J Syst Evol Microbiol* 56(Pt 1), 133-143. doi: 10.1099/ijss.0.63969-0.
- Agarwal, P., Khan, S.R., Verma, S.C., Beg, M., Singh, K., Mitra, K., et al. (2014). *Mycobacterium tuberculosis* persistence in various adipose depots of infected mice and the effect of anti-tubercular therapy. *Microbes and infection / Institut Pasteur* 16(7), 571-580. doi: 10.1016/j.micinf.2014.04.006.
- Agarwal, P., Pandey, P., Sarkar, J., and Krishnan, M.Y. (2016). *Mycobacterium tuberculosis* can gain access to adipose depots of mice infected via the intra-nasal route and to lungs of mice with an infected subcutaneous fat implant. *Microbial pathogenesis* 93, 32-37. doi: 10.1016/j.micpath.2016.01.004.
- Asmar, S., Sassi, M., Phelippeau, M., and Drancourt, M. (2016). Inverse correlation between salt tolerance and host-adaptation in mycobacteria. *BMC Res Notes* 9, 249. doi: 10.1186/s13104-016-2054-y.

- Asselineau, C., Montrozier, H., and Prome, J.C. (1969). [Structure of alpha-mycolic acids isolated from the Canetti strain of *Mycobacterium tuberculosis*]. *Bull Soc Chim Fr* 2, 592-596.
- Baker, O., Lee, O.Y., Wu, H.H., Besra, G.S., Minnikin, D.E., Llewellyn, G., et al. (2015). Human tuberculosis predates domestication in ancient Syria. *Tuberculosis (Edinb.)* 95 Suppl 1, S4-S12. doi: S1472-9792(15)00002-5 [pii];10.1016/j.tube.2015.02.001 [doi].
- Blouin, Y., Cazajous, G., Dehan, C., Soler, C., Vong, R., Hassan, M.O., et al. (2014). Progenitor "*Mycobacterium canettii*" clone responsible for lymph node tuberculosis epidemic, Djibouti. *Emerg.Infect.Dis.* 20(1), 21-28.
- Boritsch, E.C., Frigui, W., Cascioferro, A., Malaga, W., Etienne, G., Laval, F.o., et al. (2016a). pks5-recombination-mediated surface remodelling in *Mycobacterium tuberculosis* emergence. *Nature Microbiology* 1, 15019.
- Boritsch, E.C., Khanna, V., Pawlik, A., Honore, N., Navas, V.H., Ma, L., et al. (2016b). Key experimental evidence of chromosomal DNA transfer among selected tuberculosis-causing mycobacteria. *Proceedings of the National Academy of Sciences of the United States of America* 113(35), 9876-9881. doi: 10.1073/pnas.1604921113.
- Bouزيد, F., Astier, H., Osman, D.A., Javelle, E., Hassan, M.O., Simon, F., et al. (2017a). Extended spectrum of antibiotic susceptibility for tuberculosis, djibouti. *Int J Antimicrob Agents*. doi: 10.1016/j.ijantimicag.2017.07.007.
- Bouزيد, F., Bregeon, F., Lépidi, H., Donoghue, H., Minnikin, D., and Drancourt, M. (2017b). Ready experimental translocation of *Mycobacterium canettii* yields pulmonary tuberculosis. *Infection and Immunity*. Under revision.
- Bouزيد, F., Bregeon, F., Poncin, I., Weber, P., Drancourt, M., and Canaan, S. (2017c). *Mycobacterium canettii* Infection of Adipose Tissues. *Front Cell Infect Microbiol* 7, 189. doi: 10.3389/fcimb.2017.00189.

- Boyer-Cazajous, G., Martinaud, C., Dehan, C., Hassan, M.O., Gaas, Y., Chenilleau-Vidal, M.C., et al. (2014). High prevalence of multidrug resistant tuberculosis in Djibouti: a retrospective study. *J Infect Dev Ctries* 8(2), 233-236. doi: 10.3855/jidc.3837.
- Briquet, A. (2015). Étude rétrospective de 20 cas d'infections à *Mycobacterium canettii* chez des militaires français ou des membres de familles de militaires français sur une période de 17 ans (1998-2015). Medical Thesis, Marseille, France.
- Brosch, R., Gordon, S.V., Marmiesse, M., Brodin, P., Buchrieser, C., Eiglmeier, K., et al. (2002). A new evolutionary scenario for the *Mycobacterium tuberculosis* complex. *Proceedings of the National Academy of Sciences of the United States of America* 99(6), 3684-3689. doi: 10.1073/pnas.052548299.
- Bruno, D. (2006). Tuberculoses à *Mycobacterium Canetti*. Epidémiologie, clinique, microbiologie et phylogénie. Medical Thesis, Bordeaux, France.
- Caire-Brandli, I., Papadopoulos, A., Malaga, W., Marais, D., Canaan, S., Thilo, L., et al. (2014). Reversible lipid accumulation and associated division arrest of *Mycobacterium avium* in lipoprotein-induced foamy macrophages may resemble key events during latency and reactivation of tuberculosis. *Infect Immun* 82(2), 476-490. doi: 10.1128/IAI.01196-13.
- Cambau, E., and Drancourt, M. (2014). Steps towards the discovery of *Mycobacterium tuberculosis* by Robert Koch, 1882. *Clin Microbiol Infect* 20(3), 196-201. doi: 10.1111/1469-0691.12555.
- Cannon, B., and Nedergaard, J. (2004). Brown adipose tissue: function and physiological significance. *Physiological reviews* 84(1), 277-359. doi: 10.1152/physrev.00015.2003.
- CDC (2006). Emergence of *Mycobacterium tuberculosis* with extensive resistance to second-line drugs---worldwide, 2000--2004. . *MMWR* 5, 55:301.

- Coscolla, M., Lewin, A., Metzger, S., Maetz-Renning, K., Calvignac-Spencer, S., Nitsche, A., et al. (2013). Novel *Mycobacterium tuberculosis* complex isolate from a wild chimpanzee. *Emerg Infect Dis* 19(6), 969-976. doi: 10.3201/eid1906.121012.
- Daniel, J., Maamar, H., Deb, C., Sirakova, T.D., and Kolattukudy, P.E. (2011). *Mycobacterium tuberculosis* uses host triacylglycerol to accumulate lipid droplets and acquires a dormancy-like phenotype in lipid-loaded macrophages. *PLoS Pathog* 7(6), e1002093. doi: 10.1371/journal.ppat.100209310-PLPA-RA-3063 [pii].
- Drancourt, M., Berger, P., and Raoult, D. (2004). Systematic 16S rRNA gene sequencing of atypical clinical isolates identified 27 new bacterial species associated with humans. *J Clin Microbiol* 42(5), 2197-2202.
- Fabre, M., Koeck, J.L., Le, F.P., Simon, F., Herve, V., Vergnaud, G., et al. (2004). High genetic diversity revealed by variable-number tandem repeat genotyping and analysis of hsp65 gene polymorphism in a large collection of "*Mycobacterium canettii*" strains indicates that the *M. tuberculosis* complex is a recently emerged clone of "*M. canettii*". *J.Clin.Microbiol.* 42(7), 3248-3255. doi: 10.1128/JCM.42.7.3248-3255.2004 [doi];42/7/3248 [pii].
- Fan, X., Xie, L., Li, W., and Xie, J. (2014). Prophage-like elements present in *Mycobacterium* genomes. *BMC Genomics* 15, 243. doi: 10.1186/1471-2164-15-243.
- Firdessa, R., Berg, S., Hailu, E., Schelling, E., Gumi, B., Erenso, G., et al. (2013). *Mycobacterial* lineages causing pulmonary and extrapulmonary tuberculosis, Ethiopia. *Emerg Infect Dis* 19(3), 460-463. doi: 10.3201/eid1903.120256.
- Ghodbane, R., and Drancourt, M. (2013). Non-human sources of *Mycobacterium tuberculosis*. *Tuberculosis (Edinb)* 93(6), 589-595. doi: 10.1016/j.tube.2013.09.005.

- Ghodbane, R., Mba Medie, F., Lepidi, H., Nappez, C., and Drancourt, M. (2014). Long-term survival of tuberculosis complex mycobacteria in soil. *Microbiology* 160(Pt 3), 496-501. doi: 10.1099/mic.0.073379-0.
- Goh, K.S., Legrand, E., Sola, C., and Rastogi, N. (2001). Rapid differentiation of "*Mycobacterium canettii*" from other *Mycobacterium tuberculosis* complex organisms by PCR-restriction analysis of the hsp65 gene. *J Clin Microbiol* 39(10), 3705-3708. doi: 10.1128/JCM.39.10.3705-3708.2001.
- Gomez-Hernandez, A., Beneit, N., Diaz-Castroverde, S., and Escribano, O. (2016). Differential Role of Adipose Tissues in Obesity and Related Metabolic and Vascular Complications. *International journal of endocrinology* 2016, 1216783. doi: 10.1155/2016/1216783.
- Griffith, D.E., Aksamit, T., Brown-Elliott, B.A., Catanzaro, A., Daley, C., Gordin, F., et al. (2007). An official ATS/IDSA statement: diagnosis, treatment, and prevention of nontuberculous mycobacterial diseases. *Am J Respir Crit Care Med* 175(4), 367-416. doi: 10.1164/rccm.200604-571ST.
- Gutierrez, M.C., Brisse, S., Brosch, R., Fabre, M., Omais, B., Marmiesse, M., et al. (2005). Ancient origin and gene mosaicism of the progenitor of *Mycobacterium tuberculosis*. *PLoS pathogens* 1(1), e5. doi: 10.1371/journal.ppat.0010005.
- Hershkovitz, I., Donoghue, H.D., Minnikin, D.E., Besra, G.S., Lee, O.Y., Gernaey, A.M., et al. (2008). Detection and molecular characterization of 9,000-year-old *Mycobacterium tuberculosis* from a Neolithic settlement in the Eastern Mediterranean. *PLoS One*. 3(10), e3426. doi: 10.1371/journal.pone.0003426 [doi].
- Jankute, M., Nataraj, V., Lee, O.Y., Wu, H.H.T., Ridell, M., Garton, N.J., et al. (2017). The role of hydrophobicity in tuberculosis evolution and pathogenicity. *Sci Rep* 7(1), 1315. doi: 10.1038/s41598-017-01501-0.

- Koch, M.L., and Cote, R.A. (1965). Comparison of Fluorescence Microscopy with Ziehl-Neelsen Stain for Demonstration of Acid-Fast Bacilli in Smear Preparations and Tissue Sections. *Am Rev Respir Dis* 91, 283-284. doi: 10.1164/arrd.1965.91.2.283.
- Koch, R. (1882). Die Aetiologie der Tuberculose. *Berl Klin Wochenschr* 9, 221–230.
- Koeck, J.L., Bernatas, J.J., Gerome, P., Fabre, M., Houmed, A., Herve, V., et al. (2002). [Epidemiology of resistance to antituberculosis drugs in *Mycobacterium tuberculosis* complex strains isolated from adenopathies in Djibouti. Prospective study carried out in 1999]. *Med Trop (Mars)* 62(1), 70-72.
- Koeck, J.L., Fabre, M., Simon, F., Daffe, M., Garnotel, E., Matan, A.B., et al. (2011). Clinical characteristics of the smooth tubercle bacilli '*Mycobacterium canettii*' infection suggest the existence of an environmental reservoir. *Clinical microbiology and infection : the official publication of the European Society of Clinical Microbiology and Infectious Diseases* 17(7), 1013-1019. doi: 10.1111/j.1469-0691.2010.03347.x.
- Mauss, H., and Levy, F.M. (1972). [Involvement of adipose tissue in experimental tuberculosis of the mouse]. *Pathologia et microbiologia* 38(5), 333-345.
- Mba Medie, F., Ben Salah, I., Henrissat, B., Raoult, D., and Drancourt, M. (2011). *Mycobacterium tuberculosis* complex mycobacteria as amoeba-resistant organisms. *PLoS ONE* 6(6), e20499. doi: 10.1371/journal.pone.0020499.
- Millan-Lou, M.I., Olle-Goig, J.E., Tortola, M.T., Martin, C., and Samper, S. (2016). Mycobacterial diversity causing multi- and extensively drug-resistant tuberculosis in Djibouti, Horn of Africa. *Int J Tuberc Lung Dis* 20(2), 150-153. doi: 10.5588/ijtld.15.0268.
- Mitchison, D.A. (2005). The diagnosis and therapy of tuberculosis during the past 100 years. *Am J Respir Crit Care Med* 171(7), 699-706. doi: 10.1164/rccm.200411-1603OE.

- Nedergaard, J., Bengtsson, T., and Cannon, B. (2007). Unexpected evidence for active brown adipose tissue in adult humans. *Am J Physiol Endocrinol Metab* 293(2), E444-452. doi: 10.1152/ajpendo.00691.2006.
- Neyrolles, O., Hernandez-Pando, R., Pietri-Rouxel, F., Fornes, P., Tailleux, L., Payan, J.A., et al. (2006). Is Adipose Tissue a Place for *Mycobacterium tuberculosis* Persistence? *PLoS ONE* 1, e43.
- Parsons, S.D., Drewe, J.A., Gey van Pittius, N.C., Warren, R.M., and van Helden, P.D. (2013). Novel cause of tuberculosis in meerkats, South Africa. *Emerg Infect Dis* 19(12), 2004-2007. doi: 10.3201/eid1912.130268.
- Peyron, P., Vaubourgeix, J., Poquet, Y., Levillain, F., Botanch, C., Bardou, F., et al. (2008). Foamy macrophages from tuberculous patients' granulomas constitute a nutrient-rich reservoir for *M. tuberculosis* persistence. *PLoS Pathog* 4(11), e1000204. doi: 10.1371/journal.ppat.1000204.
- Pfyffer, G.E., Auckenthaler, R., van Embden, J.D., and van, S.D. (1998). *Mycobacterium canettii*, the smooth variant of *M. tuberculosis*, isolated from a Swiss patient exposed in Africa. *Emerg.Infect.Dis.* 4(4), 631-634. doi: 10.3201/eid0404.980414 [doi].
- Rastogi, S., Agarwal, P., and Krishnan, M.Y. (2016). Use of an adipocyte model to study the transcriptional adaptation of *Mycobacterium tuberculosis* to store and degrade host fat. *International journal of mycobacteriology* 5(1), 92-98. doi:10.1016/j.ijmyco.2015.10.003.
- Russell, D.G., Cardona, P.J., Kim, M.J., Allain, S., and Altare, F. (2009). Foamy macrophages and the progression of the human tuberculosis granuloma. *Nat Immunol* 10(9), 943-948. doi: ni.1781 [pii]10.1038/ni.1781.
- Santucci, P., Bouzid, F., Smichi, N., Poncin, I., Kremer, L., De Chastellier, C., et al. (2016). Experimental Models of Foamy Macrophages and Approaches for Dissecting the

- Mechanisms of Lipid Accumulation and Consumption during Dormancy and Reactivation of Tuberculosis. *Frontiers in cellular and infection microbiology* 6, 122. doi: 10.3389/fcimb.2016.00122.
- Springer, B., Lucke, K., Calligaris-Maibach, R., Ritter, C., and Bottger, E.C. (2009). Quantitative drug susceptibility testing of *Mycobacterium tuberculosis* by use of MGIT 960 and EpiCenter instrumentation. *J Clin Microbiol* 47(6), 1773-1780. doi: 10.1128/JCM.02501-08.
- Supply, P., Marceau, M., Mangenot, S., Roche, D., Rouanet, C., Khanna, V., et al. (2013). Genomic analysis of smooth tubercle bacilli provides insights into ancestry and pathoadaptation of *Mycobacterium tuberculosis*. *Nature genetics* 45(2), 172-179. doi: 10.1038/ng.2517.
- Tortoli, E., Rogasi, P.G., Fantoni, E., Beltrami, C., De Francisci, A., and Mariottini, A. (2010). Infection due to a novel mycobacterium, mimicking multidrug-resistant *Mycobacterium tuberculosis*. *Clin Microbiol Infect* 16(8), 1130-1134. doi: 10.1111/j.1469-0691.2009.03063.x.
- van Soolingen, D., Hoogenboezem, T., de Haas, P.E., Hermans, P.W., Koedam, M.A., Teppema, K.S., et al. (1997). A novel pathogenic taxon of the *Mycobacterium tuberculosis* complex, Canetti: characterization of an exceptional isolate from Africa. *Int.J.Syst.Bacteriol.* 47(4), 1236-1245. doi: 10.1099/00207713-47-4-1236 [doi].
- Wang, J., McIntosh, F., Radomski, N., Dewar, K., Simeone, R., Enninga, J., et al. (2015). Insights on the emergence of *Mycobacterium tuberculosis* from the analysis of *Mycobacterium kansasii*. *Genome Biol.Evol.* 7(3), 856-870. doi: evv035 [pii];10.1093/gbe/evv035 [doi].

- Warren, R.M., Gey van Pittius, N.C., Barnard, M., Hesselning, A., Engelke, E., de Kock, M., et al. (2006). Differentiation of *Mycobacterium tuberculosis* complex by PCR amplification of genomic regions of difference. *Int J Tuberc Lung Dis* 10(7), 818-822.
- WHO (World Health Organization). Global tuberculosis report. 2016. Available from: <http://apps.who.int/iris/bitstream/10665/250441/1/9789241565394-eng.pdf?ua=1>; 2016.
- Zeka, A.N., Tasbakan, S., and Cavusoglu, C. (2011). Evaluation of the GeneXpert MTB/RIF assay for rapid diagnosis of tuberculosis and detection of rifampin resistance in pulmonary and extrapulmonary specimens. *J Clin Microbiol* 49(12), 4138-4141. doi: 10.1128/JCM.05434-11.
- Zingue, D., Flaudrops, C., and Drancourt, M. (2016). Direct matrix-assisted laser desorption ionisation time-of-flight mass spectrometry identification of mycobacteria from colonies. *Eur J Clin Microbiol Infect Dis* 35(12), 1983-1987. doi: 10.1007/s10096-016-2750-5.